INTERNATIONAL INSTITUTE FOR INFRASTRUCTURAL, HYDRAULIC AND ENVIRONMENTAL ENGINEERING

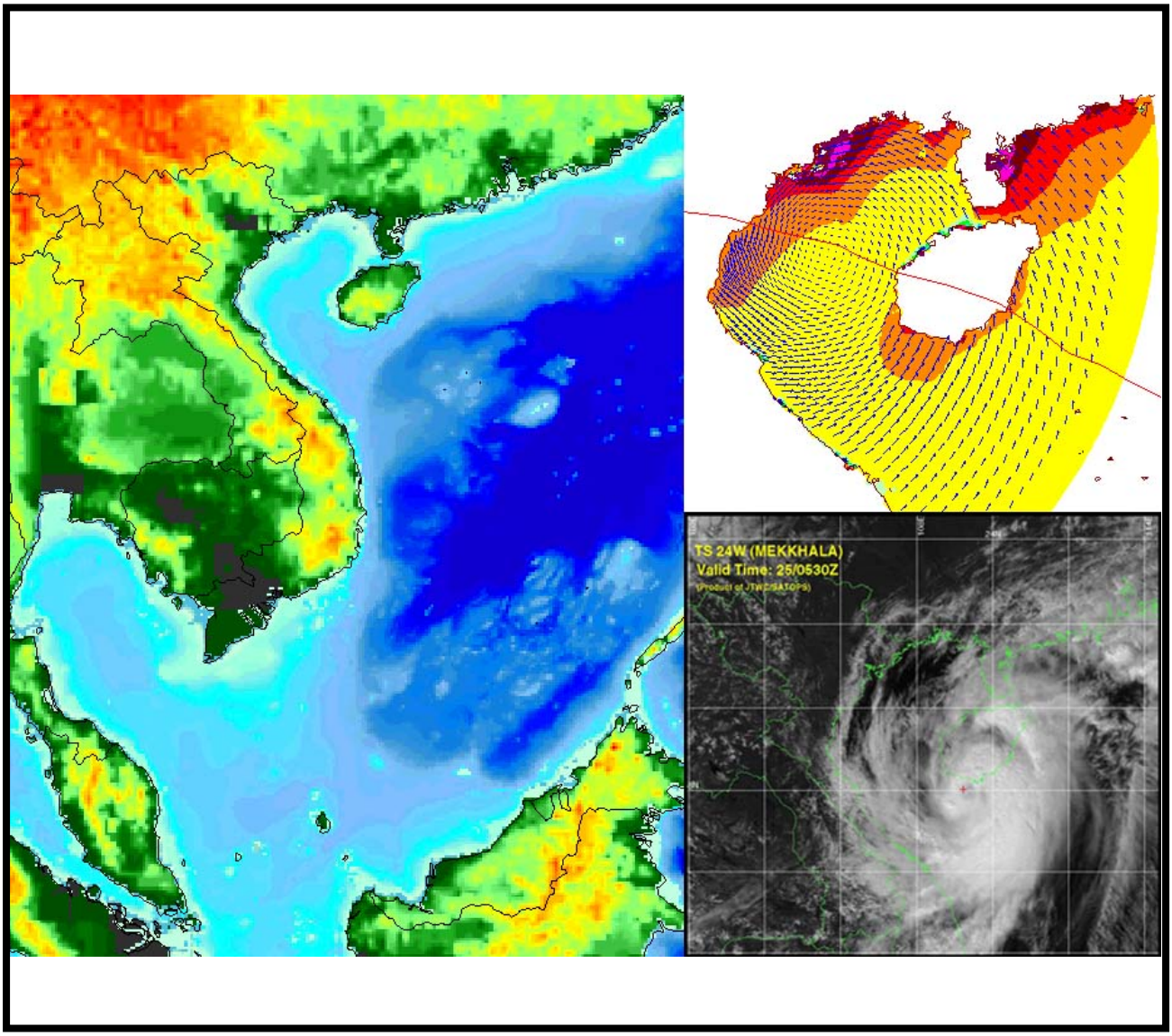

Storm Surge Modelling for Vietnam's Coast

Vu Thi Thu Thuy

M.Sc. Thesis H.E. 136
April 2003

IHE DELFT

INTERNATIONAL INSTITUTE FOR INFRASTRUCTURAL,
HYDRAULIC AND ENVIRONMENTAL ENGINEERING

Storm Surge Modelling for Vietnam's Coast

Master of Science Thesis
by
Vu Thi Thu Thuy

Supervisors

Assoc. Prof. Dr. Randa M.M. Hassan Assoc. Prof. Dr. Ir. Zheng. B. Wang

Examination Committee

Prof. B. Petry, IHE, Chairman
Prof. Dr.Ir. Marcel J.F. Stive, TU Delft
Assoc. Prof. Dr. Randa M.M. Hassan, IHE
Assoc. Prof. Dr. Ir. Zheng. B. Wang, TU Delft / WL | Delft Hydraulics

Delft, The Netherlands
April 2003

ABSTRACT

Vietnam is located near the Northwest Pacific Ocean - the largest storm basin of the world. Thus, Vietnam's coast with many coastal works, economical zones as well as high density populated regions, is the most vulnerable area under typhoons accompanied with serious storm surges. This is the main reason for the huge damages occuring in the areas. Storm surges threaten not only safety of people's lives but also coastal structures. Traditional planning, design of coastal projects and coastal zone management usually take into account these effects based on their probability distribution of very limited observed data, which results in a low reliability and safety. Therefore, improving the accuracy in determination of these abnormal water level rise during storm is essential for proper planing, design of coastal works as well as integrated coastal zone management.

The objectives of this study are: (1) Set up a storm surge model for the Vietnamese coast; (2) Compute storm surges and determine the probability distribution of storm surge for the Vietnamese coast.

To achieve these objectives, firstly various models of typhoon wind and pressure are investigated. Based on observations and criteria of root-mean-squared error, the Fujita model is selected for describing typhoon pressure field and the modified Rankine vortex model is chosen for presenting typhoon wind field. Secondly, Delft3D-FLOW is used to simulate storm surge in typhoon condition. The model is set-up for the northern part of the Vietnamese coast where high frequency of storm causing serious storm surges and severe damages occur. The hydrodynamic model is calibrated and validated for both non-storm condition and extreme condition of typhoons. The effects of boundary conditions and model parameters to the results are evaluated using sensitivity analysis. Thirdly, based on storm track information, storm surges at various locations along the north coast are computed for the years from 1951 to 2001. And then, some popular statistical distributions such as log-normal, Pearson type III, general extreme value, etc. are used to fit with set of storm surge result to model the probability distributions of storm surge and to extrapolate for long-term return period values of storm surge at these locations. Finally, by evaluation the accuracy of the result for storm surge hind-cast, some suggestions is given for storm surge forecasting in the area.

ACKNOWLEDGEMENTS

This work has been carried out to meet the requirements of the Master of Science degree at the Institute for Infrastructural, Hydraulic and Environmental Engineering (IHE), Delft under the financial support of the training project HWRU- TU Delft- IHE Delft- WL Delft Hydraulic. I would like to express my sincere gratitude to all people who have helped me in the study. I thank them all for their support and advice, which contribute to success of this study.

I sincerely thank my supervisors: Assoc. Prof. Dr. Randa M.M. Hassan and Assoc. Prof. Dr. Ir. Zheng. B. Wang for their valuable technical guidance and perpetual encouragement. My sincere thanks to Professor Dr. Le Kim Truyen – Rector of HWRU, Professor Ir. Kees d'Angremond – Team Leader of the HWRU–TU Delft–IHE Delft–WL Delft Hydraulic Training Project, Mr. Jan van der Laan – Project Co-ordinator, Assoc. Prof. Henk Jan Verhagen (TU Delft), Ir. Mick van der Wegen (IHE), and Dr. Vu Minh Cat, Department of Scientific Research and International Co-operation, HWRU. They have made efforts for the arrangement of financial support for this research work and have supported for the study of my husband beside me during my research.

I wish to express my thanks to Dr. Bui Van Duc from Hydro-Meteorological Service of Vietnam and the staff of the Marine Hydro-Meteorological Center: Dr. Nguyen The Tuong, Dr. Bui Dinh Khuoc and Dr. Vu Thanh Ca. They together with WL Delft Hydraulics are willing to help me a lot in providing data for this study.

I also wish to thank all of my colleagues and my friends for their support and encouragement during my stay in Delft.

I am grateful to my parents, my younger brother, my lovely son and my family in law for their perpetual support, help and encouragement throughout my life.

Last but not least, I am deeply grateful to my beloved husband for his perpetually technical and moral support during my entire study period, without it this research work would not have been accomplished and succeeded.

Delft, April 2003

Vu Thi Thu Thuy

TABLE OF CONTENTS

LIST OF FIGURES

LIST OF TABLES

ABBREVIATIONS

ASCE	American Society of Civil Engineers
Delft3D-FLOW	3D flow module of the Delft3D package developed by WL | Delft Hydraulics
CDF	cumulative distribution function
ETOPO2	2 minute Earth topography
EV1	Extreme Value type I distribution
EV2	Extreme Value type II distribution
EV3	Extreme Value type III distribution
GEV	General Extreme Value distribution
GLG	Generalised logistic distribution
GMT	Greenwich Mean Time
HMS	Vietnam Hydro-Meteorological Services
JTWC	Joint Typhoon Warning Center
LLG	log-logistic distribution
LN	log-normal distribution
LP3	log-Pearson type III distribution
MSL	mean sea level
NPO	Northwest Pacific Ocean
RMSE	root mean squared error
NCDC	National Climatic Data Center, USA
P3	Pearson type III distribution
PDF	probability density function
POT	peak-over-threshold
TOPEX	Topography Experiment for ocean circulation
TOPEX/Poseidon	Joint US – French orbital mission, launched in 1992 to track changes in sea-level height with radar altimeters
UNDP	United Nations Development Program
USACE	US Army Corps of Engineers
USD	US Dollars
UTM	Universal Transverse Mercator
VCM	Vietnam Coast Model
VND	Vietnam Dong, Vietnamese currency
VNT	Vietnam Local Time

LIST OF SYMBOLS

Chapter 2

F	tidal form number	(-)
f	Coriolis parameter	(-)
H_{K1}	amplitude of the K_1 (Diurnal lunar-solar declination tide) constituent	(m)
H_{M2}	amplitude of the M_2 (Semi-diurnal principle lunar tide) constituent	(m)
H_{O1}	amplitude of the O_1 (Diurnal lunar declination tide) constituent	(m)
H_{S2}	amplitude of the S_2 (Semi-diurnal principle solar tide) constituent	(m)

Chapter 3

B	parameter of Holland wind model	(-)
b	parameter of deMaria wind model	(-)
C_1	coefficient for moving typhoon center	(-)
C_2	empirical coefficient for gradient wind speed	(-)
F	adjustment coefficient for moving typhoon	(-)
H	altitude of observation station	(m)
P	atmospheric pressure	(mb)
p_0	atmospheric pressure at typhoon center	(mb)
p_a	atmospheric pressure at a specific location	(mb)
p_n	atmospheric pressure at outskirts of typhoon	(mb)
R	radius of maximum wind speed	(km)
r	distance from a specific location to typhoon center	(km)
dP	atmospheric pressure drop	(mb)
ΔP	atmospheric pressure drop	(mb)
V_f	movement speed of typhoon center	(m/s)
W	wind speed	(m/s)
W_{max}	maximum wind speed	(m/s)
W_r	gradient wind speed at a distance r from typhoon center	(m/s)
W_x	x-component of wind velocity	(m/s)
W_y	y-component of wind velocity	(m/s)
X	parameter of the modified Rankine vortex wind model	(-)
β	angle between gradient wind and isopiestic line	(deg)
ϕ	direction of typhoon movement	(deg)
φ	latitude	(deg)
π	Pi number	(-)
θ	angle of line connecting a point and typhoon center respects to x-axis	(deg)
ρ	air density	(kg/m^3)
ω	Earth angular speed	(rad/s)

Chapter 4

C	De Chézy coefficient	($m^{0.5}/s$)
C_d	wind drag coefficient	(-)
d	water depth below datum	(m)
f	Coriolis parameter	(-)
g	acceleration due to gravity	(m/s^2)
p_a	atmospheric pressure at a specific location	(mb)
t	time variable	(sec)
$\|U\|$	magnitude of total depth-averaged flow velocity	(m/s)
W	wind speed	(m/s)

W_{10}	wind speed at 10m above free surface	(m/s)
u	depth-averaged flow velocity in x-direction	(m/s)
v	depth-averaged flow velocity in y-direction	(m/s)
x	distance along west-east direction	(m)
y	distance along south-north direction	(m)
η	Water level respects to datum	(m)
ε	eddy viscosity	(m^2/s)
ρ, ρ_a	air density	(kg/m^3)
ρ_w	water density	(kg/m^3)
τ_{wx}, τ_{wy}	components of wind stress	(N/m^2)
ω	Earth angular speed	(rad/s)

Chapter 5

a	coefficient for calculating confidence interval	(-)
a_0	lower bound of random variable	(m)
C_V	coefficient of variation	(-)
C_S	coefficient of skewness	(-)
$F(x)$	cumulative distribution function	(m)
$f(x)$	probability density function	(-)
i	rank of a value in series	(-)
k	shape parameter of GEV distribution	(-)
n	length of sample series	(-)
P	probability	(-)
P_{AM}	probability of annual maximum series	(-)
P_{PD}	probability of partial duration series	(-)
S	departure parameter	(-)
X	random variable (storm surge, water level)	(m)
X_T	value corresponding to return period of T years	(m)
X_{TU}	upper limit of X_T	(m)
X_{TL}	lower limit of X_T	(m)
$\overline{X}$	mean value	(m)
x	value of random variable	(m)
α	shape parameter of pdf	(-)
β	scale parameter of pdf	(-)
Γ	gamma function	(-)
σ	standard deviation	(m)

CHAPTER 1. INTRODUCTION

1.1. General description of the area

Vietnam is located at the centre of Southeast Asia, between $8^{o}02'$N - $23^{o}23'$N and $102^{o}08'$E - $109^{o}28'$E as shown in Figure 1-1. It is located near the Northwest Pacific Ocean (NPO) where every year the highest number of storms occurs – about 30% of storm occurrences in the world (Le Van Thao et al., 2000). In recent years, the averaged number of storms in the region has increased gradually, from 22 storms per year before 1980 to currently become 31 storms per year for the time being. There are about six storms and tropical depressions on the average that hit the country annually. The highest number was reaching 12 in 1978. Therefore, Vietnam with more than 3200 km of coastline, with many coastal protection works, economical zones as well as densely populated regions along the coast, is situated in the vulnerable area by storms accompanied with serious storm surges.

1.2. Threat of storms and storm surges in Vietnam

Storms and tropical depressions in Vietnam cause strong whirlwind, gust-wind, baffling wind but also heavy rains resulting in floods and high storm surges. They have caused severe damage in terms of human life and property.

According to Le Van Thao et al. (2000), storms and floods occur in Vietnam unevenly. The most affected areas are the northern and the central parts. The southern part is the least storm affected area but some storms have serious damages to this area, of which typhoon Linda in November 1997 is an example. It is a very uncommonly strong storm in the past 100 years to the southern area, killed 788 lives, injured 1,142 others, resulted in 2,541 people missing, 2,789 boats and ships sank, and other damages. Total estimated economic loss was about 480 million USD. Another example is that in early November 1999, after a tropical depression hit land of the southern tip of the Central of Vietnam, a cold front in combination with a tropical convergence caused very heavy rains in 6 days with abnormal intensity and total amount of rainfall (2288 mm in Hue) resulting in severe floods in the central provinces. The historical floods killed 592 people, injured 204 others and damaged 235 million USD (Le Van Thao et al., 2000).

According to statistical data of the Standing Office of the Central Committee for Flood and Storm Control, damages caused by storms and tropical depressions in 10 years from 1989 to 1998 in Vietnam is as follows: about 14,674,613 million VND of economic loss and 4,730 people death.

Since storms are usually accompanied by storm surges, it is difficult to identify which damages caused by storm surge or by the storm itself. However, in qualitatively the losses due to storm surge can be realised as follows (Le Trong Dao et al., 2000):

Storm surges can cause severe inundation of a large coastal area for a long time. This leads to salt intrusion for paddy field and it takes a long time to wash out. Inundation together with salt intrusion considerably contribute to destruction of houses and solid coastal works. Moreover, storm surges cause beach erosion, displace stones or concrete amour units on jetties, groins or breakwaters, undermine structures via scouring, cut new inlets through barrier beach and shoal navigational channels. The latter shoaling problem can result in hazards to navigation thus impeding vessel traffic and hampering harbour operation. Furthermore, because of surge level, waves have more chance to destroy sea dike system by over flow or overtopping, etc.

The above evidences show the severe effects of storm surges on socio-economic activities in coastal areas. Thus it is necessary to pay more attention on survey and study storm surges.

1.3. Problem identification

According to Le Trong Dao, et al. (2000), survey campaigns in Vietnam are rather limited due to mainly economic reasons. Therefore, usually the number of observations are insufficient. For example, from 1985 to 1997, only 14 storm surges were measured. Of which 13 surveys were in the North, where the frequency of storm is highest with strongest wind and highest storm surges. Only 1 survey was carried out in the South. And there was no observation in the Centre. The measurements were executed after storm by the height of watermarks left on the wall, electric poles, etc. No one can make sure about exact time when the peak level occurred. Presently, there is no official organisation having permanent responsibility to ensure stable and timely gauging of storm surges. This means that many significant storm surges have not been measured. Moreover, in general, the gauging station networks in Vietnam are located sparsely and unevenly along the

coast. Therefore, it is difficult to get the high accurate measurement of storm surges, especially peak levels. In fact, the peak surges have been rarely measured at these stations.

Figure 1-1. Map of Vietnam and the study area

Whereas, another approach which has been developing since 1980s is calculating storm surges using numerical models. This is based on solving the common set of shallow water equations, which can be implemented by finite difference or finite element methods. There have been some models remarked for computing storm surges in different parts of Vietnamese coast such as models developed by Vietnam Institute of Mechanics (Pham Van Ninh et al., 1992), and the Vietnam Coast Model (VCM) developed by WL | Delft Hydraulics (Gerritsen et al., 2001). However, these models have been set up for different

purposes such as for prediction of storm surges levels and drift currents during typhoon activity. The study of storm surges for the purposes of coastal projects such as planning, designing of coastal structures as well as coastal zone management have not been paid much attention. These coastal projects usually require the determination of storm surges with long term return periods. The extrapolations for these values of storm surges based on very limited observed data as mentioned above may lead to a low efficiency and safety of coastal structures. This is an important reason that causes great damages to the coastal structures and high risk for the coastal area under of storm surges. Therefore, the improvement in determination of these abnormal water level rise during storms is necessary. It is also one of strategies of the Vietnamese Government for proper planing, design of coastal works as well as integrated coastal zone management and prevention of nature disasters.

1.4. Objectives of the study

To improve the reliability of storm surge determination in coastal projects, especially for long return period values, the data series of storm surges should be lengthened. Based on that, storm surges with long return periods can be extrapolated giving more safety for coastal projects. The extension of storm surge data series can be done with the help of computer models for storm surge simulation and the availability of long term information on storm tracks. Form this idea, the main objectives of this study are described as follows:

- Set up a numerical model to simulate storm surges for Vietnamese coast.

- Compute storm surges and determine the probability distributions of storm surge for Vietnamese coast based on the long term storm track information for proper planing, design of coastal works as well as integrated coastal zone management.

1.5. Approach and methodology of study

To achieve the above mentioned objectives, the methodology of this study has been developed based on the characteristics of the East Sea (South China Sea) which focuses on the interested area of Vietnamese coast. Hydrodynamic model Delft3D-FLOW for simulation storm surge and typhoon model for simulation wind and pressure field in storm are two main tools chosen to solve the problem.

The steps of the approach are:

1. Literature reviews of previous studies and information of tropical cyclones or storm surges, how to simulate and analyse them. Based on previous studies on the study area or similar cases, the possible process governing the system and related data is recognised.

2. Collect the basic data for the setting up and calibration of model such as topography and bathymetry of the East Sea, tidal information, hourly observed data of wind, pressure and water levels of main stations, information of storm tracks in the Northwest Pacific region.

3. Investigate and represent the models for pressure field and wind field based on observed data. Outcome of this step is to identify the best models and parameters for pressure field and wind field computation.

4. Set-up, calibrate and validate the flow model using Delft3D-FLOW in the normal conditions based on observed tidal data. Appropriate model parameters such as bottom roughness, computational time step, etc. are determined as the outcome of this step.

5. Validate the hydrodynamic model in the storm conditions with some observed data of water level (surge) available.

6. Compute storm surge levels at important locations of the Vietnamese coast with long term data of typhoons.

7. Determine the probability distributions and long term return period values of the storm surges at these locations by fitting the computed surge levels to some probability distributions.

8. Analyse the results and prepare the thesis report.

CHAPTER 2. DESCRIPTIONS OF THE STUDY AREA

2.1. Geographical location

Storm surges along the Vietnamese coast are mostly influenced by typhoons that are formed and developed in the East Sea. Therefore, the preliminary study area should cover the domain between 1^o North latitude and 24^o North latitude. In the West – East direction the area should cover the Gulf of Thailand and entire the Vietnamese East Sea up to the coast of Kalimantan (Figure 1.1). However the covered area focuses on specific part of Vietnam's coast which suffers from high frequency storm caused serious storm surge only.

2.2. Bathymetry

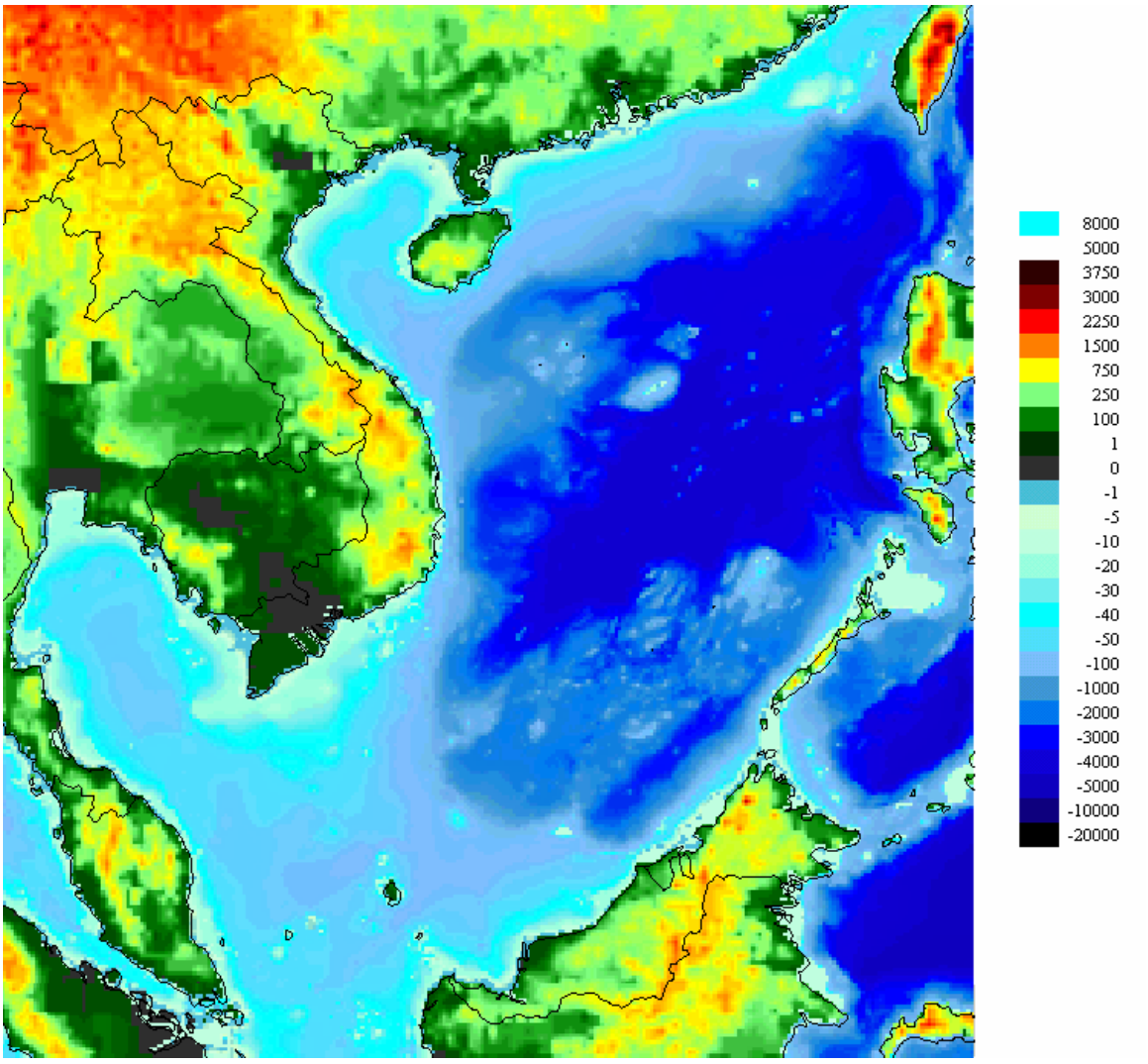

Figure 2-1. Bathymetry of the East Sea

The geometric and bathymetric data of the area were taken from VCM project (WL | Delft- Hydraulic). The depths are relative to the Hon Dau Datum (HDD). HDD is the mean sea level (MSL) at Hon Dau, it is 1.86m above the lowest astronomical tide. This datum is chosen as the standard reference level throughout this study.

Overall, the bathymetry at the study area can be divided into two parts: the continental shelf which extents from the Vietnam's coast to more or less to 100m-depth contour, and the rest of deep sea with maximum depth up to 5000m. The deep part covers half of the domain area in the East nearby the Luzon Strait, Philippine coast and one part of Malaysian coast (Figure 2-1).

The topographic characteristic of the continental shelf along the can be distinguished as three different parts which important to storm surges as follows:

+ In the Northern part (from 17°N to 22°N): It is the Tonkin Gulf with a relatively shallow continental shelf. The concave shape of coastline and the half enclose gulf seem to create good conditions to block and store water. The coastline has complex geographic features such as estuaries, lowland areas, mountains, and islands. In general the shoreline is rather flat and the slope is gentle. The depth contour line of 20m and 50m are far from the shore. These characteristics support the development of high storm surges.

+ In the Central part (from 11°N to 17°N): a number of mountain ranges stretch into the sea and are separated by river mouths. The coastal plains are very narrow and shore is rough. The continental shelf is rather narrow and steep with the depth contour line of 20m is being very close to the shore, just 10km from the shore.

+ In the Southern part: there are large tidal flats and mild slope together with shallow depths. These features are the most advantages for storm surges development. Fortunately, storms rarely occur in this part. Due to the direction of the coastline, maximum storm surges usually occur when storms get weakened after landfall.

2.3. Astronomical tides

Tidal regime is complicated and varying along the Vietnamese coast. It is governed by tide regime of the Northwest Pacific Ocean combine with a specific feature of coast and bank range. The major tidal constituents that are taken into account are O_1 (Diurnal lunar

declination tide), K_1 (Diurnal lunar-solar declination), M_2 (Semi-diurnal principle lunar), and S_2 (Principle solar semi-diurnal). The tide can be classified by the form number *F* as follows (Roos, 1997):

$$F = \frac{H_{K1} + H_{O1}}{H_{M2} + H_{S2}} \quad (2\text{-}1)$$

where:

F<0.25: fully semi-diurnal

0.25<F<1.5: mixed, mainly semi-diurnal

1.5<F<3: mixed, mainly diurnal

F>3: fully diurnal

Tidal regimes at locations along the coast are mostly mixed mainly semi-diurnal or mixed mainly diurnal. The characteristics of tide along the Vietnamese coast can be briefly described as in Table 2-1.

Table 2-1. Characteristics of tides along Vietnamese coast (Le Trong Dao et al, 2000)

(refer Figure 1.1 for the geographic locations and provinces)

Coastal part	**Province**	**Tidal type**	**Tidal range**
The Northern Coast	Mong Cai – Ninh Binh (Gulf of Tonkin)	fully diurnal	highest at spring tide up to 4m.
	Thanh Hoa – Ha Tinh	mixed, mainly diurnal	over 3m.
	Ha Tinh – Quang Binh	transition from mixed, maily semi-diurnal to fully semi- diurnal	regularly reduces
The Central Coast (the most complicated tidal regime)	Cua Tung – north of Quang Nam	transition from fully semi- diurnal to mixed maily semi-diurnal.	increase from 1m at Cua Tung to 2m at Quang nam
	Quang Nam – Binh Thuan	transition from mixed, maily semi-diurnal to mixed, mainly diurnal.	regularly increase
	Binh Thuan – South of Centre	The diurnal feature declines	increase up to 3 - 4m at Binh Thuan
The Southern Coast	Ba Ria – Ca Mau	mixed, mainly semi- diurnal.	about 3-4m (highest in Vietnam)
	Ca Mau – Ha Tien	fully diurnal	only 1 m

Tidal data of water level at many locations along the coast can be obtained from Vietnam Hydro-Meteorological Services (HMS). Tidal constants of some locations along the Vietnamese coast can be found in Service Hydrographique et Oceanographique de la Marine (1982) or in Hydrographer of the Navy (1982). Tidal information at some locations of Taiwan, Luzon strait as well as Mindoro and Singapore Borneo are available from VCM project.

2.4. Characteristic of storms

In the East Sea, there are two centres where storms frequently form and develop: the coastal north-east of the Philippines, in 15^oN-18^oN and 122^oE-127^oE, and the south-east of Hainam Island, in18^oN-20^oN and112^oE-115^oE (from report of UNDP-1999).

According to Le Trong Dao et al. (2000), the storms hitting Vietnam's coast are non-uniformly distributed, the frequency of storms reduces from North to South. The number of storms in the Northern coast is about 58.4% of total number, while in the Central coast the number of storms account for 36.85%, and the rest is belong to the South and account for only 4.8%. In general, storms on Vietnam's coastal area concentrated from June to November annually. And in reviewing the development of storm in the last 15 to 20 year, the number of storms hitting Vietnam tends to increase. The distribution of storms in terms of time and space is more erratic.

Storm is characterised by air pressure depression and intensity of wind as well as the affected radius. The characteristic of storms that hit the Vietnamese coast are small and deep, which means the storm-affected area is small but the air pressure gradient between centre and outer skirt of storm is large. In other words, the maximum wind radius is small with magnitude about from 40 to 100km, but the maximum wind speed may reach 50m/s. Compared with the high latitude area, storms have large scale of impact and wind may be weaker.

In particular, the northern area is frequently subjected to the strongest intensity storm with wind speed reaching 54-56m/s. To the south, the intensity of storm gradually decreases as close to the equator.

2.5. Features of storm surges

Storms and tropical depressions cause strong wind and heavy rains resulting in floods and high storm surge. The distribution of storm surge along the Vietnamese coast is non-uniform and the magnitude of storm surge also decreases from North to South corresponding to three different parts of storm hitting as mention above.

According to the preliminary statistic (Le Trong Dao et al., 2002), the Northern coastal area has the highest level of storm surge (3.6m), there has been frequent dangerous water surge along the coast with different intensities. Particular dangerous storm surge (≥ 2.5m) occurred in most area along this coast. Continuation of storm surge regime of the northern part is the storm surge in Central coast. The height of storm surge in this coast is not as large as northern part with highest level of 2m. About three-quarter of storm coming to the coastline caused inconsiderable storm surge. Due to the high elevation of coast bank and less population density the effects of storm surge at this coastline are not serious. Compared to the North and Centre, the storm surge in the South seem to be low, the highest storm surge in this area is only 1m and nearly 50% of total storm coming to this coastline caused inconsiderable storm surge (only 20cm-height). This is a certain result due to storm probability is low with weak intensity.

2.6. Previous studies on the area

Before 1990, there were few researches or reports related to tropical storm in large scale of North West Pacific or South China Sea, and none is for the specific Vietnamese coastal area. These researches focused mainly on the characteristics and describing storms in the area such as Holland (1980), Wang (1978).

After 1990, more attentions have been paid to the South China Sea as well as the East Sea of Vietnam that belong to the projects of surround countries or Vietnamese Government. They can be listed as follows:

- In 1992, the project UNDP VIE/87/020 developed a two-dimensional numerical model for predicting storm surge level and drift currents during typhoon activity (Pham Van Ninh et al., 1992). The model had set up for the Gulf of Tonkin and calibrated based on available data from 1960. The study used Bierknes model with correction term added to simulate pressure field and wind field. The research gave an overview of storm surges in the northern coast of Vietnam from 16ºN to 22ºN.

- In 2000, a summary report had been prepared for the Disaster Management Unit in the UNDP project VIE/97/002 by of Le Van Thao et al. (2002). The report summed the studies on storms and tropical depressions disaster in Vietnam from 1990 to 1999 of Vietnamese and overseas authors. The report gave an overview on tropical storms, the interaction of surrounding weather system with the movement of storms in the NPO, characteristic of storms in the NPO and the East Sea and the effects to Vietnam. The report also assessed the damages caused by storms in Vietnam. The solutions and guidelines for prevention and mitigation disasters caused by storms and tropical depressions by 2010 were also presented.

- It is also in the framework of Disaster Management Unit, UNDP project VIE/97/002, Le Trong Dao et al. (2000) prepared a summary report on storm surge disaster study in Vietnam. In the report, all studies on storm surge in coastal zone of Vietnam from 1990 to 1999 had been reviewed. The report has summed almost researches of authors in Vietnam. It included the analysis on the characteristics of storm surges a long the Vietnamese coast, the effects of natural conditions such as topography, tidal regime and damages caused by storm surges. An assessment on the situation of storm surge monitoring and forecasting system and difficulties (e.g. lacking of data, budget, organisation) is also made. It also presented the anticipation of storm surge situation in the future and strategies for prevention and mitigation damage caused by storm surges. These include physical and non-physical measures needed to mitigate damage from storm surges. The report clearly showed that it is necessary to do more research on storm surge in the area (including both forecasting and hindcasting) for prevention and mitigation damages caused by storm surges.

- In 2001, a project called SAT2SEA in the framework of National Remote Sensing Program of the Netherlands was carried out for the South China Sea (Gerritsen et al., 2001). The objectives of the project included quantification of the benefit of altimetry based tidal information to improve tidal modelling for the area. A hydrodynamic model was set up, calibrated and validated using tidal information from TOPEX/Poseidon. The results obtained by the model were good not only in deep but also for shallow water.

- In 2001, the VCM project supporting storm surge forecasting for Vietnam Hydrometeorological Services (HMS) had been completed (Gerritsen et al., 2000;

Gerritsen et al., 2001). A hydrodynamic model for the East Sea was set up, calibrated and validated under and without storm condition using Delft3D.

It is can bee seen that most of the studies on storm surge which have been carried out for the Vietnamese coast are mainly focused on storm surge forecasting for disaster prevention and mitigation. It is very important for a developing country like Vietnam, where the coastal area is densely populated and is concentrated for economic development. The coastal areas of Vietnam were from the areas which had not been paid much attention and development before 1990 have been very important areas and rapidly developed after economic reform since 1990s. Together with the economic development in the coastal areas, coastal structures which are mainly sea-dikes, revetments and groins are being built to protects these areas. Every year, damages of coastal structures with related to storm surges are still considerable (cf. Phan Duc Tac, 1996; HWRU, 2000; MARD, 2002). Underestimation of storm surge levels in structure design based on insufficient observation data may have responsible for that damages. Lacking of observed storm surge level is also mentioned in most of the studies above. Therefore, the improvement of storm surge level estimation is an important work. Storm surge data series lengthened by hindcasting is certainly significant not only to the processes of design and planning of coastal projects but also important for integrated coastal zone management as well as disaster prevention and mitigation.

CHAPTER 3. TYPHOON MODEL

3.1. Typhoon data

Data set for the typhoon model consists of storm tracks of more than 200 typhoons formed and developed in the East Sea before they landfell along the Vietnamese coast from 1950 to 2001. The data is obtained from The Joint Typhoon Warning Center (JTWC) and the National Climatic Data Center (NCDC), so-called Best Track. The information on track consists of time, geographical position, minimum sea level pressure at typhoon center and maximum sustained wind speed in knots every 6 hours. In addition, the observed values of pressure and wind velocity for 3 typhoons at various meteorological stations in the region were collected for calibration of typhoon model (from sources of Hydro-Meteorological Services – HMS). Greenwich Mean Time (GMT) is used throughout this study, which can be converted from local time as follows GMT = VNT - 7.

3.2. Typhoon pressure model

A storm as defined by USACE (1986) is an atmospheric disturbance characterised by one or more low-pressure centers and high wind. All storms formed in the East Sea, i.e. originated in the tropics are called tropical storms. A severe tropical storm is referred to as a hurricane, a tropical cyclone or a typhoon when the maximum sustained wind speed equals to or exceeds 33m/s. Hurricanes are well organised in terms of the wind patterns. The wind patterns of a hurricane are nearly circular except in the eye with wind revolving counter clockwise (in the Northern Hemisphere). Winds in a hurricane blow spirally inward and not along a circle concentric with the storm center. The eye is characterised as an area of low atmospheric pressure and light wind. Atmospheric pressure increases with distance from the eye to the outskirts of a hurricane.

In order to simulate flows under typhoon condition, it is necessary to set up a typhoon model to simulate storms including two separately parts: pressure field and wind field. The results of the model are pressure field and wind field on the sea surface under storm condition that will be the data set required putting into hydrodynamic model.

3.2.1. Review existing typhoon pressure models

The decrease of pressure causes a rise of water level. In the equilibrium state, a water level has one centimetre increase for every millibar (mb) decline of atmospheric pressure. The larger the water depth the stronger the influence of atmospheric pressure field. In shallow water although the effect of atmospheric pressure itself exerts the water surface is small compared to wind stress, it plays an important role in driving wind field. Therefore, setting up a model to simulate pressure field under typhoon condition is an important work.

An atmospheric pressure field can be given based on observation or on forecast. In the absence of data, we may use a field associated with an ideal typhoon (hurricane) or cyclone model such as

a). Bierknes model (1921):

The atmospheric pressure in mb at a distance r in km from the center of a typhoon can be estimated by

$$p_a(r) = p_n - \frac{p_n - p_0}{1 + \left(\frac{r}{R}\right)^2} \tag{3-1}$$

Where:

p_n [mb] is the environmental (outskirts) atmospheric pressure not affected by the typhoon;

p_0 [mb] is the atmospheric pressure at the center (eye) of the typhoon;

R [km] is the radius associated with maximum wind speed.

b). Takahashi model (1939):

$$p_a(r) = p_n - \frac{p_n - p_0}{1 + \frac{r}{R}} \tag{3-2}$$

c). Fujita model (1952):

$$p_a(r) = p_n - \frac{p_n - p_0}{\sqrt{1+\left(\frac{r}{R}\right)^2}} \tag{3-3}$$

d). Mayers model (1954):

$$p_a(r) = p_n - (p_n - p_0)\left(1 - e^{-\frac{R}{r}}\right) \tag{3-4}$$

e). Jelesnianski model (1965):

$$p_a(r) = \begin{cases} p_n - \frac{3}{4}(p_n - p_0)\frac{R}{r} & (r \geq R) \\ p_0 + \frac{1}{4}(p_n - p_0)\left(\frac{r}{R}\right)^2, & (r < R) \end{cases} \tag{3-5}$$

For all of the above models, p_n has a value of p_n = 1atm = 1013mb (Tan, 1992) and (Ou, 2002). The value of p_0 is obtained from Best Track. Therefore, only parameter R is still unknown.

The magnitude of R varies in time during the development of a typhoon. It can be taken directly from observed data of atmospheric pressure field or estimated by minimising the error between the observations and computed values.

The root-mean-squared error (RMSE) between observed pressures and computed values by the models is

$$RMSE = \sqrt{\frac{\sum_{i=1}^{N}\left[P_i - f(r_i, R)\right]^2}{N}} \tag{3-6}$$

In which

$f(r_i,R)$: the pressure calculated by models at an observation station i, as a function of r_i and parameter R;

r_i: the distance from the station i to the typhoon center;

N: number of observation points

Radius of maximum wind speed *R* is achieved by using Microsoft Excel Solver with the objective function of optimisation *R* to minimise RMSE.

3.2.2. Inspection of typhoon pressure model

An investigation to identify which model is the most suitable with typhoons in the East Sea has been carried out by comparing the fitting level between observed values and calculated values. The information of storm track and observed data of three typhoons namely Dan, Frankie and Wukong are available and have been used for this study (Table 3-1). The storm tracks of these typhoons and locations of meteorological stations are presented in Figure 3.1.

Table 3-1. Typhoons with observations available

Typhoon name	Occurred period	Land fall
Dan	12/10/1989-13/10/1989	North of Centre coast
Frankie	22/7/1996-23/7/1996	The Gulf of Tonkin
Wukong	8/9/2000-10/9/2000	North of Centre coast

The observed pressure at the station were transferred to the pressure at sea surface if it is not given, by using the formula

$$P_{sea-surface} = P(H) \times 10^{\frac{0.014837H}{273+H/400+30}} \quad (3\text{-}7)$$

Where: *H* is altitude of observation station.

Through the development of typhoon in time and space, the pressure field within the influence of typhoon was simulated. The results of *R* and RMSE using different models for typhoons Dan, Frankie and Wukong are presented in Table 3-2, 3-3 and 3-4 respectively. Time step of 6 hours has been used in the calculation.

Figure 3-1. Best track of typhoon Dan (8929), Frankie (9609), Wukong(0023) and locations of meteorological stations

Table 3-2. Radius of max. wind (*R*) and pressure error of typhoon Dan

Formula	*R*(km)					RMSE(mb)				
Date-time	Bierknes	Takahashi	Fujita	Mayers	Jelesnianski	Bierknes	Takahashi	Fujita	Mayers	Jelesnianski
12-10-89 18:00	159	71	61	65	80	1.6	3.0	2.7	2.8	2.6
13-10-89 00:00	141	75	61	67	79	0.9	1.6	1.1	1.3	1.0
13-10-89 06:00	132	89	64	73	77	2.3	1.7	1.1	1.2	1.5
13-10-89 12:00	124	88	57	65	65	4.3	1.9	2.4	2.1	3.5
13-10-89 18:00	192	141	94	109	110	2.7	1.7	1.9	1.8	2.4
					Average RMSE	2.4	2.0	**1.8**	1.9	2.2

Table 3-3. Radius of max. wind (*R*) and pressure error of typhoon Frankie

Formula	*R*(km)					RMSE(mb)				
Date	Bierknes	Takahashi	Fujita	Mayers	Jelesnianski	Bierknes	Takahashi	Fujita	Mayers	Jelesnianski
22-07-96 06:00	504	532	295	355	329	1.5	1.1	1.2	1.1	1.6
22-07-96 12:00	470	530	281	340	305	1.1	0.9	0.8	0.8	1.3
22-07-96 18:00	337	333	193	231	220	1.6	1.0	1.2	1.1	1.9
23-07-96 00:00	290	300	168	202	189	1.6	1.0	1.0	0.9	1.9
23-07-96 06:00	273	315	162	195	169	2.6	1.6	1.7	1.8	3.0
23-07-96 12:00	222	234	127	152	134	3.7	2.0	2.2	2.2	3.7
23-07-96 18:00	191	203	106	125	112	4.8	2.7	2.7	2.9	4.8
					Average RMSE	2.4	**1.5**	**1.5**	**1.5**	2.6

Table 3-4. Radius of max. wind (*R*) and pressure error of typhoon Wukong

Formula	*R*(km)					RMSE(mb)				
Date	Bierknes	Takahashi	Fujita	Mayers	Jelesnianski	Bierknes	Takahashi	Fujita	Mayers	Jelesnianski
08-09-00 18:00	182	63	57	60	76	0.7	0.7	0.7	0.7	0.7
09-09-00 00:00	154	56	50	53	66	0.8	0.7	0.7	0.7	0.7
09-09-00 06:00	174	88	72	78	93	1.3	0.7	0.7	0.7	0.8
09-09-00 12:00	174	104	79	89	101	2.1	0.9	1.2	1.1	1.3
09-09-00 18:00	186	140	96	111	118	2.2	1.4	1.6	1.5	1.9
10-09-00 00:00	152	119	79	92	91	1.8	1.2	0.5	0.6	1.3
10-09-00 06:00	134	99	63	72	71	3.7	0.9	2.2	2.1	3.2
					Average RMSE	1.8	**0.9**	1.1	1.1	1.4

Figure 3-2 is an example to illustrate the results indicated in Table 3-2 at 06h00 13/10/1989. More detail of the results can be referred to Appendix A. The figures present the agreement between the measurements and computed atmospheric pressures by 5 pressure models at certain times. The observed pressure data sets were taken at about 30 stations located along the Vietnamese coast. However, the chosen observation points to inspect typhoon models were selected such that they are within the influence area of typhoons. This means that the magnitude of a measured pressure must be less than the value at outskirts of a typhoon (1013mb). Thus, the distance from these points to the center of storm is around 500km.

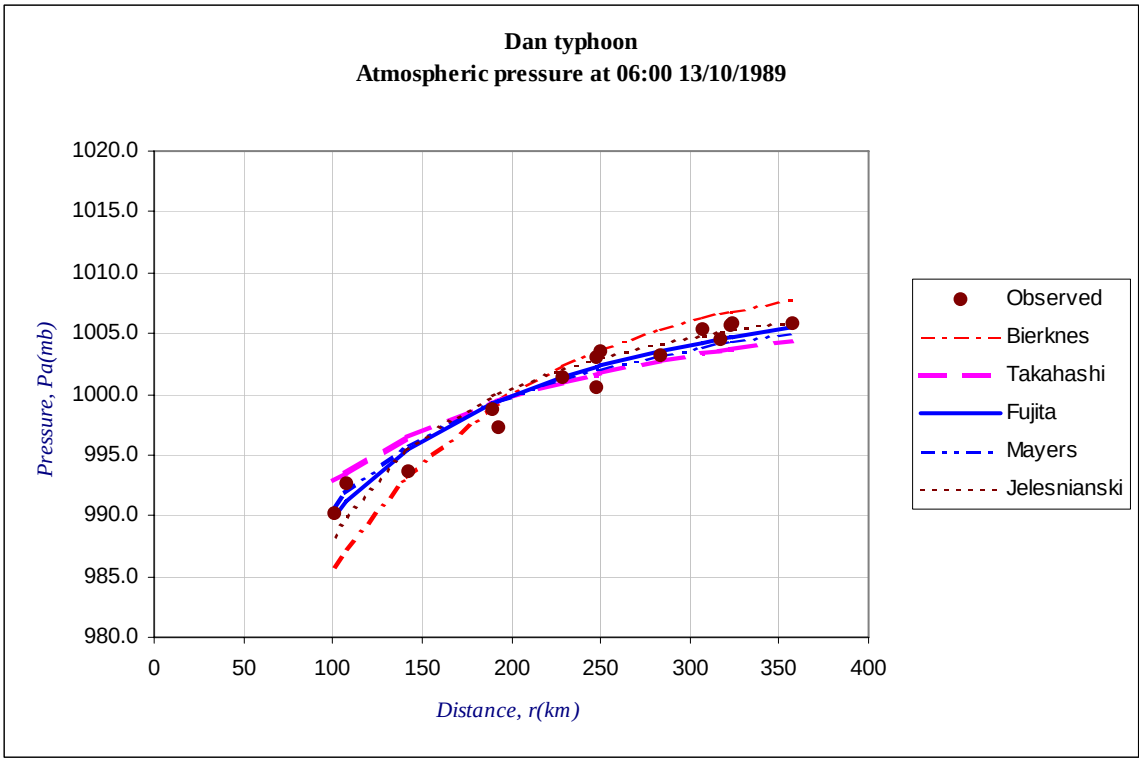

Figure 3-2. The relation between observed and computed pressure of Dan typhoon

In general, it is concluded from Table 3-1 to 3-3 that the RMSE using five models are very small in the order of 0.9 to 2.5 mb compared to the central pressure drop of 35 to 55 mb. The error of the pressure models for three typhoons is only about 0.2% of the normal pressure and about 4% of average pressure drop. In addition, Figure 3.2 shows that these five pressure models are in good agreements with observations. This indicates that all five pressure models can be applied for the simulation of the pressure field in typhoon condition in this area. From the result of simulation pressure field and the enclose chart, the positions of each simulation line by model are relatively fixed. The lines of Takahashi and Bierknes model always are bounds, this means they give the highest or lowest value of pressure compared to other. As shown in Figure 3.2, within 200 km from the center the deviation among the results of fives models is larger than beyond this area. Inside this area pressure decreases faster than outside. Far away from center the value of pressure comes up to stable value of 1013mb. The agreement is worse for the locations located close to the typhoon center.

In particular three pressure models Takahashi, Fujita and Mayers have the lowest value of average RMSE for three typhoons with the order of 1.5mb. Each of those models best fit with observations at least for two of three typhoons. It was followed by Jelesnianski

model and the last one is Bierknes with largest RMSE. To choose which one is the best fit model it is necessary to take into account other aspects such as *R*.

Regarding the magnitude of radius associated with maximum wind speed, all models give high value for the radii of typhoon Frankie compared to the corresponding values for typhoons Dan and Wukong with order of hundreds of km. In fact, typhoon Frankie was a special case, which was different from the common characteristics of rather small *R* in East Sea. However, sometimes this could be occurred in this area. It is noticed that the value of *R* calculated using Bierknes model are usually higher than corresponding values using the other pressure models. The calculated values of *R* using Bierknes model are not in accordance with the values for tropical cyclones in this area. *R* of Jelesnianski model is the second largest and Takahashi model give the intermediate value of *R*. Mayers and Fujita give rather small values of radius, in which the smallest one is from Fujita model in the order of 50 to 90km except for Frankie. The value of *R* given by Fujita is the closest and most realistic with the common feature of *R* in this area with the same range (from 50 to 100 km).

Moreover, the results of *R* optimised by fitting with observed data by different model for three typhoons show that *R* are various in time during the development of a typhoon. However, in general the values of radius maximum wind speed tend to decrease in time corresponding to the reduction of central pressure drop (ΔP is referred to Table 3-4, 3-5). This means the less the central pressure depression is, the smaller the value of *R* is. The explanation for some larger values of *R*, which did not follow the relation, is that at that time the storms went through or near by Hai Nan island, or almost landfell. This condition makes the vortex structure of tropical cyclone more or less destroy, after that period the structure of storm as well as *R* gradually return to normal state. Some examples for this case are the values of *R* for typhoon Dan at 18:00 13/10/1989 (almost landfell) or typhoon Frankie 12:00 to 22/7/1996, Wukong at 6:00 to 18:00 9/9/2000 (storms went through or near by Hainan island).

As a conclusion, with respect to radius associated with maximum wind speed and the agreement between observed and computed pressure through RMSE error as well as the reality, Fujita model can be considered the best model for simulation pressure field in typhoon condition.

3.2.3. Calibration and validation of typhoon pressure model

In case of no information is available on R due to lack of pressure observations, then another method to calculate or estimate R should be used. Pham Van Ninh (1992) presented a relationship between R and ΔP (referred as the Chinese table). The relationship can be represented as follows:

$$R = 5.4436 \times (p_n - p_0)^{0.5034} \quad (3\text{-}8)$$

It is released from equation (3-9) that the greater the pressure drop between the ambient and the central pressure is, the larger radius of maximum wind speed is. This relation suitable with the common tendency of R as mentioned in 3.2.2. Radii computed by this formula for each time instant of Dan and Wukong are rather appropriate with the optimised value from observations by Fujita model (as seen Table 3-5, 3-6). To ensure its accuracy, the application value of R by formula (3-8), so-called $R_{(3\text{-}8)}$, have been calibrated and validated for typhoons Dan and Wukong. The results of pressure error (RMSE) by using not only Fujita model but also for other four models are presented in Table 3-5 and 3-6 enclosed by Figure 3.3. It is concluded that Fujita model is still the best pressure model even in case of without observation data with smallest errors of 2.5 mb equal 0.25% of the normal pressure and 5% of the average pressure drop. Moreover, from Figure 3.3 the Fujita model has the best agreement with measurements, while other models are far from observation points.

Table 3-5. RMSE for pressure of typhoon Dan

Formula	Po	ΔP	$R_{(3\text{-}8)}$	R_{Fujita}	RMSE (mb)				
Date-time	(mb)	(mb)	(km)	(km)	Bierknes	Takahashi	**Fujita**	Mayers	Jelesnianski
12-10-89 18:00	960	53	65	61	7.2	3.0	2.7	2.8	3.1
13-10-89 00:00	965	48	61	61	7.8	2.2	1.2	1.5	2.5
13-10-89 06:00	970	43	58	64	9.1	3.8	1.5	2.5	3.5
13-10-89 12:00	975	38	55	57	7.5	3.8	2.4	2.6	3.7
13-10-89 18:00	990	23	42	94	7.2	4.9	4.3	4.6	5.1
Average RMSE					7.7	3.5	**2.4**	2.8	3.6

Table 3-6. RMSE for pressure of typhoon Wukong

Formula	Po	ΔP	$R_{(3-8)}$	R_{Fujita}	RMSE (mb)				
Date-time	(mb)	(mb)	(km)	(km)	Bierknes	Takahashi	**Fujita**	Mayers	Jelesnianski
08-09-00 18:00	960	53	65	57	4.9	0.7	1.0	0.8	1.1
09-09-00 00:00	960	53	65	50	5.0	1.1	1.9	1.5	0.7
09-09-00 06:00	970	43	58	72	7.4	2.6	1.7	2.1	3.3
09-09-00 12:00	975	38	55	79	8.4	4.0	3.1	3.5	4.6
09-09-00 18:00	980	33	51	96	9.4	5.3	4.2	4.7	5.7
10-09-00 00:00	980	33	51	79	9.8	5.6	3.9	4.7	5.6
10-09-00 06:00	980	33	51	63	7.4	4.0	2.7	3.1	4.1
Average RMSE					7.5	3.3	**2.6**	2.9	3.6

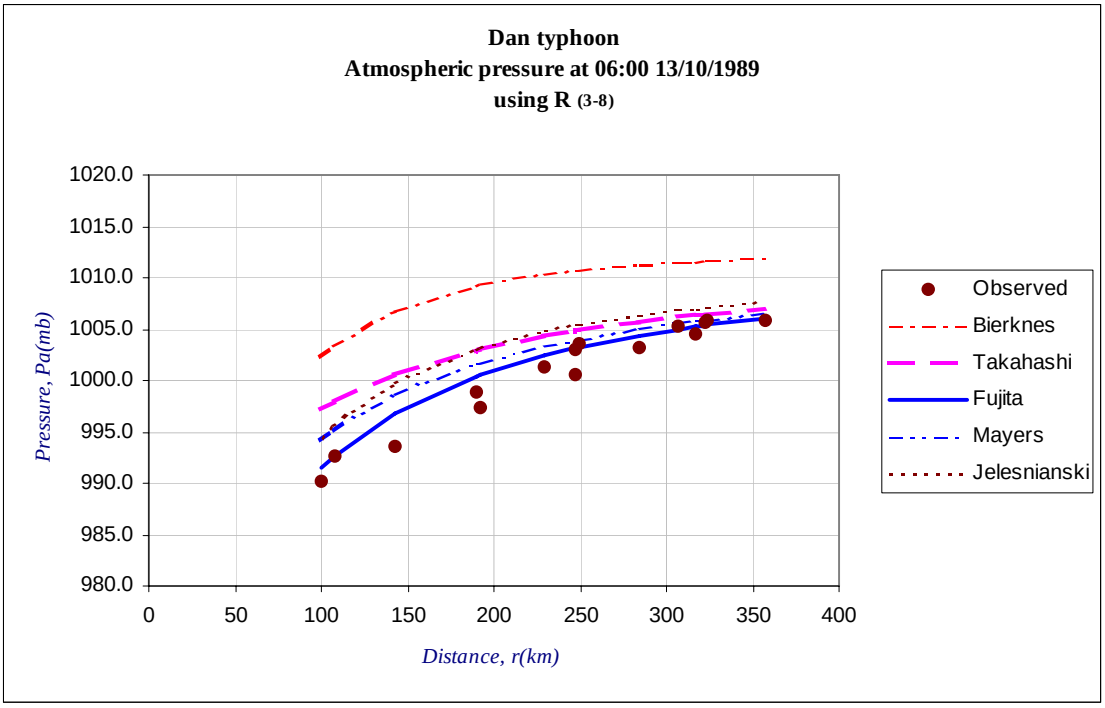

Figure 3-3. The relation between observed and computed pressure of Dan typhoon

Pham Van Ninh (1992) investigated many storms and concluded that the relation (i.e. formula 3-8) give acceptable values of *R* in the Gulf of Tonkin.

Therefore, Fujita model is confirmed to be the best-fit model for simulation pressure field under typhoon condition in this area. And formula (3-8) for estimation *R* can be applied in case of lack or no information of pressure observations available.

3.3. Typhoon wind model

3.3.1. Review existing typhoon wind models

Surface wind stress terms represent the drag force produced by wind over the water surface. This is important for shallow water areas in storm conditions where very strong winds occur. It is even much more important than the role of pressure in driving storm surges. Actually, typhoon wind fields are usually intensive, spatially inhomogeneous and directionally varying. The large gradients in wind speed and rapidly varying wind directions of typhoon vortex can generate very complicated flow. However, for practical application, the wind field data may be taken from observation or forecasts using several simple parametric wind models as an ideal typhoon model.

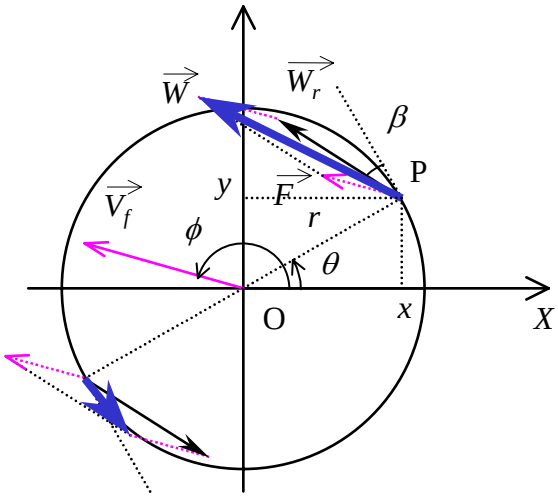

Figure 3-4. Sketch of wind velocity field for a moving cyclone

♦ Actually the wind speed (W) has two components: one is related to the typhoon center movement and the other is the gradient wind speed, which is driven by the pressure gradient. Combine these two vectors of wind speed components and present in Cartesian co-ordination. Fully wind speed model is described in (3-9)

$$\begin{cases} W_x = F_x + W_{rx} = F\cos\phi + C_2 W_r \cos(90^o + \theta + \beta) \\ W_y = F_y + W_{ry} = F\sin\phi + C_2 W_r \sin(90^o + \theta + \beta) \end{cases} \quad (3\text{-}10)$$

Where

W_x,W_y: x- (east), y- (north) components of the typhoon wind speed at altitude of 10m above sea level.

F: wind speed component related to moving center of typhoon at a distance r from the center of the typhoon

F_x,F_y: x-, y- components of velocity related to moving center of typhoon

W_r: typhoon gradient wind speed at a distance r from the center of the typhoon

W_{rx},W_{ry}: x-, y- components of typhoon gradient wind speed

θ: angle between x-axis and the line connecting calculation point and typhoon center (see figure 3.4)

β: angle made by the gradient wind speed with isopiestic line.

ϕ: angle between x-axis and typhoon track

C_2: empirical coefficient in the range of 0.6 to 0.8

♦ The first component of wind speed in formula (3-9) related to moving center can be calculated by following formula (Masami, 1962)

$$F = C_1 V_f e^{\left(-\frac{\pi r}{500}\right)} \tag{3-11}$$

Where C_1 is a coefficient in the order of 4/7 to 6/7 and depends on R. C_1=4/7 if R is relatively large, otherwise its value is 6/7. V_f: velocity of center movement. According to this formula, wind speed caused by moving typhoon center decrease from $C_1 \times V_f$ at center to $C_1 \times e^{-\pi}$ at r = 500km.

While Jelesnianski suggested the wind speed part as a correction term (Phadke et al., 2002).

$$F = \frac{Rr}{R^2 + r^2} V_f \tag{3-12}$$

According to this formula, F = 0 at the center of storm and increase to the maximum value of $0.5V_f$ at R and then decrease radially outward to zero.

♦ The second component in formula (3-9) is determined from the equilibrium between the centrifugal force of rotating air mass with atmospheric pressure gradient and the Coriolis forces. It is

$$W_r = \sqrt{\left(\frac{fr}{2}\right)^2 + \frac{r}{\rho}\frac{\partial P}{\partial r}} - \frac{fr}{2} \tag{3-13}$$

where

ρ: air density ρ =1.293kg/m^3 at 0^{o}C and 1atm;

f: Coriolis coefficient; $f = 2\omega\sin\varphi = 0.525\sin\varphi$ in which ω is the angular speed of Earth; φ is the latitude.

The Coriolis forces are relatively small compared to the pressure gradient and centrifugal forces near *R*, sometimes it can be negligible.

With geostrophic winds determined based on the atmospheric pressure field, surface winds are then estimated by using some empirical relation between geostrophic winds and surface wind speeds (Tan, 1992).

There are some well-known parametric wind models presented as follow: (Phadke et al., 2002; Bode, L.and Thomas et al., 1997; Holland, 1980,1997).

a) The modified Rankine vortex model (1947):

$$W(r) = \begin{cases} W_{\max}\left(\frac{R}{r}\right)^X, & (r \geq R) \\ W_{\max}\left(\frac{r}{R}\right), & (r < R) \end{cases} \qquad (3\text{-}14)$$

In which W_{max}: the maximum wind speed. X is shape parameter ranging $0.3 < X < 0.8$ (Hughes, 1952) to adjust the wind speed distribution in radial direction can be determined empirically from observed data.

b) SLOSH model

$$W(r) = W_{\max}\frac{2Rr}{R^2 + r^2} \qquad (3\text{-}15)$$

Above two models require user specified *R* and W_{max}. *R* is taken from fitting with pressure observation or relation (3-8). W_{max} is available from best track

c) Holland model (1980)

$$W(r) = \sqrt{B\frac{p_\infty - p_0}{\rho_a}\left(\frac{R}{r}\right)^B \exp\left[-\left(\frac{R}{r}\right)^B\right] + \left(\frac{fr}{2}\right)^2} - \frac{fr}{2} \tag{3-16}$$

Where B is a parameter and can be obtained from

$$B = 2 - \frac{p_0 - 900}{160} \qquad \text{for } 1.0 < B < 2.5 \tag{3-17}$$

d) DeMaria et al (1992)

$$W(r) = W_{\max}\left(\frac{r}{R}\right)\exp\left[\frac{1}{b}\left(1 - \left[\frac{r}{R}\right]^b\right)\right] \tag{3-18}$$

b is a parameter change the shape of the profile, which can be vary from 0.2<b<0.8

e) Fujita model (Tan,1992)

$$W_r = \left[\sqrt{\left(\frac{fr}{2}\right)^2 + \frac{r^2 \Delta p R}{\rho(R^2 + r^2)^{1.5}}} - \frac{fr}{2}\right] \tag{3-19}$$

♦ To estimate the wind direction, it is necessary to take into consideration a bias angle β between geostrophic wind and real wind (see Figure 3-4) (e.g., about 18º counter clockwise in the Northern Hemisphere). As regards typhoons, in the literature it is sometimes assumed that the wind velocity is directed toward its center and makes an angle with the isobar lines, which is taken as 30º for moderate-latitude zone in the Northern Hemisphere (Tan , 1992). For a stationery tropical cyclone, the inflow angle at the surface is approximated as Bretschneider in (Phadke at al., 2002).

$$\beta(r) = \begin{cases} 10^\circ\left(1 + \dfrac{r}{R}\right), & (0 \le r < R) \\ 20^\circ + 25^\circ\left(\dfrac{r}{R} - 1\right), & (R \le r < 1.2R) \\ 25^\circ, & (r \ge 1.2R) \end{cases} \tag{3-20}$$

β varies from 10^o at the center to 20^o at *R* and then increase linearly to 25^o at 1.2 *R* and remains at 25^o beyond 1.2R.

3.3.2. Inspection typhoon wind models

The investigation for the predictive capability of the models is carried out by comparison the fitting level between the magnitudes of observed and calculated wind speeds. In this part, to simplify the magnitude of wind speed, only the main value of the gradient wind speed is used. The part related to moving center of typhoon was not yet considered due to small compared to the gradient wind speed. The maximum value of this part is only $0.5V_f$ with the order of 1.5 to 2 m/s for three storms, it reduces very fast from center. While the average value of wind speed in the order of more than 15 m/s. Moreover, wind direction is not concerned because all five models are based on the same rule. Those models have some coefficients that require adjustment with measurements, adjust these coefficients of model itself together with C_2 to get best agreement with observations. The available information of storm track and observed data of wind speed for three typhoons Dan, Frankie and Wukong are used. Besides that, heritage of the previous part results, the parameter *R* optimised by Fujita model with observed pressure is applied for wind models. The results of model parameters and errors (RMSE) between the observed and computed wind speed are presented in table 3-7, 3-8 and 3-9 accompanied with Figure 3.5.

Table 3-7. The parameters and RMSE of wind simulation for Frankie

Formula	Wmax	X	b	B	RMSE(m/s)				
Date-time	(m/s)	Rankine	DeMaria	Holland	Rankine	SLOSH	DeMaria	Holland	Fujita
22-07-96 06:00	23.15	1	0.6	1.47	4.43	4.16	4.25	4.17	4.13
22-07-96 12:00	23.15	1	0.6	1.47	4.02	3.32	3.43	3.30	3.16
22-07-96 18:00	23.15	1	0.6	1.50	3.32	3.57	3.71	3.78	3.88
23-07-96 00:00	23.15	1	0.6	1.50	4.70	5.41	5.44	5.36	5.77
23-07-96 06:00	23.15	1	0.6	1.50	4.16	4.97	4.88	5.03	5.48
23-07-96 12:00	25.72	1	0.6	1.53	5.27	6.03	5.91	6.33	6.61
23-07-96 18:00	28.29	1	0.6	1.53	7.84	8.48	8.27	8.99	9.49
Average RMSE					**4.82**	5.13	5.13	5.28	5.50

Table 3-8. The model parameters and RMSE of wind simulation for typhoon Dan

Formula	Wmax	X	b	B	RMSE(m/s)				
Date-time	(m/s)	Rankine	DeMaria	Holland	Rankine	SLOSH	DeMaria	Holland	Fujita
12-10-89 18:00	38.6	0.8	0.6	1.63	2.92	2.77	3.13	2.95	3.71
13-10-89 00:00	36.0	0.8	0.6	1.59	5.53	5.27	5.87	5.55	5.55
13-10-89 06:00	33.4	0.8	0.6	1.56	6.32	6.48	6.52	6.26	6.71
13-10-89 12:00	30.9	0.8	0.6	1.53	8.55	8.39	7.74	9.03	9.05
13-10-89 18:00	15.4	0.8	0.6	1.44	6.42	7.07	6.54	6.12	6.11
Average RMSE					**5.95**	6.00	5.96	5.98	6.23

Table 3-9. The parameters and RMSE of wind simulation for Wukong

Formula	Wmax	X	b	B	RMSE(m/s)				
Date-time	(m/s)	Rankine	DeMaria	Holland	Rankine	SLOSH	DeMaria	Holland	Fujita
08-09-00 18:00	36.0	0.8	0.6	1.63	3.39	3.37	3.72	3.42	3.80
09-09-00 00:00	36.0	0.8	0.6	1.63	3.40	3.57	4.29	3.33	3.35
09-09-00 06:00	30.9	0.8	0.6	1.56	3.34	3.36	3.35	3.44	3.50
09-09-00 12:00	28.3	0.8	0.6	1.53	4.27	4.24	4.62	4.52	4.38
09-09-00 18:00	25.7	0.8	0.6	1.50	4.80	4.79	5.27	4.90	4.80
10-09-00 00:00	25.7	0.8	0.6	1.50	5.41	5.72	5.78	5.55	5.93
10-09-00 06:00	25.7	0.8	0.6	1.50	3.85	3.89	3.92	4.27	4.62
Average RMSE					**4.07**	4.13	4.42	4.20	4.34

Overall, the empirical coefficient C_2 plays most important role for accuracy of wind models, without multiply C2, all models are overestimated in simulation wind field except the modified Rankine vortex model (refer Table A-1 in appendix). Especially, the errors of wind speed of Holland and Fujita models can be up to 13 to 15m/s that are unacceptable. Whereas, the modified Rankine vortex model gives the lowest error of wind speed with the order of 5.5m/s. This model has a quite good agreement with observations even W_{max} by model is close to measured highest wind speed. However, to make sure that the comparison is fair for every model, C_2 is taken into account so that each model can get the best fit with measurements. It is recognised that different model requires different value of C_2 that much depend on specific typhoon except the Rankine model. For example Holand and Fujita require very low value of C2 even lower than usual range of 0.6 to 0.8, especially for typhoon Frankie.

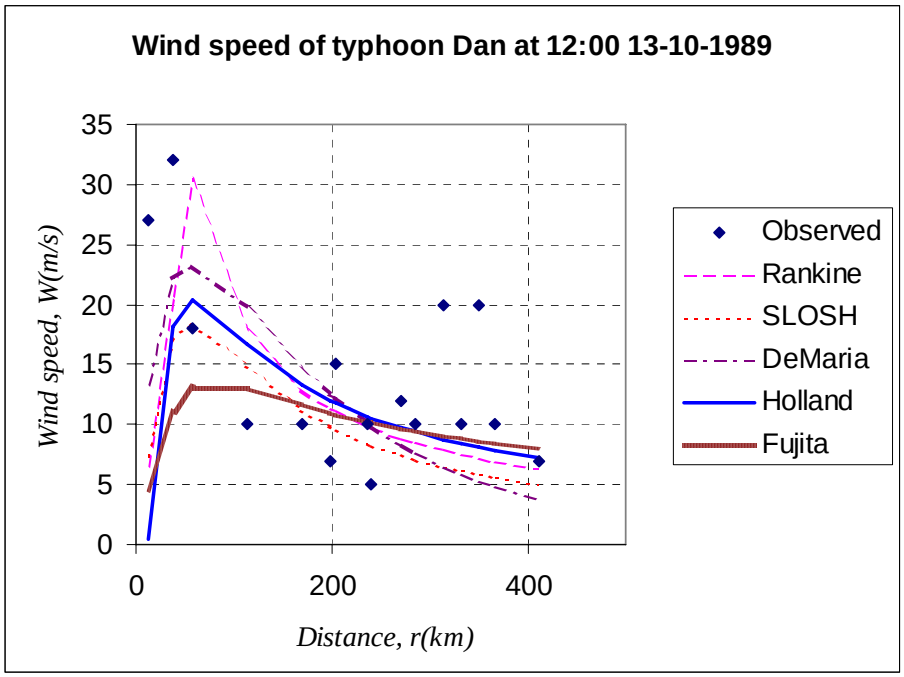

Figure 3-5. The relations between observations and computed wind speed for typhoon Dan after optimised model parameters and C_2 coefficient

Finally, after optimising C_2 all models turn to well simulate wind field with nearly the same average error of wind speed in the order from 4 to 6m/s that are equivalent to 10% to 15% of W_{max}. In particular, for typhoon Wukong the model describe better than typhoons Dan and Frankie with a better agreement with observations. The reasons are the groups of observation points are closer to each other, and the values of *R* of typhoon Wukong obtained more fitting with pressure observations than Dan and Frankie. The variations among different simulations are not much within 35km from the center and far from the center of typhoon as well. In contrast, the differences become significant at the peak of computed wind speed or in other word, within the area of maximum wind speed.

In particular, the modified Rankine vortex model and DeMaria model always give higher peaks than other models, while Fujita model always presents lowest value of maximum wind speed, the rest two models of Holand and Slosh are in the middle. Thus, Rankine often catches the highest value of real wind speed, whereas other models especially Fujita model is far from the measured $W_{max.}$ The peak by Fujita is most obtuse and the tail is higher than the other, consequently it has the largest error of wind speed. As can be seen from the Tables and Figure, it is easy to recognise that the modified Rankine vortex model gives the lowest error of wind speed of about 5 m/s equivalent to 10% of $W_{max.}$ In

comparison to other models, it produces the narrowest peak and more attenuation wind speed from the center and gives the best overall agreement with measurement even the highest value of wind speed. Therefore the modified Rankine vortex model is chosen to simulate wind field.

3.3.3. Calibration and validation of typhoon wind model

In the previous part of inspection wind model, to simplify for calculation and comparison, some minor parts were neglected. But in this part, in contrast after choosing the best wind model, it is necessary to focus in more detail. The part of wind speed relating to movement of center will be taken into account to improve the accuracy of wind model and make it more realistic.

The application of full formula of the model modified Rankine vortex with the correction term has been done to achieve the best agreement with observations. The relation between computed and observed wind speeds for typhoon Dan is shown in the figure 3.6.

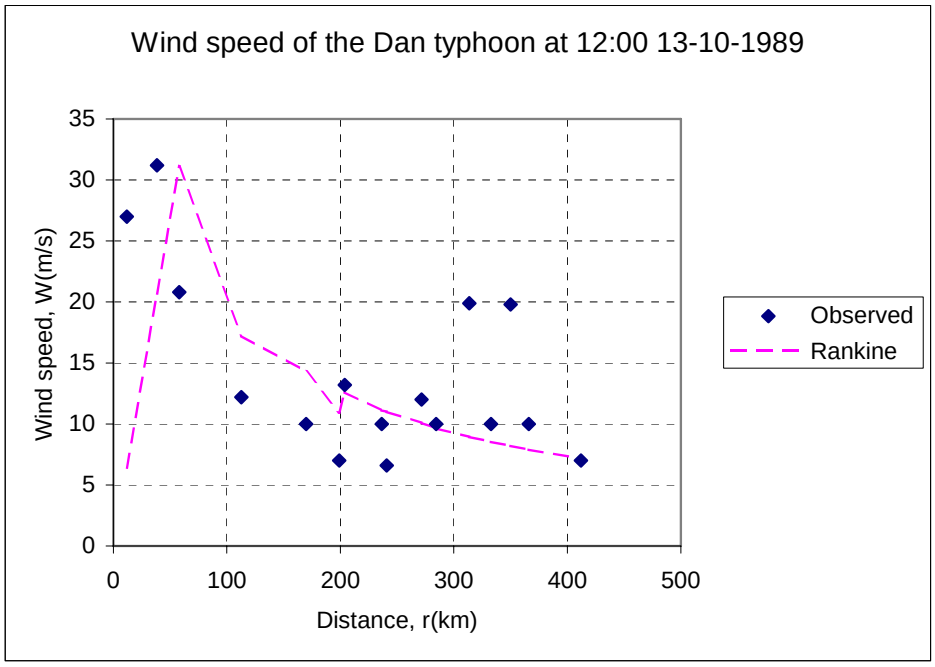

Figure 3-6. The relation between observation and simulation wind field for Dan by using the modified Rankine vortex model.

It should be recognised that the distribution of wind speeds of typhoon in Northern Hemisphere is asymmetrical. The maximum wind on the right side of the storm track due to the tropical cyclone's forward motion (same direction) is being added to gradient wind

speed; whereas, on the left side we can get the minimum value of wind with opposite direction.

As can be seen from Figure 3-6, the simulation wind filed is not a smooth line as before due to the additional the wind speed related to the movement of the typhoon center. This makes the wind field more realistic and better agree with observation points. However, this part is small compared to gradient wind speed, so the effect is inconsiderable especially for the distance larger than 200km. The value of wind speed given by (3-11) are larger and more suitable in comparison with (3-10), with the tendency of model to achieve the best fit with observations. Thus, (3-11) will be used for better simulation with lower error a little bit. Besides that, the parameter X and coefficient C_2 pay more important role to the accuracy of model, the results of wind speed by the model are improved a little bit and have the best agreement when X=0.8 and C_2=0.8 are applied. These parameters of the model are calibrated and verified for three typhoons, the results of W_{max} computed by the modified Rankine vortex model are appropriate with measurements and the error now reduces slightly to 5.2m/s for Dan and increased little to 4.3 m/s for Wukong. The error can not as low as expect but it should be accepted because the fact it is. Observed wind speeds depend on the elevation of gauge that is influenced by surrounding landscape. Moreover, the wind speeds measured by stations located on the left side of storm track are always much lower than computed values due to the friction of land when wind direction is seaward. While, some observations that carried out on islands and on the right side of storm track are much higher than calculated despite they are far from the typhoon center. The reason is that the friction on island is less than on land. In the area within the radius of maximum wind speed, it is more difficult to evaluate the accuracy of model since the number of observations is usually few. Whereas, far away from the center the number of observations are much more and the deviation among observations is not much, consequently the model simulated wind field is more reliable.

3.4. Summary

In conclusion, the Fujita model is chosen for simulation pressure field and the modified Rankine vortex model is the best- fit model to describe wind field. These results will be used as input surface boundary for the hydrodynamic model.

CHAPTER 4. HYDRODYNAMIC MODEL

4.1. Description of the hydrodynamic model

Storm surge is a long gravity wave with a length scale similar to the size of generating tropical storm, and last for several hours depending on the size and speed of movement. This produces sustained elevation of the water surface above the levels caused by the normal astronomical tides. However, its behaviour is different in deep water and in shallow. In deep water, far from a coast, the surface wind stress by a tropical creates a rotating mound, or vortex, of water by diffusing momentum downward. The ocean elevation is small, approximately the hydrostatic uplift in response to the low central pressure (the inverted barometer effect) and some minor long term Coriolis effect. On entering the shallow water of continental shelf, dynamic effects become pronounced, conservation of the potential vorticity of the mound requires development of marked divergence. Local bathymetry reflections from the coast also contribute to substantially amplify the surge high. To calculate the extreme water level, a hydrodynamic model Delft 3D- FLOW for continental shelf is used.

4.1.1. Basic equations

The hydrodynamics of the continent shelf in the storm conditions is simulated by solving the system of two-dimensional of shallow water equations that consists two horizontal momentum equations and one continuity equation:

Conservation of momentum in x-direction (depth and density averaged)

$$\frac{\partial u}{\partial t} + u\frac{\partial u}{\partial x} + v\frac{\partial u}{\partial y} + g\frac{\partial \eta}{\partial x} - fv + \frac{1}{\rho}\frac{\partial p_a}{\partial x} + \frac{g|U|u}{C^2(d+\eta)} - \frac{\tau_{wx}}{\rho_w(d+\eta)} - \varepsilon\left(\frac{\partial^2 u}{\partial x^2} + \frac{\partial^2 u}{\partial y^2}\right) = 0 \quad (4\text{-}1)$$

Conservation of momentum in y-direction (depth and density averaged)

$$\frac{\partial v}{\partial t} + u\frac{\partial v}{\partial x} + v\frac{\partial v}{\partial y} + g\frac{\partial \eta}{\partial y} + fu + \frac{1}{\rho}\frac{\partial p_a}{\partial y} + \frac{g|U|v}{C^2(d+\eta)} - \frac{\tau_{wy}}{\rho_w(d+\eta)} - \varepsilon\left(\frac{\partial^2 v}{\partial x^2} + \frac{\partial^2 v}{\partial y^2}\right) = 0 \quad (4\text{-}2)$$

(1) (2) (3) (4) (5) (6) (7) (8) (9)

The depth and density averaged continuity equation is given by:

$$\frac{\partial \eta}{\partial t} + \frac{\partial (d+\eta)u}{\partial x} + \frac{\partial (d+\eta)v}{\partial y} = 0 \quad (4\text{-}3)$$

In these formulas we have the following terms

(1)	local accelerations	(6)	atmospheric pressure gradient
(2),(3)	convective accelerations	(7)	bottom friction
(4)	surface slope	(8)	external force by wind
(5)	Coriolis force	(9)	depth averaged turbulent viscosity

In which:

C	Chézy coefficient	η	water level above a referent level
d	bottom depth	u,v	depth averaged velocity
f	Coriolis parameter	ρ_W	mass density of water

ε diffusion coefficient (eddy viscosity)

U absolute magnitude of total velocity, $U = (u^2 + v^2)^{1/2}$

τ_{wx}, τ_{wy}: x-,y- components of wind shear stress. Wind shear stress is determined by the widely used quadratic expression, $\tau_w = \rho_a C_d W^2$, where ρ_a: air density; C_d: wind drag coefficient; W: wind speed at 10m above the free surface.

4.1.2. Assumptions

In Delft3D-FLOW the following assumptions are applied:

The vertical momentum equation is reduced to the hydrostatic pressure relation. Vertical accelerations are small compared to the gravitational acceleration (g) and negligible. The fluid is incompressible and using Bussinesq approximation. No dynamic coupling between changes in topography and flow. In small-scale flow, complete Reynolds stress tensor is used. In vertical direction, the so-called σ–coordinate is used that means the number of layer is constant over the horizontal computational area. In this study, only depth-averaged model is used corresponding to one layer in vertical.

Figure 4-1. The model grid and boundary locations

4.2. Set up the hydrodynamic model

In the preliminary stage, the model was set up for the large area of the East Sea with ambition of using tidal information available at some locations of Taiwan, Luzon strait as well as Mindoro and Singapore Borneo as the model boundary conditions. It is realised later that because the computational domain is too large, the grid size becomes coarse. Thus, the bathymetry have been distorted and not present the real local topography especially in coast area that sensitive and play important role to the accuracy of computed storm surge. Consequently, it leads to unacceptable error, while using fine grid that cover such large area is over capability of Delft3D. Moreover, because the model grid is too coarse and the distortion of, the effects of boundary conditions as well as bottom roughness and time step to the computed water levels at the Vietnamese coast are very small. Therefore, it is recognised that the model grid should be as fine as possible to reflect the bottom topography, especially for continental shelf and the Vietnamese coast. Due to the limitation of computer capacity, the computational domain hence, is reduced correspondingly. Beside that, along Vietnamese coast the storm surges in the north coast is more serious than other parts as described in Chapter 2, so the Gulf of Tonkin is selected for storm surge modelling.

Finally, the hydrodynamic model was set up for smaller area of about 450,000km^2 in between the 14^o N to 22^o N and 105^{o}E to 113^{o}E. It consists entire the Gulf of Tonkin and extends further covering Hainan island of China (see figure 4.1).

- *Computational grid*

The model grid is curvilinear in UTM co-ordinate system with dimension of 145 by 180 grid points and one layer, of which about 90% points were active that shown in Figure 4.1. Curvilinear grid with high grid resolution (2km×2km) in the interested area along coast from 17^o N up to the North and low grid resolution (8km×8km) from 17^o N down to the south boundary and far away. By choosing such kind of grid the computational effort can be minimised and the presentation of coastline by staircase can be avoided. Besides, the grid spacing vary smoothly over the computational domain help minimise inaccuracy errors in the finite difference operators.

- *Bathymetry*

There were two sources of bathymetric data. The first one is from VCM project (WL| Delft- Hydraulic) which was digitised from 15'×15' nautical charts of the area. But it is too coarse that just suit for larger scale of the East Sea as mentioned in chapter 2. Another one is high resolution obtained from 2'×2' oceanic bathymetry (ETOPO2), which are relative to mean sea level (MSL) compiled by the U.S. Naval Oceanographic Office. Both of them are used to evaluate the influence of bathymetry to the results of model and to choose the suitable one. In the model area, most area is shallower than 100m. Nevertheless, there is a small part in the middle of the Gulf of Tonkin with 200m- depth and the part located between location 5 to location 7 at open boundary is rather deep with the order of 500m (see Figure 4.1 for locations 4 to 7).

- *Boundary conditions*

The open boundary has the shape of an arc that went though two tidal gauges: one is Qui Nhon station on the Central Vietnamese coast, another one is the station on Paracel island in deep sea. The open boundary consists 8 sections between from location 1 to location 9 as defined in Table 4-1 and presented in figure 4.1. At each location, water level was prescribed by specifying the tidal constituents in terms of amplitude (denoted by A in meters) and phase (denoted by G in degrees) taken from Global Ocean Tides (Schwiderski, 1979) that was shown in Table 4-2. At location 9, the tidal constituents are taken from Qui Nhon station.

Table 4-1. Definition of the open boundary

Section	Location	M	N	Latitude	Long
1	1	13	180	21.81	112.9
2	2	32	180	20.51	112.94
3	3	47	180	19.5	112.82
4	4	62	180	18.5	112.58
5	5	77	180	17.5	112.23
6	6	94	180	16.49	111.66
7	7	111	180	15.5	110.94
8	8	131	180	14.5	109.97
	9	144	180	13.9	109.3

Table 4-2. Tidal constituent at open boundary (case B00)

Location	1		2		3		4		5		6		7		8		9	
Consti-tuent	A	G	A	G	A	G	A	G	A	G	A	G	A	G	A	G	A	G
M2	0.51	68	0.32	78	0.2	46	0.2	51	0.21	60	0.17	69	0.19	77	0.17	92	0.17	89
S2	0.16	73	0.11	91	0.08	80	0.08	89	0.09	97	0.07	110	0.09	116	0.08	126	0.07	127
K1	0.37	188	0.3	193	0.26	187	0.27	188	0.28	189	0.26	185	0.26	191	0.27	188	0.3	195
O1	0.32	155	0.28	151	0.27	146	0.27	149	0.27	152	0.23	150	0.26	153	0.23	150	0.3	154
N2	0.08	51	0.05	50	0.03	39	0.03	44	0.03	55	0.03	58	0.03	70	0.03	79	—	—
P1	0.13	191	0.1	189	0.08	182	0.08	183	0.09	183	0.09	185	0.08	187	0.06	176	—	—
K2	0.06	74	0.04	95	0.02	85	0.02	92	0.02	101	0.02	110	0.02	120	0.021	125	—	—
Q1	0.06	135	0.05	138	0.05	128	0.05	134	0.05	142	0.05	150	0.04	144	0.035	141	—	—

- *Other parameters*

The calibration period for tidal computation is chosen from 31/06/1996 to 1/8/1996 to make use the available data. This period includes two spring tides and two neap tides in addition to 2 days for spin up model. To obtain tidal constants, the simulation period should be at least 29 days. The simulation period for extreme condition was chosen at the time of Wukong typhoon from 5/9/2000 to 11/9/2000 and Frankie from 19/7/1996 to 26/7/1996.

The roughness coefficient chosen is Manning's roughness coefficient with normal value of 0.026 for whole model area. This value will be checked again in the part of calibration to make sure it is properly with the model.

Water density is 1025kg/m^3.

A time step at first time was taken as 5 minutes. And initial condition was chosen cold start with a uniform water level of 0m.

4.3. Calibration and validation of the hydrodynamic model

4.3.1. Calibration, sensitivity analysis for tide

- Data for calibration

The tidal data used for forcing and calibration were taken from a set of tidal constants for major tidal constituents. Four sources of tidal constants were used:

- Set of tidal constants from Service Hydrographique de la Marine, 1982
- Tide tables from the Marine Hydrometeorological Center, 1999
- Global Ocean Tides, Atlas of tidal charts and map (Schwiderski, 1979).
- Set of tidal constants obtained from applying the response method to 8 years of TOPEX/ Poseidon altimeter data.

With these available tidal data, it was decided to do a sensitivity analysis on the 2D barotropic tidal representation to investigate whether the existing tidal representation could be improved.

- Criteria for evaluating results

The criterion for evaluation of the tidal representation of the model was to minimise the error between computed by model and harmonic predicted water level by RMSE in m $RMSE = \sqrt{\frac{\sum_{i=1}^{N}(\eta_i - \tilde{\eta}_i)^2}{N}}$, in which η: harmonic predicted water level and $\tilde{\eta}$ computed water level. The criterion for ideal case are the ratio of A_c/A_o = 1 and $G_c - G_o = 0$. Subscripts *c* and *o* denote computed and observed values, respectively.

- Some evaluations from calibration

At first time, the model was set up using bathymetric data from VCM project. The results show that water levels at almost stations were overestimated more than 20% compared to harmonic predicted water level. Then the bathymetry data ETOPO2 (2 minute Worldwide Bathymetry/Topography) with higher resolution is applied for the model, so-called B00. Consequently, the results of water level at many stations are improved with only 10-15% overestimation depending on stations and time. It is realised that coarse bathymetry can increase smoothness of bottom artificially, leading a high model roughness required to resist this tendency.

From the results of B00, at some locations such as Hon Dau, Bach Long Vi and Hai Phong, their phase were really appropriate. Other stations have good agreements with part of diurnal but not well for part of mix mainly diurnal such as Hon Ne , Hon Ngu. The rest ones are different in phase. In conclusion, behaviour of the diurnal constituent, i.e O_1 and

K_1, is generally over predicted by the model especially for the coast from 20^o N up to the North. On the other hand, the amplitude of the semidiurnal constituent was underestimated for the coast from 18^oN to 20^o N. In neap tide, more than half of number of stations also needs to adjust. This leads to the conclusion that some aspects that impact to the result of model should be changed to fit.

By process of sensitivity analysis the results when changing many factors, the remarks in tendency to improve the computed result are drawn out.

The influence of time step and time for spin up

Time step is chosen small enough to ensure sufficient accuracy. To investigate the impact of time step, a time step of 3, 5,10 and 15 minutes are applied in B00~B03 and computational results are compared. The results show that a time step of 5 minutes produced results almost the same as results of a time step of 3 minutes, while with other time steps the result still change. Therefore, a time step of 5 minutes is chosen for the model simulations. The results also proved that one days is enough for model to adjust from cold start with zero water level come up to the stable state.

The influence of bottom roughness

The model calibration is carried out with the investigation on bottom roughness. Different values of roughness such as 0.015, 0.02, 0.03 and 0.035 are applied in B00, B04~B07. The results of computation show that the higher value of roughness the lower of water level are even change the phase in neap tide and the variation between various options are significant to consider. Since B00 with Manning coefficient of 0.026, the results of water level are overestimated, so the higher value of bottom roughness can be chosen for the whole model. However, simply increasing bottom roughness also impacts the phase, therefore the final value of bottom roughness should be obtained in adjusting process together with tidal constituents at boundary to get the best results.

The influence of latitude

Regarding to the Coriolis force that depend on the latitude of study area, and because the model stretch from 14^oN to 22^oN, so which latitude is the appropriate for the model. Three values of latitude corresponding to the north, middle and south of model are 20^oN,

18^oN and 16^oN that are applied respectively in B08, B00, B09. The results of water level just change a little bit except in neap tide. In comparison among three alternatives, the latitude of 20^oN seem to be good for neap tide of some stations in the North but not good in phase for water level at neap tide of some stations in the South. The contrast also occurs with latitude of 16^oN. On the other hand, the results of water level are suitable for both North and South stations in case of latitude of 18^oN. Therefore, it is chosen for the model.

Comment about the influence open boundaries:

Recognised that although changing time step, bottom roughness and latitude of model, the results of model are still far from agreement with harmonic predicted water levels. Thus, a usual way, adjustment open boundary is carried out to improve results. To see how sensitive of each tidal constituent at open boundary, many alternatives of increasing and decreasing separately amplitude and phase of four main constituents (M_2, S_2, O_1, K_1) have done at each location. Some following remarks are found out from comparison and analysis these results of H01~H54 and G01~G60:

It is evidential that tides propagating from deep water produce better results than from shallow water. The proofs were that in spite of changing in amplitude of every constituent, no response from water level at stations is obtained with locations 1, 2 and 3. With locations 4, 8 and 9 the results change a little bit; whereas at locations 5, 6 and 7 the results change much. As known, locations 5, 6, 7 situated in the deeper part with water depth about 500m, while other locations are on the shallower part with water depth less than 200m. Hence, the effort to adjust boundary lately just focus on the deeper sections of boundary.

The impact of amplitude of the semidiurnal constituents at open boundary is much less than the impact of amplitude of diurnal constituents even in deep water. In particular (H01~ H54), in spite of increasing or reduce 50% amplitude of M_2 or S_2 at all locations, the results seem no change or change inconsiderably. In contrast, the results are very sensitive with diurnal constituents even with only their small change. Furthermore, decreasing amplitude of O_1 and increasing K_1 are not only good for amplitude but also for phase especially in neap tide at many stations for example at Hon Dau, Bach Long Vi,

Hai Phong, Chan May, Hon Ne, , Hon Ngu. As a consequence, by applying this tendency, the results of B13 are much improved for those stations that represent diurnal water level.

Besides that, the model results are sensitive with changing of phase in open boundary even in shallow water; nevertheless in deep water the impact could be seen more clearly. In general, increasing phase of semi-diurnal constituents improve both amplitude and phase of stations Hon Dau, Hai Phong especially in neap tide, while reduction phase of M_2, S_2 only improve amplitude at Hon Ne, Hon Ngu stations. On the other hand, the phases of diurnal constituents play important role in adjustment of the model, by reducing phases of K_1, O_1 at boundary, the better agreements in amplitude of water level are obtained at Hon Me, Hon Ne, Hon Nieu stations. In summary, by changing phase of tidal constituents the results of G01 ~ G60 are not better than the results of B13. In order to get an acceptable model that well represent water level at all stations are so difficult and require much more effort to adjust very careful and a little by little in phase.

After that the different alternatives are tested with combined changing amplitude and phase simultaneously at all locations and group of locations. The results have better agreement but not yet as good as expected especially in neap tide and some stations that require put more semidiurnal constituents.

The conclusion is drawn out that the model set up with boundary conditions taken from source of Global Ocean tides is not good enough. Therefore, other set of tidal constant from TOPEX/Poseidon, that is found out later, is chosen for open boundary. The differences between two data sets are not much, specifically the variations of each tidal constituent are less than 5 cm in amplitude and 10 degree in phase. However, according to Gerritsen (2000) when calibration for the South China Sea model, this source presents rather properly for deep open sea and shallow areas. The best final model is obtained by using the new source and adjusts with reference to some good tend of tidal sensitivity as mentioned above.

Finally, the chosen hydrodynamic model has following parameters:

- A time step of 5 minutes, time for spin up 1 day.
- Bottom roughness of Manning coefficient = 0.026
- Latitude of 18^0N .

- Grid and bathymetry of (ETOPO2) are preserved for the Gulf of Tonkin

- Open boundary condition has four segments in which section 1 (location 1, 4), section 2 (location 4, 6), section 3 (location 6, 8) and section 4(location 8, 9). Water levels in tidal constants of boundary condition are shown in table 4-3.

The errors between computed and harmonic predicted water levels are presented in Table 4-4. The relation and agreement between computed and harmonic predicted water levels at some stations are shown in Appendix B.

Table 4-3. Tidal constituents at open boundary of the final model

Tidal consti-tuents	Location-1		Location-4		Location-6		Location-8		Location-9	
	A	G	A	G	A	G	A	G	A	G
M2	0.489	69.88	0.154	60.71	0.161	71.94	0.159	81.31	0.153	93.45
S2	0.203	83.25	0.052	93.12	0.058	103.64	0.063	111.86	0.063	133.35
K1	0.253	193.06	0.184	199.12	0.187	200.55	0.199	200.71	0.195	204.75
O1	0.210	152.64	0.165	155.67	0.165	156.49	0.175	156.94	0.195	161.70
P1	0.082	189.68	0.062	195.33	0.063	196.35	0.067	196.00	0.000	0.00
Q1	0.041	135.78	0.033	139.71	0.032	141.29	0.031	142.99	0.000	0.00

Table 4-4. Error of model calibration for tides

No	Station	Max error (m)	RMSE (m)	No	Station	Max error (m)	RMSE (m)
1	Do Son	0.24	0.10	7	Da Nang	0.14	0.05
2	Bac Long Vi	0.22	0.10	8	Hoi An	0.08	0.03
3	Hon Ne	0.28	0.11	9	Duc Pho	0.04	0.02
4	Hon Me	0.26	0.10	10	Dung Quat	0.07	0.03
5	Hon Ngu	0.30	0.17	11	Tam Quan	0.06	0.03
6	Cua Tung	0.15	0.08	12	Paracel	0.02	0.01
Average maximum error : 0.16m				Average RMSE error : 0.07m			

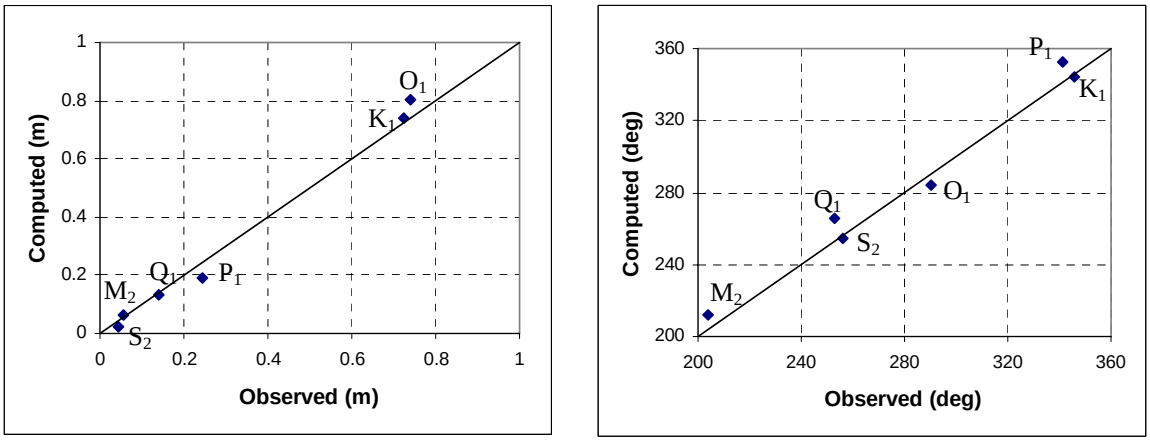

Figure 4-2. Model calibration for tides at Do Son (amplitude on the left; phase lag in GMT on the right)

As can be seen from the table, the maximum error occur at the spin up period, when water level in a transition period from zero to stable state. Overall, most computed water levels are underestimated or overestimated compared to predicted tidal depend on time and station. The average error is just less than 10cm, of which majority errors are in high and low water. At spring tides, the calculated water levels have better agreement than at neap tide. The phases are almost appropriate. By doing tidal analysis at each station, the results of amplitude and phase nearly concentrate to bisector of right angle. Figure 4-2 shows an example of the good agreement between observed and computed in each tidal constituent at Do Son station. This shows that these criteria posed are met.

In short, the model with acceptable error will be used for simulation tidal level at the stations along coast of North Vietnam.

4.3.2. Calibration and validation for tide plus typhoon

- Data for calibration

The available data for sensitivity study and calibration – validation model under extreme condition are information of storm track, observations of pressure, wind speed and water levels of two typhoons Frankie and Wukong at various stations along North Vietnamese coast. These are supplied by NCDC, JTWC and WL | Delft Hydraulic. The number of stations having measured water level for Frankie typhoon is six, while for Wukong were only three.

- Wind and pressure fields for the storm surge model

In order to calculate extreme water levels under typhoon condition, the model is driven by tides, wind and pressure fields. The input files are provided by results of wind and pressure models, which have been calibrated in previous chapter, at each grid point of the model. The given data only in every six hours; whereas the storm surge model runs required wind and pressure in every simulation time-step in the order of minutes. The strong gradients in associated with the cyclone do not allow for straightforward temporal interpolation because this can destroy the structure of actual cyclone with wrong direction and magnitude. Hence, a program is developed to transfer from wind and pressure field in every six hours to every time step required in Delft3D..

Basically, storm surge simulation is executed with following steps:

- Read the specified parameters of storm track for two consecutive times such as P_0, W_{max}, V_f, location of center ….
- Interpolate intermediate values for those parameters in short time interval
- Using Fujita model to compute pressure field and using the Rankine model to present wind field for each time step at every grid points of model.
- Out put the results under format of Delft3D-flow input file.
- Execute Delft3D-flow to compute water level.

- Sensitivity analysis wind drag coefficient

Wind drag coefficient (C_d) is an important parameter that depends on wind velocity, and reflects roughness of sea surface corresponding to wind speed. The influence of this parameter can be found out by a sensitivity analysis. It may be specified by an empirical formula:

$$C_d = \begin{cases} C_d^{(1)} & W \le W_1 \\ C_d^{(1)} + (C_d^{(2)} - C_d^{(1)}) \dfrac{W - W_1}{W_2 - W_1} & W_1 < W \le W_2 \\ C_d^{(2)} & W > W_2 \end{cases} \quad (4\text{-}4)$$

Where

$C_d^{(1)}$, $C_d^{(2)}$: specified drag coefficients at wind speed W_1, W_2 respectively

W_1,W_2: thresholds of wind speed

To investigate the sensitivity of model with changing of wind drag coefficient, many tests have been done (run W2i to W2f) based on some empirical formulas such as Wilson (1960), Smith-Banke (1975), Garratt (1971), Heaps (1965), Rijkswaterstaat for two typhoons. The relationship between wind speed and wind drag coefficient by different formulas is shown in Figure 4-3. Within 40m/s of wind speed, the maximum error of C_d by various formulas is only 0.001 causing not much variation on water level. When wind speed is larger than that value, the differences become significant. Actually, two typhoons with maximum wind speeds were only 30m/s and 38m/s respectively for typhoons Frankie and Wukong. The variations of computed water level by different formulas are very small. However, Smith-Banke and Garratt formulas give a little bit lower results compared to other ones. In fact those formula are just specific cases of equation (4-4). The mater is to find out which wind drag coefficients $C_d^{(1)}$, $C_d^{(2)}$ are suitable at wind speed W_1, W_2 so that the best fit can be obtained between computed and observed water levels. Also it is recognised that intermediate values are linear interpolated from two values of $C_d^{(1)}$, $C_d^{(2)}$. If the transition line is too steep, that means C_d grows too fast associate with wind speed, this easily leads to unstable in the results. The evidence are shown in the results of W2a to W2f corresponding with $C_d^{(1)} = 0.00063$ at $W_1 = 0$m/s, $C_d^{(2)} = 0.00723$ and changing W_2 to 10, 20, 30, 40, 50 m/s, respectively.

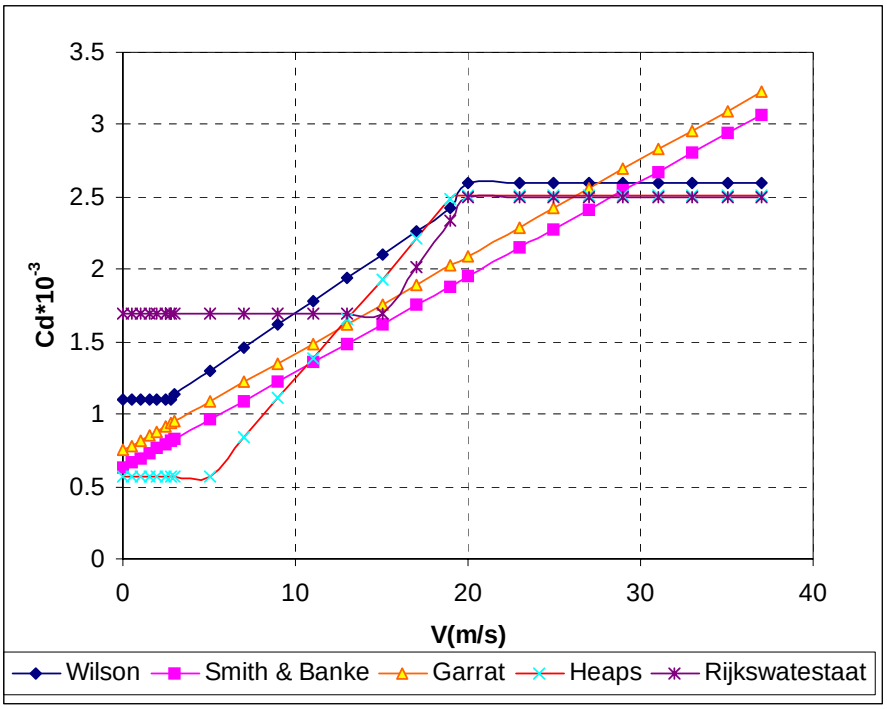

Figure 4-3. The relationships between V and C_d by different formulas

Finally, after many adjustments, the wind drag coefficients are chosen as follow:

$C_d^{(1)} =$ 0.0010 at $W_1 =$ 6 m/s

$C_d^{(2)} =$ 0.00723 at $W_2 =$ 50 m/s

- Comments from calibration process

The relation between the computed water levels and observed water levels for five stations during typhoon Frankie and three stations during typhoon Wukong are presented in appendix B and the results of error is shown in Table 4-5. The criterion for evaluating the accuracy of model is also RMSE as before. In general, the simulated water levels under typhoon condition are underestimated in comparison to observation especially at station Hon Dau during typhoon Wukong. The more typhoon affect on water level, the higher error of water level occurs, for example the maximum error at Hon Dau is up to 0.3 m in typhoon Wukong. And the error of water level in case of tide plus typhoon is larger than only tidal forcing. In particular, the results show that one-day after starting simulation the water level become stable and the average error is around 22 cm. There is one stations out side the influence area of typhoon such as Qui Nhon whereas at Hon Dau had the largest affect on the water level. In addition, the big errors usually occur at neap tide than at spring tide and at high water than low water.

Table 4-5. Error of model calibration for tides plus typhoon

Typhoon Frankie				Typhoon Wukong			
No	Station	Max error (m)	RMSE (m)	No	Station	Max error (m)	RMSE (m)
1	Hon Dau	0.23	0.09	1	Hon Dau	0.30	0.13
2	Hon Ngu	0.29	0.1	2	Hon Ngu	0.29	0.12
3	Son Tra	0.12	0.06	3	Son Tra	0.15	0.06
4	Dong Hoi	0.21	0.09	Average maximum error: 0.22m			
5	Cua Hoi	0.22	0.09	Average RMSE: 0.09m			

During typhoon period, the water levels increased (decreased) gradually at some stations on the right (left) side of storm track until landfall time, after that water level considerably rise (reduce) and maintain in a strong fluctuation within about one day, then return steadily to normal state. This is corresponding to the change of wind speed in terms of magnitude and direction.

In consideration the variation of water level and position of stations with respect to storm track, the typhoon influence area can be more than two times of radius of maximum wind speed. It is evident that the water levels still change at stations Dong Hoi and Da Nang to the left of Frankie track, which are more than 350 km from the track- equivalent to 3 times of R at landfall time. Similarly, although Hon Dau station is about 300km far from Wukong track to the right, the water levels were impacted.

The highest water levels under typhoon condition were obtained at stations Hon Dau for typhoon Frankie and Cua Hoi for Wukong. Both of them are on the right of the storm track, with the distance more or less radius of maximum wind speed.

Starting with uniform initial condition, the model takes time to reach at a dynamic equilibrium. One day before typhoon event is enough for spin up the model, nevertheless the simulation period for running storm surge model were chosen as soon as getting information from best track. Fortunately, to calibrate two typhoons, wind and pressure data are available for this period at the meteorological stations along the coast, in case of without observation the daily data will be used. Thus, wind and pressure fields are used at the beginning of simulation.

In this study, the results of storm surge should be better if the effect of waves is incorporated. The specification of surface stress, as a function of wind speed only, under-estimates the important role that surface wind waves play in transfer of momentum across the air–sea interface. However, the interaction between surge and wave is very complicated and required more effort in computation and time, so it is not taken into account in this study. Nevertheless, according to Mastenbroek et al (1993), a simple increase in drag coefficient also gives much the same improvement in results as the full surge-wave calculations. Therefore, although without consideration wind–wave interaction, the hydrodynamic model has been able to hindcast storm surge with acceptable accuracy as calibration.

The limitation of the model is that the open boundary in case of plus typhoon is kept the same as without typhoon. This may leads to the error of water level due to without the consideration of the influence of swell caused by typhoon in case typhoon formed outside the model domain. To take it into account, the water level at open boundary can be obtained from results of larger model, but it is beyond the scope of the study.

4.4. Summary

The hydrodynamic model for two cases with and without typhoon has been set up, calibrated and validated. Finally, the parameters of model such as time step, bottom roughness, tidal constituents at open boundary, wind drag coefficient were found based on sensitivity analysis method by comparison between simulation and harmonic predicted or observed water level. The model is able to represent the characteristic water level variation due the typhoon-induced surge.

CHAPTER 5. RESULTS OF STORM SURGE SIMULATION AND PROBABILITY DISTRIBUTION

5.1. Results of storm surge simulation

Storm surge is obtained by subtracting the predicted tide from the total water level. Figure 5-1 and 5-2 show the extreme water level and storm surge during typhoon Frankie at Hon Dau, located approximately 110 km to the right of storm track at the time of landfall. The highest water level produced by a storm at any coast location in the absence of astronomical tide effect is referred to as the "maximum surge", while the highest water level produced during the course of the storm is referred to as the "peak surge". For example, peak surge during typhoon Frankie occurred at around 20:00 23/07/1996 at Hon Dau, as can be seen in Figure 5-1.

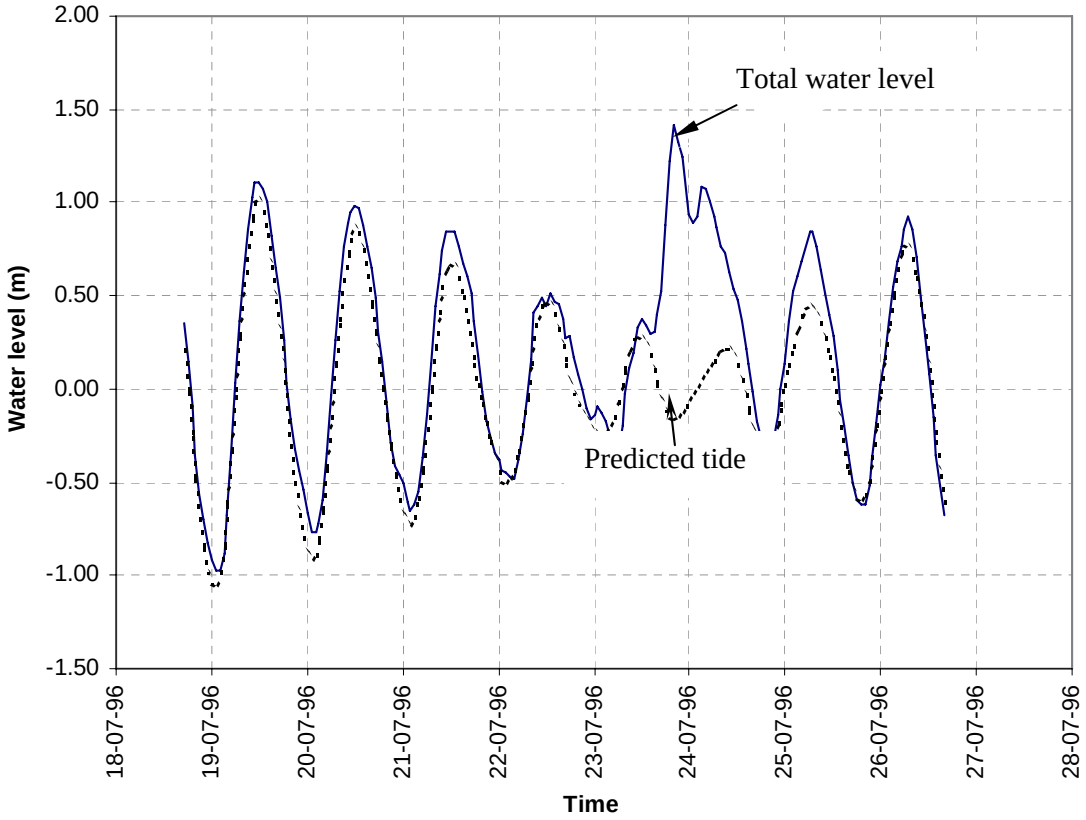

Figure 5-1. Water level at Hon Dau during typhoon Frankie

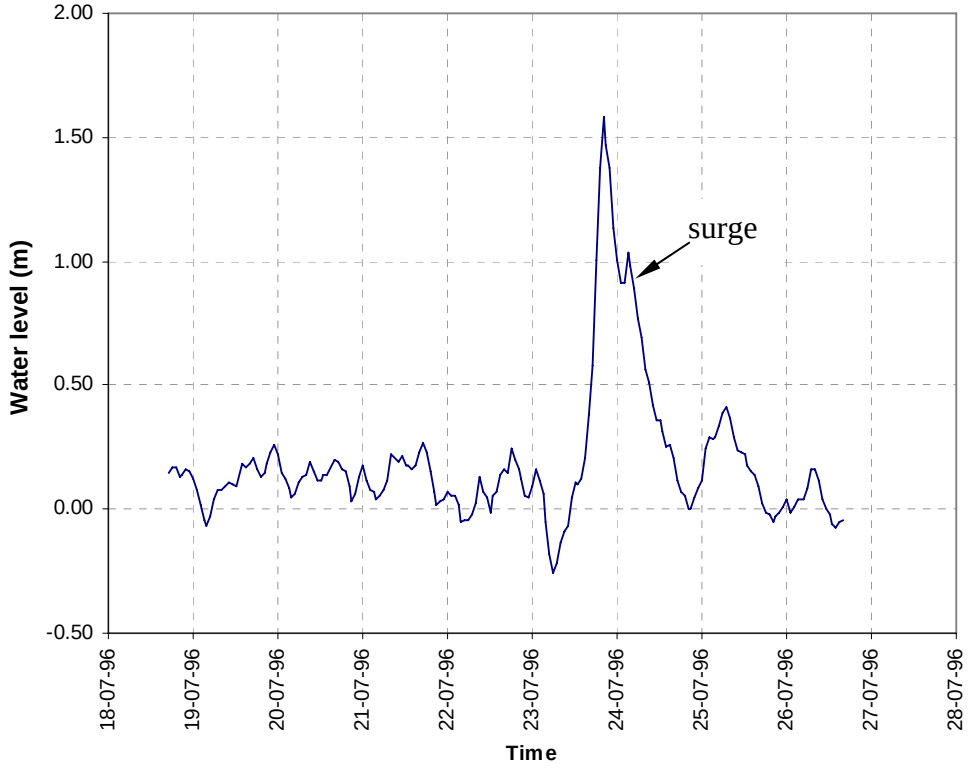

Figure 5-2. Storm surge at Hon Dau during typhoon Frankie

The storm surge calculation is based on the available information of storm tracks and weather data from 1950 to 2002. There are 174 storms sorted out that can induce storm surge in the study area. Most of them formed outside the study area and landfell in the coast area of the northern Vietnam. In general, the range of central pressure depression of those storms is from 20 to 112 mb and the range of maximum wind speed is from 24 to 72m/s. The duration of storm movement from the boundary of the area to the coast is about three days. The storm having largest central pressure depression of 112mb occurred from 3 to 5/11/1995 that did not landfall and dissipated at about 80 km nearby Hon Nieu. It is also the storm with the strongest wind intensity of W_{max} = 72m/s. The storm with the highest movement speed of 30m/s occurred from 27 to 28/06/1993 that landfell in Quang Ninh.

By using hydrodynamic model with input data of pressure field described by Fujita formula and wind field calculated by the modified Rankine vortex model, extreme water levels of each storm are computed for about 30 locations along the coast. Predicted tide during a storm can be computed from tidal constituents at those locations. Tidal

constituents at some of the main stations are already available, tidal constituents at the other locations are obtained from tidal analysis the results of water levels run for one month of July 1996. The results of storm surges at the locations for 174 storms from 1951 to 2001 are computed by subtracting the predicted tide from the total water levels. The process to synthesise and analyse the results has been carried out. The positive value and maximum value of storm surge are sorted out and prepared for determining probability distributions at each location. The brief summary of storm surge modelling results is given in Table 5-1, Figure 5-3, and Figure 5-4. Table 5-1 presents the occurrence frequency corresponding to different grade of storm surges at each location from 1951 to 2001. Figure 5-3 shows the time series of annual maximum storm surge for this period. Figure 5-4 shows a plot for the magnitude of maximum storm surge at some main locations along the coast.

- *Evaluation for results of simulated storm surge*

By synthesising and analysing the computed results of maximum storm surge for 174 storms, it is concluded that storm surge in the coastal line of northern Vietnam are rather high. It is evident that about 45% of typhoons cause maximum storm surges higher than 1.0m, 30% of storms cause maximum surges higher than 1.5m, 20% of storms cause maximum storm surges higher than 2.0m and 3% having highest surges greater than 3.0m. The high frequency of typhoon occurrence with high storm surge indicates that it is necessary to pay more attention to this dangerous phenomenon.

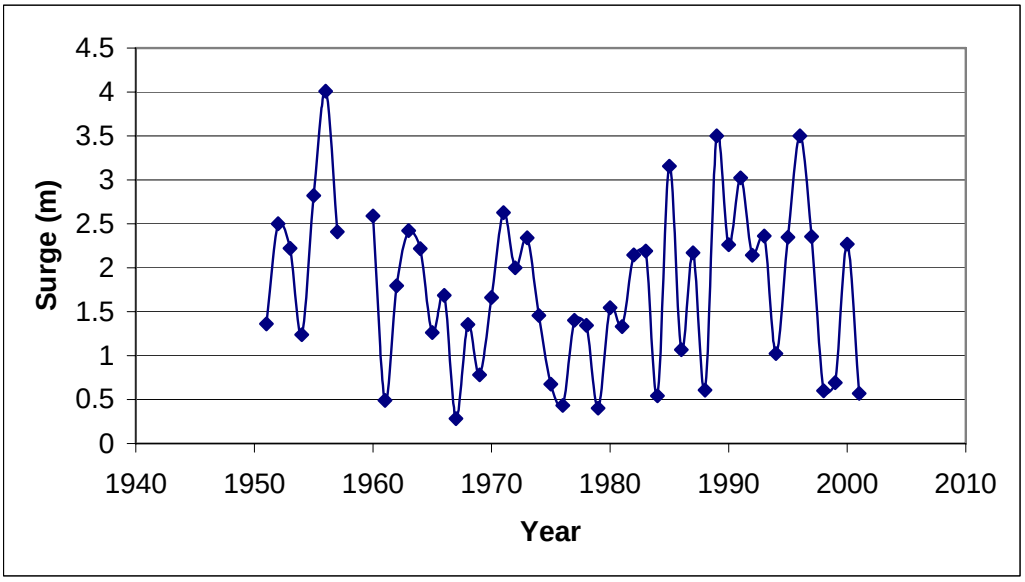

Figure 5-3. Annual maximum storm surge from 1951 to 2001

From the results of storm surge simulation, the maximum surge of 4.01m is found at Cua Hoi during a typhoon from 29/8 to 1/9/1956 landfell near Cua Khau with maximum central pressure drop of 77.4mb. This is not the storm with largest central pressure depression and strongest wind intensity because that typhoon did not landfall. Another typhoon namely Dan (10/1989) with a central pressure depression of 56.7mb caused a 3.5m surge, which is close to the storm surge reported at Cua Hoi (3.6m).

Overall, 96% of totally 174 storms caused the surge with the order more than 20cm. From Table 5-1, only a minor number of typhoons cause high surge, most of typhoons (about 80% of typhoons) induce storm surges less than 1 m at all locations along the coast. The spatial distribution of high storm surge along the coast is unevenly. Storm surges higher than 2.5 m are mainly distributed in the northern coast from Diem Dien, the coastal area of Nghe An province near Cua Hoi and the coastal area of Quang Tri province near Cua Viet. The region from Diem Dien up to the north and especially at Hon Nieu, Cua Hoi, Cua Sot stations had suffered from influence of storm much more than other regions. Although the levels of surges less than 1m are less than other parts, the higher surges even up to 4m occur frequently in these areas. Along the coastline from north to south, the occurrence of storm surge less than 0.5m tends to increase from 45% to 98%, while the occurrence of storm surge higher from 0.5m to 1.5m is decreasing from 51% to 1.2%. The storm surge in the range of 1.5 m to 2.0m is about 2% spatially distributed more evenly except the area from Dien Chau to Hon Nieu that is more or less 6%. The surge levels higher than 2m are not found at some locations such as Yen Dinh, Chan May, Duc Pho and Tam Quan. In contrast, the highest percentage of occurrences such high surge are found at Hon Nieu and Cua Hoi. In fact, the area of Cua Hoi is the most vulnerable coastal area of Vietnam. In the last 51 years, 35 out of 174 storms caught the highest value of storm surge at Cua Hoi. The southern part (Duc Pho, Tam Quan) has least suffered from influence of storm. The magnitude of storm surge in this part is only about 0.5m, rarely up to 1m or 1.5m. This part is close to the model boundary so may be influenced by the boundary conditions. For fully assessment, it may require larger model to consider those storm which can influence on the southern region.

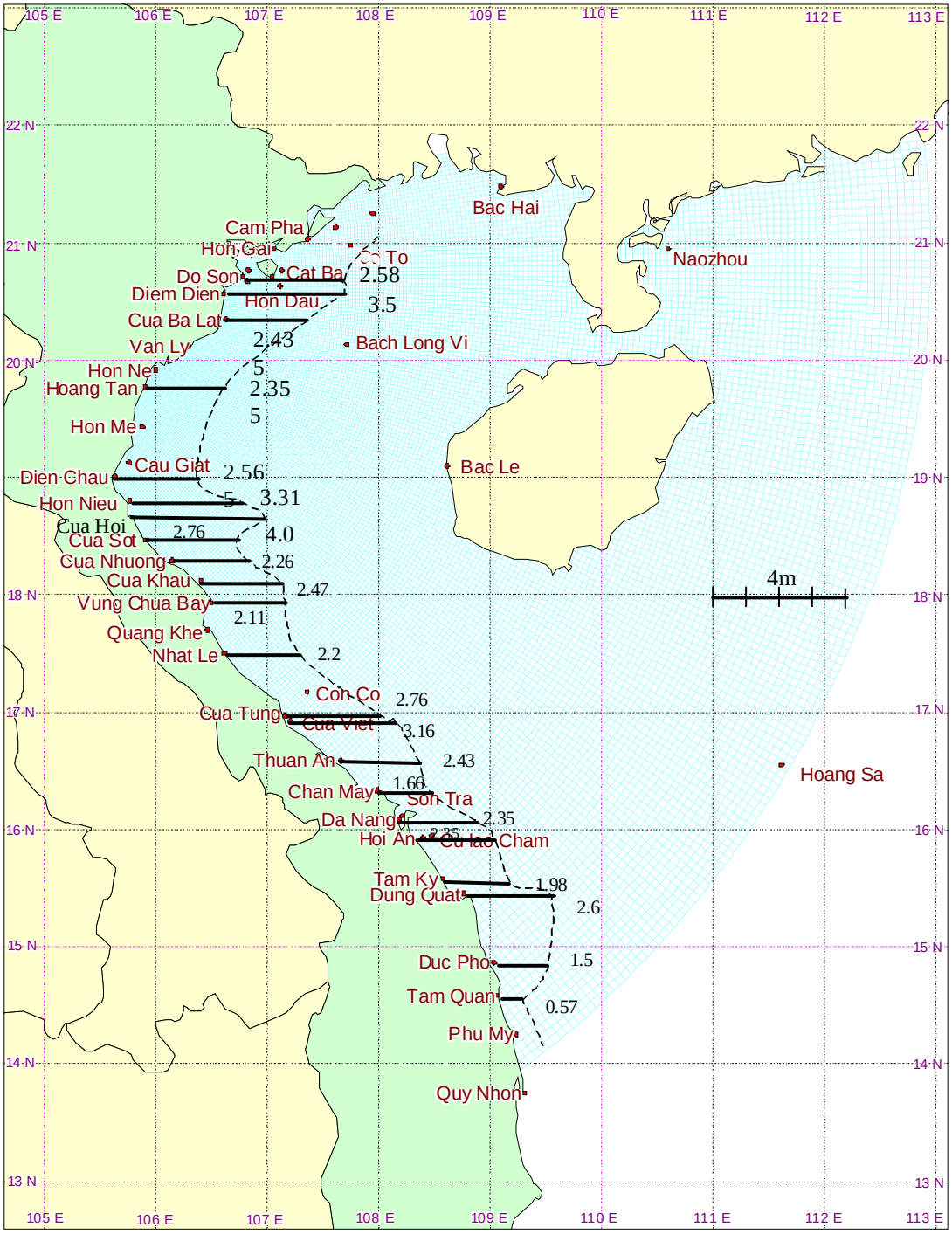

Figure 5-4. Magnitude of maximum storm surge along the coast

Table 5-1. Percentage of storm surge occurrence in % by grade

No	Station	Range of storm surges in meters						
		< 0.5	0.5 to 1	1 to 1.5	1.5 to 2	2 to 2.5	2.5 to 3	≥ 3
1	Cua Nam Trieu	49.7	34.7	10.8	1.8	2.4	0.6	
2	Do Son	44.9	42.5	9.6	1.2	1.2	0.6	
3	Hon Dau	46.7	41.3	9.0	1.2	1.2	0.6	
4	Diem Dien	41.3	44.3	7.8	4.2	1.2	0.6	0.6
5	Cua Ba Lat	48.5	40.1	6.0	3.6	1.8		
6	Yen Dinh	58.7	36.5	3.6	1.2			
7	Hoang Tan	52.7	37.1	6.6	2.4	1.2		
8	Tinh Gia	55.1	34.7	7.2	1.2	1.8		
9	Cau Giat	57.5	31.7	7.2	3.0	0.6		
10	Dien Chau	53.3	32.9	7.2	5.4	0.6	0.6	
11	Thanh Hoa (NA)	59.3	29.9	7.2	3.6			
12	Hon Nieu	52.1	30.5	6.0	6.6	3.0	1.2	0.6
13	Cua Hoi	47.9	34.1	6.6	3.0	6.0	0.6	1.8
14	Cua Sot	59.3	27.5	6.0	4.2	1.8	1.2	
15	Cua Nhuong	65.9	24.6	6.0	2.4	1.2		
16	Cua Khau	68.3	20.4	4.8	6.0	0.6		
17	Vung Chua	74.9	22.2	1.2	0.6	1.2		
18	Cua Gianh	77.8	20.4		1.2	0.6		
19	Dong Hoi	77.2	19.8	1.2	1.2	0.6		
20	Nhat Le	76.0	21.6	0.6	1.2	0.6		
21	Cua Tung	82.0	15.6	0.6	0.6	0.6	0.6	
22	Cua Viet	83.2	13.8	1.2	0.6		0.6	0.6
23	Thuan An	83.2	9.6	5.4	1.2	0.6		
24	Chan May	87.4	7.2	3.6	1.8			
25	Da Nang	87.4	6.0	3.0	2.4	1.2		
26	Hoi An	87.4	6.0	2.4	2.4	1.8		
27	Tam Ky	91.0	4.2	3.0	1.8			
28	Dung Quat	88.6	4.8	1.8	2.4	1.8	0.6	
29	Duc Pho	97.6	1.2	1.2				
30	Tam Quan	98.8	1.2					

It is recognised that for typhoon moving more or less perpendicular to the coast, the peak surge usually occurs at or near the point where the region of maximum winds intersects the shoreline. The distance is about the radius measured from the typhoon centre to the region of maximum winds, which is in the right side of storm track in the Northern Hemisphere. For instance the typhoon Dan (10/1989), despite its central pressure drop was only 56.7mb, which was less than three other typhoons with central pressure depression of more than 62mb, the maximum surge of typhoon Dan at Cua Hoi was 0.5m higher than max surges of those three typhoons at Diem Dien or Cua Hoi. The reason is that Cua Hoi has an auspicious geographic condition of concave coastline, depth contours nearly parallel to the coast. Moreover, it is on the right of storm track with the distance form the typhoon center of 70km (equals R at landfall) when typhoon approaching the coast with the angle of more or less 90 degree. Those features were together at the same time made the onshore wind field becoming highest in magnitude and normal in direction, that focus highest energy to push mass of water causing high surge.

It is realised that about 13% of typhoons even with very strong wind intensity have only small surges (less than 1.5m). The reasons are, these typhoons did not landfall or landfell but far from the interested area such as they landfell too far in the north from Cam Pha up to the border between Vietnam and China or too far from Qui Nhon to the south. One more reason is that their approaching angle were small, this means the highest wind speed did not occur at the landfall time. Weaker approaching wind in combination with destruction of vortex structure due to going along the land for period of time before hitting lead to small surge.

A typhoon has onshore wind, with positive surge, to the right and offshore winds, with negative surge to the left of storm track looking from sea to land (in the Northern Hemisphere). This is clearly corresponding with counter-clockwise of tropical cyclones. Positive surges usually dominate in the coast area on the right of storm track, then it decreases at the center, and then negative surge occurs in the coast area on the left of storm track (only at landfall time), far away from the center surge re-increase. However, we just interested in the positive surge because it causes more damage and more meaningful for searching and practical application, so only the positive and maximum value of surge in storm period are taken for study. Figure 5-5 shows the envelop of maximum surges along the shoreline of typhoon occurred from 13 to16/10/1985.

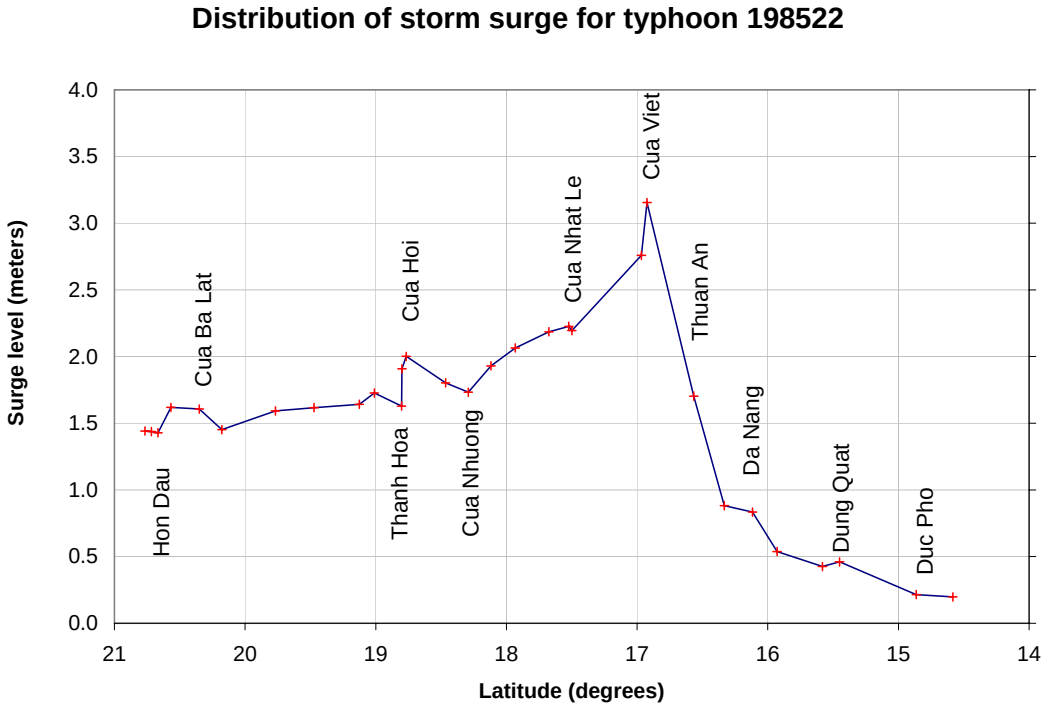

Figure 5-5. Envelop of maximum surges along the coast of typhoon 13-16/10/1985

From the computed results, the maximum storm surge can occur in any different phase of tide. In fact, 34% of maximum storm surges occur at high water, 33% of maximum storm surges occur at low water and the rest one occur in between low and high water. The highest water level does not mean that highest storm surge occur at that time. However, the storm surges with high magnitude are usually found at low water. Because the water levels are the results of interaction between surge and tide, so the relative phases of the surge and tidal components affect the peak-sustained water level. The peak surge will become significant (6m) when maximum surge occur at the same time at high water at spring tide of the region with highest tidal range of 4m. Fortunately, from the results of computation as well as in practical, this case has not yet occurred. The highest water level is 4.2 m corresponding with maximum surge of 4m at Cua Hoi of typhoon 8/1956.

The duration of storm surge maintains approximately from half a day to one and a half of days, but most of storm surge periods are less than one day. The maximum surge and high surge which are equivalent to or larger than 80% of maximum surge are kept for 2 or 3 hours. The time for water level rising up is usually less than the time for going down.

From the results of maximum storm surge from 1951 to 2001, it is clear that the occurrence frequency of storm surge higher than 2m tends to increase. The occurrence frequency of such high surge increases from 16% in the first 20 years of the period to 21% in the recent 30 years. Four of five typhoons having surge higher than 3m are in recent years. The storm surges higher than 2m usually occur in October, September and August than other time in year.

Tropical cyclone size, intensity, movement speed, maintaining duration on the continental shelf and angle of landfall together with local offshore bathymetry and inland topography all play significant roles in surge generation. Besides that, the accuracy of results of storm surge simulated by model depends on the accuracy of information of those factors as well as the accuracy of the model itself.

5.2. Determination of storm surge probability distribution

As presented in previous chapters, the occurrence and magnitude of storm surges at a specific location depend on many governing factors. The occurrences and combined influence of these factors on storm surge are very complicated which cannot be predicted precisely in long-term using physical laws. In general, the occurrence and magnitude of some typhoon parameters can be considered as random variables. The occurrence and magnitude of storm surges, either actually observed or model simulated, can be also considered as random variable and can be described using statistical distributions. In fact, storm surges or maximum water levels during typhoons are joint probability distributions of those influencing factors. The determination of those component distributions may suffer many difficulties of data available and statistical modelling, and therefore, is left outside the scope of this study. In this chapter, storm surge is considered as an independent random variable.

5.2.1. Commonly used probability distributions

Probability distributions are commonly used for extreme events like flood or storm surge analysis including

- Log-normal (LN),
- Pearson type III (P3),
- Extreme value type I (Gumbel type I) (EV1),
- Extreme value type II (Gumbel type II) (EV2),

- Extreme value type III (Gumbel type III) (EV3),
- Gamma,
- Log-Pearson type III (LP3),
- General extreme value (GEV),
- Weibull,
- Generalised logistic (GLG), and
- Log-logistic (LLG)

Among the distributions, only the log-normal has had any theoretical support elicited for it but then only after 40 years of prior use in hydrology (Cunnane, 1989). Chow (1954) stated that if an extreme phenomenon (e.g. flood) could be considered to be the product of a large number of random effects then it would be log-normal distributed, because the logarithm of the variate could be considered to be the sum of large number of random effects and would therefore be normally distributed by the central limit theorem.

Probability density function (PDF) of the log-normal distribution is:

$$f(x) = \frac{1}{\sigma_{\ln x}\sqrt{2\pi}} \exp\left\{-\frac{1}{2}\left(\frac{\ln x - \overline{\ln x}}{\sigma_{\ln x}}\right)^2\right\} \tag{5-1}$$

Where

x random variable

$f(x)$ probability of x

Some probability distributions are the special cases of others. For example, the probability density function for the Pearson type III (P3) distribution is given as

$$f(x) = \frac{1}{\beta\Gamma(\alpha)}\left(\frac{x-a_0}{\beta}\right)^{\alpha-1} \exp\left\{-\frac{x-a_0}{\beta}\right\} \tag{5-2}$$

Where

a_0 lower bound of x

α, β parameters to the distribution

$\Gamma(\alpha)$ the Gamma function, $\Gamma(\alpha) = \int_0^\infty t^{\alpha-1}e^{-t}dt$

This distribution may reduce to the Gamma distribution if the lower bound $a_0 = 0$. It becomes the normal distribution if the skewness is zero. P3 also reduces to exponential with specific values of its parameters as $\alpha = 1$. In the tradition and design criteria of Vietnam, P3 is the most common used probability distribution in design of water resources projects.

Other example, GEV is the generalised form of EV1, EV2 and EV3 with the cumulative distribution function (CDF) is given as

$$F(x) = \begin{cases} \exp\left\{-\left(1-k\dfrac{x-a_0}{\beta}\right)^{\frac{1}{k}}\right\} & k \neq 0 \\ \exp\left\{-\exp\left(-\dfrac{x-a_0}{\beta}\right)\right\} & k = 0 \end{cases} \qquad (5\text{-}3)$$

Where

$F(x)$ exceedance probability of x

k, β parameters to the distribution

To know more information about other distributions see specific books listed in reference.

As the results from the hydrodynamic model, information includes storm surge and maximum water level at each location along the coast. This information can be used for determining probability distribution in two forms of annual maximum series and partial duration series (i.e. series of storm surges from each typhoon). The partial duration series of storm surges can be constructed by selecting a fixed number of typhoon per year (method of n-largest values) or by selecting all values exceeding a specific threshold (method of peak-over-threshold – POT).

The conversion from partial duration series to annual maximum series according to Langbein (1949) is as follows

$$P_{AM} = 1 - \exp\{-P_{PD}\} \qquad (5\text{-}4)$$

Where

P_{AM} Probability respects to annual maximum series

P_{PD} Probability respects to partial duration series

The annual maximum series of storm surge at each location obtained from the hydrodynamic model has a length of about 50 years with the standard error of estimated standard deviation $\Delta\sigma_{n-1}$ is small, says less than 0.05, can be accepted as sufficiently long for determining its statistical distribution.

The LN and P3 distribution is plotted on a probability paper of normal distribution (Hazen probability paper). The plotting positions of those distribution is calculated using Weibull formula

$$P_i = \frac{i}{n+1} \tag{5-5}$$

Where

P_i Exceedance probability of the i^{th} value in the series sorted descending

i Rank of the value in the series

n Length of the series

The GEV distribution is plotted on a logarithmic scale and plotting position is used type weighting function (Cunnane, 1989)

$$P_i = \frac{n - i + 0.35}{n} \tag{5-6}$$

The statistical parameters of the distribution are determined initially using the method of moments. The final values of these parameters (mainly coefficient of skewness (C_S) and coefficient of deviation (C_V)) are obtained by changing the values within the confidence limits of estimates (standard errors) to get the fit with data samples. The mean value of a series X = (x1, x2, ..., xn) is given as the first moment about the origin and estimated by

$$\overline{X} = \frac{1}{n}\sum_{i=1}^{n} x_i \tag{5-7}$$

The standard deviation can be estimated from the second moment about the mean as

$$\sigma_{n-1} = \sqrt{\frac{\sum_{i=1}^{n}\left(x_i - \overline{X}\right)^2}{n-1}} \tag{5-8}$$

The variation coefficient C_V is calculated as

$$C_V = \frac{\sigma_{n-1}}{\overline{X}} \tag{5-9}$$

The parameters of the GEV distribution are estimated from probability weighted moments (PWM) (Cunnane, 1989).

The confidence limits of an estimate XT is calculated as follows

$$X_{TU} = X_T + S\frac{\sigma_{n-1}}{\sqrt{n}}a \tag{5-10}$$

$$X_{TL} = X_T - S\frac{\sigma_{n-1}}{\sqrt{n}}a \tag{5-11}$$

X_{TU} and X_{TL} are upper limit and lower limit of the estimate X_T, respectively; a is a coefficient calculated on the basic of the frequency factor; σ_{n-1} is the standard deviation and S is the departure parameter computed from normal distribution depending on the confidence level. For the confidence limit of 95%, the value of S = 1.96 is used.

Probability distributions of LN, P3 and GEV for storm surge with 95%-confidence limits at some location are presented in Figure 5-6 to Figure 5-8.

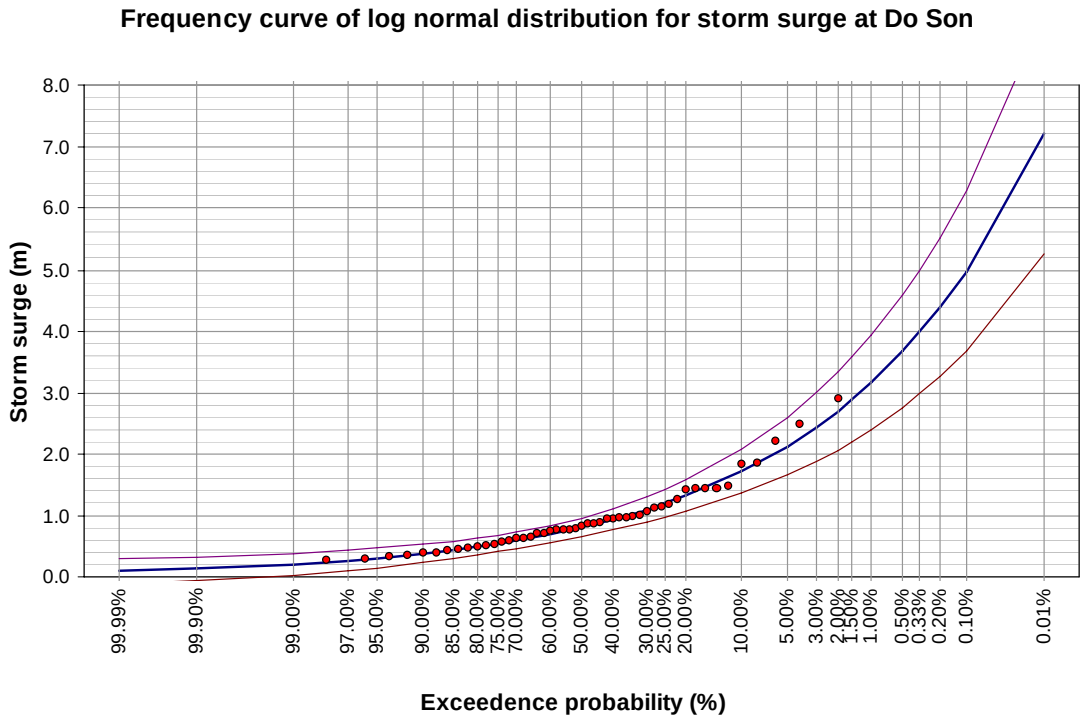

Figure 5-6. Log-normal distribution of storm surge at Do Son

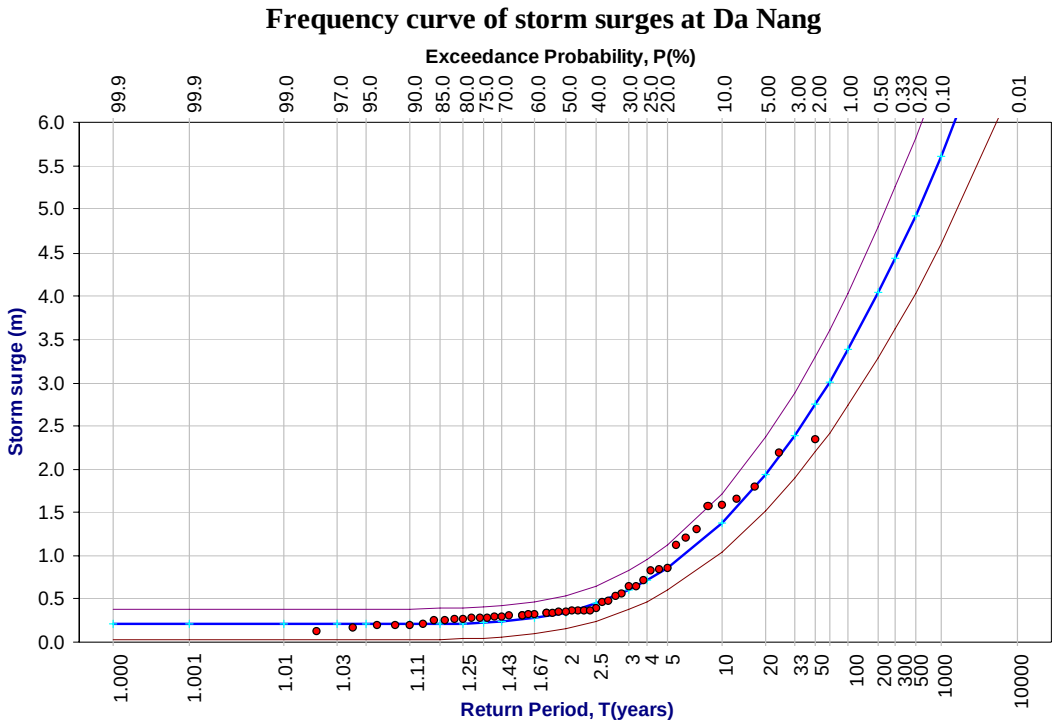

Figure 5-7. Pearson type III distribution of surge at Da Nang

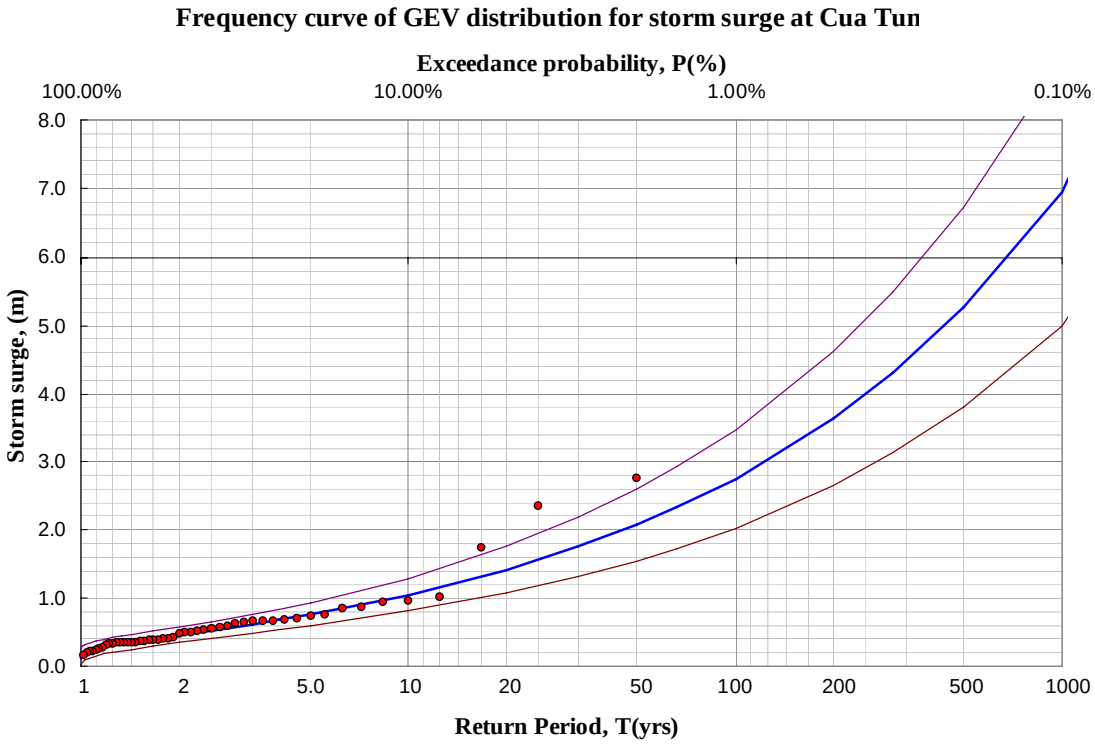

Figure 5-8. Generalised extreme value distribution of surge at Cua Tung

5.2.2. Statistical criteria and selection of probability distribution.

Visual inspection shows that LN and P3 distributions of storm surge at most locations are inside the 95%-confidence limits, while GEV distributions are not. The goodness-of-fit of the distributions can be evaluated using some statistical tests. The most common tests are the Chi-Square (χ^2) Test and the Kolmogorov-Smirnov (K-S) Test. The chi-square test for goodness-of-fit is a measurement to know how well the sample data fit a hypothesised probability density function. But the disadvantage of this test is the data must be grouped (or classified) before it is applied. Such a grouping results naturally in loss of information. The Kolmogorov-Smirnov test for goodness-of-fit compares an empirical distribution function with the distribution of the hypothesised function. This test does not require grouping the data in any way, and it is valid for any sample size *n* when all parameters are known. The Kolmogorov-Smirnov test tends to be more powerful than chi-square tests against many alternative distributions. Therefore, the K-S test is chosen for goodness-of-fit tests.

The K-S test is conducted as follows (Haan,1982):

1) Let $P_x(x)$ be the completely specified theoretical cumulative distribution function under the null hypothesis.

2) Let $S_n(x)$ be the sample cumulative density function based on n observations. For any observed x, $S_n(x)=k/n$ where k is the number of observations less than or equal to x.

3) Determine the maximum deviation (D) defined by

$$D = \max \left| P_x(x) - S_n(x) \right| \qquad (5\text{-}11)$$

4) If for the chosen significance level, the observed value of D is greater than or equal to the critical value of the K-S test, the hypothesis is rejected. The critical value of K-S test for the sample size of 48 years and the significant level of 95% is 0.196.

The K-S tests for goodness-of-fit of probability distributions are carried out using a computer program BestFit developed by Palisade Corporation. The results of tests with various distributions for data series of storm surges and maximum water level are arranged in Table 5-2 and Table 5-3.

Table 5-2. K-S test for goodness-of-fit for distributions of storm surge

Location	Log normal	Pearson3	GEV	Logistic	Normal
Ba Lat	**0.103**	0.124	0.155	0.208	0.196
Cau Giat	0.079	**0.077**	0.098	0.258	0.118
Chan May	0.175	**0.165**	0.201	0.264	0.240
Cua Hoi	**0.147**	0.164	0.189	0.394	0.303
Cua Khau	**0.118**	0.145	0.175	0.269	0.234
Cua Sot	**0.124**	0.145	0.175	0.424	0.188
Cua Tung	**0.142**	0.141	0.145	0.205	0.205
Cua Viet	**0.130**	0.212	0.146	0.212	0.216
Cua Gianh	**0.132**	0.139	0.166	0.212	0.208
Cua Nhuong	**0.100**	0.111	0.144	0.183	0.189
Da Nang	0.204	**0.180**	0.220	0.246	0.258
Diem Dien	**0.064**	0.085	0.115	0.173	0.159
Dien Chau	**0.087**	0.090	0.112	0.297	0.213
Do Son	**0.054**	0.085	0.117	0.160	0.156
Dong Hoi	**0.096**	0.136	0.160	0.213	0.206
Duc Pho	0.308	**0.179**	0.189	0.264	0.260
Dung Quat	**0.165**	0.248	0.185	0.227	0.240
Hoang Tan	**0.080**	0.110	0.143	0.186	0.180
Hoi An	**0.159**	0.202	0.193	0.231	0.254
Hon Dau	**0.051**	0.081	0.113	0.259	0.149
Hon Nieu	**0.130**	0.144	0.167	0.380	0.287
Cua Nam Trieu	**0.096**	0.114	0.143	0.324	0.151
Nhat Le	**0.098**	0.133	0.165	0.215	0.210
Tam Ky	**0.149**	0.199	0.176	0.218	0.232
Tam Quan	**0.094**	0.115	0.142	0.182	0.169
Thanh Hoa	**0.068**	0.071	0.083	0.244	0.113
Thuan An	**0.118**	0.137	0.170	0.457	0.221
Tinh Gia	**0.089**	0.122	0.155	0.189	0.189
Vung Chua	**0.110**	0.128	0.143	0.177	0.168
Yen Dinh	**0.078**	0.083	0.120	0.138	0.139

Table 5-3. K-S test for goodness-of-fit for distributions of maximum water level

Location	Log normal	Pearson3	GEV	Logistic	Normal
Ba Lat	**0.083**	0.101	0.140	0.122	0.129
Cau Giat	**0.108**	0.127	0.161	0.150	0.157
Chan May	**0.129**	0.150	0.187	0.218	0.206
Cua Hoi	**0.142**	0.149	0.175	0.194	0.200
Cua Khau	**0.175**	0.198	0.227	0.238	0.237
Cua Sot	**0.165**	0.182	0.209	0.235	0.227
Cua Tung	0.228	**0.182**	0.219	0.204	0.217
Cua Viet	0.208	**0.195**	0.223	0.222	0.232
Cua Gianh	**0.102**	0.127	0.165	0.143	0.154
Cua Nhuong	**0.147**	0.170	0.202	0.197	0.202
Da Nang	0.165	**0.163**	0.197	0.258	0.236
Diem Dien	0.155	**0.131**	0.171	0.167	0.166
Dien Chau	**0.113**	0.133	0.166	0.172	0.171
Do Son	**0.158**	0.178	0.219	0.181	0.198
Dong Hoi	**0.137**	0.153	0.204	0.176	0.184
Duc Pho	**0.187**	0.216	0.253	0.255	0.260
Dung Quat	**0.183**	0.222	0.222	0.278	0.255
Hoang Tan	**0.122**	0.143	0.184	0.151	0.166
Hoi An	0.208	**0.195**	0.227	0.242	0.257
Hon Dau	**0.143**	0.159	0.203	0.158	0.176
Hon Nieu	**0.148**	0.162	0.190	0.220	0.207
Cua Nam Trieu	**0.143**	0.168	0.207	0.187	0.198
Nhat Le	**0.123**	0.142	0.187	0.161	0.172
Tam Ky	**0.190**	0.215	0.253	0.283	0.273
Tam Quan	0.183	**0.110**	0.130	0.125	0.135
Thanh Hoa	**0.101**	0.110	0.156	0.125	0.134
Thuan An	**0.139**	0.147	0.181	0.217	0.203
Tinh Gia	**0.096**	0.116	0.158	0.134	0.142
Vung Chua	**0.073**	0.094	0.138	0.109	0.120
Yen Dinh	0.141	**0.096**	0.106	0.098	0.106

Bold number shows the lowest value of K-S by best-fit distribution at each location

From these tables, we can see that at almost locations the log-normal (LN) distribution is likely having the best fit with the data series with the test statistic is smaller than the critical value of the K-S test. The second good distribution is P3. Generally speaking for all locations, the goodness-of-fit of the distributions of storm surge sorted descending are LN (occupied 87% number of locations), P3 (13%), GEV, Normal and logistic. The order of goodness-of-fit of the distributions of maximum water level sorted descending are LN (occupied 77% number of locations), P3 (23%), GEV, logistic and Normal.

Also it is can be seen that the LN distribution has a goodness-of-fit for extreme samples of storm surge better than maximum water level. P3 distribution has a goodness-of-fit for extreme samples of maximum water level better than storm surge.

From this result, the best fit distribution for each data series is selected. The chosen distribution at almost locations is log-normal. Some other locations use P3 distribution such as Cau Giat, Chan May, Da Nang, Duc Pho for storm surge and and Diem Dien, Cua Tung, Cua Viet, Da Nang, Hoi An, Tam Quan, Yen Dinh for maximum water level. The remaining distributions have not got best fit for any location, so they are rejected.

5.2.3. Results of storm surge and water level corresponding return period.

The statistical parameters and values of storm surge corresponding to the return period of 100 years at each location are shown in Table 5-4.

From this table, it is can be seen that at most locations the values of 100-year maximum water level are greater than the values of 100-year storm surge. There are small number of location that the values of 100-year storm surge are greater than the values of 100-year maximum water level. It does not mean that maximum storm surges always occur during low tide or in other words 100-year surge-only not always accompanied with 100-year maximum water level, since it depends on tide-surge interaction. It is can be explained by the variation coefficients C_V of the surge-only series and the maximum water level series at each location. The coefficients of variation C_V of the surges are commonly 1.5 to 3 times greater than those of maximum water levels at all locations. We can also see that the value of C_V and the value of 100-year storm surge at Cua Hoi are largest along the Vietnamese coast. Normally, the P3 distribution gives higher values of storm surge than the GEV distribution does, except at Cua Hoi (refer more detail in appendix).

Therefore, for precisely design of coastal structures the best-fit distribution as mentioned above (or Table 5-4) are applied. Otherwise, P3 distribution also can be suggested to give more safety for design of coastal structures. The results of maximum water level corresponding to various return periods can also be presented in GIS maps based on topographical data for coastal zone planning, management or disaster mitigation.

Table 5-4. Statistical parameters and 100-year values of storm surges (meters)

Station	**Storm surge** (tide subtracted)				**Max. water level** (tide included)			
	Mean	**C_V**	**LN**	**P3**	**Mean**	**C_V**	**LN**	**P3**
Cua Nam Trieu	1.01	0.66	3.18		1.63	0.32	3.39	
Hon Dau	0.92	0.68	2.76		1.54	0.26	2.83	
Do Son	0.96	0.69	2.94		1.56	0.27	2.95	
Diem Dien	1.03	0.76	3.38		1.62	0.34		3.51
Cua Ba Lat	0.95	0.66	2.98		1.56	0.28	3.00	
Yen Dinh	0.71	0.53	1.76		1.38	0.18		2.13
Hoang Tan	0.82	0.66	2.43		1.47	0.28	2.80	
Tinh Gia	0.84	0.67	2.50		1.46	0.29	2.83	
Cau Giat	0.84	0.66		2.85	1.42	0.29	2.76	
Dien Chau	0.92	0.71	2.86		1.49	0.35	3.17	
Thanh Hoa	0.79	0.64	2.30		1.38	0.27	2.59	
Hon Nieu	1.10	0.84	3.91		1.60	0.43	3.89	
Cua Hoi	1.22	0.82	4.61		1.70	0.49	4.59	
Cua Sot	0.94	0.88	3.47		1.46	0.41	3.47	
Cua Nhuong	0.77	0.79	2.62		1.35	0.31	2.70	
Cua Khau	0.81	0.88	2.99		1.35	0.37	2.97	
Vung Chua	0.63	0.77	2.08		1.12	0.27	2.07	
Dong Hoi	0.60	0.79	2.05		1.11	0.33	2.28	
Da Nang	0.61	1.09		3.39	0.67	0.79		2.99
Dung Quat	0.61	1.36	3.24		0.84	0.74	2.88	
Duc Pho	0.25	1.25		1.61	0.67	0.47	1.62	
Tam Quan	0.21	0.56	0.55		0.62	0.28		1.18
Cua Gianh	0.58	0.75	1.92		1.10	0.29	2.11	
Nhat Le	0.60	0.79	2.04		1.11	0.32	2.24	
Cua Tung	0.61	0.98	2.47		0.93	0.47		2.57
Cua Viet	0.63	1.08	2.76		0.93	0.54		2.89
Thuan An	0.66	0.89	2.48		0.81	0.53	2.17	
Chan May	0.56	0.89		2.50	0.64	0.53	1.68	
Hoi An	0.62	1.13	3.06		0.74	0.84		3.47
Tam Ky	0.48	1.22	2.34		0.71	0.57	1.98	

CHAPTER 6. CONCLUSIONS AND RECOMMENDATIONS

6.1. Conclusions

In general, the objectives of the study have been achieved. These include investigation and selection of the appropriate typhoon models; set-up, calibration and validation of a storm surge model for Northern Vietnamese coast using Delf3d-FLOW; calculation and evaluation the results of storm surges for typhoons from 1951 to 2001 and determination of probability distribution for storm surge. In particular, the major results of the study are summarised as follows:

1. For representing typhoons in the area, the Fujita model has been selected for describing typhoon pressure field and the modified Rankine vortex model has been chosen for simulating typhoon wind field. These have been selected among various models and provide best fit with observations according to root-mean-squared error criteria. RMSE is about 1.5mb for the pressure model and it is approximately 4m/s for the wind model.
2. The hydrodynamic model has been set up for the most vulnerable area under storm surge of Vietnam. The model has been calibrated and validated by using method of sensitivity analysis to investigate effects of boundary conditions and model parameters on water level simulation for both cases of with and without typhoon. The errors between computed and observed water levels are less than 0.1m and more or less 0.2 m for cases of without and with typhoon effect, respectively.
3. The hydrodynamic model has been used to simulate storm surges of 174 storms at main locations along the coast based on storm track information from 1951 to 2001. The resultant sets obtained from the hydrodynamic model have been used to determine probability distributions at the locations.
4. The most suitable probability distribution has been selected using the Kolmogorov-Smirnov test to statistically model each data set of both storm surge and maximum water level at each location along the coast. The best-fit distribution at almost locations is log-normal distribution. At the rest locations, Pearson type III is the best-fit distribution. The values corresponding to the 100-year occurrences as well as other different return periods of storm surge and maximum water level at each location have been estimated.

Besides main achievements as mentioned above, the following conclusions have been drawn from the study:

- The accuracy of typhoon simulation, which mainly depends on estimation of radius of maximum wind speed *R*, plays most important role on magnitude of storm surge and

location of maximum surge occurrence. In case of lacking or without observations, value of *R* can be estimated from the relationship with central pressure drop, with an acceptable error.

- A coarse grid size as well as coarse bathymetry cause enormous error and difficulty for model calibration due to the distortion of bottom topography. Coarse grid sizes also increase smoothness of bottom artificially, leading to a high model roughness required to resist this tendency. Therefore, the selection of a suitable model grid and data set of bathymetry is important.
- According to the characteristics of tidal propagation in the area, model boundary has been separated in many sections corresponding to deep or shallow parts as long as the phase in each section varies linearly to get more efficiency in calibration. In the study area, diurnal components are dominant and more sensitive than semi-diurnal constituents.
- To avoid incorrectly interpolation of wind field in Delft3D, a program is developed to create wind and pressure fields in every time step of the hydrodynamic model.
- Hydrodynamic simulation in typhoon condition requires coupling with a wave model to present effect of wind waves. In the simple case of without wind wave simulation, the wind drag coefficient (depends on wind speed) should be increased to give much the same improvement in results as the full surge-wave calculations.
- The peak surge usually occurs at or near the point where maximum winds intersects the shoreline. Typhoons move more or less perpendicular to the coast also induce high surge.
- The maximum storm surge can occur in any phase of tide due to the results of interaction between surge and tide. The relative phases of the surge and tidal components affect the peak-sustained water level. Similarly, the maximum water level with 100-year return period is not always accompanied with 100-year surge-only.
- The region from Diem Dien up to the north and especially at the locations of Hon Nieu, Cua Hoi, Cua Sot are being suffered from influence of storm surges much more than other regions. Cua Hoi is the most vulnerable coastal area of Vietnam that should be paid more attention here to mitigate the damage.

6.2. Recommendations

1. The model can be used for computing storm surge in the northern coastal area of Vietnam for different purposes of coastal engineering or integrated coastal zone management. For enhancement of model results, more observation data of pressure

and wind speed of each storm induced surge should be taken to give the more precise value of *R* as well as other parameters of typhoon model.

2. High resolution of local bathymetry should be applied especially in shallow water near shoreline in order to improve the results of hydrodynamic model as well as the model itself.
3. For further study storm surge in this area, surge–wave interaction model should be carried out. Then the results of that model should be compared to the results of the present model, which is surge–tide only, to choose the more suitable model.
4. In fact, storm surges or maximum water levels during typhoons are joint probability distributions of many influencing factors. The determination of those component distributions may be done in case of meteorological observed data and statistical modelling are available. The results can be compared with the case, in which storm surge is considered as an independent random variable.
5. The model can be used for hindcasting storm surge for normal coastal line. Because of model grid size, it should not be used for special coastline associated with bays, estuaries, canals, barriers because for these fragmentary. A more detailed bathymetry and inflow data is required for these areas.
6. The model can be used not only for storm surge hindcasting but also for forecasting. However, to consider the error of storm surge caused by inaccurate storm track forecasting, the storm surge model should run with several alternative tracks, varying on either side of forecast landfall point. Similarly, many options of storm parameters such as maximum wind speed and radius of maximum wind speed during a forecast period should be applied. By this way, a range of possible surge values is produced corresponding with the range of meteorological imprecision.
7. To estimate storm surge with a long-term return period for coastal engineering, the approach of probabilistic design should be applied. However, at this time because of scarce database or observed data is non-existent in most regions, the method of construction probability distribution for storm surge presented in this study could be used.

REFERENCES

1. American Society for Oceanography, 1966. Hurricane symposium, Houston, Texas
2. Ao Chu, 2002. Study of Extreme hydrodynamic conditions in the Yangtze Estuary, MSc thesis, IHE, Delft.
3. As-Salek, J.A. et al, 1995. Comparative study of storm surge models proposed for Bangladesh: Last developments and research needs, Journal of Wind Engineering and Industrial Aerodynamics 54/55, pp 595-610.
4. Bijl, W., 1995. Impact of a wind climate change on the surge in the southern part of the North Sea, report. RIKZ-95.016, EU- project IMPACTS, Rijksinstituut voor Kust en Zee/RIKZ
5. Bijlsma, A.C.,1989. Investigation of surge- tide interaction in the storm surge model CSM-16, Delft Hydraulics
6. Bode, L. and Hardy, T.A., 1997. Process and Recent Developments in Storm Surge Modelling, Journal of Hydraulic Engineering, Vol. 123, No. 4, pp 315-330.
7. Bunpapong, M., Reid R. O. and Whitaker, R.E., 1985. An investigation of hurricane-induced forerunner surge in the Gulf of Mexico, Technical report CERC-85-5, USACE, Washington, DC.
8. Cunnane, C., 1989. Statistical distributions for flood frequency analysis, Operational Hydrology Report No. 33, World Meteorological Organisation, Geneva.
9. Do Cao Dam (editor), 1993. Applied hydrology, Agricultural publishing, Hanoi.
10. De Vries, J.W., 1991. The implementation of the WAQUA/ CSM-16 model for real time storm surge forecasting, De Bilt
11. Disaster Management Unit, 1999. Storm and Tropical Depression Study in Vietnam, UNDP Project /VIE/97/002 - Support to Disaster Management System in Viet Nam
12. Gerritsen, H., Hulsen, L.J.M., van der Kaaij and Verploegh, D., 2001. The SCM regional model and VCM detailed model – set-up, calibration and validation, WL | Delft Hydraulics, Delft.
13. Gerritsen, H., Schrama, E.J.O., Uittenbogaard, R.E., van den Boogaard, H.F.P., van der Kaaij, Th., 2001. SAT2SEA, WL | Delft Hydraulics, Delft.
14. Gerritsen, H., Vatvani, D.K., 2000. Inception and data Gathering mission, WL | Delft Hydraulics, Delft.
15. Haan, C. T., 1982. Statistical methods in Hydrology, Third printing, The Lowa State University Pree/ Ames
16. Hanoi Water Resources University (HWRU), 2000. Summary and evaluation on types of toe-protection for sea dike revetments – a study on suitable types of toe-protection. Hanoi
17. Heemink, A.W., 1986. Storm surge prediction using Kalman filtering, Rijkswaterstraat communications, No. 46, Twente University of Technology, The Hague.
18. Holand, G.J., 1980. An Analytic Model of the Wind and Pressure profiles in Hurricanes. Monthly Weather Review, Vol. 108, pp 1213-1218.
19. Holand, G.J., 1997. Wind field dynamics of landfalling tropical cyclone, http://www.bbsr.edu/rpi/meetpart/land/holland2.html
20. Le Bac Huynh, Nguyen Viet Thi, Bui Duc Long, Dang Thanh Mai, 1999, Flood Disaster Study, Disaster Management Unit, UNDP Project VIE/97/002, Hanoi.

21. Le Trong Dao, Nguyen Tai Hoi, Truong Van Bon, Bui Xuan Thong, 2000, Storm Surge Disaster Study, Disaster Management Unit, UNDP Project VIE/97/002, Hanoi.

22. Le Van Thao, Bui Thi Bich, Pham Duc Thi, 2000, Storms and Tropical Depressions Disaster Study in Vietnam, Disaster Management Unit, UNDP Project VIE/97/002, Hanoi.

23. Masami, M., et al,1962, Numerical calculations of storm surge in Daban Bay and West part of Laihu Sea, conf., Coast Engineering, No.9, Japan.

24. Mastenbroek, C., Burgers, G., and Janssen, P.A.E.M., 1993. The dynamical coupling of a wave model and a storm surge model through the atmospheric boundary layer. Journal of Physical Oceanography, Vol. 23. pp 1856-1866

25. McGregor, G. R., 1995. The tropical cyclone hazard over the South China Sea 1970- 1989, Applied Geography, pp 35- 52.

26. Pham Van Ninh, 1992. The storm surge models, UNDP Project VIE/87/020, Hanoi.

27. Phan Duc Tac, 1996. A study on solutions for sea dike revetments in Vietnam by flexible mattresses of concrete units. Doctorate dissertation. Hanoi

28. Ou, S.H., Liau, J.M., Hsu, T.W., Tzang, S.Y., 2002. Simulating typhoon wave by SWAN wave model in coastal waters of Taiwan, Ocean Engineering 29, pp 947-971.

29. Phadke, A.C., Martino, C.D., Cheung, K.F., Houston, S.H., 2002, Modeling of tropical cyclone winds and waves for emergency management, Ocean Engineering, pp 4-6.

30. Roos, A., 1997, Tides and Tidal Currents, Lecture Notes, IHE Delft.

31. Schwiderski, E.W., 1979. Global Ocean Tides. Naval Surface Weapons Center. Virginia

32. Service Hydrographique et Oceanographique de la Marine, 1982. Table des Marees des Grands Ports du Monde, No. 540, Paris.

33. Seyhan, E., 1980. Application of statistical methods to hydrology, Institute of Earth Sciences – Free University, Amsterdam.

34. Shi, F et al, 1997. A WDM method on a generalized curvilinear grid for calculation of storm surge flooding, Applied Ocean Research, pp 275-282.

35. Tan, W., 1992. Shallow water hydrodynamics, Nanjing research Institute of Hydrology and Water resources, Beijing.

36. The Hydrographer of the Navy, 1982. Admiralty Tide Tables Volume 3-1983, Pacific Ocean and Adjacent Seas, Britain.

37. USACE (US Army Corps of Engineers), 1986. Engineering and design - storm surge analysis, Engineer manual EM 1110-2-1412, Washington, DC.

38. WL Delft Hydraulics, 2001. Delft 3D-FLOW Manual, version 2.2

39. Zhang, M. Y. and Li, Y. S., 1996. The synchronous coupling of a third-generation wave model and a two-dimensional storm surge model, Ocean Engineering Vol. 23. No. 6, pp533-543.

Appendix A. Models of typhoon wind and pressure

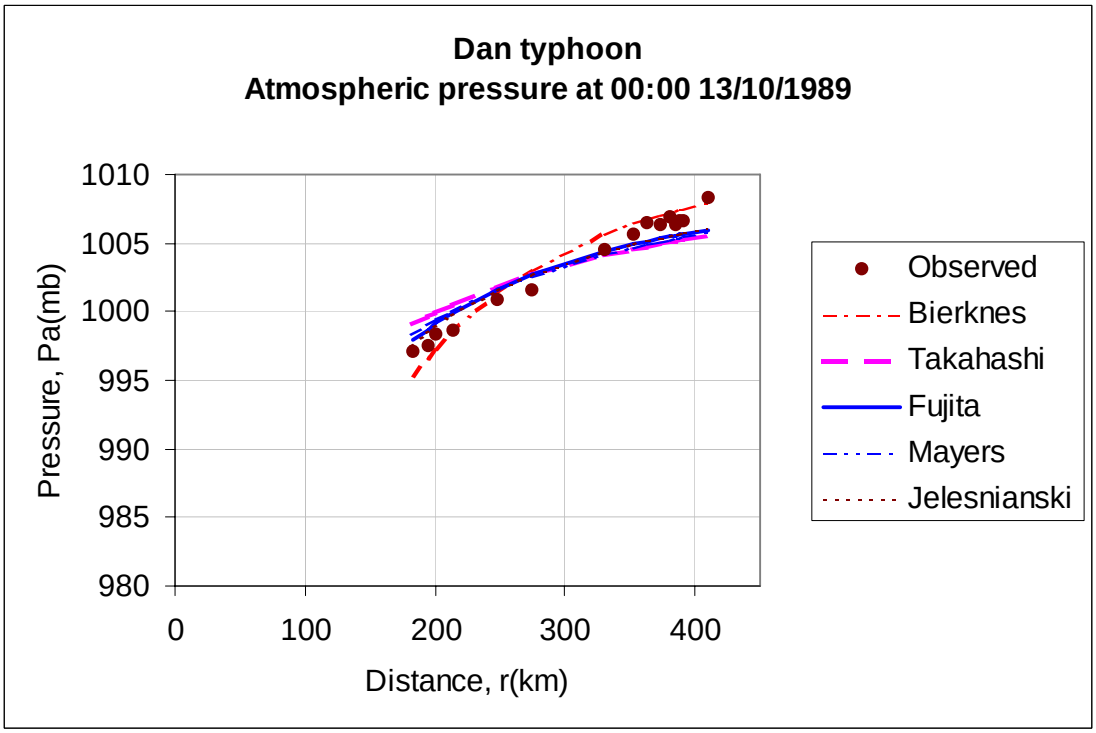

Figure A-1. Atmospheric pressure of typhoon Dan at 00:00 13/10/1989

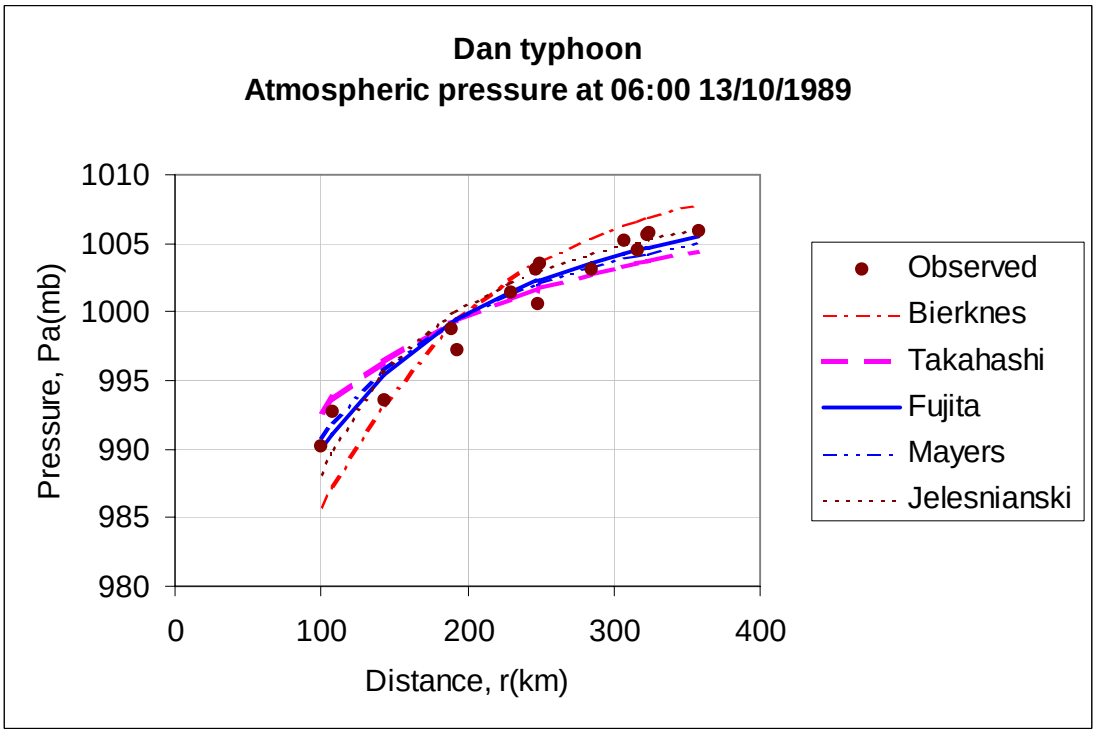

Figure A-2. Atmospheric pressure of typhoon Dan at 06:00 13/10/1989

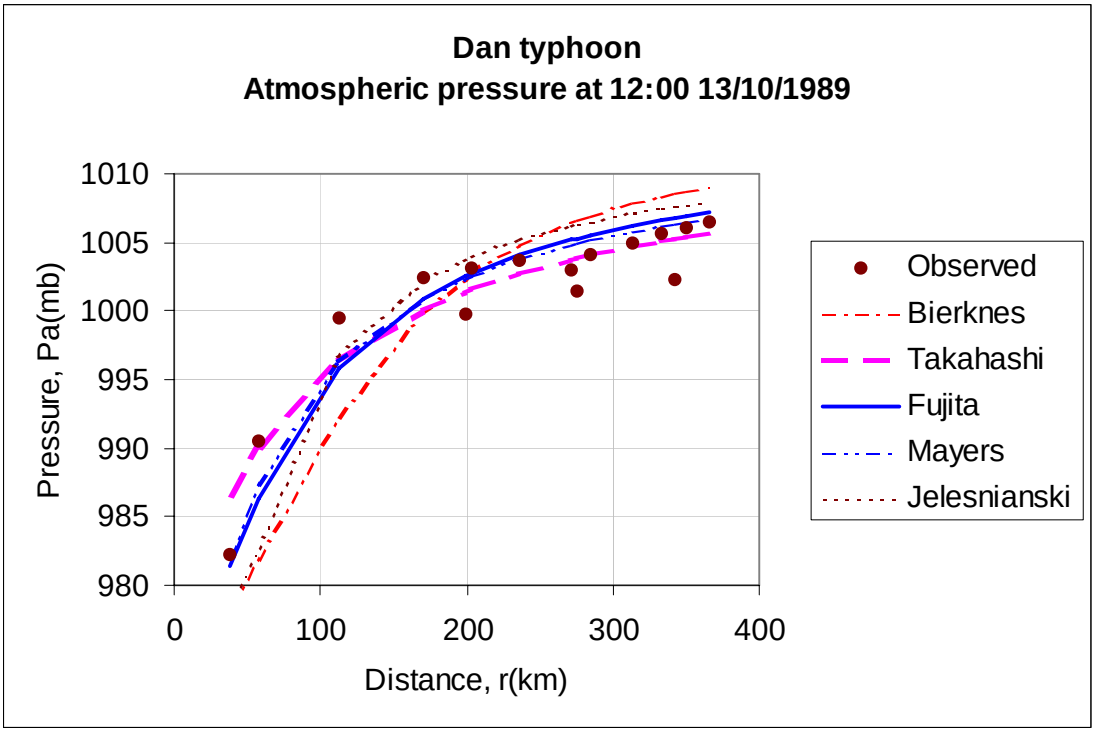

Figure A-3. Atmospheric pressure of typhoon Dan at 12:00 13/10/1989

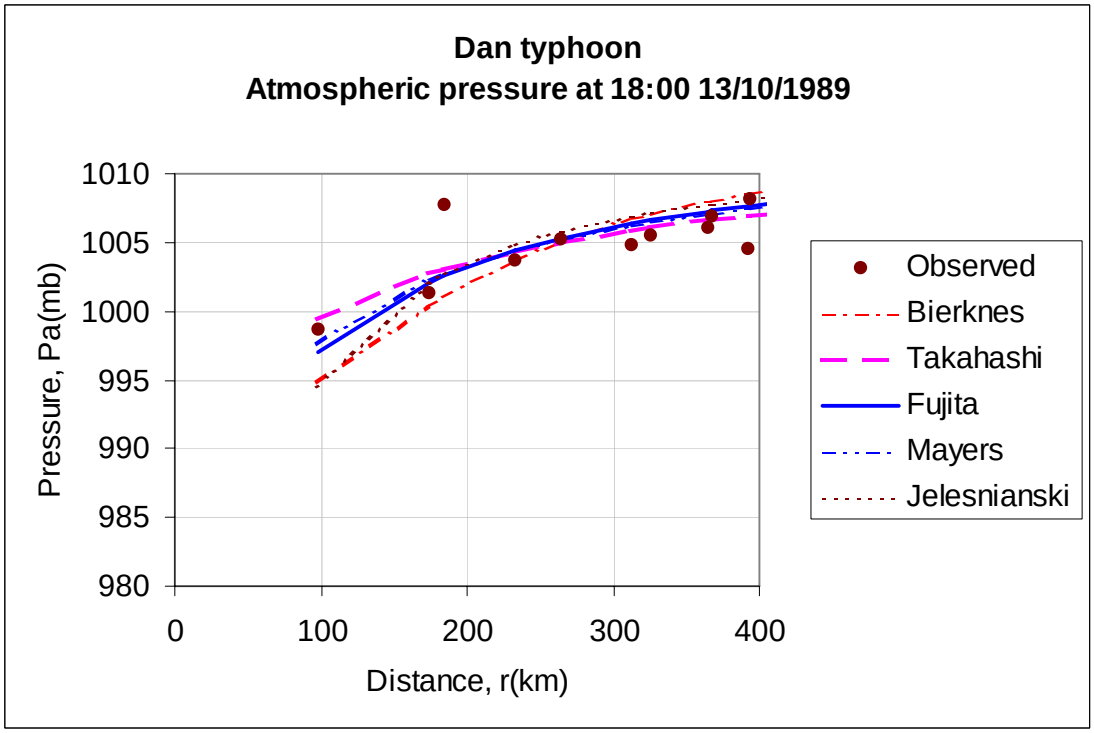

Figure A-4. Atmospheric pressure of typhoon Dan at 18:00 13/10/1989

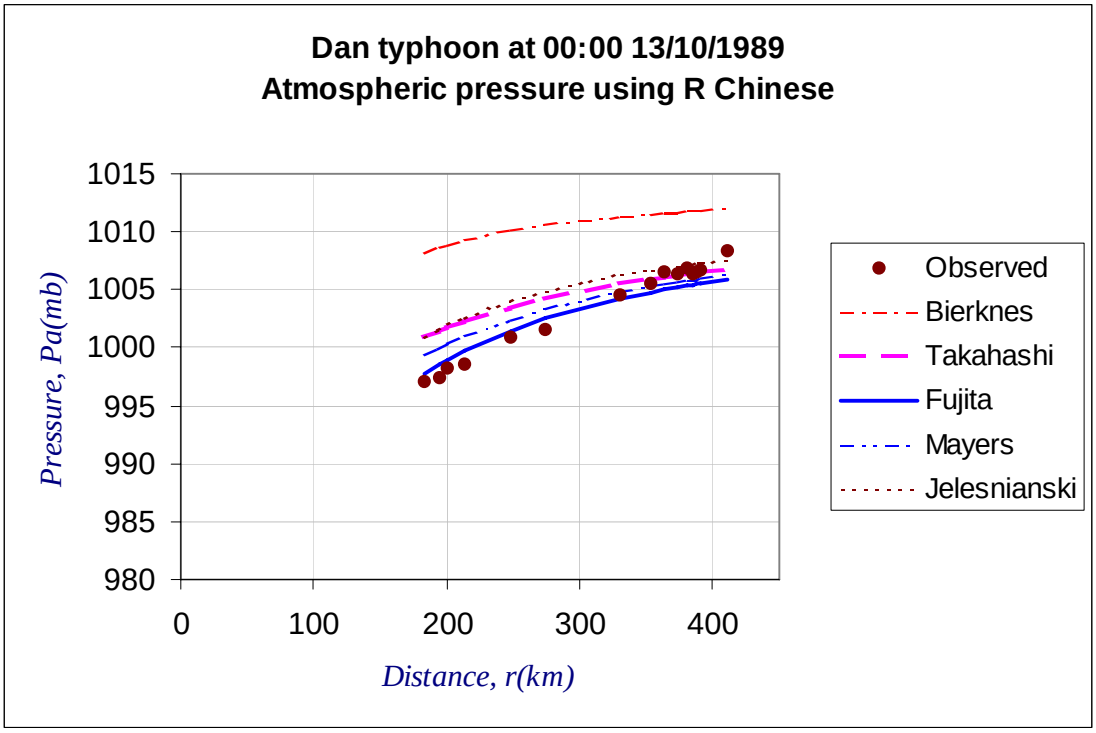

Figure A-5. Atmospheric pressure of typhoon Dan at 00:00 13/10/1989

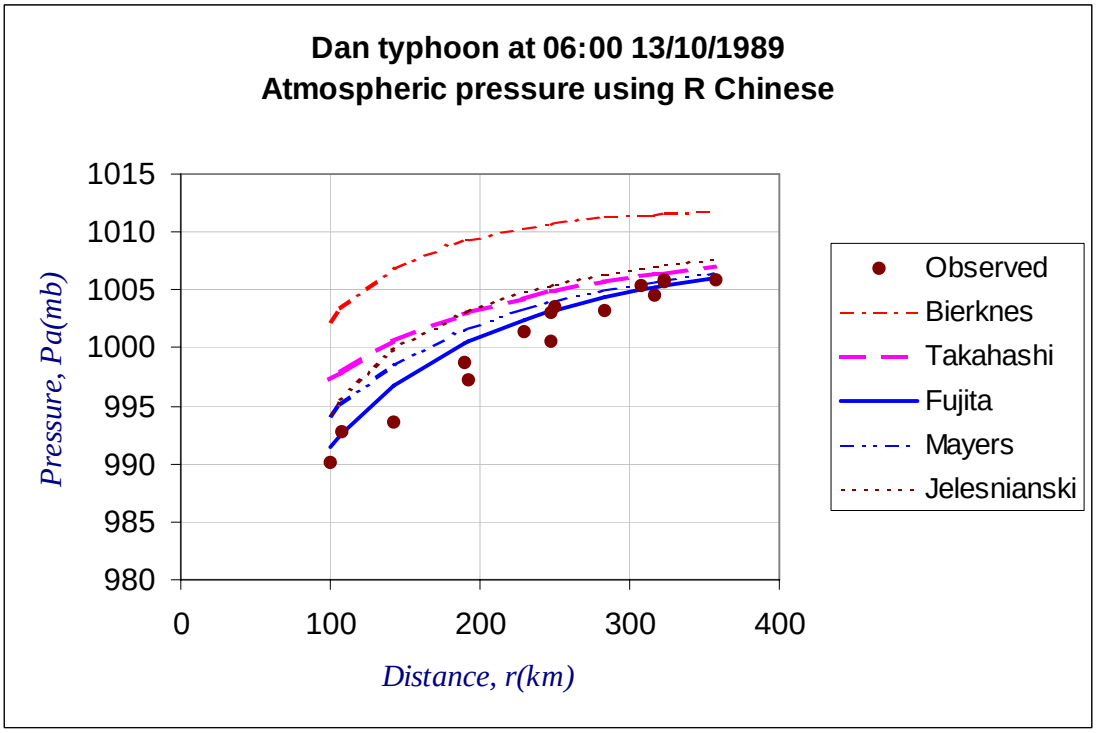

Figure A-6. Atmospheric pressure of typhoon Dan at 06:00 13/10/1989

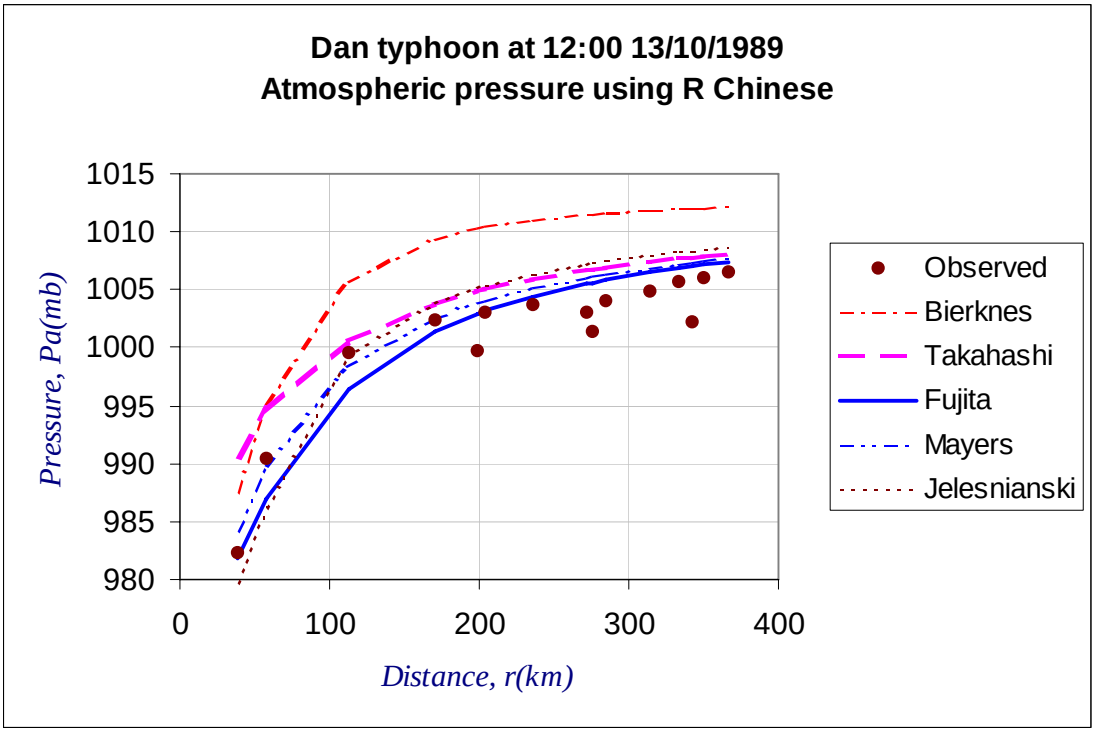

Figure A-7. Atmospheric pressure of typhoon Dan at 12:00 13/10/1989

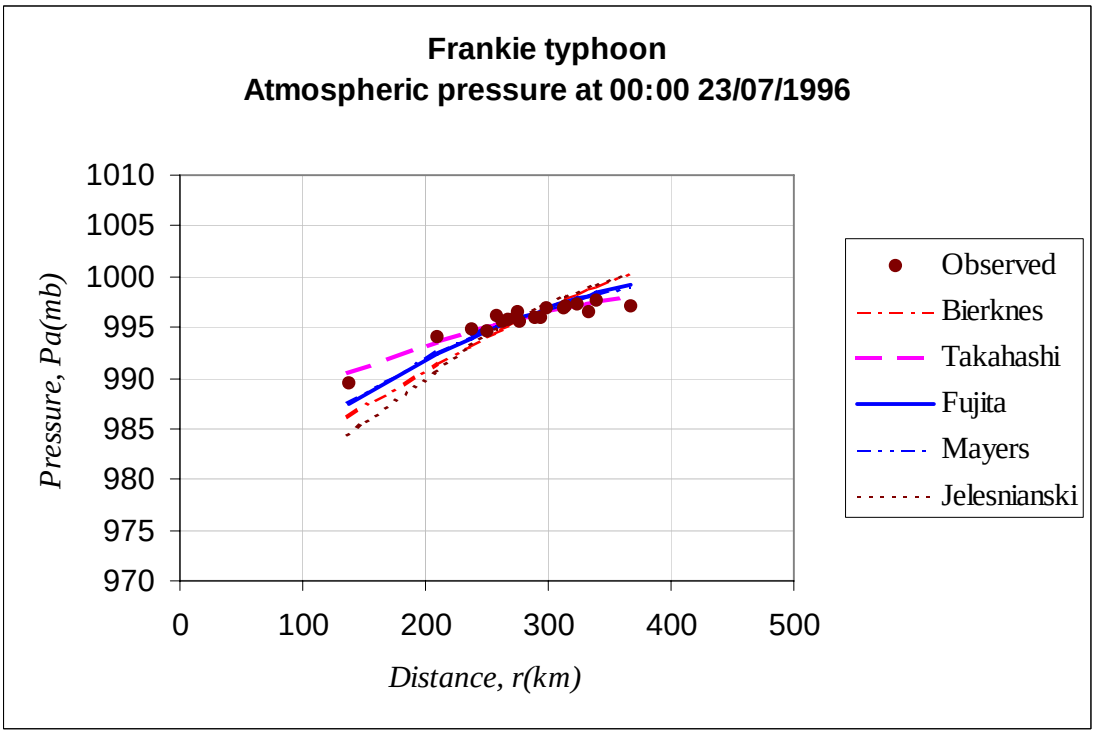

Figure A-8. Atmospheric pressure of typhoon Frankie at 00:00 23/07/1996

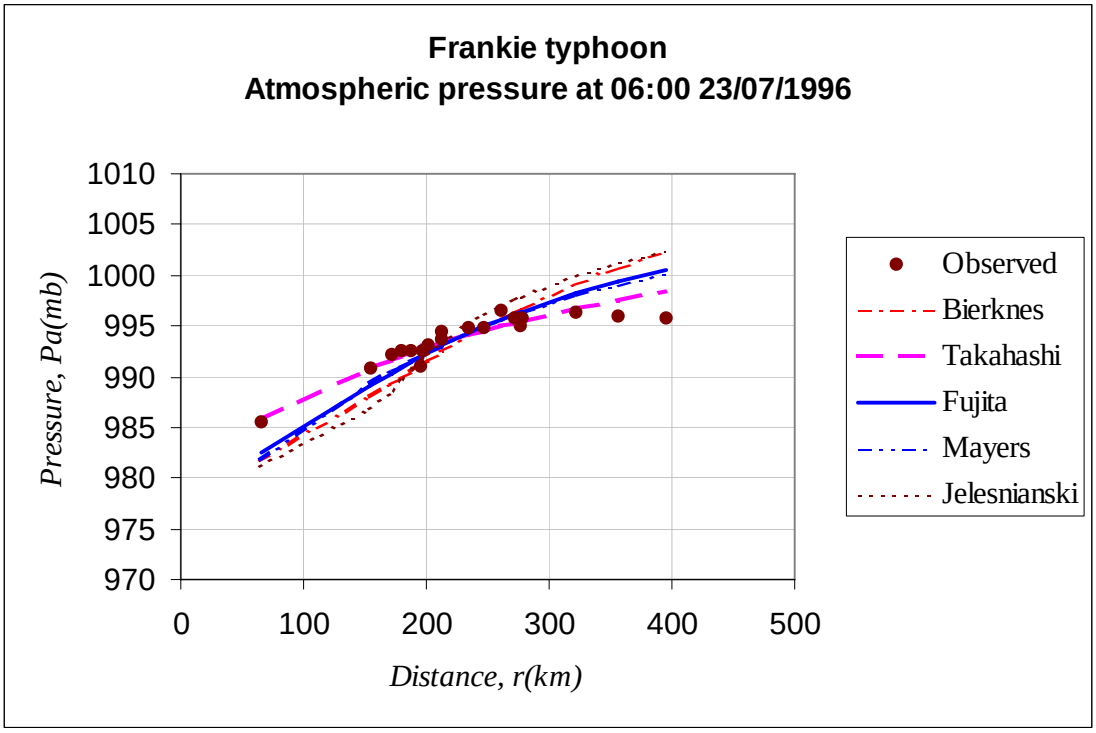

Figure A-9. Atmospheric pressure of typhoon Frankie at 06:00 23/07/1996

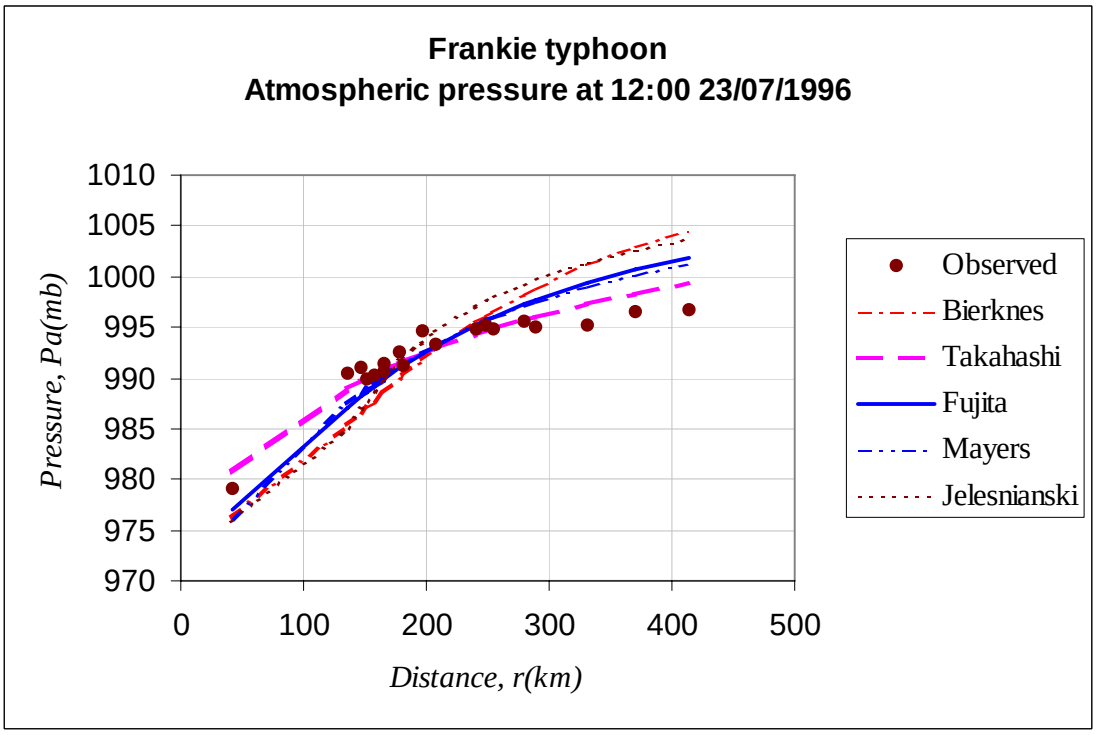

Figure A-10. Atmospheric pressure of typhoon Frankie at 12:00 23/07/1996

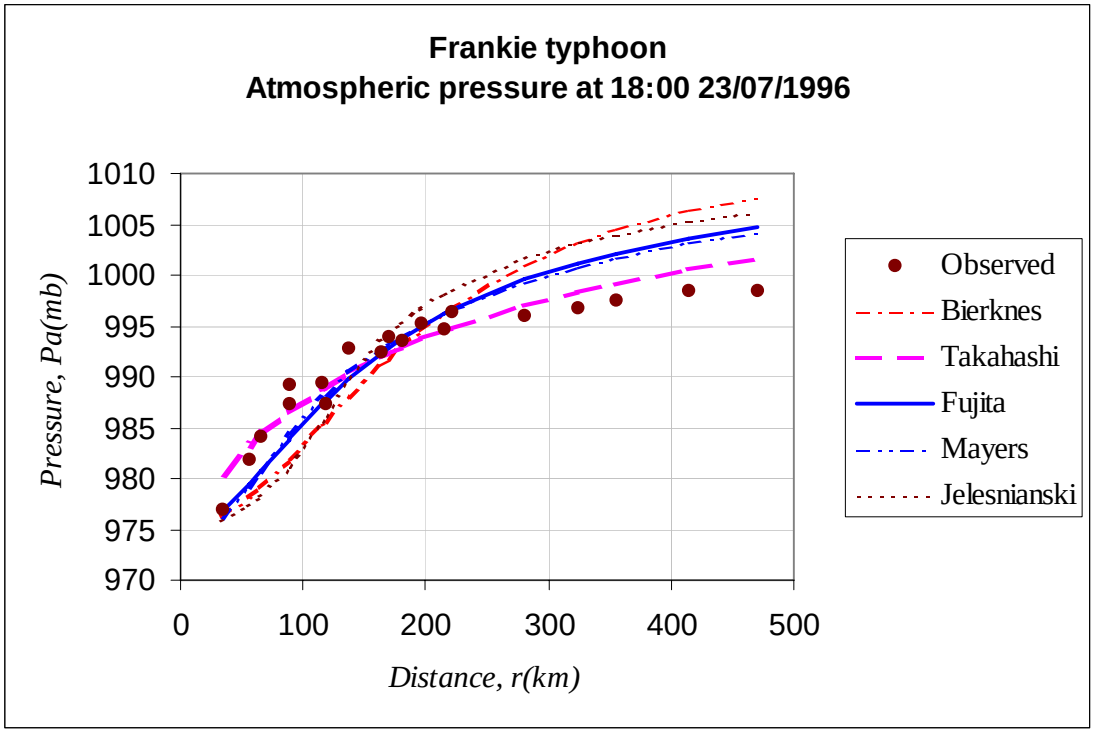

Figure A-11. Atmospheric pressure of typhoon Frankie at 18:00 23/07/1996

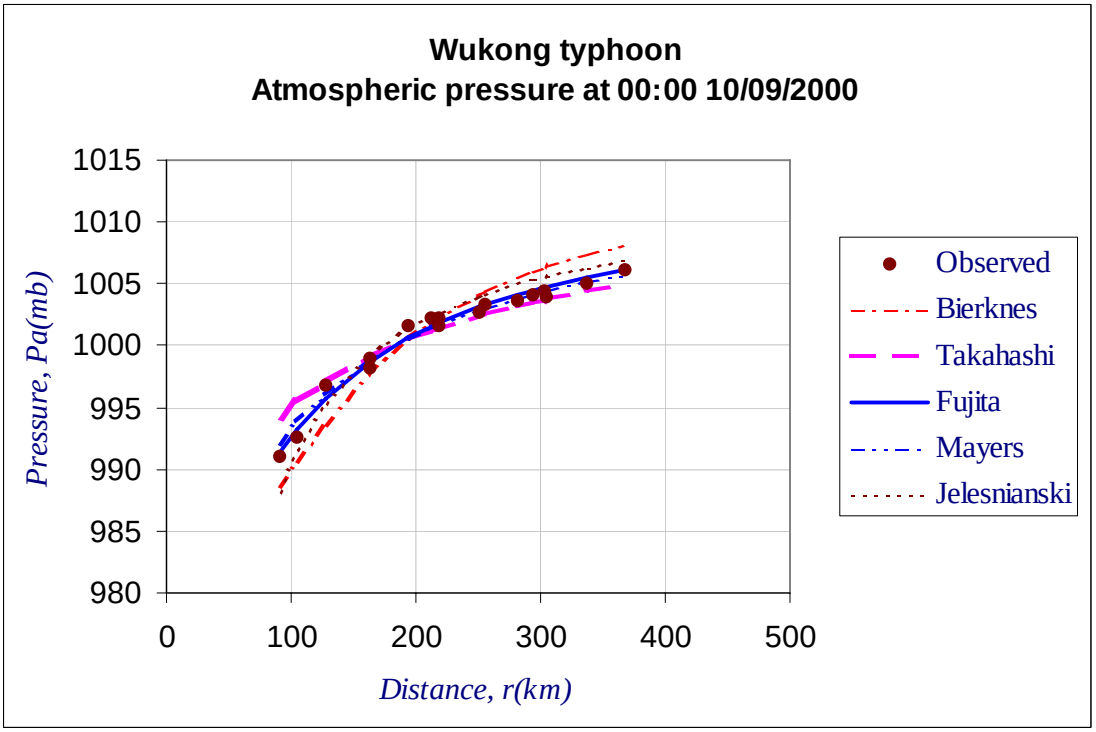

Figure A-12. Atmospheric pressure of typhoon Wukong at 00:00 10/09/2000

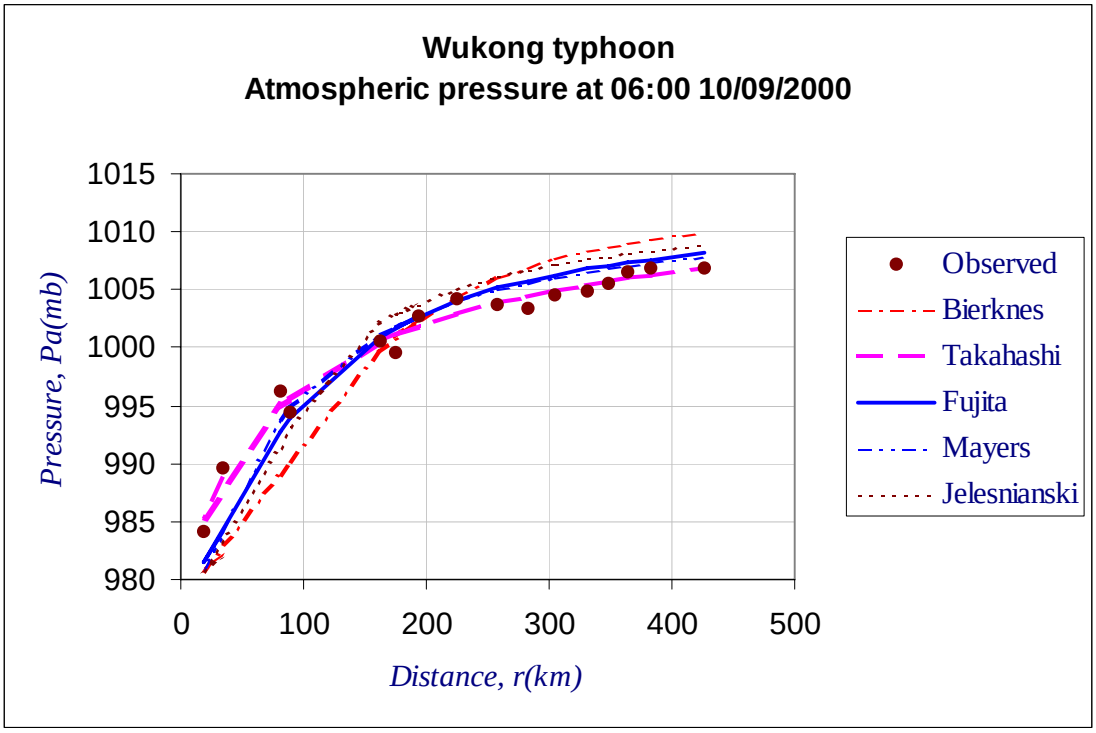

Figure A-13. Atmospheric pressure of typhoon Wukong at 06:00 10/09/2000

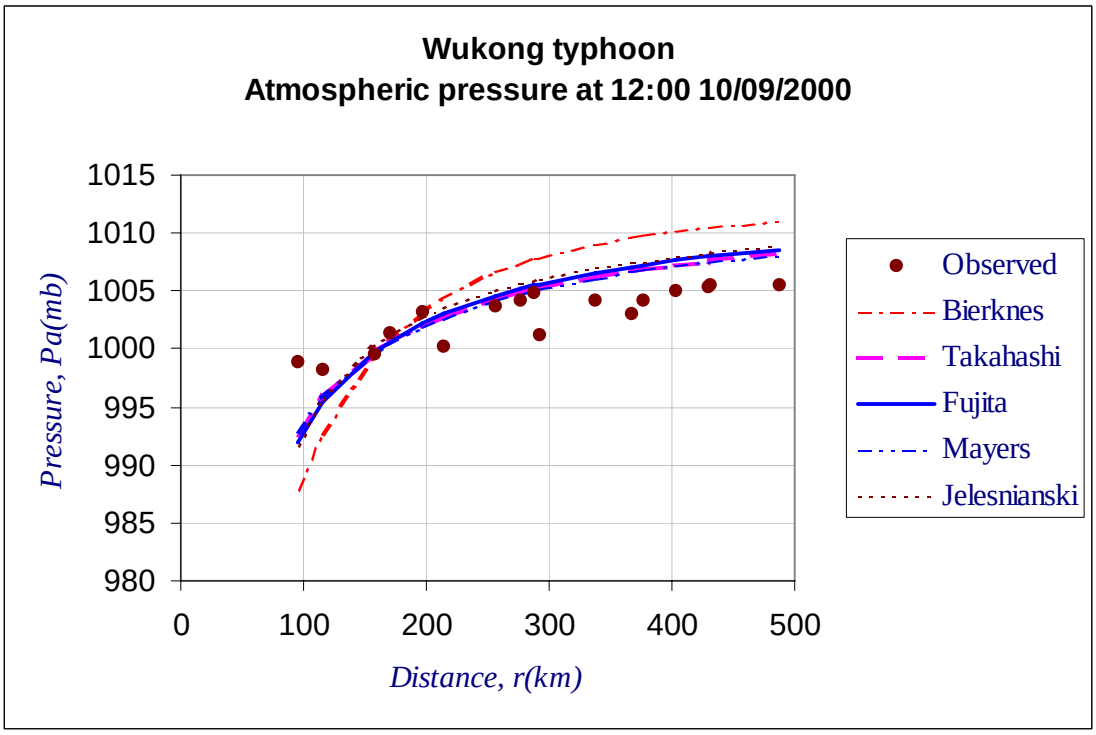

Figure A-14. Atmospheric pressure of typhoon Wukong at 12:00 10/09/2000

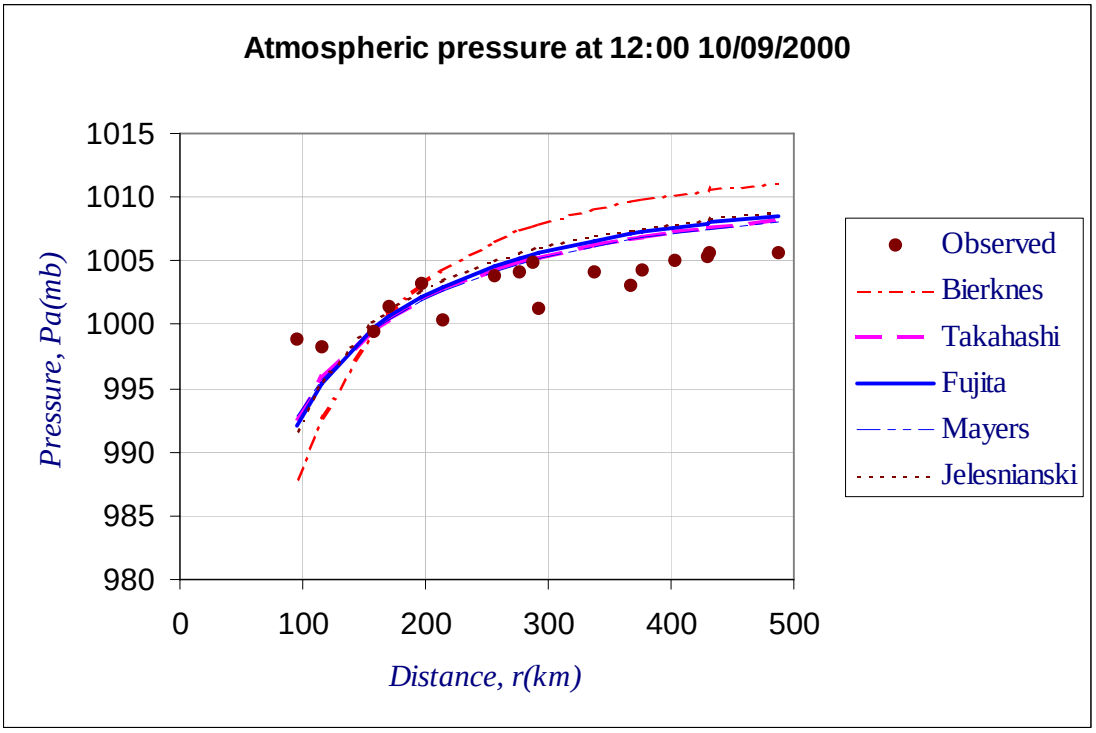

Figure A-15. Atmospheric pressure of typhoon Wukong at 18:00 10/09/2000

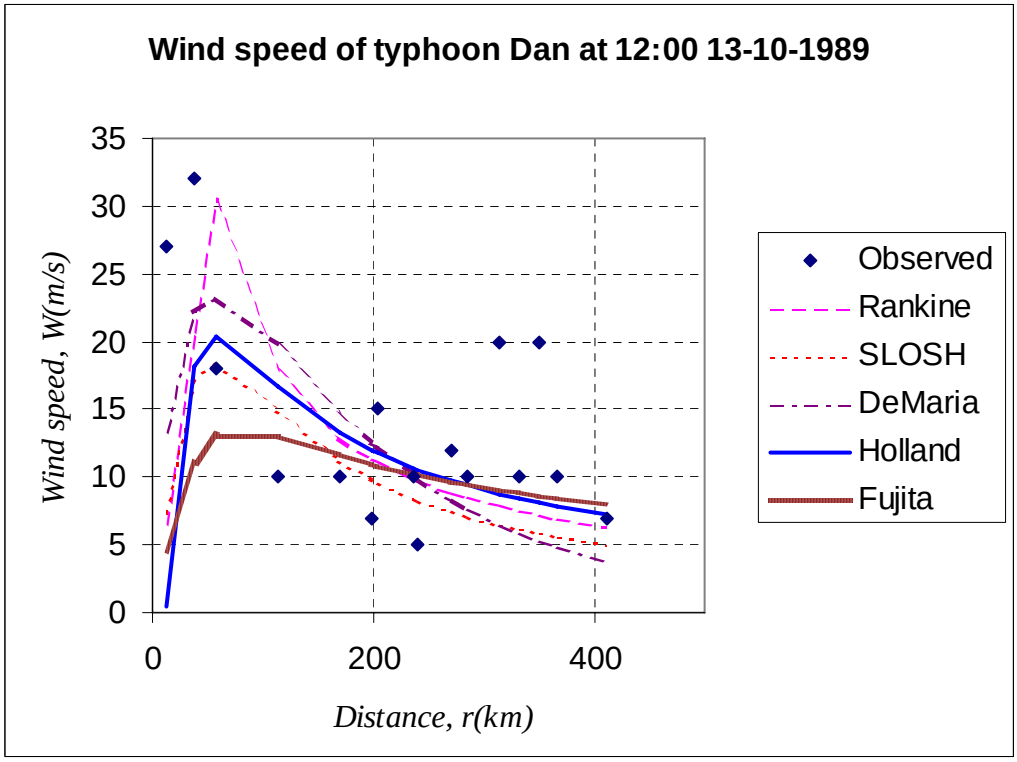

Figure A-16. Wind speed of typhoon Dan at 12:00 13/10/1989

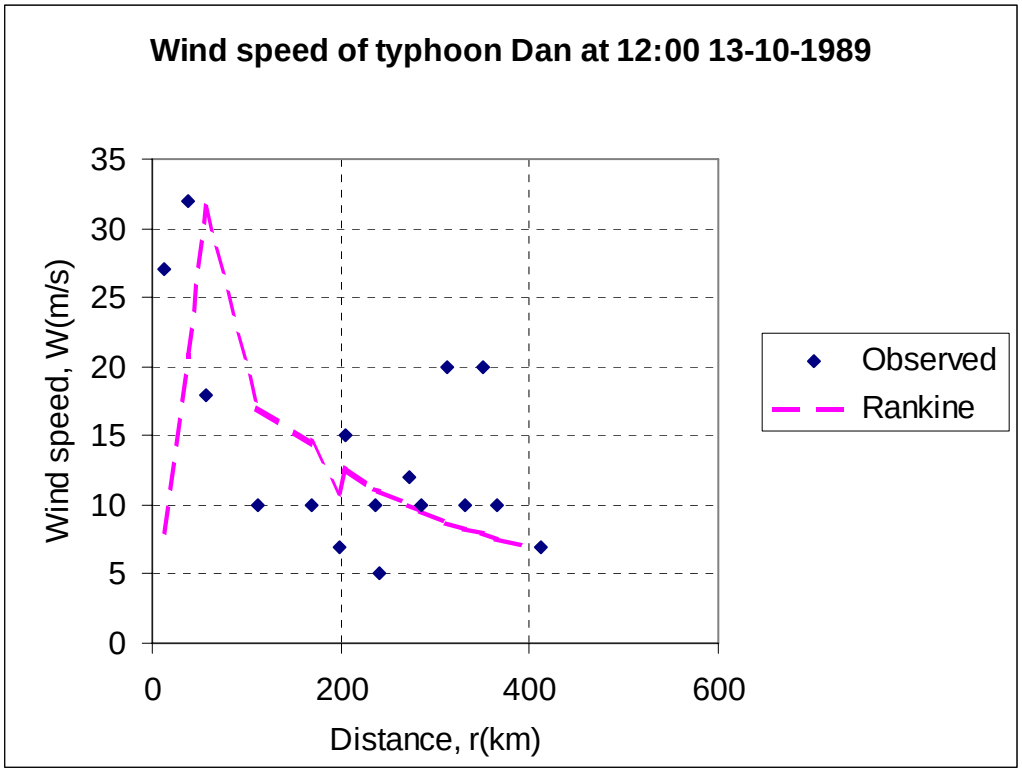

Figure A-17. Wind speed of typhoon Dan at 12:00 13/10/1989

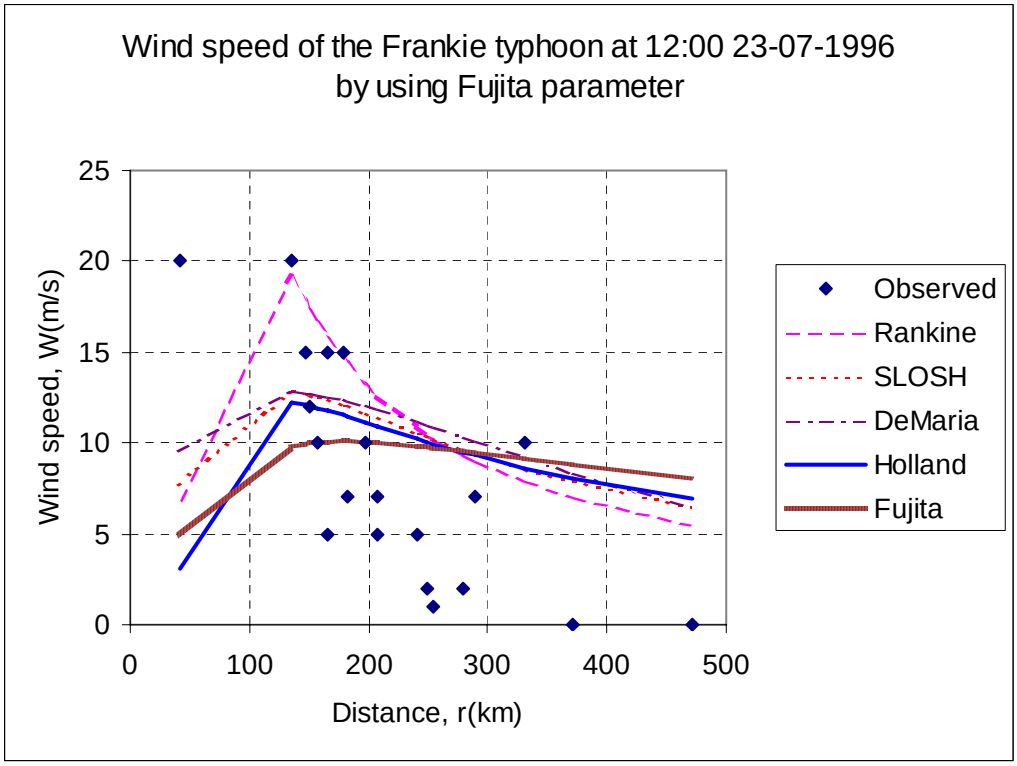

Figure A-18. Wind speed of typhoon Frankie at 12:00 23/07/1996

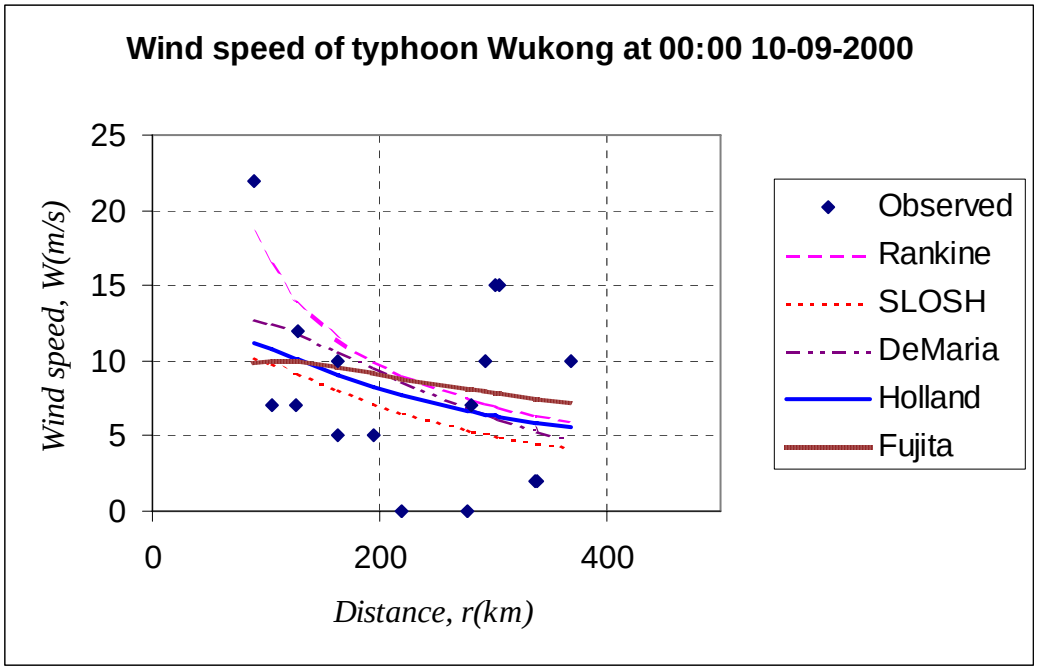

Figure A-19. Wind speed of typhoon Wukong at 00:00 10/09/2000

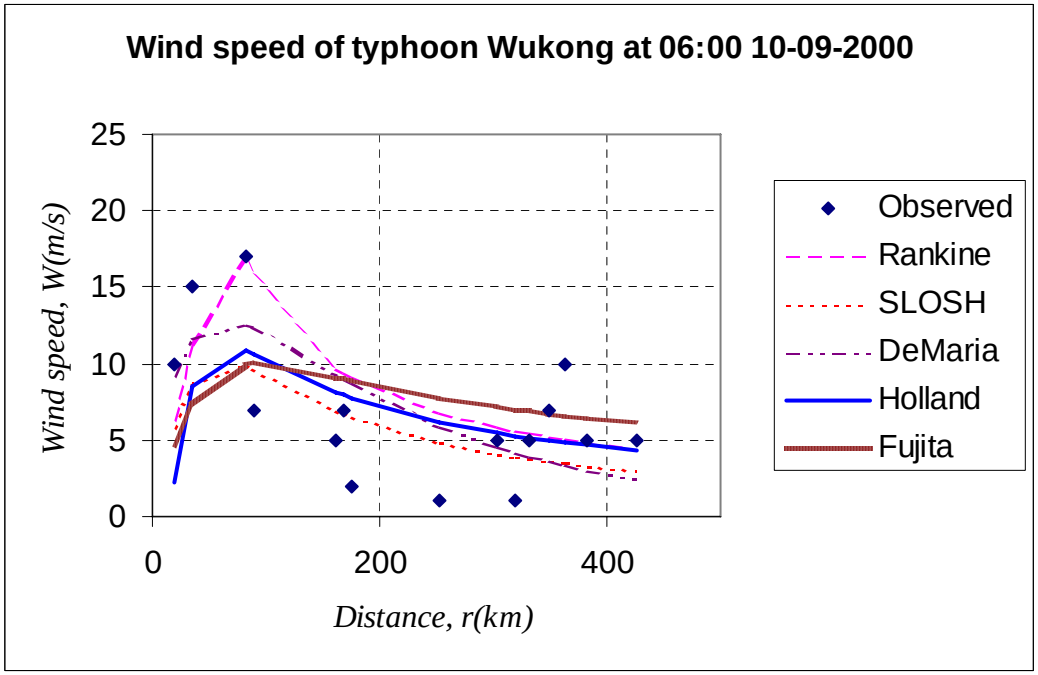

Figure A-20. Wind speed of typhoon Wukong at 06:00 10/09/2000

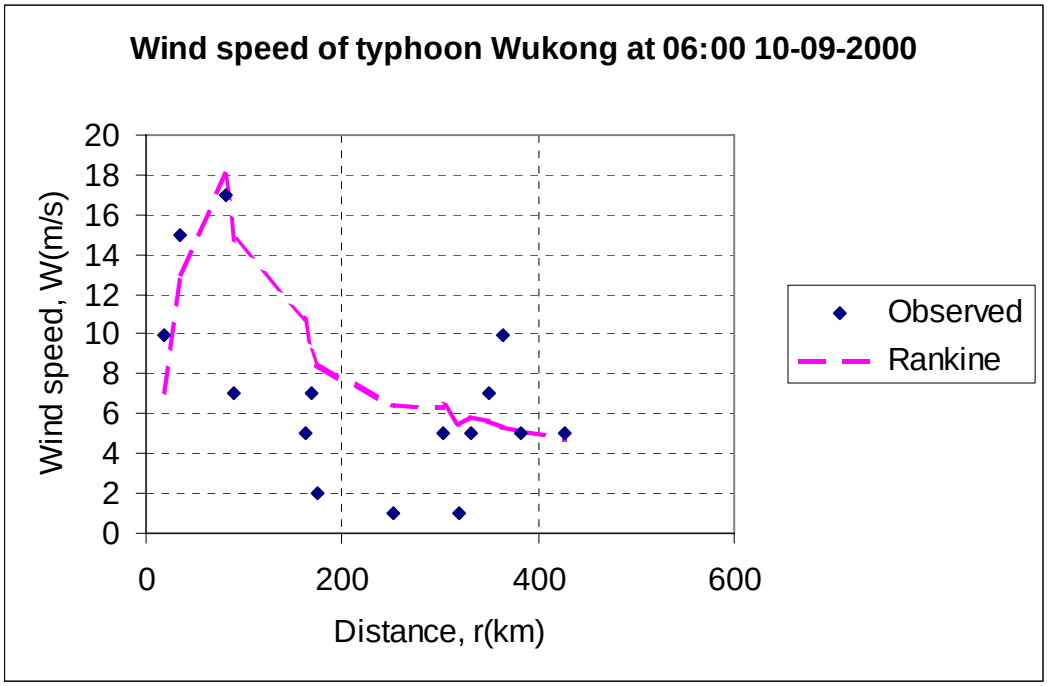

Figure A-21. Wind speed of typhoon Wukong at 06:00 10/09/2000

Table A-1. Error of computed wind speed if apply R Fujita, Po from best track and Pn=1013mb

And coeffiecient

Dan typhoon

Formula	Wmax	C2					X	b	B	RMSE(m/s)				
Date-time	(m/s)	Rankine	SLOSH	DeMaria	Holland	Fujita	Rankine	DeMaria	Holland	Rankine	SLOSH	DeMaria	Holland	Fujita
12-10-89 18:00	38.6	1	0.6	0.8	0.5	0.4	0.8	0.6	1.63	2.92	2.77	3.13	2.95	3.71
13-10-89 00:00	36.0	1	0.6	0.8	0.5	0.4	0.8	0.6	1.59	5.53	5.27	5.87	5.55	5.55
13-10-89 06:00	33.4	1	0.6	0.8	0.5	0.4	0.8	0.6	1.56	6.32	6.48	6.52	6.26	6.71
13-10-89 12:00	30.9	1	0.6	0.8	0.5	0.4	0.8	0.6	1.53	8.55	8.39	7.74	9.03	9.05
13-10-89 18:00	15.4	1	0.6	0.8	0.5	0.4	0.8	0.6	1.44	6.42	7.07	6.54	6.12	6.11
Average RMSE										5.95	6.00	5.96	5.98	6.23

Wukong typhoon

Formula	Wmax	C2					X	b	B	RMSE(m/s)				
Date-time	(m/s)	Rankine	SLOSH	DeMaria	Holland	Fujita	Rankine	DeMaria	Holland	Rankine	SLOSH	DeMaria	Holland	Fujita
08-09-00 18:00	36.01	1	0.4	0.5	0.3	0.4	0.8	0.6	1.63	3.39	3.37	3.72	3.42	3.80
09-09-00 00:00	36.01	1	0.4	0.5	0.3	0.4	0.8	0.6	1.63	3.40	3.57	4.29	3.33	3.35
09-09-00 06:00	30.87	1	0.4	0.5	0.3	0.4	0.8	0.6	1.56	3.34	3.36	3.35	3.44	3.50
09-09-00 12:00	28.29	1	0.4	0.5	0.3	0.4	0.8	0.6	1.53	4.27	4.24	4.62	4.52	4.38
09-09-00 18:00	25.72	1	0.4	0.5	0.3	0.4	0.8	0.6	1.50	4.80	4.79	5.27	4.90	4.80
10-09-00 00:00	25.72	1	0.4	0.5	0.3	0.4	0.8	0.6	1.50	5.41	5.72	5.78	5.55	5.93
10-09-00 06:00	25.72	1	0.4	0.5	0.3	0.4	0.8	0.6	1.50	3.85	3.89	3.92	4.27	4.62
Average RMSE										4.07	4.13	4.42	4.20	4.34

Frankie typhoon

Formula	Wmax	C2					X	b	B	RMSE(m/s)				
Date-time	(m/s)	Rankine	SLOSH	DeMaria	Holland	Fujita	Rankine	DeMaria	Holland	Rankine	SLOSH	DeMaria	Holland	Fujita
22-07-96 06:00	23.15	0.7	0.5	0.5	0.3	0.3	1	0.6	1.47	4.43	4.16	4.25	4.17	4.13
22-07-96 12:00	23.15	0.7	0.5	0.5	0.3	0.3	1	0.6	1.47	4.02	3.32	3.43	3.30	3.16
22-07-96 18:00	23.15	0.7	0.5	0.5	0.3	0.3	1	0.6	1.50	3.32	3.57	3.71	3.78	3.88
23-07-96 00:00	23.15	0.7	0.5	0.5	0.3	0.3	1	0.6	1.50	4.70	5.41	5.44	5.36	5.77
23-07-96 06:00	23.15	0.7	0.5	0.5	0.3	0.3	1	0.6	1.50	4.16	4.97	4.88	5.03	5.48
23-07-96 12:00	25.72	0.7	0.5	0.5	0.3	0.3	1	0.6	1.53	5.27	6.03	5.91	6.33	6.61
23-07-96 18:00	28.29	0.7	0.5	0.5	0.3	0.3	1	0.6	1.53	7.84	8.48	8.27	8.99	9.49
Average RMSE										4.82	5.13	5.13	5.28	5.50

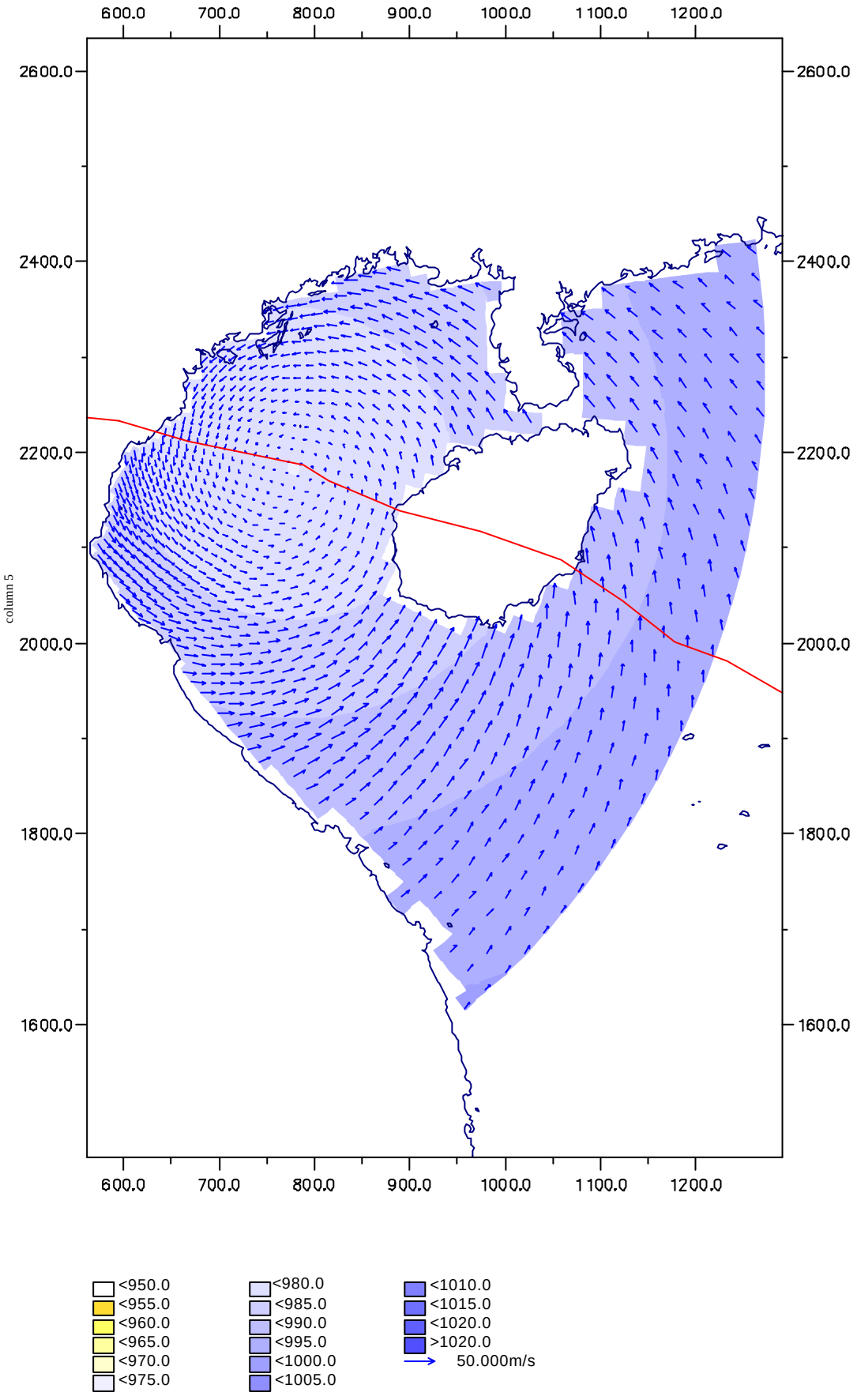

Figure B-1. Wind field and atmospheric pressure field of typhoon Frankie at 18h:00 23/07/1996

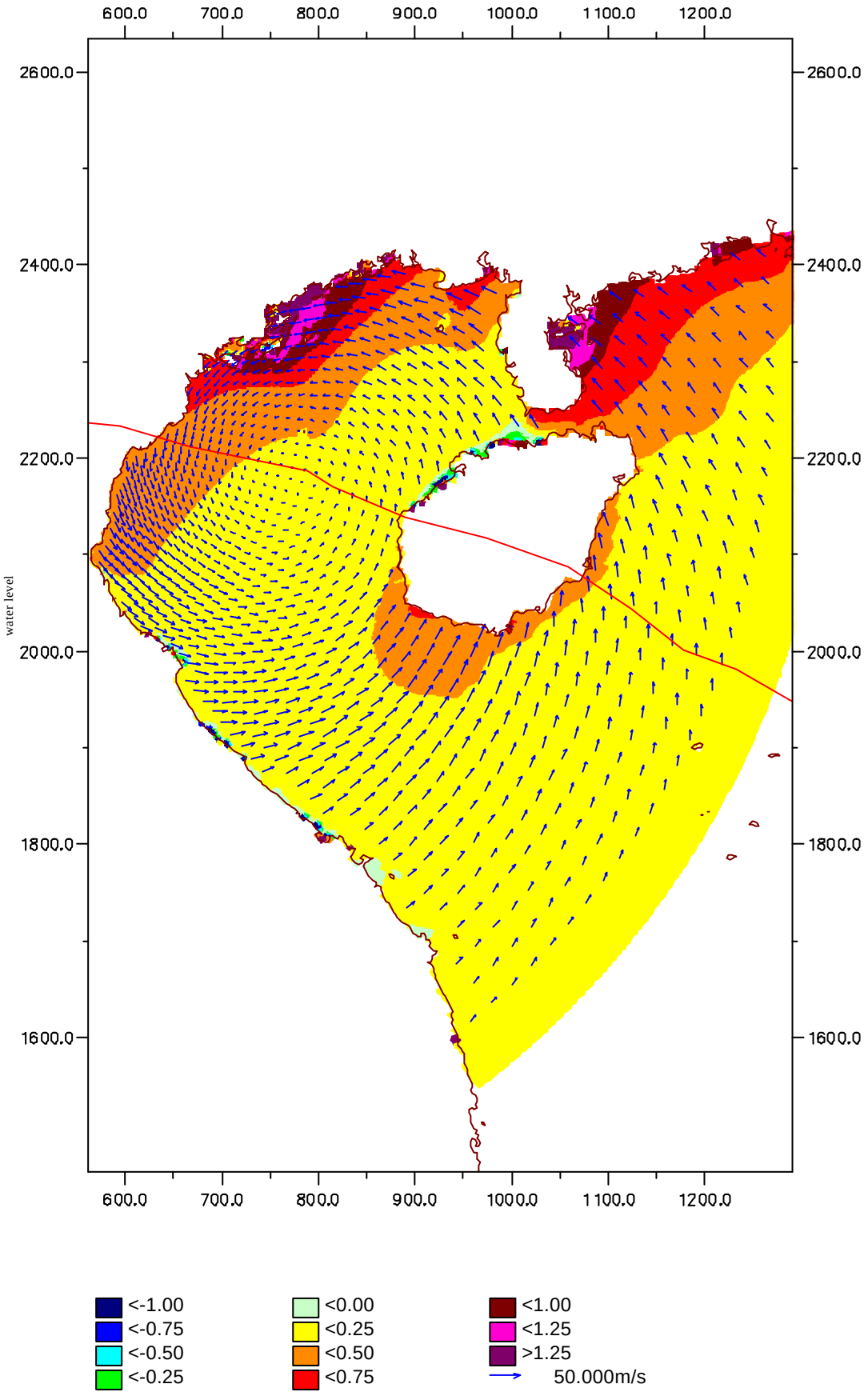

Figure B-2. Wind field and water level during typhoon Frankie at 18h:00 23/07/1996

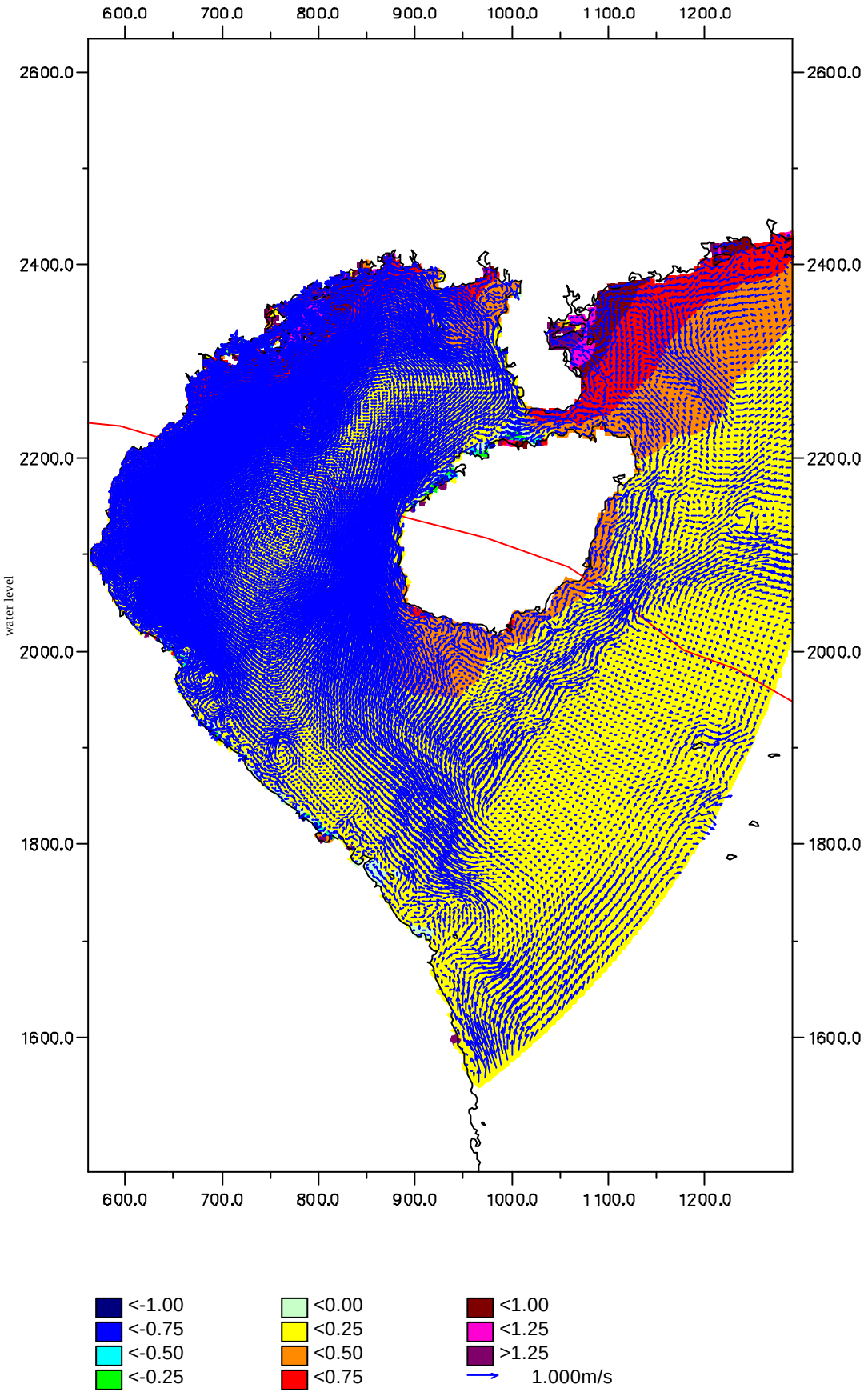

Figure B-3. Water level and flow velocity field during typhoon Frankie at 18h:00 23/07/1996

Figure B-4. Model calibration for tidal forcing - Water level at Bach Long Vi

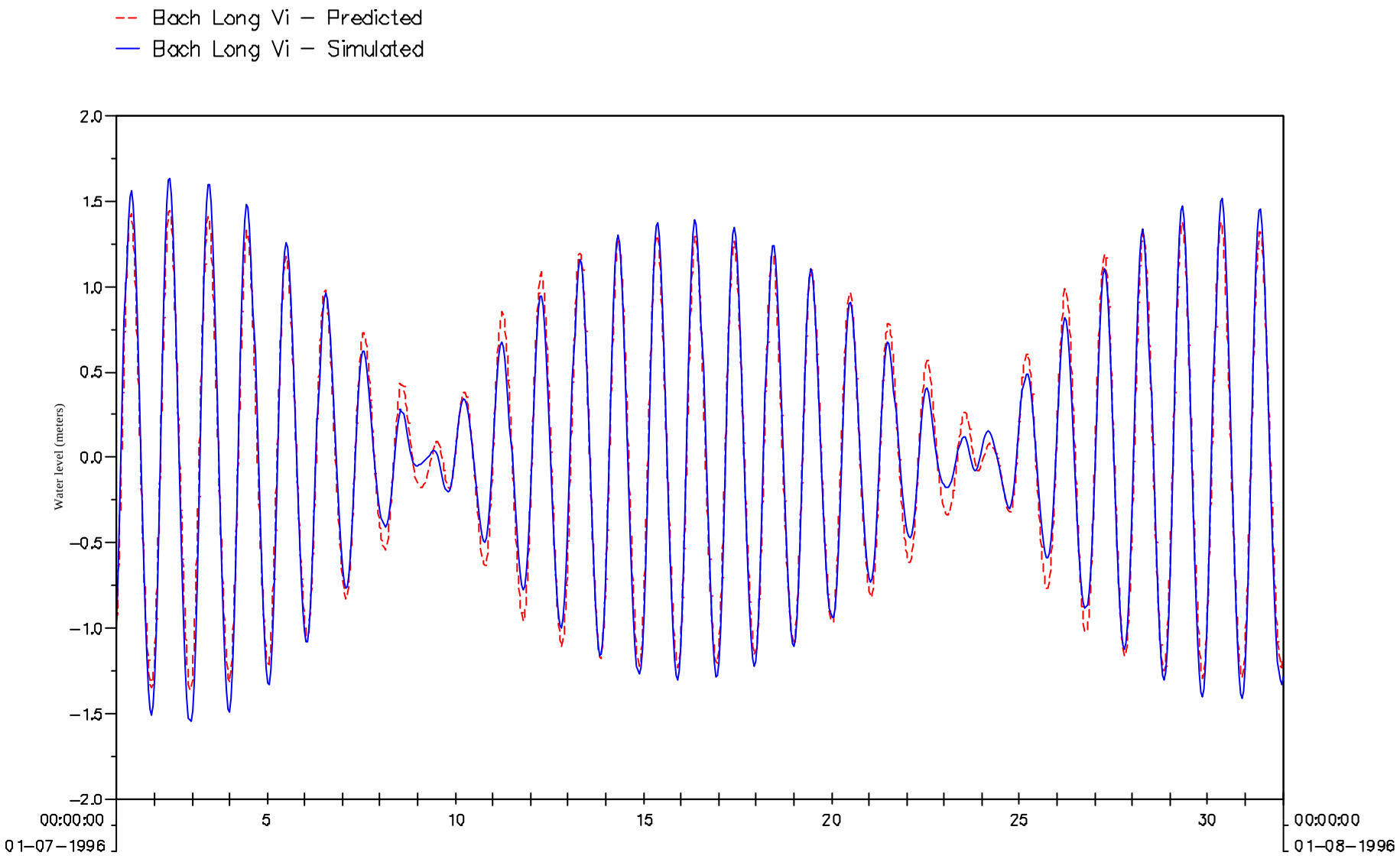

Figure B-5. Model calibration for tidal forcing - Water level at Do Son

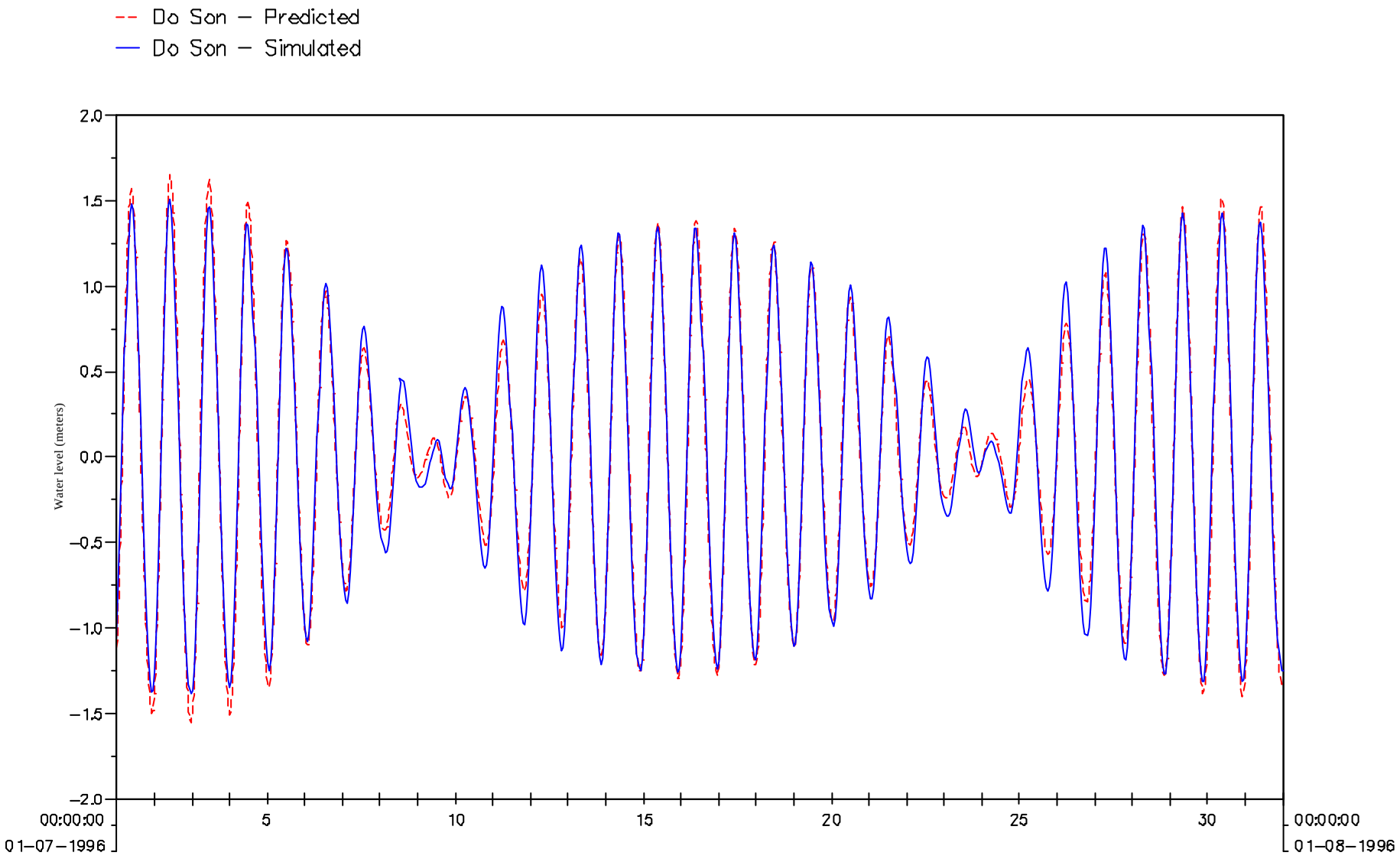

Figure B-6. Model calibration for tidal forcing - Water level at Hon Ne

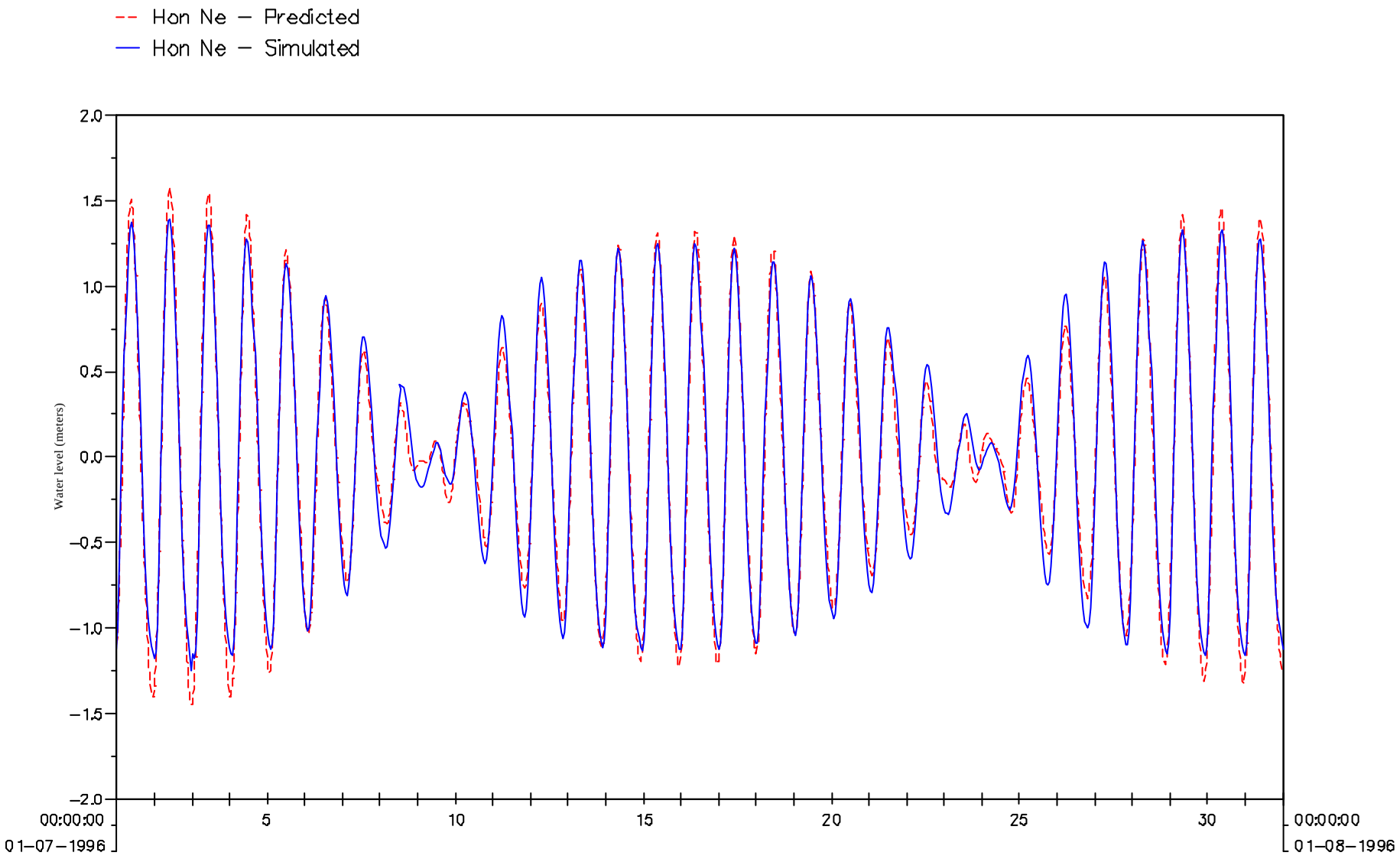

Figure B-7. Model calibration for tidal forcing - Water level at Hon Me

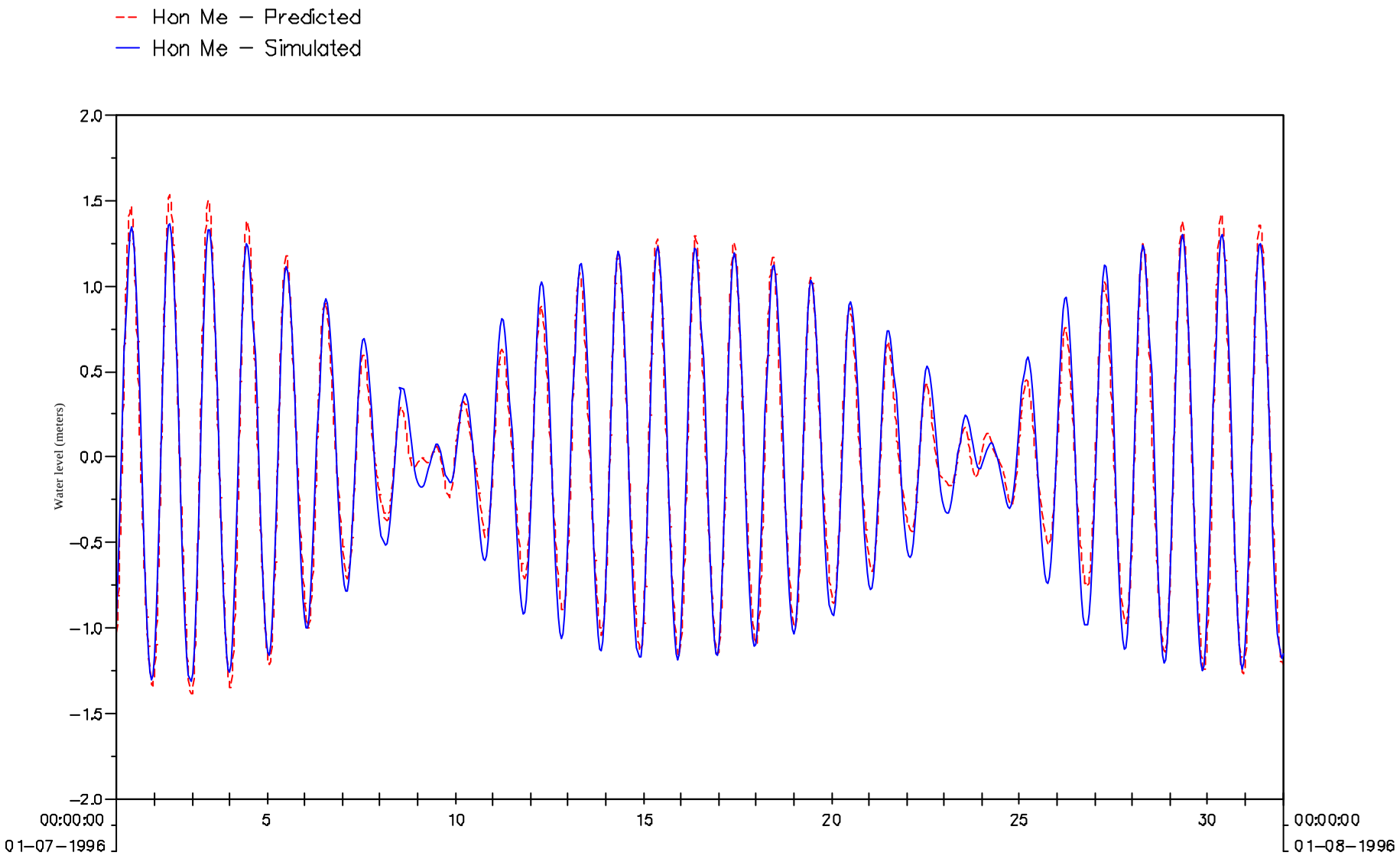

Figure B-8. Model calibration for tidal forcing - Water level at Hon Ngu

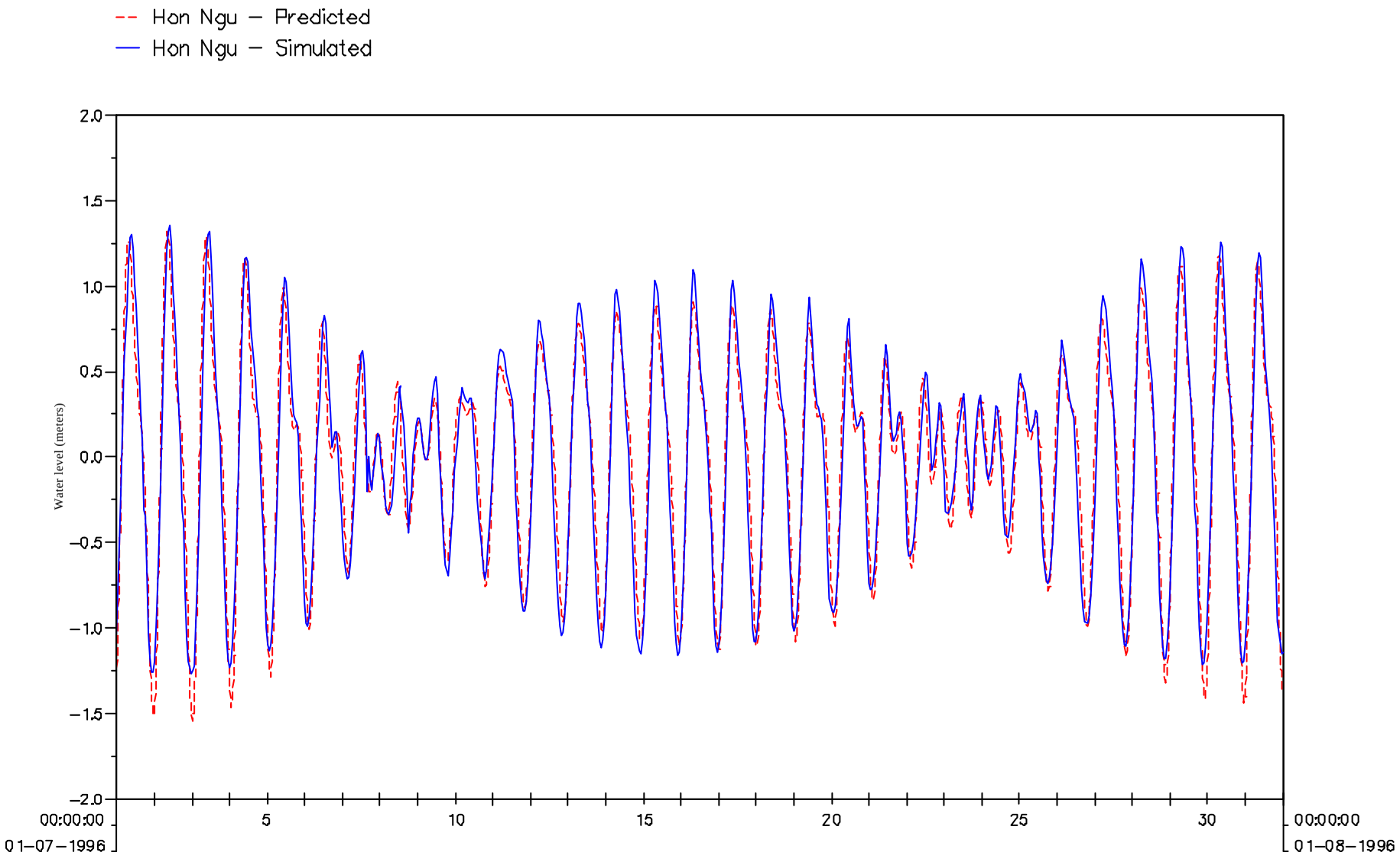

Figure B-9. Model calibration for tidal forcing - Water level at Cua Tung

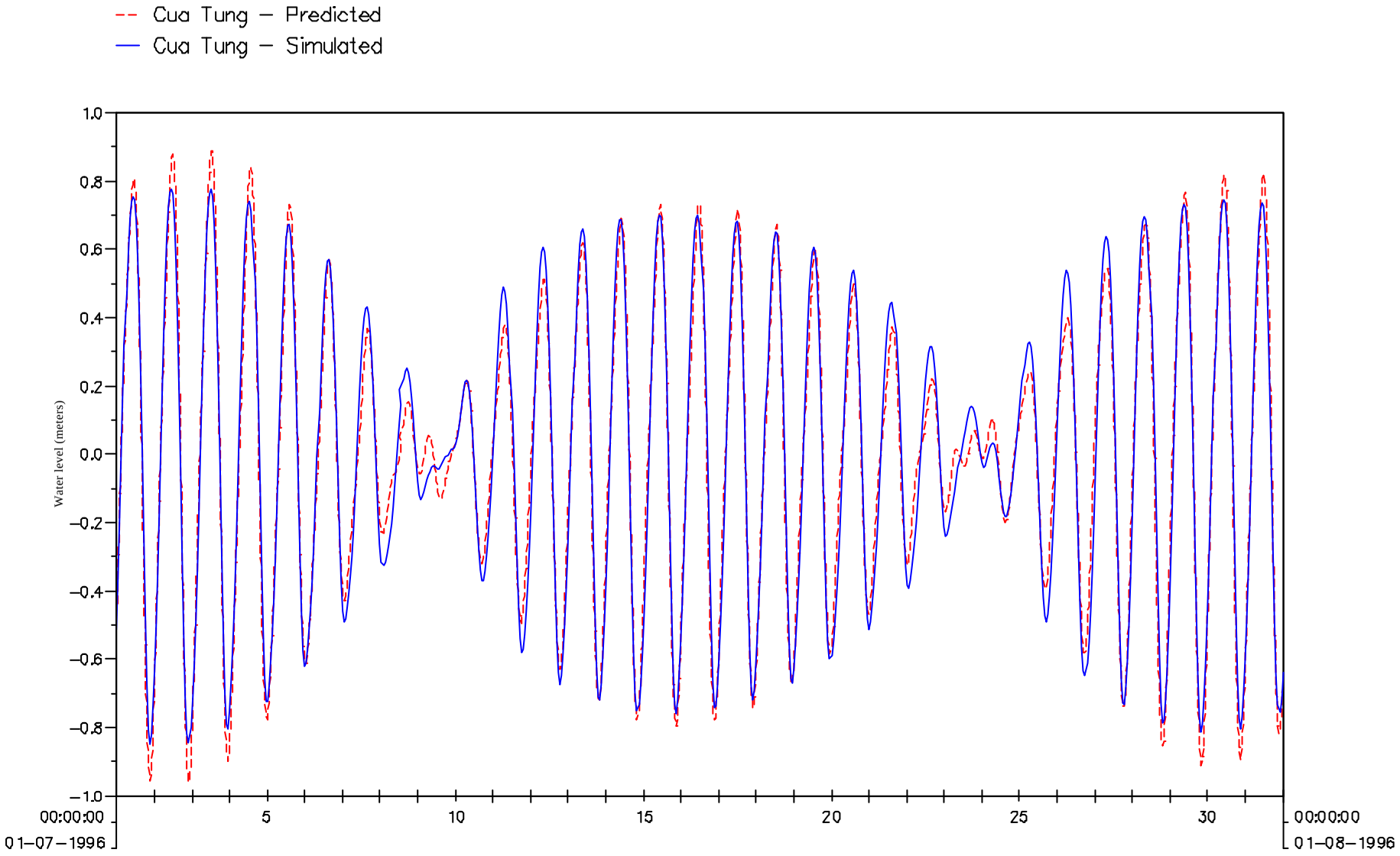

Figure B-10. Model calibration for tidal forcing - Water level at Da Nang

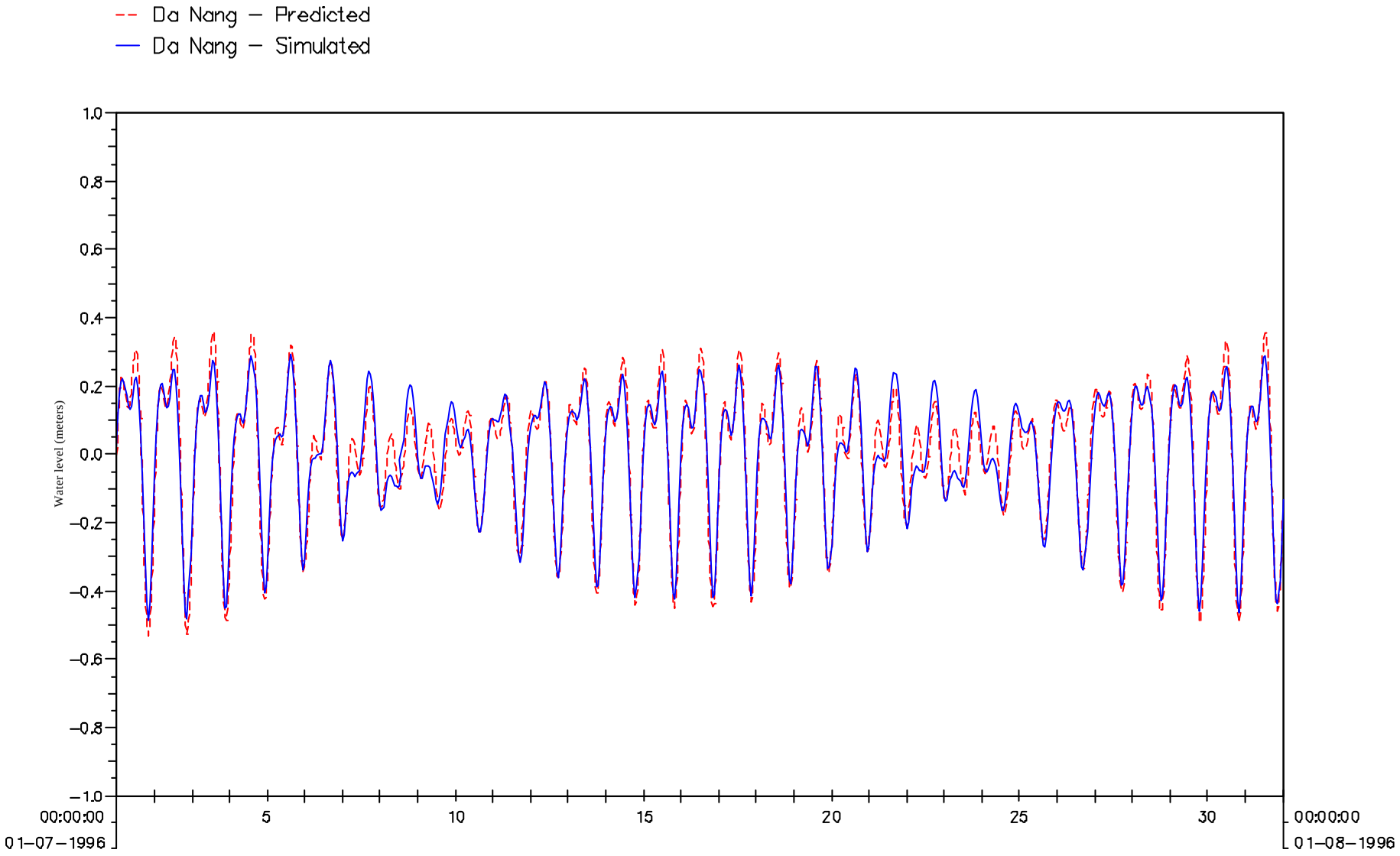

Figure B-11. Model calibration for tidal forcing - Water level at Hoi An

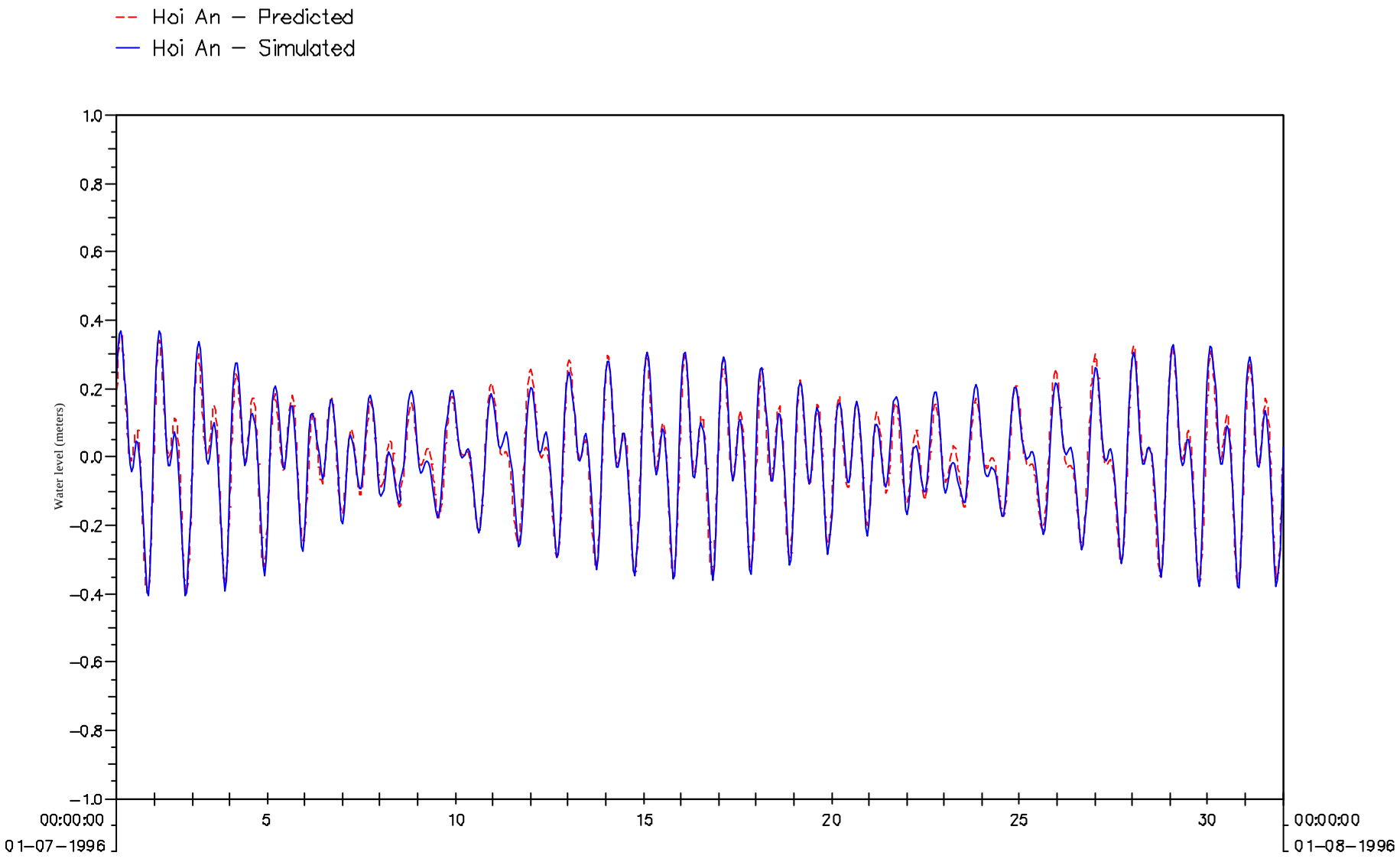

Figure B-12. Model calibration for tidal forcing - Water level at Dung Quat

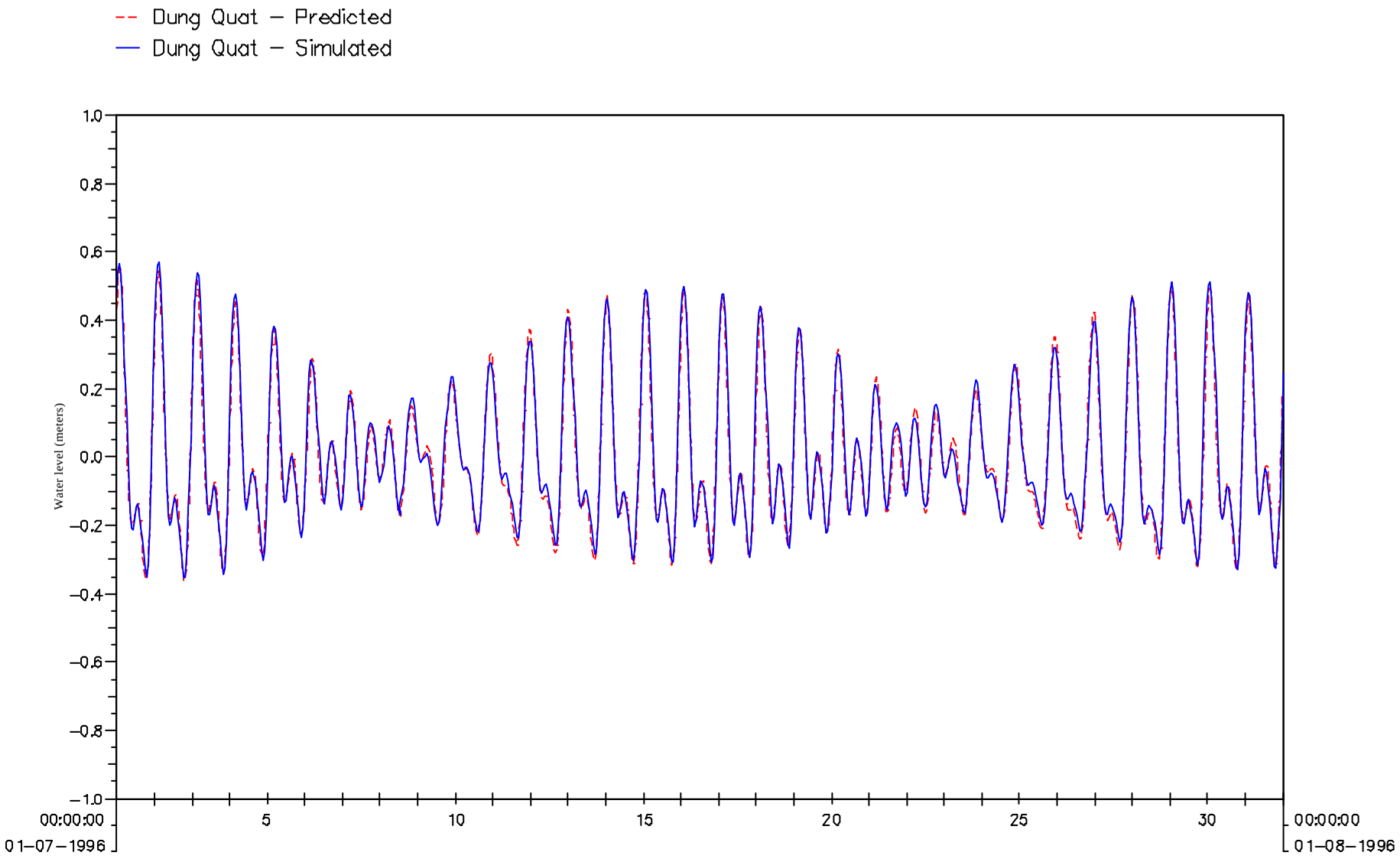

Figure B-13. Model calibration for tidal forcing - Water level at Duc Pho

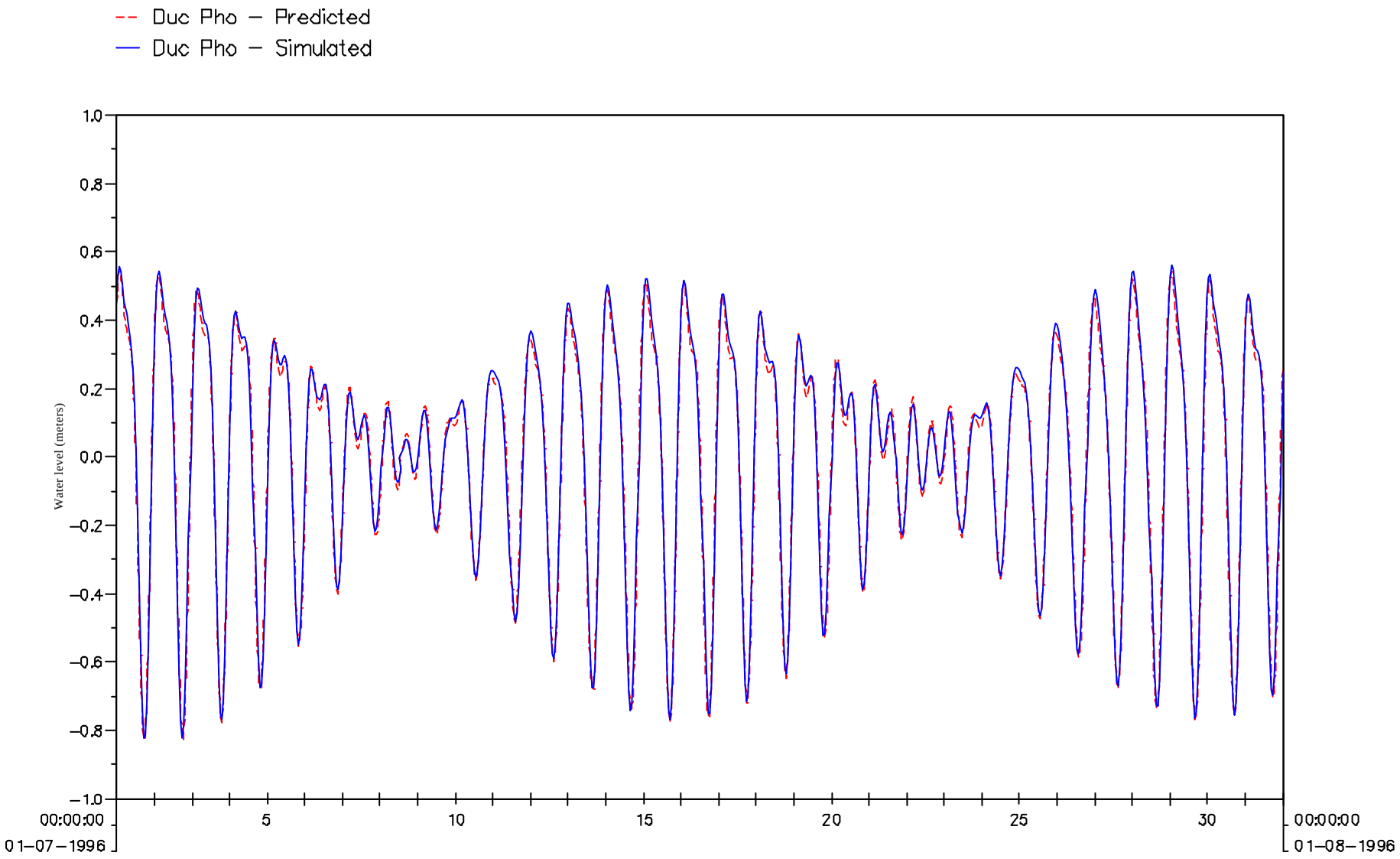

Figure B-14. Model calibration for tidal forcing - Water level at Tam Quan

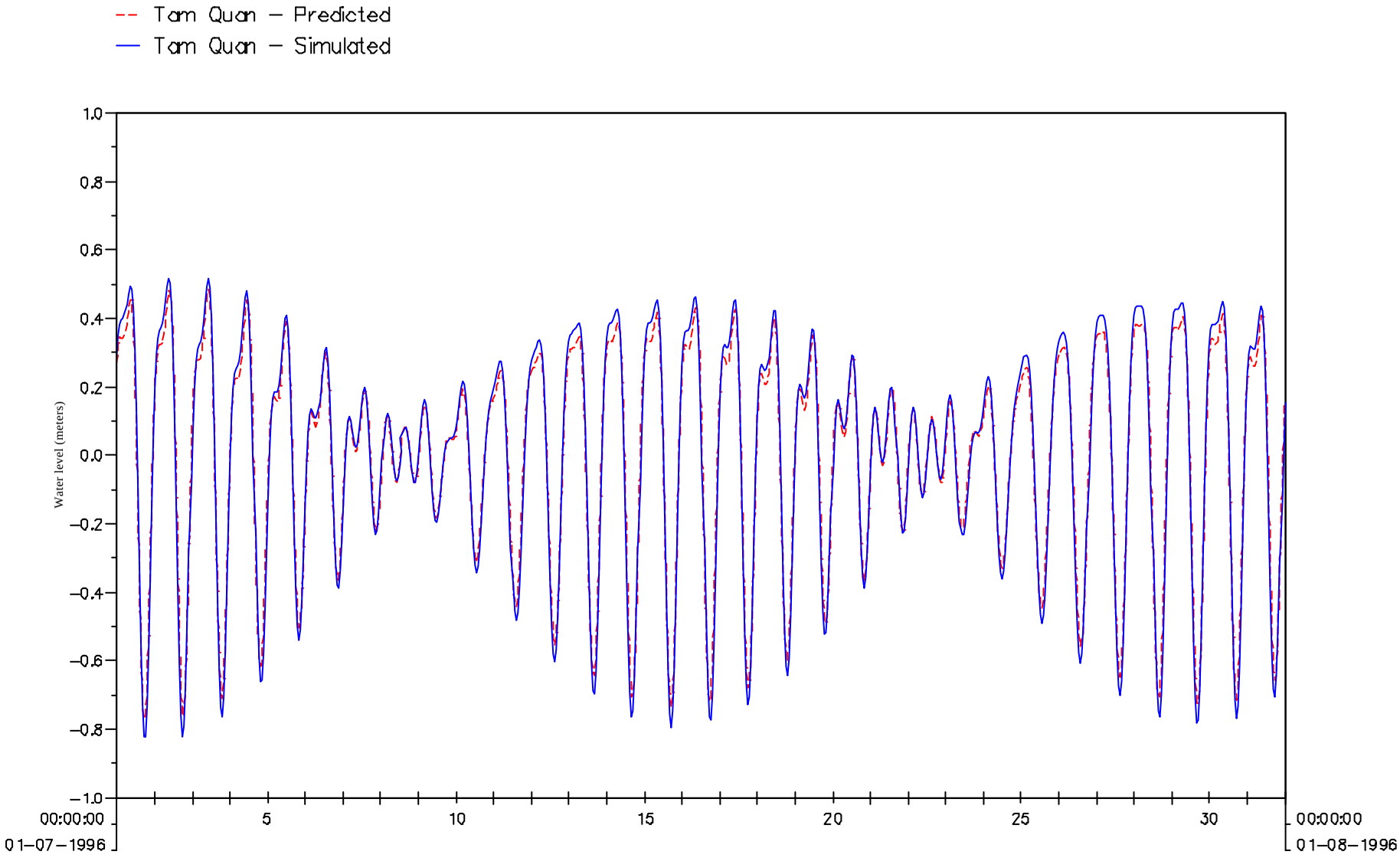

Figure B-15. Model calibration for tidal forcing - Water level at Paracel Islands

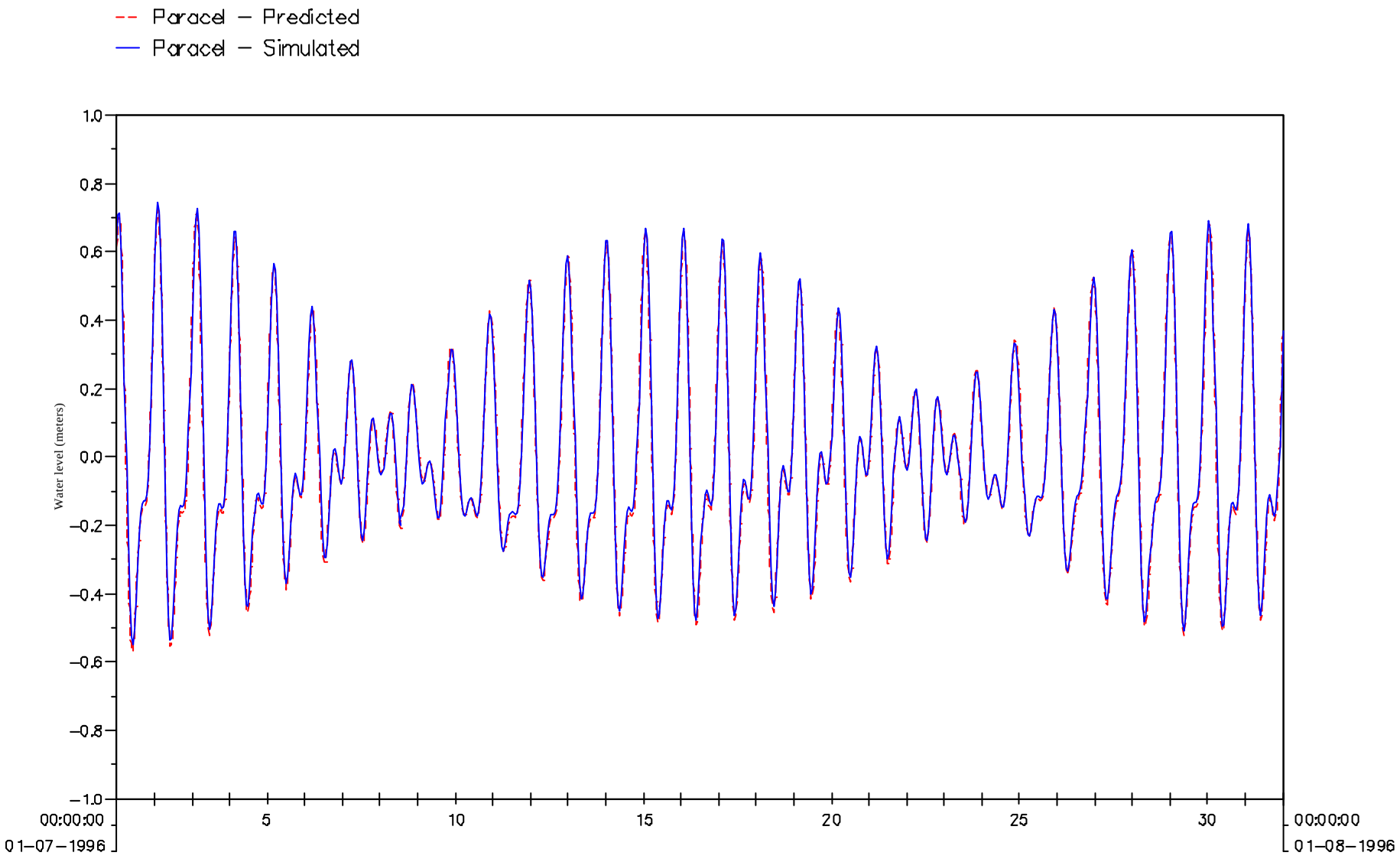

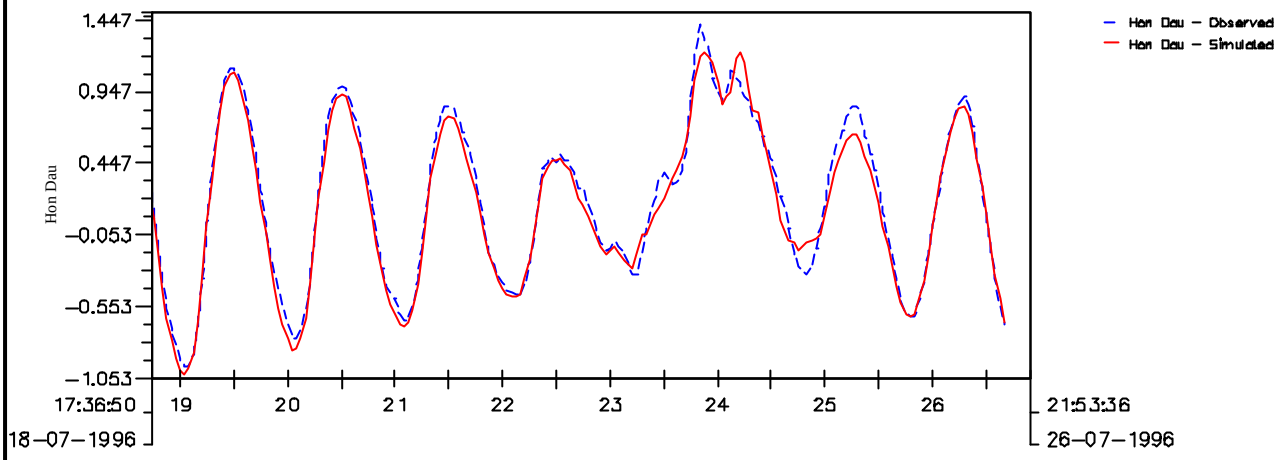

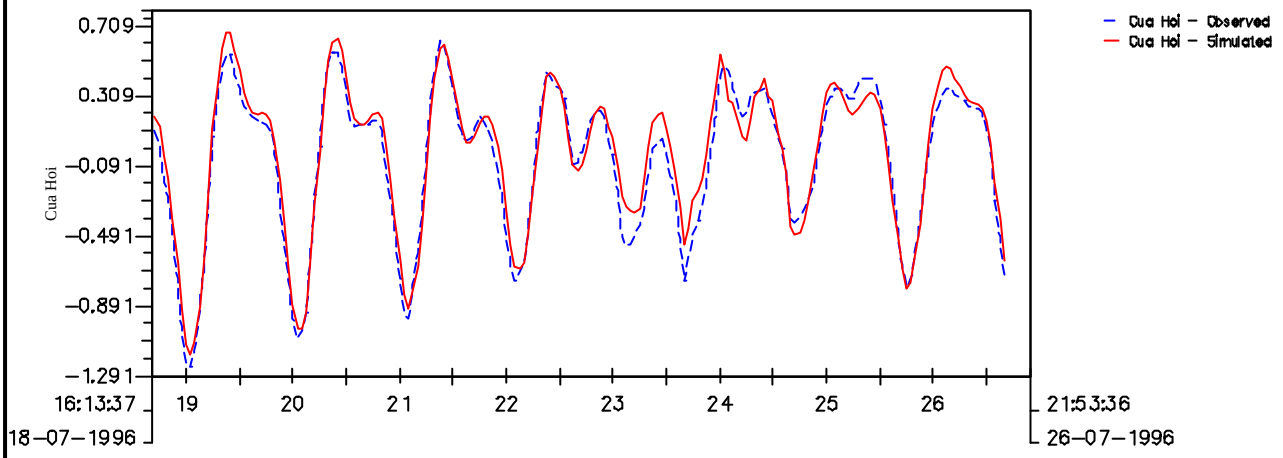

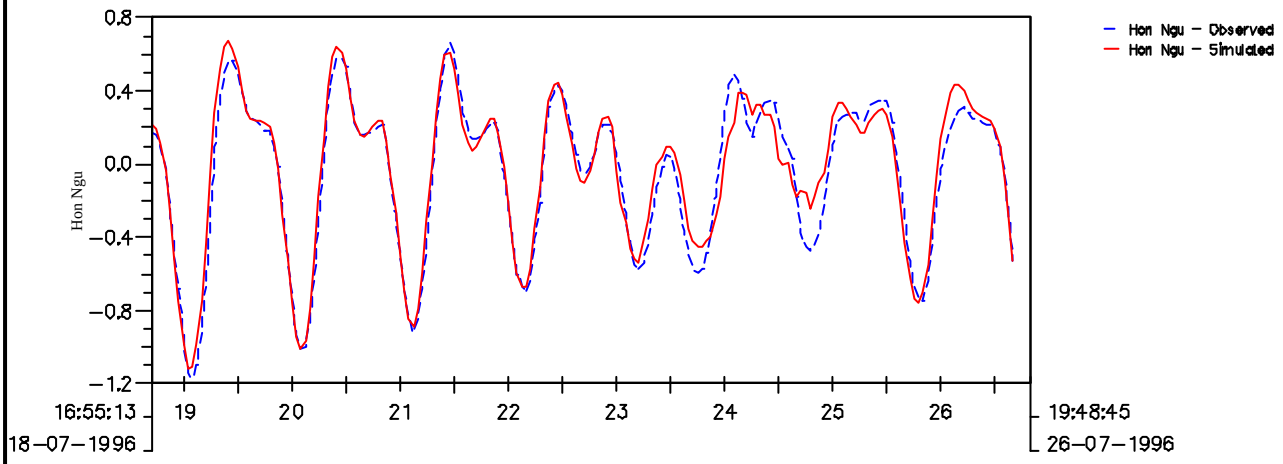

Figure B-16. Water levels at Hon Dau, Cua Hoi and Hon Ngu during typhoon Frankie (1996)

WL | DELFT HYDRAULICS

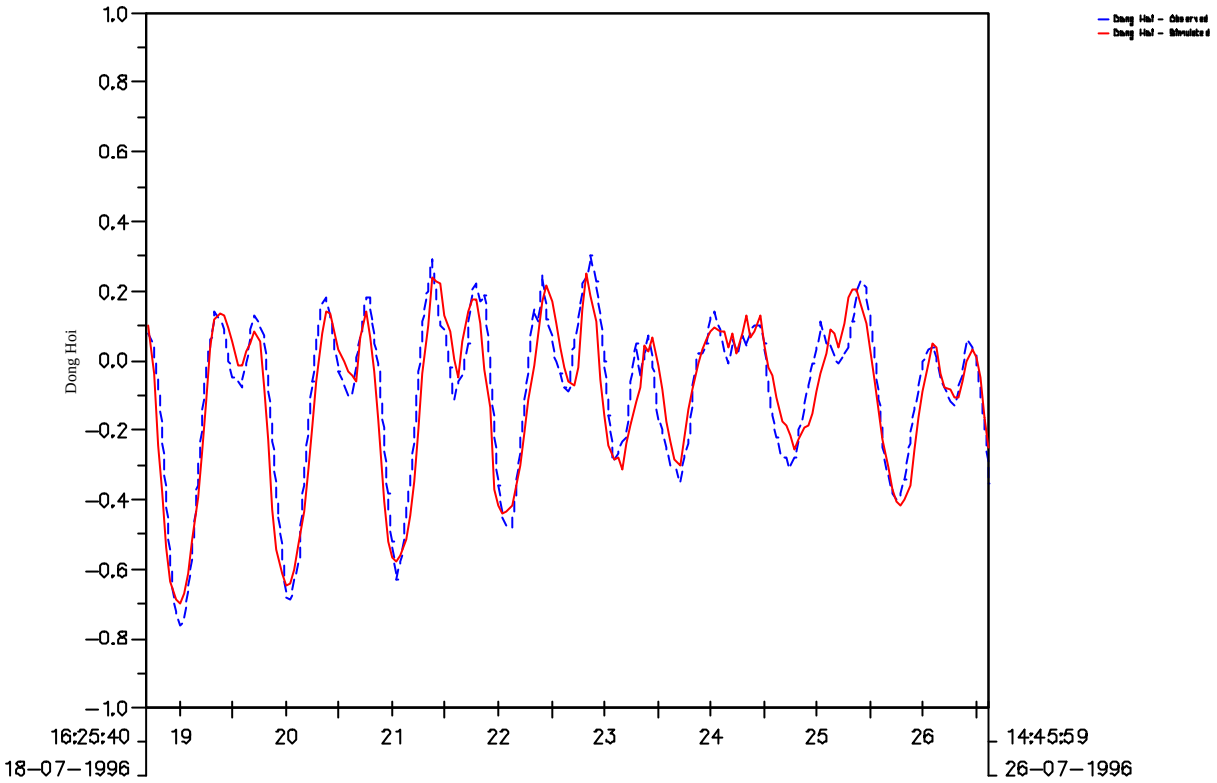

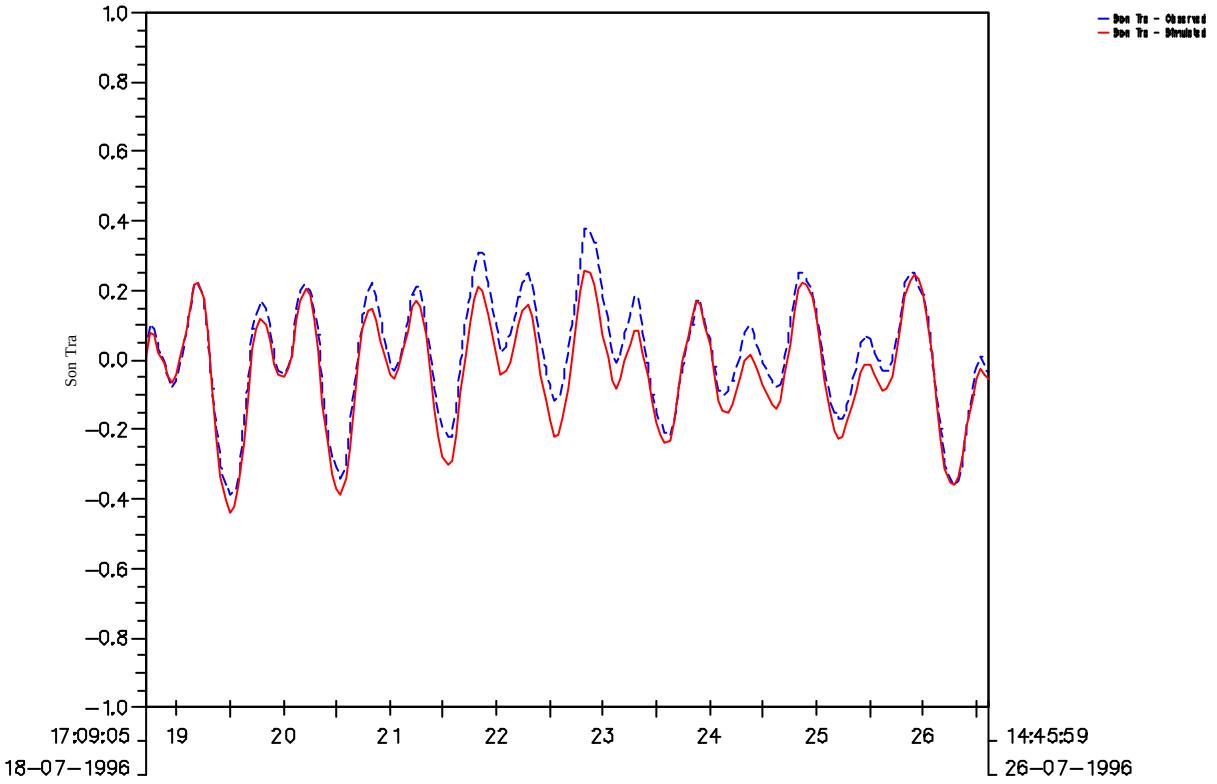

Figure B−17. Water level at Dong Hoi and Son Tra during typhoon Frankie (1996)

WL | DELFT HYDRAULICS

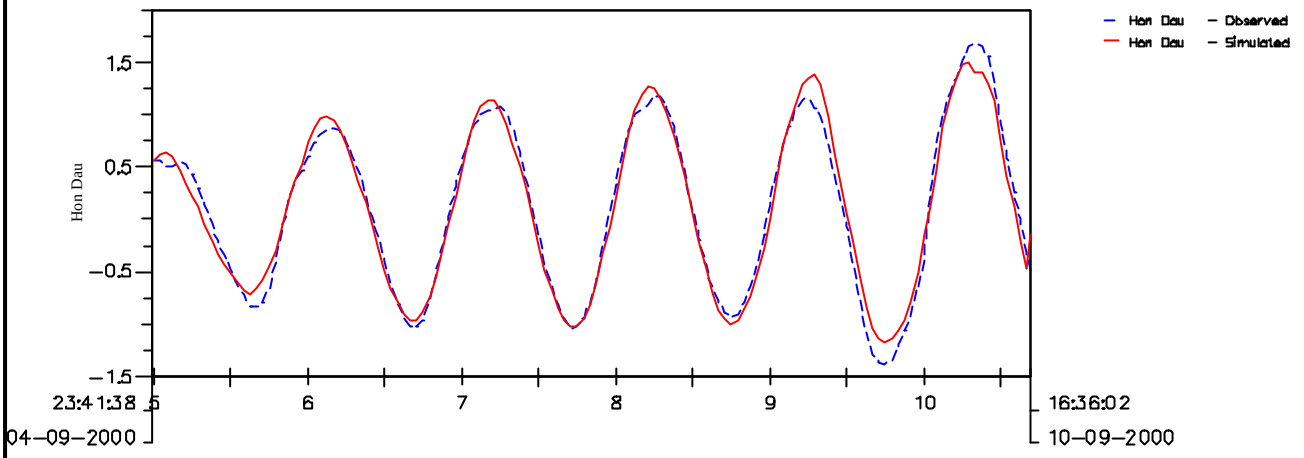

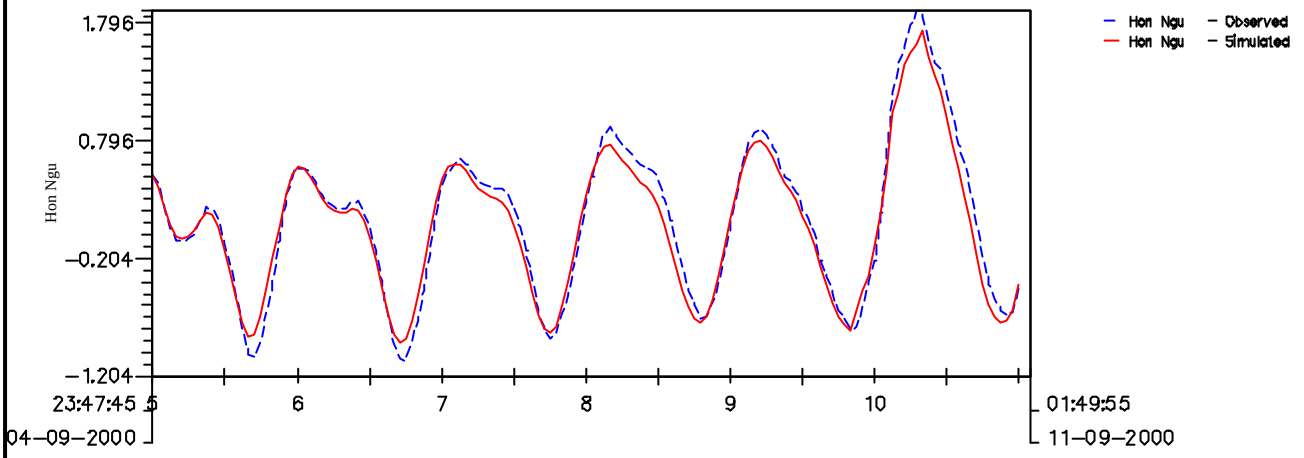

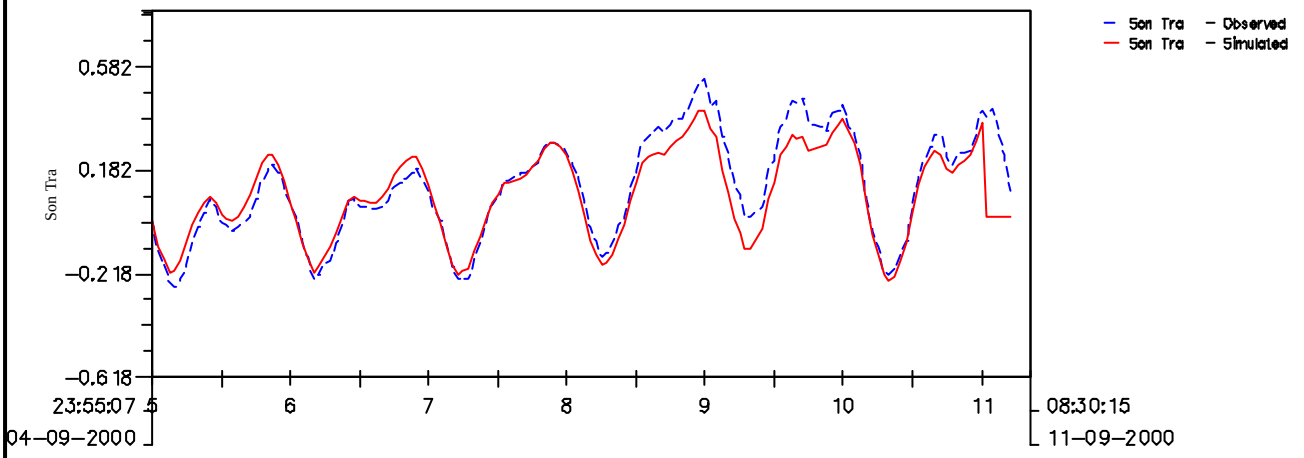

Figure B-18. Water levels at Hon Dau, Hon Ngu and Son Tra during typhoon Wukong (2000)

WL | DELFT HYDRAULICS

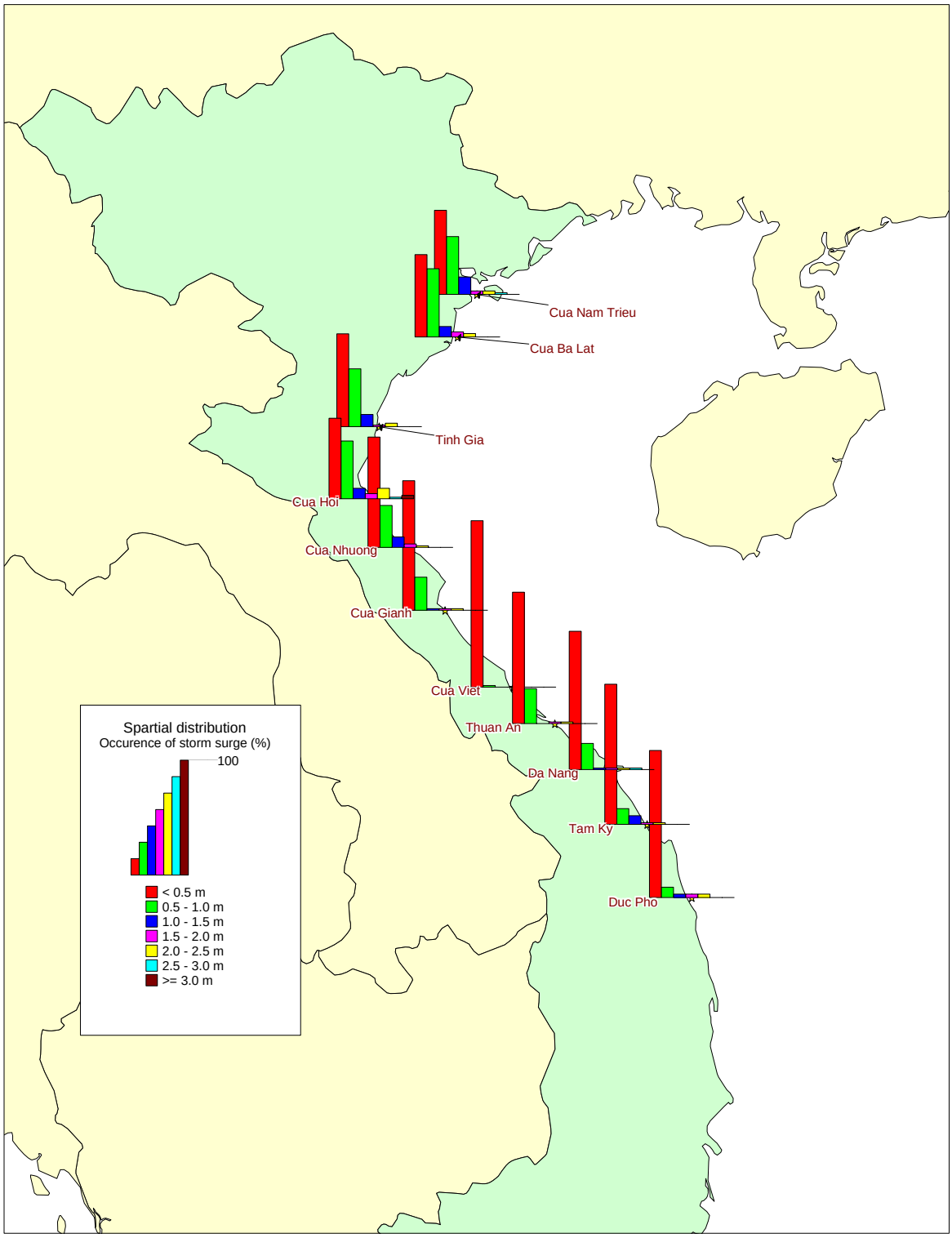

Figure C-0. Distribution of storm surge along the coast (illustration of Table 5-1)

Table C-1. Log normal distribution of storm surge

	Cua Nam Trieu	Hon Dau	Do Son	Diem Dien	Cua Ba Lat	Yen Dinh	Hoang Tan	Tinh Gia	Cau Giat	Dien Chau	Thanh Hoa	Hon Nieu	Cua Hoi	Cua Sot	Cua Nhuong	Cua Khau	Vung Chua	Dong Hoi	Da Nang	Dung Quat	Duc Pho	Tam Quan	Cua Gianh	Nhat Le	Cua Tung	Cua Viet	Thuan An	Chan May	Hoi An	Tam Ky
X	1.01	0.92	0.96	1.03	0.95	0.71	0.82	0.84	0.84	0.92	0.79	1.10	1.22	0.94	0.77	0.81	0.63	0.60	0.61	0.61	0.25	0.21	0.58	0.60	0.61	0.63	0.66	0.56	0.62	0.48
Sx	0.67	0.58	0.62	0.72	0.63	0.34	0.50	0.52	0.51	0.60	0.47	0.85	1.01	0.75	0.55	0.64	0.43	0.42	0.58	0.71	0.26	0.10	0.39	0.42	0.52	0.59	0.52	0.44	0.66	0.50
Cv	0.66	0.63	0.64	0.70	0.66	0.49	0.61	0.62	0.61	0.65	0.59	0.77	0.83	0.80	0.71	0.79	0.69	0.70	0.95	1.15	1.04	0.49	0.67	0.70	0.86	0.94	0.79	0.78	1.07	1.04
Y	-0.17	-0.25	-0.21	-0.17	-0.24	-0.46	-0.36	-0.34	-0.33	-0.26	-0.38	-0.14	-0.06	-0.31	-0.47	-0.46	-0.66	-0.71	-0.81	-0.91	-1.74	-1.67	-0.72	-0.71	-0.77	-0.79	-0.65	-0.82	-0.86	-1.10
Sy	0.60	0.57	0.59	0.63	0.60	0.46	0.56	0.57	0.56	0.59	0.55	0.68	0.72	0.70	0.64	0.70	0.62	0.64	0.80	0.92	0.85	0.47	0.61	0.63	0.74	0.80	0.70	0.69	0.87	0.86
0.01%	8.00	6.62	7.21	8.82	7.42	3.53	5.69	5.88	5.83	7.04	5.25	11.04	13.90	9.95	6.83	8.43	5.21	5.22	8.72	12.24	4.21	1.07	4.73	5.20	7.34	8.82	6.90	5.75	10.85	8.03
0.10%	5.46	4.61	4.98	5.93	5.08	2.64	3.99	4.11	4.09	4.84	3.72	7.18	8.81	6.40	4.56	5.44	3.52	3.50	5.28	6.87	2.46	0.79	3.22	3.49	4.60	5.34	4.46	3.72	6.26	4.69
0.20%	4.81	4.08	4.39	5.19	4.47	2.40	3.54	3.65	3.63	4.27	3.31	6.21	7.55	5.52	3.98	4.69	3.09	3.06	4.45	5.65	2.05	0.72	2.83	3.05	3.92	4.51	3.85	3.21	5.21	3.91
0.33%	4.36	3.72	3.99	4.68	4.06	2.22	3.24	3.33	3.31	3.88	3.03	5.56	6.72	4.93	3.59	4.19	2.79	2.76	3.91	4.87	1.79	0.67	2.56	2.75	3.48	3.97	3.44	2.87	4.52	3.40
0.50%	4.00	3.43	3.68	4.28	3.73	2.08	2.99	3.07	3.06	3.57	2.81	5.05	6.07	4.46	3.28	3.80	2.56	2.52	3.50	4.28	1.59	0.62	2.35	2.52	3.13	3.55	3.12	2.61	4.00	3.02
1.00%	3.44	2.97	3.17	3.66	3.21	1.86	2.60	2.67	2.66	3.07	2.45	4.26	5.06	3.75	2.79	3.20	2.19	2.15	2.87	3.40	1.28	0.56	2.02	2.15	2.60	2.91	2.62	2.20	3.21	2.44
1.50%	3.13	2.72	2.89	3.32	2.92	1.73	2.38	2.44	2.44	2.80	2.25	3.83	4.52	3.36	2.52	2.87	1.99	1.95	2.53	2.95	1.12	0.52	1.83	1.95	2.32	2.57	2.35	1.97	2.80	2.13
2.00%	2.92	2.54	2.70	3.08	2.72	1.64	2.23	2.28	2.28	2.61	2.11	3.53	4.16	3.10	2.34	2.64	1.85	1.81	2.30	2.65	1.02	0.49	1.71	1.81	2.13	2.34	2.17	1.82	2.53	1.93
3.00%	2.63	2.30	2.44	2.76	2.45	1.51	2.02	2.07	2.07	2.36	1.92	3.14	3.67	2.74	2.10	2.34	1.66	1.62	2.01	2.26	0.88	0.45	1.53	1.62	1.87	2.04	1.92	1.61	2.18	1.67
5.00%	2.28	2.01	2.12	2.38	2.13	1.36	1.77	1.81	1.81	2.05	1.68	2.67	3.09	2.32	1.80	1.99	1.43	1.40	1.66	1.82	0.72	0.40	1.33	1.40	1.57	1.69	1.63	1.37	1.77	1.36
10.00%	1.83	1.63	1.72	1.89	1.71	1.15	1.44	1.47	1.48	1.65	1.38	2.08	2.38	1.80	1.43	1.54	1.14	1.11	1.24	1.30	0.52	0.34	1.06	1.11	1.20	1.26	1.27	1.07	1.29	1.00
20.00%	1.40	1.27	1.32	1.43	1.31	0.94	1.13	1.15	1.15	1.27	1.08	1.54	1.73	1.32	1.08	1.14	0.87	0.84	0.87	0.87	0.36	0.28	0.81	0.84	0.86	0.89	0.93	0.79	0.88	0.68
25.00%	1.27	1.15	1.20	1.29	1.19	0.87	1.02	1.04	1.05	1.15	0.99	1.37	1.53	1.18	0.97	1.01	0.78	0.75	0.77	0.75	0.31	0.26	0.73	0.75	0.76	0.78	0.83	0.70	0.76	0.59
30.00%	1.16	1.05	1.10	1.17	1.08	0.81	0.94	0.96	0.96	1.05	0.91	1.24	1.37	1.06	0.88	0.91	0.71	0.69	0.68	0.65	0.27	0.24	0.67	0.69	0.68	0.69	0.75	0.63	0.67	0.52
40.00%	0.98	0.90	0.94	0.99	0.92	0.71	0.81	0.82	0.83	0.90	0.78	1.03	1.13	0.88	0.74	0.75	0.60	0.58	0.55	0.51	0.22	0.21	0.57	0.58	0.56	0.56	0.62	0.52	0.53	0.41
50.00%	0.84	0.78	0.81	0.84	0.79	0.63	0.70	0.71	0.72	0.77	0.68	0.87	0.94	0.73	0.63	0.63	0.52	0.49	0.45	0.40	0.18	0.19	0.48	0.49	0.46	0.46	0.52	0.44	0.42	0.33
60.00%	0.72	0.67	0.70	0.72	0.68	0.56	0.61	0.62	0.62	0.66	0.59	0.73	0.78	0.61	0.53	0.53	0.44	0.42	0.36	0.32	0.14	0.17	0.42	0.42	0.38	0.37	0.44	0.37	0.34	0.27
70.00%	0.61	0.58	0.59	0.60	0.58	0.50	0.52	0.53	0.53	0.56	0.51	0.61	0.64	0.51	0.45	0.44	0.37	0.35	0.29	0.25	0.11	0.15	0.35	0.35	0.31	0.30	0.36	0.31	0.27	0.21
75.00%	0.56	0.53	0.54	0.55	0.53	0.46	0.48	0.48	0.49	0.52	0.47	0.55	0.58	0.46	0.41	0.40	0.34	0.32	0.26	0.22	0.10	0.14	0.32	0.32	0.28	0.27	0.33	0.28	0.23	0.19
80.00%	0.51	0.48	0.49	0.49	0.48	0.43	0.44	0.44	0.45	0.47	0.43	0.49	0.51	0.41	0.36	0.35	0.31	0.29	0.23	0.19	0.09	0.13	0.29	0.29	0.25	0.23	0.29	0.25	0.20	0.16
85.00%	0.45	0.43	0.44	0.44	0.42	0.39	0.39	0.39	0.40	0.42	0.39	0.43	0.44	0.35	0.32	0.31	0.27	0.25	0.20	0.15	0.07	0.12	0.26	0.25	0.21	0.20	0.25	0.22	0.17	0.14
90.00%	0.39	0.37	0.38	0.37	0.36	0.35	0.34	0.34	0.35	0.36	0.34	0.36	0.37	0.30	0.27	0.26	0.23	0.22	0.16	0.12	0.06	0.10	0.22	0.22	0.18	0.16	0.21	0.18	0.14	0.11
95.00%	0.31	0.30	0.31	0.30	0.29	0.30	0.28	0.28	0.28	0.29	0.28	0.28	0.28	0.23	0.22	0.20	0.19	0.17	0.12	0.09	0.04	0.09	0.18	0.17	0.14	0.12	0.17	0.14	0.10	0.08
97.00%	0.27	0.26	0.27	0.26	0.25	0.27	0.24	0.24	0.25	0.25	0.24	0.24	0.24	0.20	0.19	0.17	0.16	0.15	0.10	0.07	0.04	0.08	0.15	0.15	0.11	0.10	0.14	0.12	0.08	0.07
99.00%	0.21	0.20	0.21	0.19	0.19	0.22	0.19	0.19	0.19	0.19	0.19	0.18	0.17	0.14	0.14	0.13	0.12	0.11	0.07	0.05	0.02	0.06	0.12	0.11	0.08	0.07	0.10	0.09	0.06	0.05
99.90%	0.13	0.13	0.13	0.12	0.12	0.15	0.12	0.12	0.13	0.12	0.13	0.10	0.10	0.08	0.09	0.07	0.08	0.07	0.04	0.02	0.01	0.04	0.07	0.07	0.05	0.04	0.06	0.05	0.03	0.02
99.99%	0.09	0.09	0.09	0.08	0.08	0.11	0.09	0.09	0.09	0.08	0.09	0.07	0.06	0.05	0.06	0.05	0.05	0.05	0.02	0.01	0.01	0.03	0.05	0.05	0.03	0.02	0.04	0.03	0.02	0.01

Table C-2. Log-normal distribution of maximum water level

	Cua Nam Trieu	Hon Dau	Do Son	Diem Dien	Cua Ba Lat	Yen Dinh	Hoang Tan	Tinh Gia	Cau Giat	Dien Chau	Thanh Hoa	Hon Nieu	Cua Hoi	Cua Sot	Cua Nhuong	Cua Khau	Vung Chua	Dong Hoi	Da Nang	Dung Quat	Duc Pho	Tam Quan	Cua Gianh	Nhat Le	Cua Tung	Cua Viet	Thuan An	Chan May	Hoi An	Tam Ky
X	1.60	1.51	1.53	1.59	1.53	1.35	1.44	1.44	1.39	1.46	1.36	1.57	1.67	1.44	1.33	1.32	1.10	1.09	0.67	0.83	0.66	0.61	1.09	1.09	0.91	0.92	0.80	0.63	0.73	0.71
Sx	0.58	0.45	0.47	0.59	0.48	0.31	0.45	0.46	0.45	0.55	0.41	0.71	0.86	0.62	0.45	0.52	0.33	0.38	0.48	0.57	0.29	0.17	0.34	0.37	0.42	0.48	0.41	0.31	0.55	0.37
Cv	0.36	0.29	0.31	0.37	0.32	0.23	0.31	0.32	0.32	0.37	0.30	0.45	0.52	0.43	0.34	0.39	0.30	0.35	0.72	0.68	0.44	0.27	0.31	0.34	0.46	0.52	0.51	0.50	0.75	0.53
Y	0.41	0.37	0.38	0.40	0.38	0.28	0.32	0.32	0.28	0.31	0.26	0.36	0.39	0.28	0.23	0.21	0.06	0.03	-0.61	-0.38	-0.50	-0.53	0.03	0.03	-0.19	-0.21	-0.34	-0.57	-0.54	-0.47
Sy	0.35	0.29	0.30	0.36	0.31	0.23	0.31	0.31	0.31	0.36	0.30	0.43	0.49	0.42	0.33	0.38	0.29	0.34	0.64	0.62	0.42	0.27	0.31	0.33	0.44	0.49	0.48	0.47	0.67	0.50
0.01%	5.51	4.24	4.49	5.68	4.61	3.05	4.29	4.37	4.27	5.26	3.91	7.09	9.02	6.19	4.28	5.02	3.11	3.67	5.91	6.83	2.93	1.60	3.23	3.58	4.27	5.04	4.23	3.22	7.09	3.95
0.10%	4.42	3.53	3.71	4.53	3.80	2.65	3.54	3.59	3.51	4.19	3.25	5.41	6.65	4.76	3.48	3.96	2.59	2.96	3.94	4.63	2.24	1.35	2.67	2.90	3.23	3.70	3.13	2.40	4.65	2.89
0.20%	4.11	3.32	3.48	4.20	3.56	2.53	3.32	3.36	3.28	3.88	3.05	4.93	6.00	4.36	3.24	3.65	2.43	2.75	3.44	4.06	2.05	1.27	2.50	2.70	2.95	3.34	2.82	2.17	4.03	2.60
0.33%	3.88	3.17	3.32	3.96	3.38	2.44	3.16	3.19	3.12	3.66	2.91	4.60	5.54	4.08	3.07	3.44	2.32	2.60	3.10	3.67	1.91	1.22	2.38	2.56	2.74	3.08	2.61	2.01	3.62	2.40
0.50%	3.70	3.05	3.18	3.76	3.24	2.36	3.02	3.06	2.98	3.47	2.79	4.33	5.18	3.85	2.93	3.26	2.23	2.48	2.83	3.36	1.80	1.18	2.28	2.44	2.58	2.88	2.44	1.88	3.29	2.24
1.00%	3.39	2.83	2.95	3.44	3.00	2.23	2.80	2.83	2.76	3.17	2.59	3.89	4.59	3.47	2.70	2.97	2.07	2.28	2.41	2.88	1.62	1.10	2.11	2.24	2.31	2.54	2.17	1.68	2.78	1.98
1.50%	3.21	2.71	2.81	3.25	2.86	2.15	2.67	2.70	2.62	3.00	2.47	3.64	4.25	3.25	2.57	2.80	1.98	2.16	2.18	2.62	1.52	1.05	2.01	2.13	2.16	2.36	2.01	1.56	2.51	1.83
2.00%	3.08	2.62	2.72	3.12	2.76	2.10	2.58	2.60	2.53	2.88	2.39	3.46	4.02	3.09	2.47	2.68	1.92	2.07	2.03	2.43	1.45	1.02	1.94	2.05	2.05	2.23	1.90	1.47	2.32	1.73
3.00%	2.90	2.49	2.58	2.93	2.61	2.02	2.45	2.46	2.40	2.70	2.27	3.21	3.69	2.88	2.33	2.51	1.82	1.95	1.81	2.19	1.34	0.98	1.84	1.93	1.90	2.04	1.75	1.36	2.06	1.59
5.00%	2.67	2.33	2.40	2.69	2.43	1.91	2.28	2.29	2.22	2.48	2.12	2.90	3.29	2.61	2.16	2.29	1.70	1.80	1.56	1.89	1.22	0.92	1.71	1.79	1.71	1.82	1.56	1.22	1.76	1.41
10.00%	2.36	2.10	2.15	2.37	2.17	1.76	2.04	2.04	1.98	2.17	1.90	2.48	2.76	2.24	1.92	2.00	1.53	1.59	1.23	1.51	1.04	0.83	1.53	1.58	1.46	1.52	1.31	1.03	1.38	1.18
20.00%	2.02	1.85	1.89	2.02	1.90	1.59	1.78	1.78	1.73	1.85	1.67	2.05	2.23	1.87	1.66	1.69	1.35	1.37	0.93	1.15	0.87	0.74	1.34	1.37	1.20	1.23	1.06	0.84	1.03	0.95
25.00%	1.91	1.76	1.79	1.90	1.80	1.54	1.69	1.69	1.64	1.74	1.59	1.91	2.05	1.74	1.57	1.59	1.28	1.29	0.83	1.03	0.81	0.71	1.27	1.29	1.12	1.13	0.98	0.77	0.92	0.87
30.00%	1.81	1.68	1.71	1.80	1.72	1.48	1.62	1.61	1.56	1.65	1.52	1.79	1.91	1.64	1.49	1.50	1.23	1.23	0.76	0.94	0.76	0.68	1.22	1.23	1.04	1.05	0.91	0.72	0.83	0.81
40.00%	1.65	1.56	1.58	1.64	1.58	1.40	1.49	1.48	1.43	1.50	1.40	1.59	1.67	1.46	1.36	1.36	1.14	1.12	0.64	0.80	0.67	0.63	1.12	1.12	0.93	0.92	0.80	0.63	0.69	0.71
50.00%	1.51	1.45	1.46	1.49	1.46	1.32	1.38	1.37	1.32	1.37	1.30	1.43	1.48	1.32	1.26	1.23	1.06	1.03	0.54	0.68	0.61	0.59	1.04	1.03	0.83	0.81	0.71	0.56	0.58	0.63
60.00%	1.38	1.35	1.36	1.36	1.35	1.25	1.27	1.27	1.22	1.25	1.21	1.28	1.31	1.19	1.15	1.12	0.98	0.94	0.46	0.58	0.54	0.55	0.96	0.95	0.74	0.72	0.63	0.50	0.49	0.55
70.00%	1.26	1.24	1.25	1.24	1.24	1.17	1.17	1.16	1.12	1.13	1.11	1.14	1.15	1.06	1.06	1.01	0.91	0.86	0.39	0.49	0.48	0.51	0.88	0.87	0.66	0.63	0.55	0.44	0.41	0.48
75.00%	1.19	1.19	1.19	1.17	1.19	1.13	1.12	1.11	1.07	1.07	1.07	1.07	1.07	1.00	1.00	0.96	0.87	0.81	0.35	0.45	0.46	0.49	0.84	0.82	0.62	0.58	0.51	0.41	0.37	0.45
80.00%	1.13	1.14	1.14	1.10	1.13	1.09	1.06	1.05	1.02	1.01	1.01	1.00	0.98	0.93	0.95	0.90	0.83	0.77	0.32	0.40	0.42	0.47	0.80	0.78	0.57	0.54	0.47	0.38	0.33	0.41
85.00%	1.05	1.07	1.07	1.03	1.06	1.04	1.00	0.99	0.96	0.94	0.96	0.92	0.89	0.86	0.89	0.83	0.78	0.72	0.28	0.36	0.39	0.45	0.75	0.73	0.52	0.49	0.43	0.35	0.29	0.37
90.00%	0.97	1.00	0.99	0.94	0.99	0.99	0.93	0.92	0.89	0.86	0.89	0.82	0.79	0.77	0.82	0.76	0.73	0.66	0.24	0.31	0.35	0.42	0.70	0.67	0.47	0.43	0.38	0.31	0.25	0.33
95.00%	0.85	0.90	0.89	0.83	0.88	0.91	0.83	0.82	0.79	0.75	0.80	0.70	0.67	0.66	0.73	0.66	0.66	0.58	0.19	0.25	0.30	0.38	0.63	0.59	0.40	0.36	0.32	0.26	0.19	0.28
97.00%	0.78	0.84	0.83	0.76	0.82	0.86	0.77	0.76	0.73	0.69	0.75	0.64	0.59	0.60	0.68	0.61	0.61	0.54	0.16	0.21	0.27	0.36	0.58	0.55	0.36	0.32	0.29	0.23	0.17	0.25
99.00%	0.67	0.74	0.73	0.65	0.71	0.78	0.68	0.66	0.64	0.59	0.65	0.53	0.48	0.50	0.58	0.51	0.54	0.46	0.12	0.16	0.23	0.32	0.51	0.47	0.30	0.26	0.23	0.19	0.12	0.20
99.90%	0.51	0.59	0.58	0.49	0.56	0.66	0.54	0.52	0.50	0.45	0.52	0.38	0.33	0.36	0.45	0.38	0.43	0.36	0.07	0.10	0.16	0.26	0.40	0.37	0.21	0.18	0.16	0.13	0.07	0.14
99.99%	0.41	0.49	0.48	0.39	0.46	0.57	0.44	0.43	0.41	0.35	0.43	0.29	0.24	0.28	0.37	0.30	0.36	0.29	0.05	0.07	0.13	0.22	0.33	0.30	0.16	0.13	0.12	0.10	0.05	0.10

Table C-3. Pearson type III distribution of storm surge

P%	Cua Nam Trieu	Hon Dau	Do Son	Diem Dien	Cua Ba Lat	Yen Dinh	Hoang Tan	Tinh Gia	Cau Giat	Dien Chau	Thanh Hoa	Hon Nieu	Cua Hoi	Cua Sot	Cua Nhuong	Cua Khau	Vung Chua	Dong Hoi	Da Nang	Dung Quat	Duc Pho	Tam Quan	Cua Gianh	Nhat Le	Cua Tung	Cua Viet	Thuan An	Chan May	Hoi An	Tam Ky
XTB	1.01	0.92	0.96	1.03	0.95	0.71	0.82	0.84	0.84	0.92	0.79	1.10	1.22	0.94	0.77	0.81	0.63	0.60	0.61	0.61	0.25	0.21	0.58	0.60	0.61	0.63	0.66	0.56	0.62	0.48
σ	0.61	0.53	0.57	0.66	0.57	0.32	0.46	0.48	0.47	0.55	0.44	0.77	0.91	0.69	0.51	0.59	0.40	0.40	0.55	0.67	0.26	0.10	0.37	0.40	0.49	0.56	0.49	0.41	0.62	0.48
CV	0.66	0.68	0.69	0.76	0.66	0.53	0.66	0.67	0.66	0.71	0.64	0.84	0.82	0.88	0.79	0.88	0.77	0.79	1.09	1.36	1.25	0.56	0.75	0.79	0.98	1.08	0.89	0.89	1.13	1.22
CS	1.98	2.03	2.08	2.27	1.98	1.59	1.99	2.01	1.99	2.12	1.93	2.51	2.47	2.63	2.37	2.63	2.30	2.37	3.26	4.08	3.75	1.69	2.26	2.36	2.94	3.25	2.66	2.66	3.39	3.67
m	3.00	3.00	3.00	3.00	3.00	3.00	3.00	3.00	3.00	3.00	3.00	3.00	3.00	3.00	3.00	3.00	3.00	3.00	3.00	3.00	3.00	3.00	3.00	3.00	3.00	3.00	3.00	3.00	3.00	3.00
ao	0.34	0.31	0.32	0.34	0.32	0.24	0.27	0.28	0.28	0.31	0.26	0.37	0.41	0.31	0.26	0.27	0.21	0.20	0.20	0.20	0.08	0.07	0.19	0.20	0.20	0.21	0.22	0.19	0.21	0.16
α	1.02	0.97	0.92	0.78	1.02	1.58	1.01	0.99	1.01	0.89	1.07	0.64	0.66	0.58	0.71	0.58	0.76	0.71	0.38	0.24	0.28	1.40	0.78	0.72	0.46	0.38	0.57	0.57	0.35	0.30
β	1.51	1.59	1.44	1.14	1.61	3.37	1.84	1.77	1.81	1.46	2.02	0.87	0.81	0.93	1.39	1.07	1.81	1.78	0.92	0.59	1.68	10.03	2.00	1.78	1.14	0.91	1.28	1.52	0.85	0.93
0.01%	6.47	6.06	6.54	7.85	6.06	3.43	5.29	5.45	5.40	6.41	4.92	9.63	10.50	8.80	6.25	7.58	4.88	4.89	7.90	11.04	4.01	1.10	4.47	4.87	6.70	7.98	6.32	5.34	8.40	7.38
0.10%	4.95	4.61	4.96	5.88	4.63	2.71	4.04	4.15	4.13	4.85	3.77	7.10	7.77	6.45	4.65	5.55	3.65	3.63	5.60	7.56	2.78	0.86	3.34	3.63	4.83	5.66	4.62	3.90	5.92	5.13
0.20%	4.49	4.18	4.49	5.29	4.20	2.49	3.66	3.76	3.74	4.38	3.43	6.35	6.95	5.75	4.17	4.95	3.28	3.26	4.92	6.54	2.42	0.78	3.01	3.25	4.27	4.98	4.12	3.48	5.19	4.48
0.33%	4.15	3.87	4.14	4.87	3.89	2.33	3.39	3.48	3.46	4.04	3.18	5.81	6.36	5.24	3.83	4.51	3.01	2.99	4.44	5.82	2.17	0.73	2.77	2.99	3.88	4.49	3.75	3.17	4.67	4.01
0.50%	3.88	3.60	3.86	4.51	3.63	2.19	3.16	3.25	3.23	3.76	2.97	5.36	5.88	4.83	3.54	4.16	2.79	2.77	4.04	5.23	1.96	0.69	2.57	2.76	3.55	4.09	3.45	2.92	4.24	3.62
1.00%	3.42	3.17	3.39	3.93	3.20	1.97	2.79	2.86	2.85	3.30	2.62	4.62	5.07	4.14	3.07	3.57	2.43	2.40	3.39	4.27	1.61	0.61	2.23	2.40	3.01	3.43	2.96	2.50	3.54	3.00
1.50%	3.15	2.92	3.11	3.59	2.94	1.84	2.56	2.63	2.62	3.02	2.42	4.19	4.61	3.74	2.80	3.22	2.21	2.19	3.01	3.72	1.42	0.57	2.04	2.18	2.70	3.05	2.67	2.26	3.14	2.64
2.00%	2.96	2.74	2.91	3.35	2.76	1.74	2.41	2.47	2.46	2.83	2.27	3.89	4.28	3.47	2.60	2.98	2.06	2.03	2.75	3.34	1.28	0.54	1.90	2.03	2.48	2.79	2.47	2.09	2.86	2.39
3.00%	2.69	2.48	2.64	3.01	2.51	1.61	2.19	2.24	2.24	2.56	2.07	3.46	3.82	3.07	2.33	2.65	1.85	1.82	2.39	2.83	1.10	0.50	1.71	1.82	2.18	2.42	2.19	1.85	2.47	2.05
5.00%	2.35	2.16	2.29	2.59	2.19	1.44	1.91	1.95	1.95	2.22	1.81	2.94	3.24	2.59	1.99	2.23	1.59	1.56	1.94	2.20	0.87	0.44	1.47	1.55	1.80	1.97	1.84	1.56	2.00	1.63
10.00%	1.88	1.73	1.82	2.02	1.76	1.20	1.53	1.56	1.57	1.76	1.46	2.24	2.48	1.95	1.54	1.68	1.24	1.20	1.37	1.43	0.58	0.37	1.15	1.20	1.32	1.40	1.38	1.17	1.39	1.11
20.00%	1.42	1.30	1.36	1.46	1.33	0.96	1.15	1.18	1.18	1.30	1.11	1.57	1.75	1.34	1.10	1.15	0.89	0.86	0.86	0.79	0.34	0.29	0.83	0.86	0.87	0.88	0.95	0.80	0.86	0.65
25.00%	1.27	1.16	1.21	1.29	1.19	0.88	1.03	1.05	1.06	1.16	1.00	1.36	1.52	1.16	0.96	0.99	0.78	0.75	0.71	0.62	0.27	0.26	0.73	0.75	0.73	0.73	0.82	0.69	0.70	0.52
30.00%	1.15	1.04	1.09	1.15	1.08	0.81	0.93	0.95	0.96	1.04	0.90	1.20	1.34	1.01	0.85	0.87	0.70	0.67	0.60	0.50	0.22	0.24	0.65	0.67	0.63	0.61	0.71	0.60	0.59	0.43
40.00%	0.96	0.87	0.90	0.93	0.90	0.70	0.78	0.79	0.80	0.85	0.76	0.95	1.06	0.79	0.68	0.68	0.56	0.53	0.44	0.35	0.16	0.21	0.53	0.53	0.48	0.45	0.55	0.47	0.43	0.31
50.00%	0.81	0.73	0.75	0.77	0.76	0.61	0.65	0.66	0.67	0.71	0.64	0.76	0.86	0.63	0.56	0.54	0.46	0.44	0.34	0.27	0.12	0.18	0.44	0.44	0.37	0.35	0.44	0.37	0.33	0.24
60.00%	0.69	0.62	0.63	0.64	0.64	0.53	0.55	0.56	0.57	0.60	0.55	0.63	0.71	0.52	0.46	0.44	0.38	0.36	0.28	0.23	0.10	0.15	0.36	0.36	0.30	0.28	0.36	0.31	0.27	0.20
70.00%	0.58	0.52	0.53	0.53	0.54	0.47	0.47	0.47	0.48	0.50	0.46	0.52	0.59	0.43	0.39	0.37	0.32	0.30	0.24	0.21	0.09	0.13	0.30	0.30	0.25	0.24	0.30	0.25	0.23	0.17
75.00%	0.54	0.48	0.49	0.49	0.50	0.43	0.43	0.44	0.44	0.46	0.43	0.48	0.54	0.40	0.35	0.34	0.29	0.28	0.22	0.21	0.09	0.12	0.28	0.28	0.24	0.23	0.28	0.23	0.22	0.17
80.00%	0.49	0.44	0.45	0.45	0.46	0.40	0.40	0.40	0.41	0.42	0.39	0.45	0.50	0.37	0.33	0.32	0.27	0.26	0.22	0.21	0.09	0.11	0.26	0.26	0.22	0.22	0.26	0.22	0.21	0.16
85.00%	0.45	0.40	0.41	0.42	0.42	0.37	0.36	0.37	0.37	0.39	0.36	0.42	0.47	0.35	0.30	0.30	0.25	0.24	0.21	0.20	0.08	0.10	0.24	0.24	0.21	0.21	0.24	0.21	0.21	0.16
90.00%	0.41	0.37	0.38	0.38	0.38	0.33	0.33	0.34	0.34	0.36	0.33	0.39	0.44	0.33	0.28	0.28	0.23	0.22	0.21	0.20	0.08	0.09	0.22	0.22	0.21	0.21	0.23	0.20	0.21	0.16
95.00%	0.37	0.34	0.35	0.36	0.35	0.30	0.30	0.31	0.31	0.33	0.30	0.37	0.42	0.32	0.27	0.27	0.22	0.21	0.21	0.20	0.08	0.08	0.20	0.21	0.20	0.21	0.22	0.19	0.21	0.16
97.00%	0.36	0.32	0.34	0.35	0.34	0.28	0.29	0.29	0.30	0.32	0.28	0.37	0.41	0.31	0.26	0.27	0.21	0.20	0.20	0.20	0.08	0.08	0.20	0.20	0.20	0.21	0.22	0.19	0.21	0.16
99.00%	0.34	0.31	0.32	0.34	0.32	0.26	0.28	0.28	0.29	0.31	0.27	0.37	0.41	0.31	0.26	0.27	0.21	0.20	0.20	0.20	0.08	0.07	0.20	0.20	0.20	0.21	0.22	0.19	0.21	0.16
99.90%	0.34	0.31	0.32	0.34	0.32	0.24	0.27	0.28	0.28	0.31	0.27	0.37	0.41	0.31	0.26	0.27	0.21	0.20	0.20	0.20	0.08	0.07	0.19	0.20	0.20	0.21	0.22	0.19	0.21	0.16
99.99%	0.34	0.31	0.32	0.34	0.32	0.24	0.27	0.28	0.28	0.31	0.26	0.37	0.41	0.31	0.26	0.27	0.21	0.20	0.20	0.20	0.08	0.07	0.19	0.20	0.20	0.21	0.22	0.19	0.21	0.16

Table C-4. Pearson type III distribution of maximum water level

P%	Cua Nam Trieu	Hon Dau	Do Son	Diem Dien	Cua Ba Lat	Yen Dinh	Hoang Tan	Tinh Gia	Cau Giat	Dien Chau	Thanh Hoa	Hon Nieu	Cua Hoi	Cua Sot	Cua Nhuong	Cua Khau	Vung Chua	Dong Hoi	Da Nang	Dung Quat	Duc Pho	Tam Quan	Cua Gianh	Nhat Le	Cua Tung	Cua Viet	Thuan An	Chan May	Hoi An	Tam Ky
XTB	1.63	1.54	1.56	1.62	1.56	1.38	1.47	1.46	1.42	1.49	1.38	1.60	1.70	1.46	1.35	1.35	1.12	1.11	0.67	0.84	0.67	0.62	1.10	1.11	0.93	0.93	0.81	0.64	0.74	0.71
σ	0.46	0.34	0.37	0.48	0.38	0.22	0.36	0.36	0.36	0.45	0.32	0.59	0.72	0.52	0.36	0.43	0.26	0.32	0.45	0.52	0.27	0.15	0.28	0.31	0.38	0.43	0.37	0.29	0.52	0.35
CV	0.32	0.26	0.27	0.34	0.28	0.18	0.28	0.29	0.29	0.35	0.27	0.43	0.49	0.41	0.31	0.37	0.27	0.33	0.79	0.74	0.47	0.28	0.29	0.32	0.47	0.54	0.53	0.53	0.84	0.57
CS	1.61	1.28	1.35	1.69	1.12	0.92	1.39	1.14	1.45	1.73	1.07	1.49	1.72	2.06	1.86	1.85	1.34	1.67	3.95	3.72	2.35	1.38	1.45	1.62	2.35	2.69	2.67	2.66	4.18	2.85
m	5.00	5.00	5.00	5.00	4.00	5.00	5.00	4.00	5.00	5.00	4.00	3.50	3.50	5.00	6.00	5.00	5.00	5.00	5.00	5.00	5.00	5.00	5.00	5.00	5.00	5.00	5.00	5.00	5.00	5.00
ao	0.98	0.92	0.94	0.97	0.78	0.83	0.88	0.73	0.85	0.89	0.69	0.68	0.73	0.88	0.90	0.81	0.67	0.66	0.40	0.50	0.40	0.37	0.66	0.67	0.56	0.56	0.48	0.38	0.44	0.43
α	1.54	2.45	2.19	1.40	3.21	4.70	2.06	3.07	1.90	1.34	3.49	1.81	1.35	0.94	1.15	1.17	2.22	1.43	0.26	0.29	0.72	2.11	1.91	1.52	0.73	0.55	0.56	0.56	0.23	0.49
β	2.36	3.98	3.52	2.16	4.10	8.55	3.51	4.19	3.35	2.26	5.04	1.98	1.39	1.61	2.56	2.18	4.96	3.23	0.95	0.87	2.70	8.51	4.33	3.43	1.96	1.49	1.74	2.22	0.78	1.73
0.01%	5.49	4.13	4.40	5.75	4.28	2.84	4.27	4.09	4.29	5.38	3.65	6.40	8.05	6.50	4.66	5.26	3.15	3.88	7.21	8.17	3.50	1.78	3.33	3.76	4.84	5.78	4.97	3.90	8.58	4.80
0.10%	4.46	3.47	3.67	4.63	3.61	2.50	3.55	3.44	3.54	4.33	3.10	5.14	6.33	5.08	3.75	4.18	2.63	3.13	5.04	5.78	2.68	1.48	2.75	3.05	3.70	4.32	3.72	2.92	5.95	3.55
0.20%	4.15	3.27	3.45	4.30	3.41	2.39	3.33	3.24	3.31	4.01	2.93	4.76	5.81	4.65	3.47	3.86	2.47	2.91	4.41	5.08	2.43	1.39	2.58	2.84	3.36	3.89	3.35	2.63	5.18	3.18
0.33%	3.92	3.12	3.29	4.05	3.25	2.31	3.17	3.10	3.15	3.77	2.80	4.48	5.43	4.34	3.27	3.62	2.36	2.74	3.96	4.58	2.25	1.33	2.45	2.68	3.11	3.58	3.08	2.42	4.64	2.92
0.50%	3.73	3.00	3.15	3.85	3.13	2.24	3.03	2.97	3.01	3.58	2.70	4.25	5.12	4.09	3.11	3.43	2.26	2.61	3.59	4.17	2.11	1.27	2.34	2.55	2.91	3.32	2.86	2.25	4.19	2.70
1.00%	3.42	2.79	2.92	3.51	2.91	2.13	2.80	2.77	2.77	3.26	2.52	3.85	4.59	3.66	2.83	3.10	2.10	2.38	2.99	3.50	1.86	1.18	2.16	2.33	2.57	2.89	2.50	1.96	3.47	2.34
1.50%	3.23	2.67	2.79	3.31	2.78	2.06	2.67	2.64	2.64	3.07	2.41	3.62	4.28	3.41	2.67	2.91	2.00	2.24	2.65	3.12	1.72	1.12	2.05	2.20	2.38	2.65	2.29	1.80	3.06	2.13
2.00%	3.10	2.58	2.69	3.16	2.69	2.01	2.57	2.55	2.54	2.93	2.34	3.46	4.06	3.23	2.55	2.77	1.93	2.15	2.42	2.85	1.62	1.08	1.97	2.11	2.24	2.48	2.14	1.68	2.77	1.99
3.00%	2.91	2.45	2.55	2.96	2.56	1.94	2.44	2.42	2.40	2.74	2.23	3.22	3.74	2.98	2.39	2.58	1.83	2.01	2.09	2.49	1.48	1.02	1.87	1.98	2.05	2.24	1.93	1.52	2.38	1.78
5.00%	2.66	2.29	2.37	2.70	2.39	1.85	2.26	2.26	2.22	2.50	2.08	2.92	3.35	2.67	2.18	2.34	1.70	1.84	1.70	2.05	1.30	0.95	1.73	1.82	1.80	1.94	1.67	1.32	1.91	1.53
10.00%	2.33	2.06	2.12	2.35	2.15	1.72	2.01	2.02	1.97	2.16	1.88	2.50	2.80	2.25	1.90	2.00	1.52	1.60	1.21	1.49	1.07	0.85	1.53	1.59	1.48	1.54	1.34	1.05	1.34	1.20
20.00%	1.99	1.82	1.86	1.98	1.89	1.57	1.76	1.77	1.70	1.82	1.66	2.07	2.25	1.82	1.61	1.66	1.34	1.35	0.80	1.01	0.84	0.74	1.33	1.35	1.17	1.17	1.02	0.80	0.86	0.90
25.00%	1.87	1.74	1.77	1.86	1.80	1.52	1.67	1.69	1.62	1.71	1.58	1.92	2.06	1.69	1.52	1.55	1.27	1.27	0.69	0.88	0.77	0.70	1.26	1.27	1.07	1.06	0.92	0.72	0.74	0.81
30.00%	1.78	1.67	1.69	1.76	1.72	1.48	1.60	1.61	1.54	1.62	1.52	1.80	1.91	1.58	1.45	1.46	1.22	1.21	0.61	0.78	0.71	0.67	1.20	1.21	0.99	0.97	0.84	0.66	0.65	0.73
40.00%	1.62	1.55	1.57	1.60	1.59	1.40	1.48	1.49	1.42	1.47	1.41	1.60	1.67	1.41	1.32	1.32	1.13	1.10	0.51	0.65	0.63	0.62	1.11	1.10	0.87	0.84	0.73	0.57	0.54	0.63
50.00%	1.50	1.46	1.47	1.47	1.48	1.34	1.38	1.39	1.32	1.35	1.32	1.44	1.47	1.27	1.23	1.20	1.06	1.01	0.45	0.58	0.56	0.58	1.03	1.02	0.78	0.74	0.65	0.51	0.49	0.56
60.00%	1.39	1.37	1.38	1.36	1.38	1.28	1.29	1.29	1.23	1.24	1.23	1.29	1.30	1.17	1.15	1.11	0.99	0.93	0.42	0.54	0.51	0.54	0.96	0.94	0.71	0.67	0.59	0.46	0.46	0.51
70.00%	1.29	1.29	1.29	1.27	1.29	1.22	1.21	1.20	1.15	1.15	1.15	1.16	1.16	1.07	1.08	1.03	0.93	0.87	0.41	0.51	0.47	0.51	0.90	0.88	0.65	0.62	0.54	0.43	0.45	0.47
75.00%	1.25	1.25	1.25	1.22	1.24	1.19	1.17	1.16	1.12	1.11	1.11	1.10	1.09	1.04	1.05	0.99	0.90	0.84	0.41	0.51	0.45	0.49	0.87	0.85	0.63	0.61	0.53	0.41	0.45	0.46
80.00%	1.20	1.21	1.21	1.18	1.19	1.16	1.13	1.11	1.08	1.07	1.07	1.04	1.02	1.00	1.02	0.95	0.87	0.81	0.41	0.50	0.44	0.48	0.84	0.82	0.61	0.59	0.51	0.40	0.44	0.45
85.00%	1.16	1.16	1.16	1.13	1.14	1.12	1.09	1.06	1.04	1.03	1.02	0.97	0.96	0.96	0.99	0.92	0.84	0.78	0.40	0.50	0.43	0.46	0.81	0.79	0.59	0.58	0.50	0.39	0.44	0.44
90.00%	1.11	1.12	1.12	1.09	1.08	1.09	1.04	1.01	0.99	0.99	0.97	0.90	0.89	0.93	0.96	0.88	0.80	0.75	0.40	0.50	0.42	0.44	0.78	0.75	0.58	0.57	0.49	0.39	0.44	0.43
95.00%	1.06	1.06	1.06	1.04	1.01	1.03	0.99	0.94	0.94	0.95	0.91	0.83	0.82	0.90	0.93	0.85	0.76	0.71	0.40	0.50	0.41	0.42	0.74	0.72	0.56	0.56	0.49	0.38	0.44	0.43
97.00%	1.04	1.03	1.03	1.02	0.97	1.01	0.96	0.90	0.92	0.93	0.87	0.79	0.79	0.89	0.92	0.83	0.74	0.70	0.40	0.50	0.41	0.41	0.72	0.70	0.56	0.56	0.49	0.38	0.44	0.43
99.00%	1.01	0.99	0.99	0.99	0.90	0.96	0.93	0.84	0.89	0.91	0.81	0.74	0.75	0.88	0.91	0.82	0.71	0.68	0.40	0.50	0.40	0.39	0.69	0.68	0.56	0.56	0.48	0.38	0.44	0.43
99.90%	0.99	0.95	0.95	0.98	0.84	0.90	0.90	0.78	0.86	0.89	0.75	0.70	0.73	0.88	0.90	0.81	0.69	0.67	0.40	0.50	0.40	0.38	0.67	0.67	0.56	0.56	0.48	0.38	0.44	0.43
99.99%	0.98	0.93	0.94	0.97	0.81	0.87	0.89	0.75	0.85	0.89	0.72	0.69	0.73	0.88	0.90	0.81	0.68	0.66	0.40	0.50	0.40	0.37	0.67	0.67	0.56	0.56	0.48	0.38	0.44	0.43

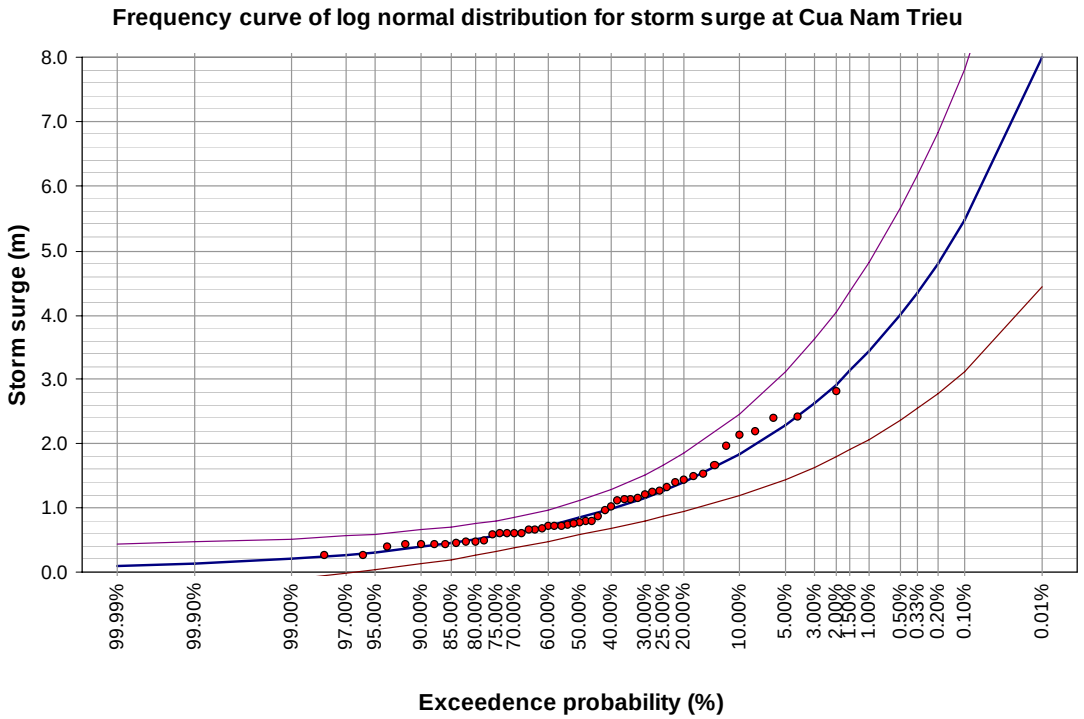

Figure C-1. Log-normal distribution for storm surge at Cua Nam Trieu

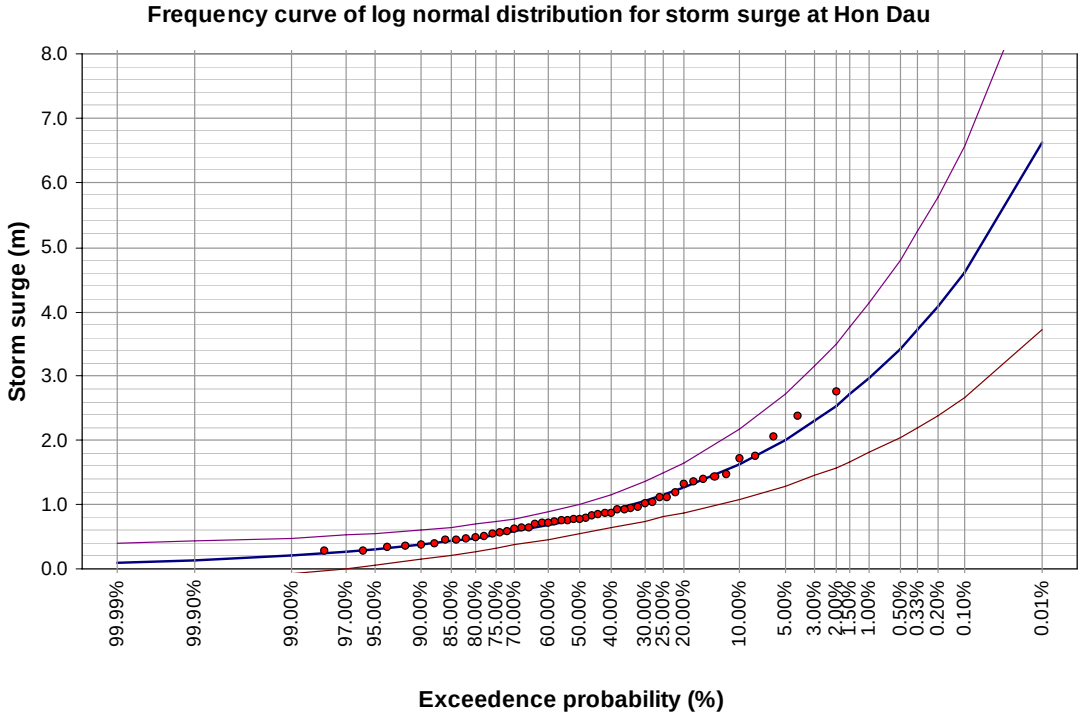

Figure C-2. Log-normal distribution for storm surge at Hon Dau

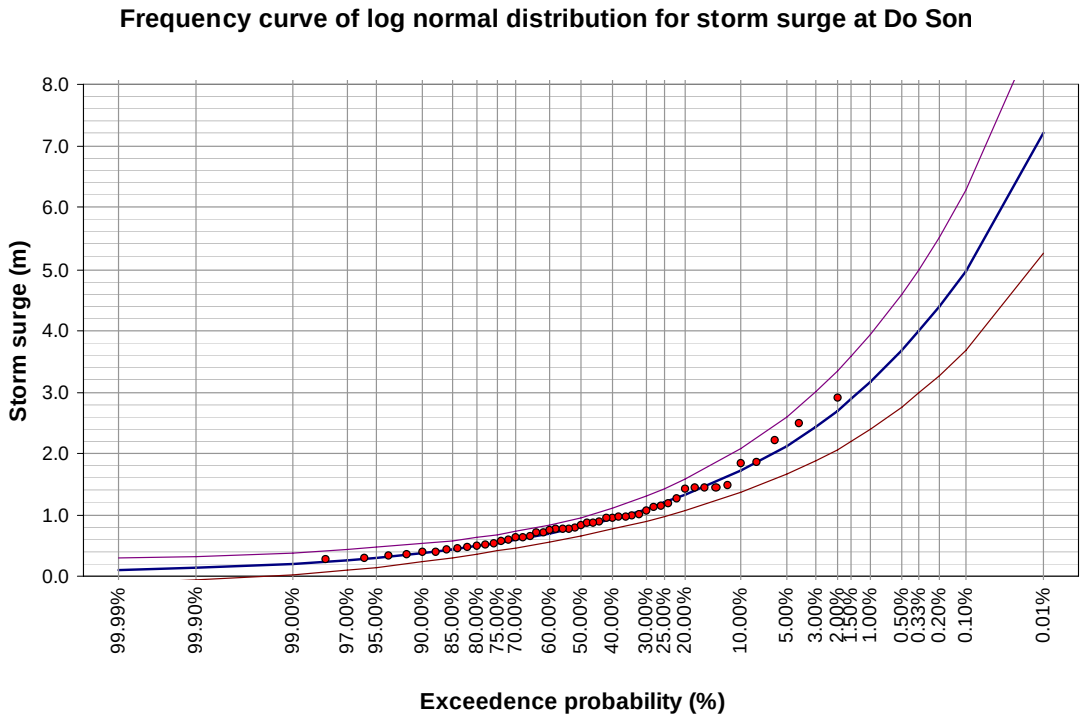

Figure C-3. Log-normal distribution for storm surge at Do Son

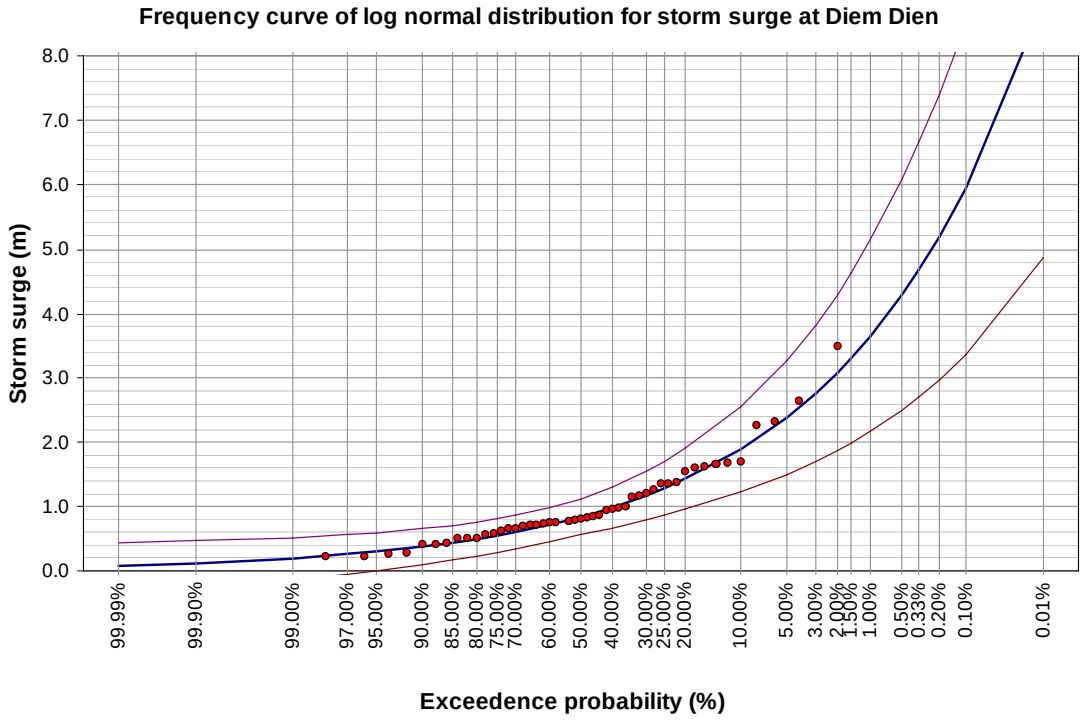

Figure C-4. Log-normal distribution for storm surge at Diem Dien

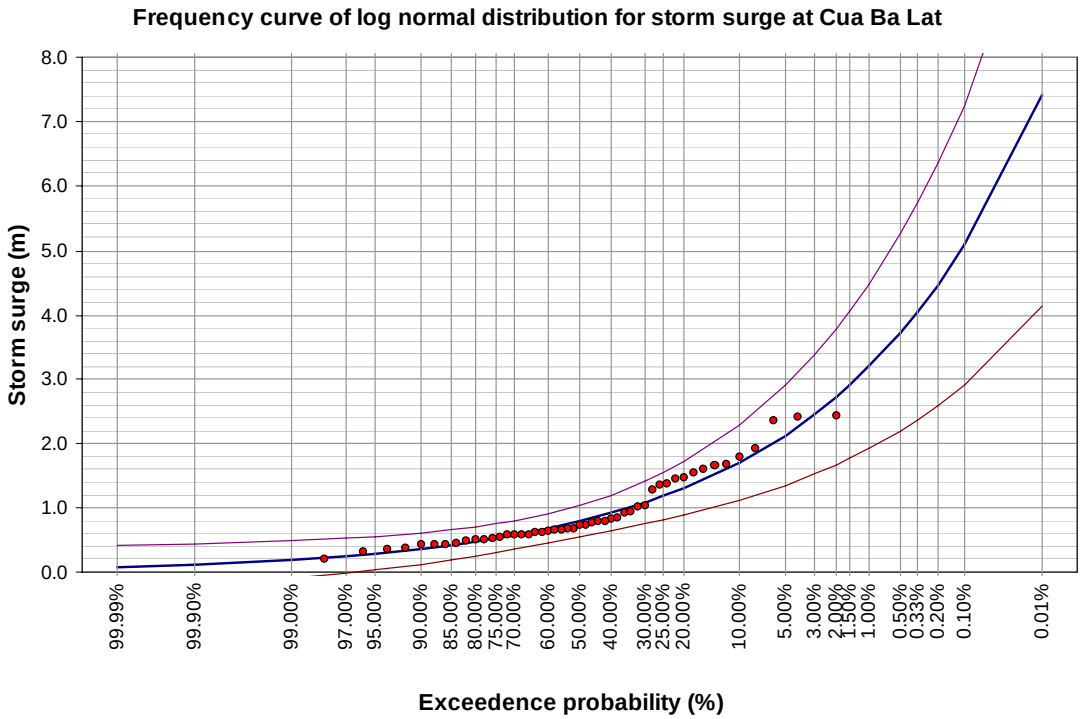

Figure C-5. Log-normal distribution for storm surge at Cua Ba Lat

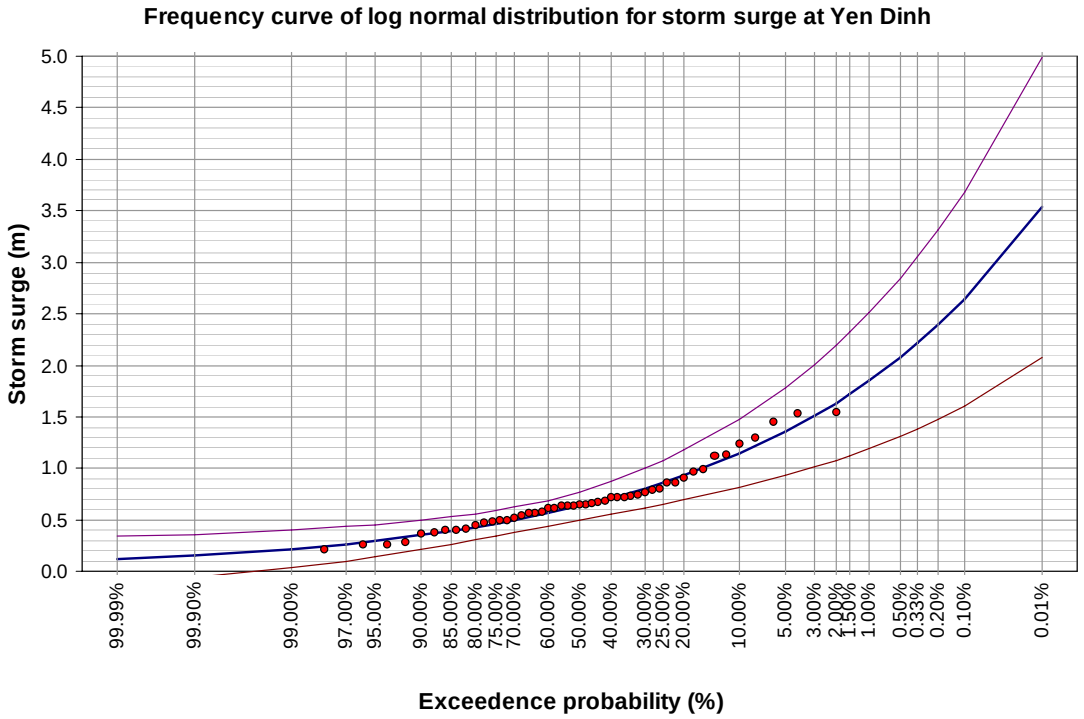

Figure C-6. Log-normal distribution for storm surge at Yen Dinh

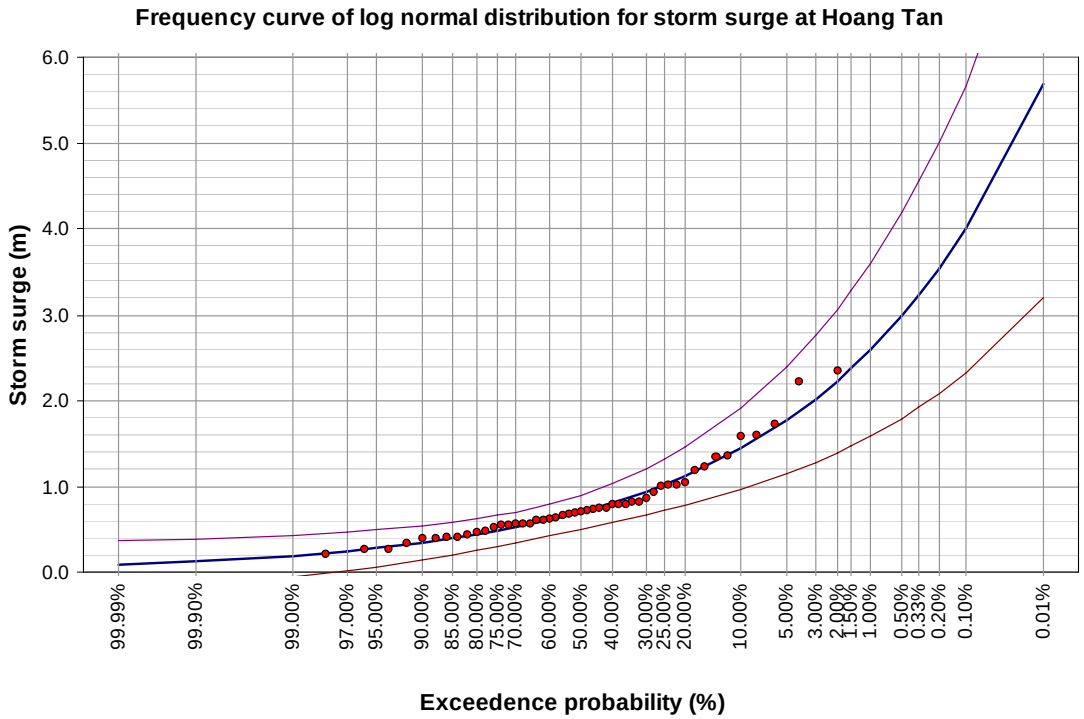

Figure C-7. Log-normal distribution for storm surge at Hoang Tan

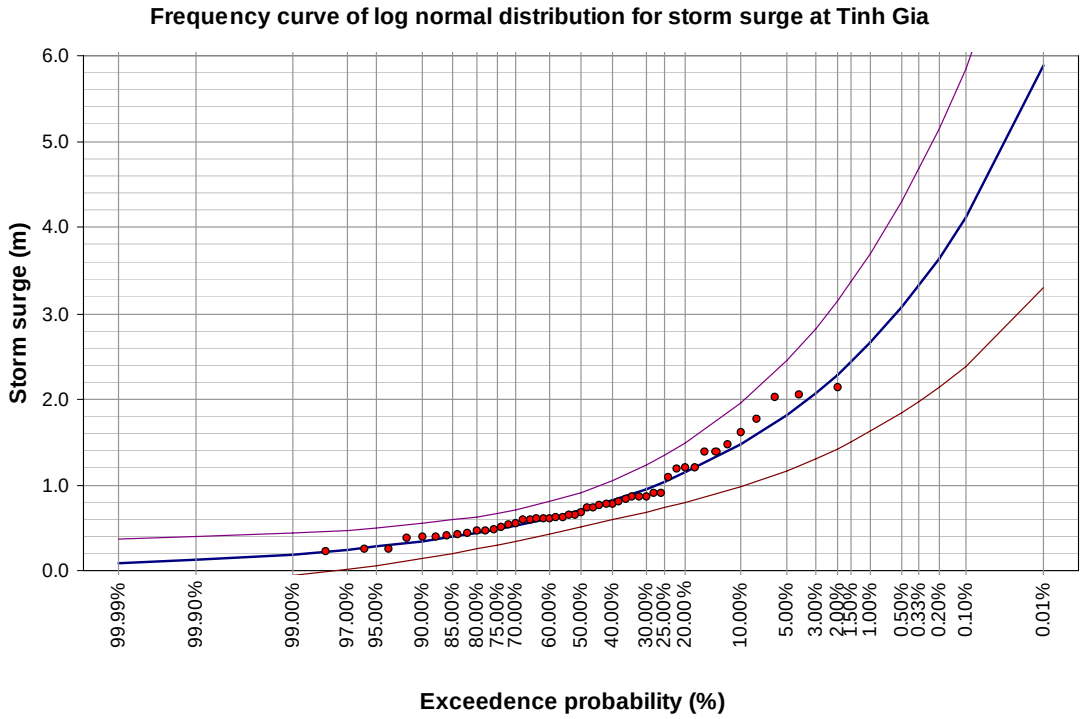

Figure C-8. Log-normal distribution for storm surge at Tinh Gia

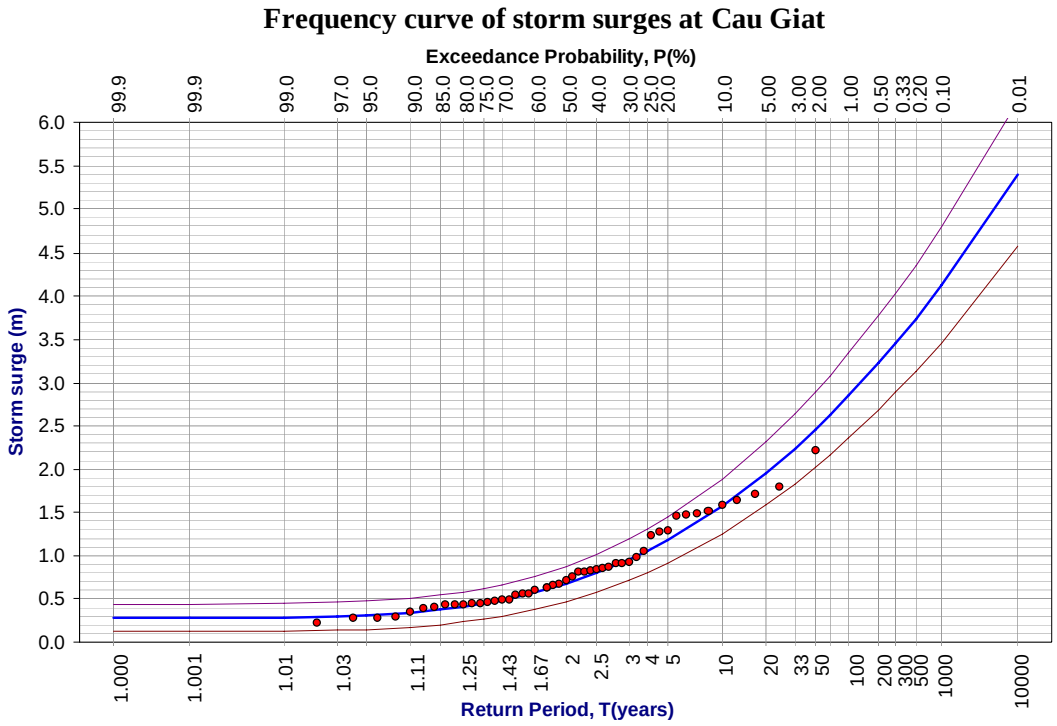

Figure C-9. Pearson type III distribution for storm surge at Cau Giat

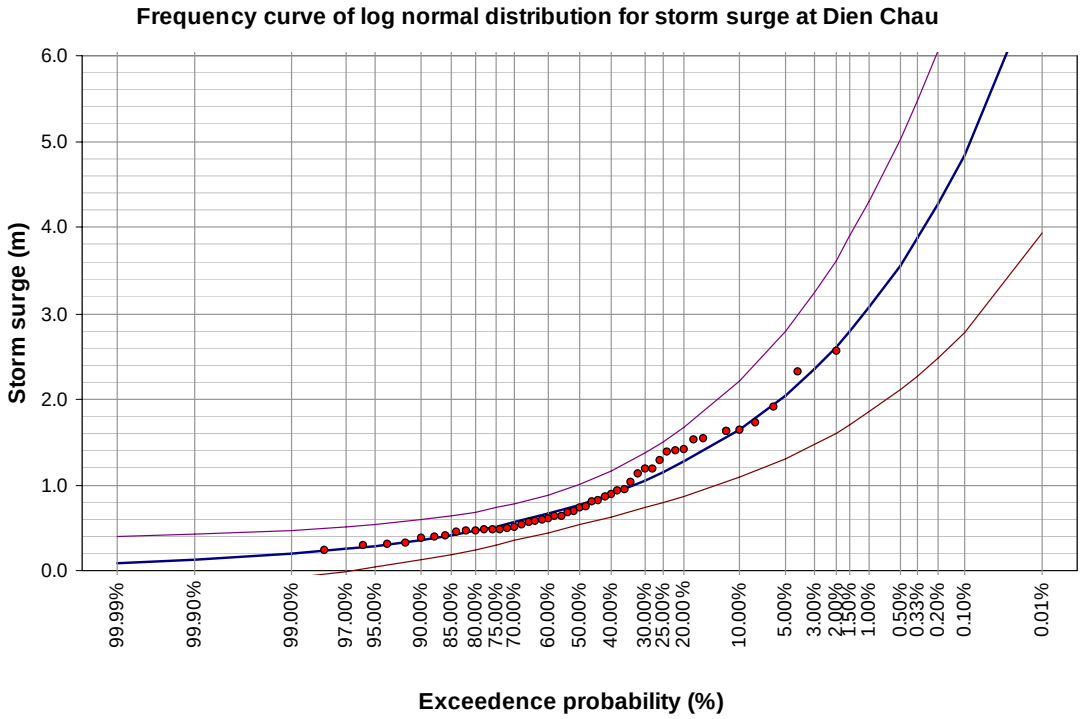

Figure C-10. Log-normal distribution for storm surge at Dien Chau

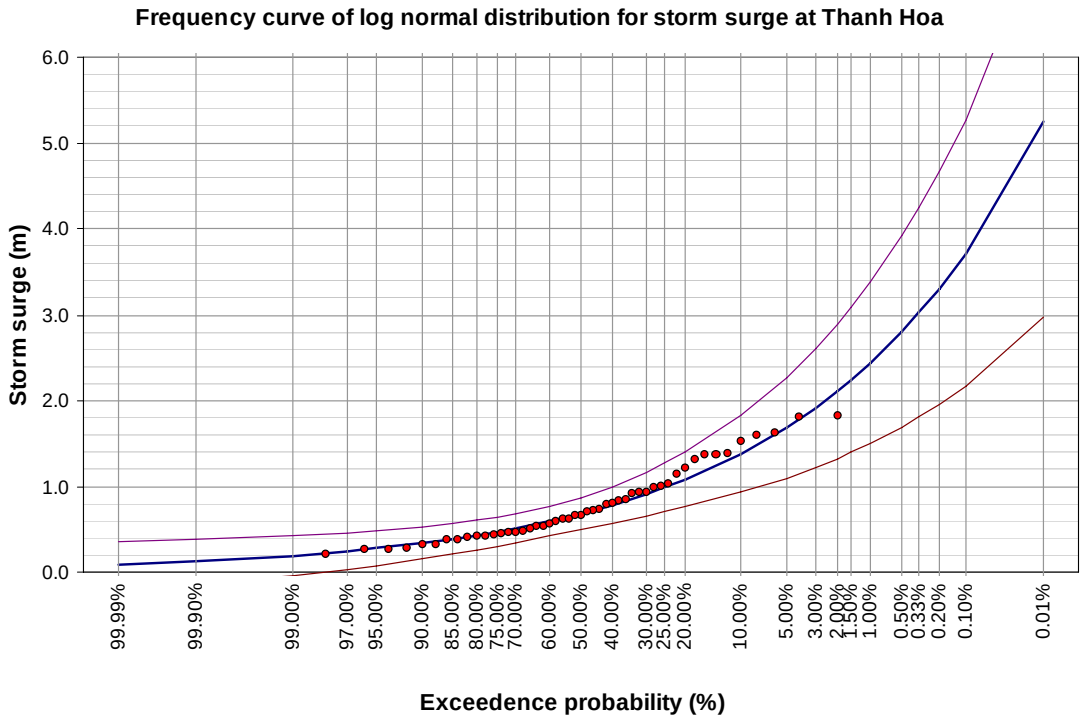

Figure C-11. Log-normal distribution for storm surge at Thanh Hoa

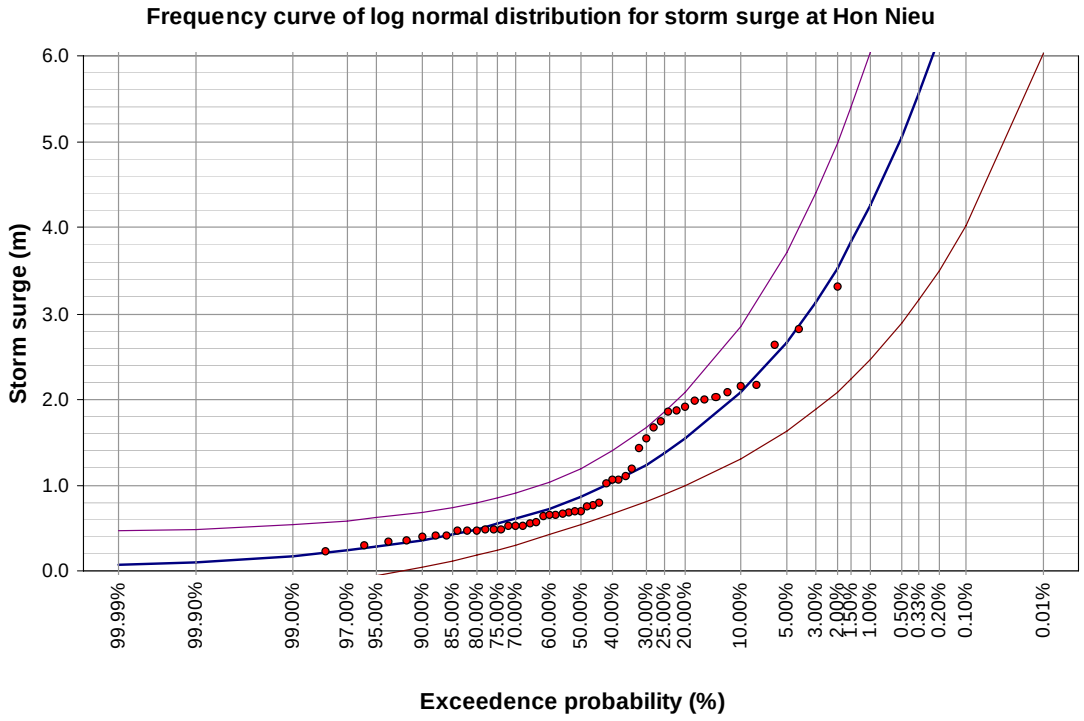

Figure C-12. Log-normal distribution for storm surge at Hon Nieu

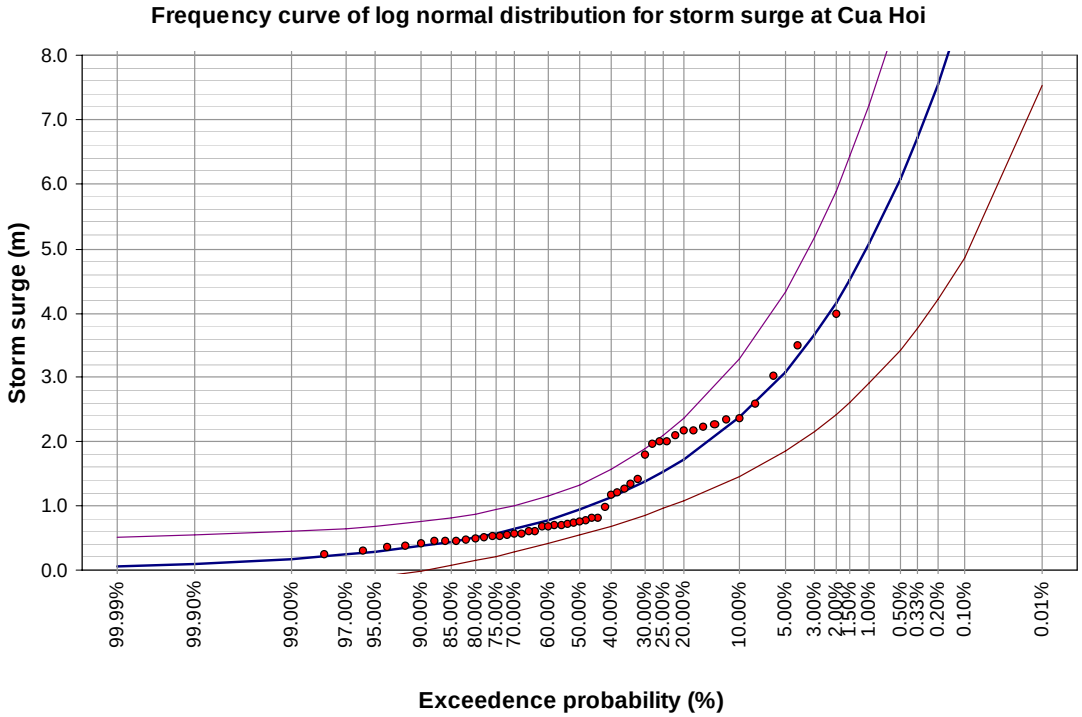

Figure C-13. Log-normal distribution for storm surge at Cua Hoi

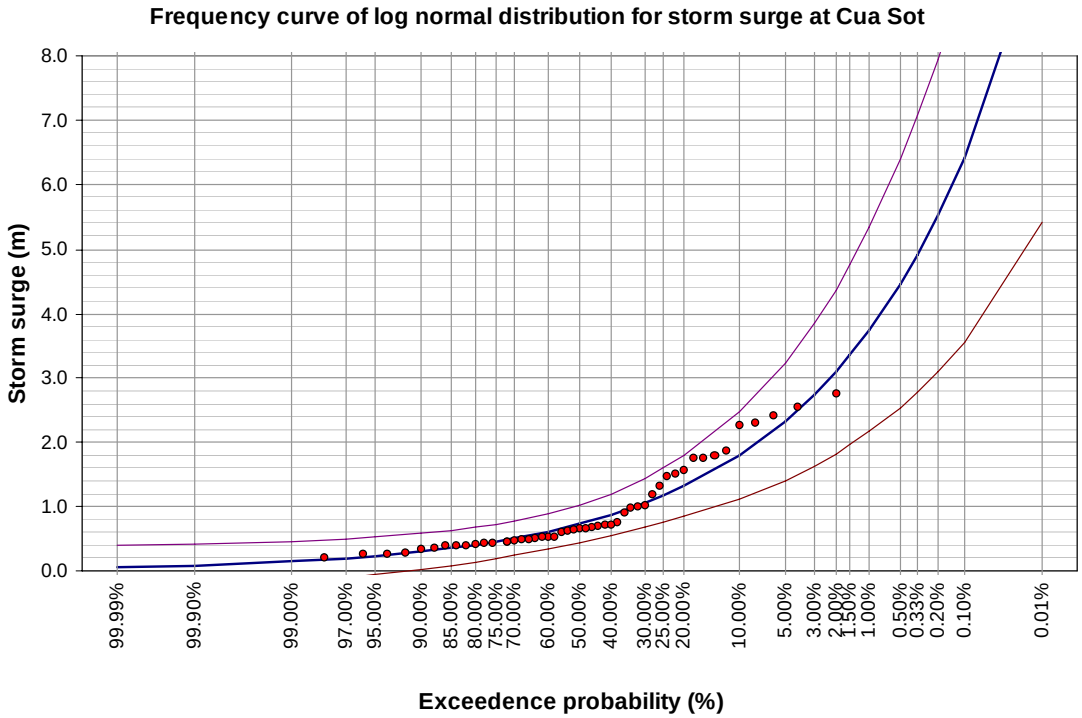

Figure C-14. Log-normal distribution for storm surge at Cua Sot

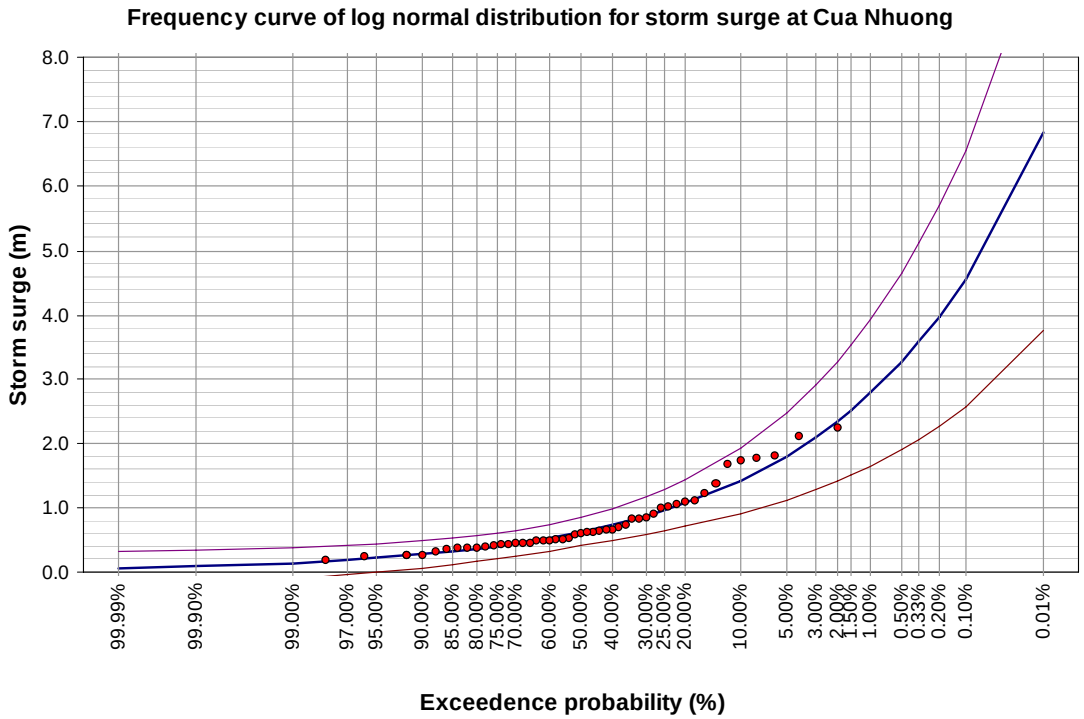

Figure C-15. Log-normal distribution for storm surge at Cua Nhuong

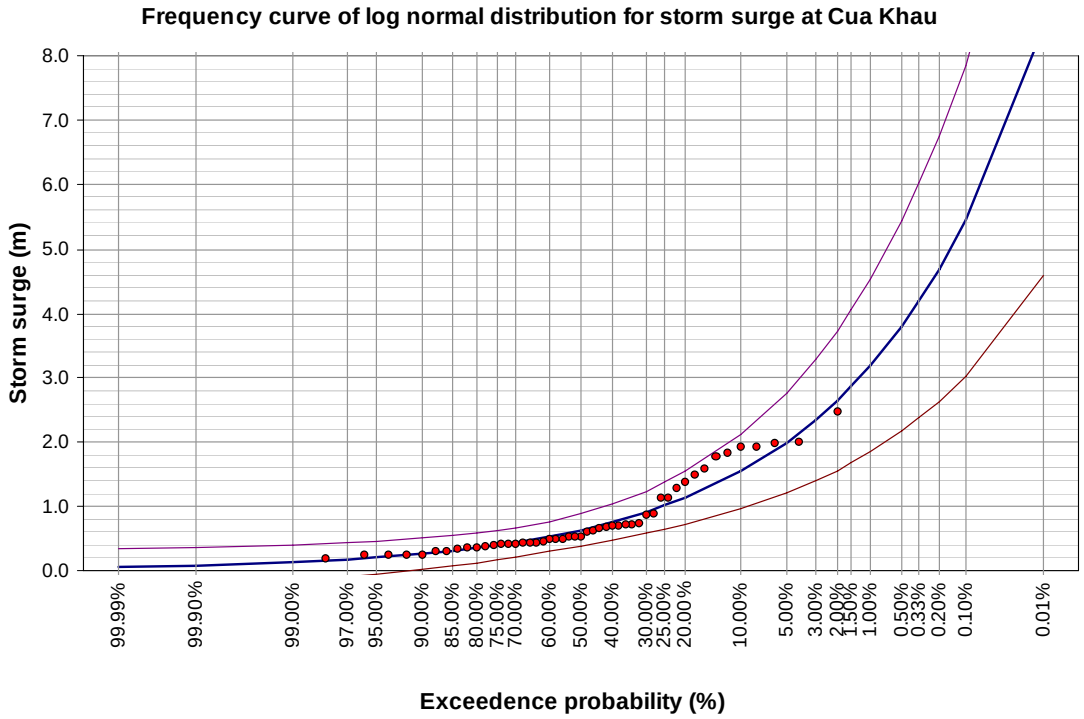

Figure C-16. Log-normal distribution for storm surge at Cua Khau

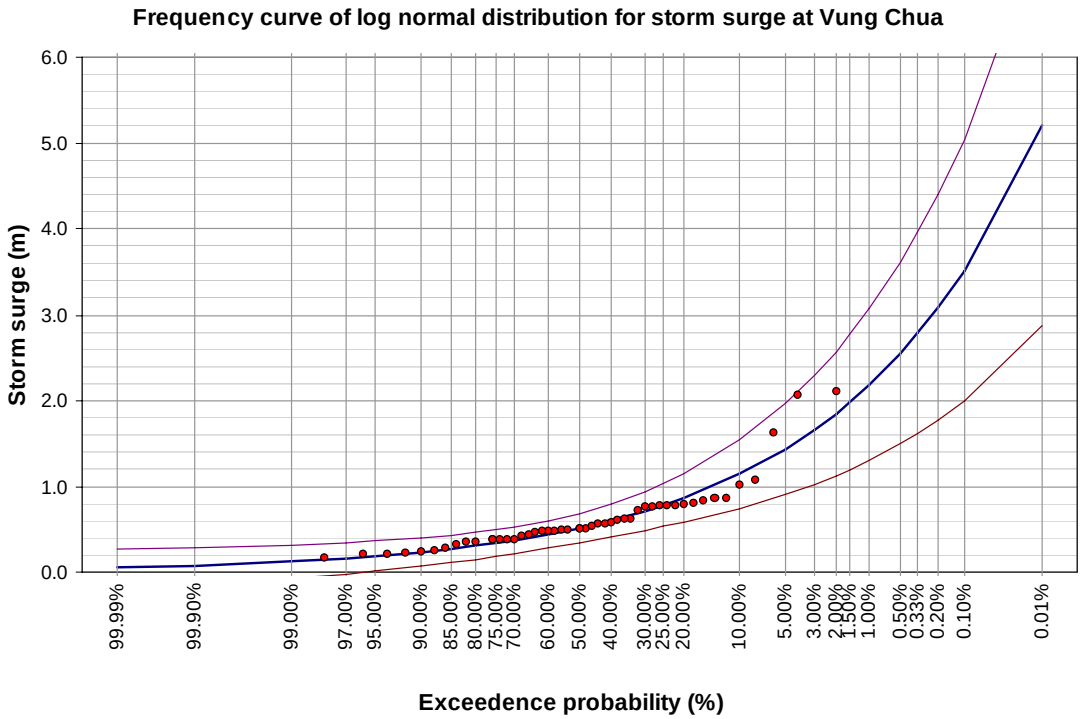

Figure C-17. Log-normal distribution for storm surge at Vung Chua

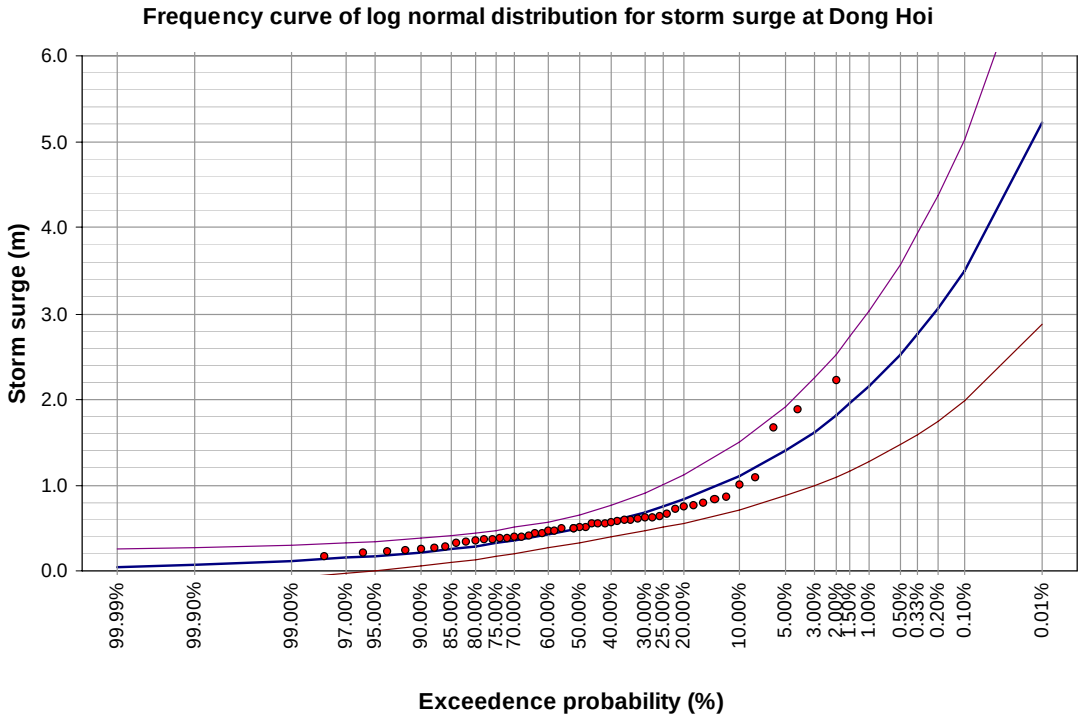

Figure C-18. Log-normal distribution for storm surge at Dong Hoi

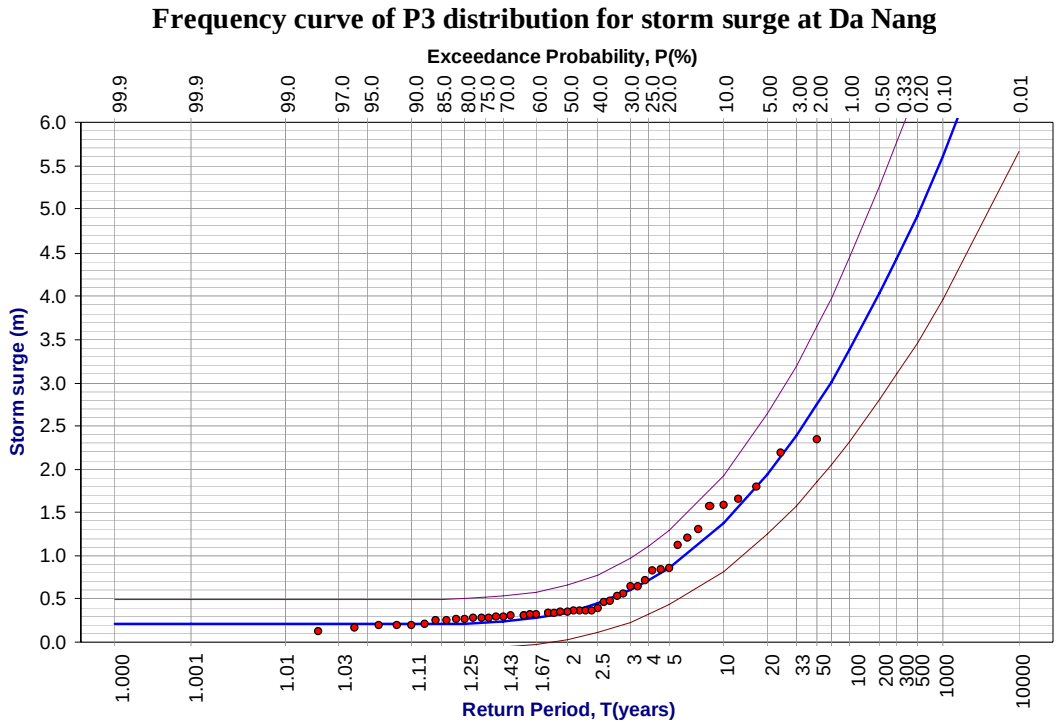

Figure C-19. Pearson type III distribution for storm surge at Da Nang

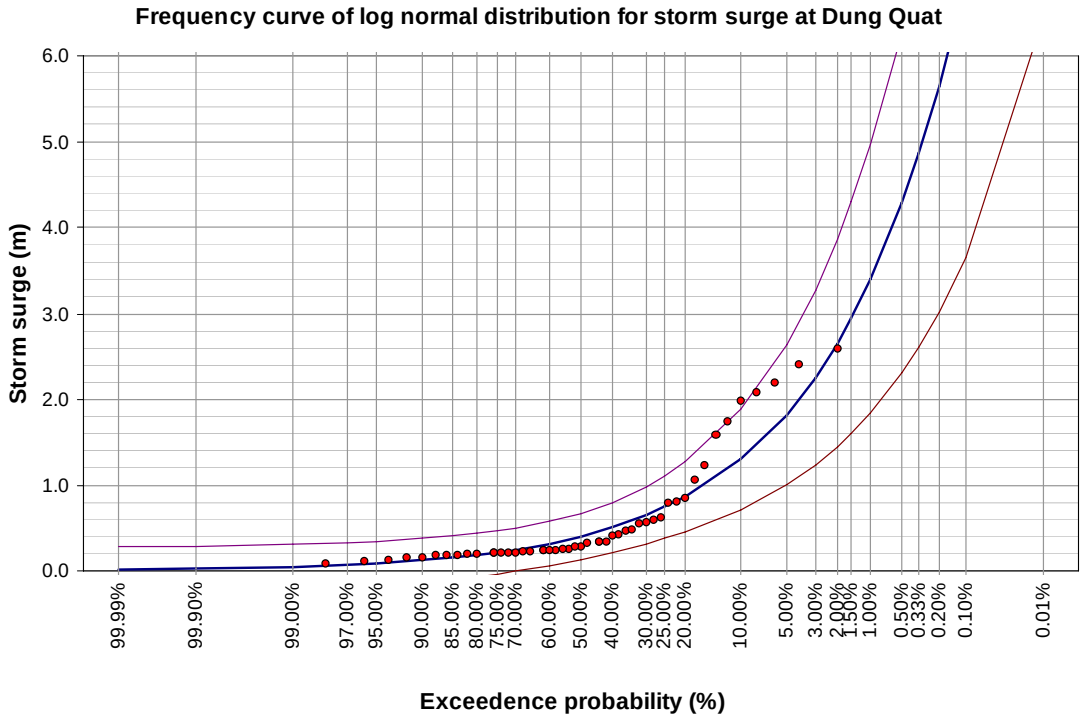

Figure C-20. Log-normal distribution for storm surge at Dung Quat

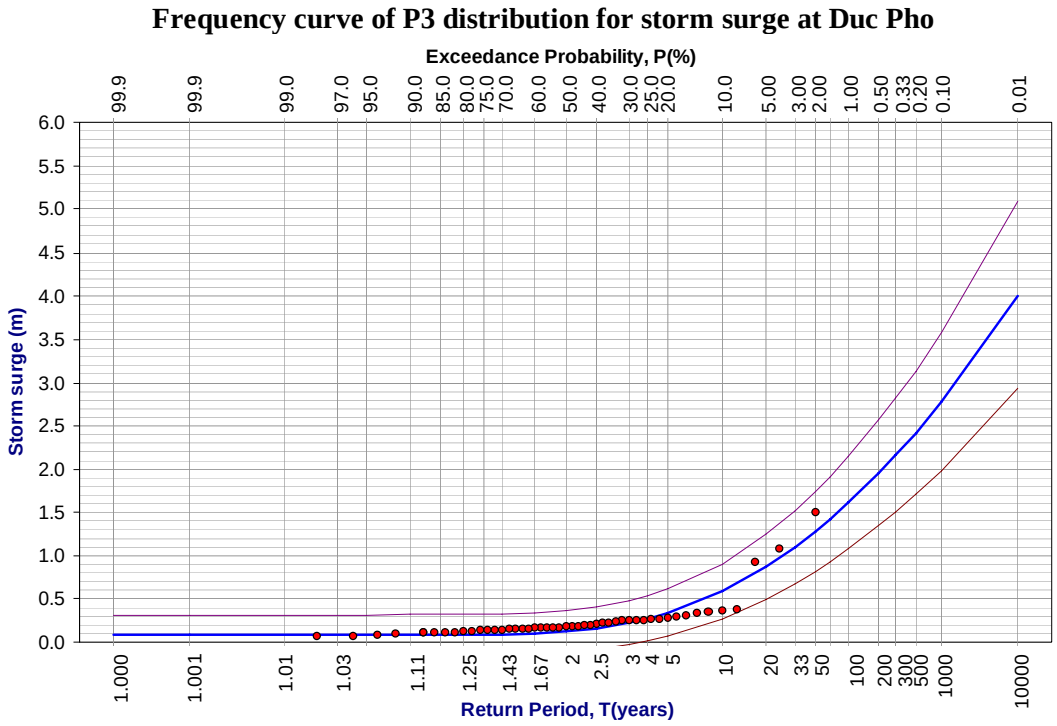

Figure C-21. Pearson type III distribution for storm surge at Duc Pho

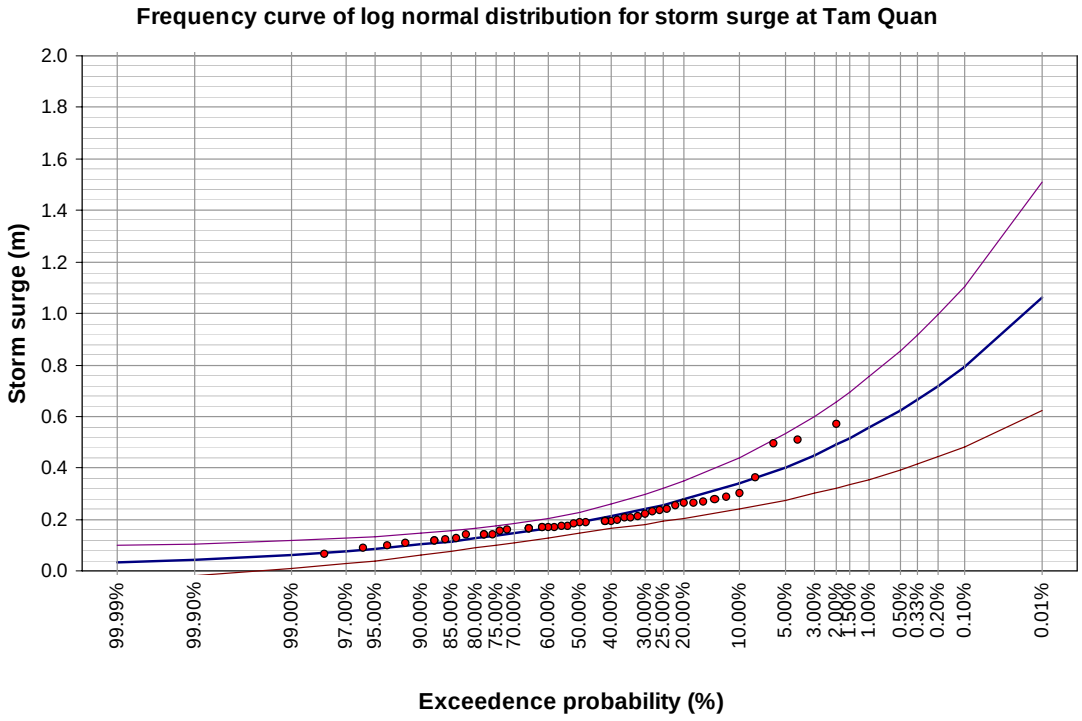

Figure C-22. Log-normal distribution for storm surge at Tam Quan

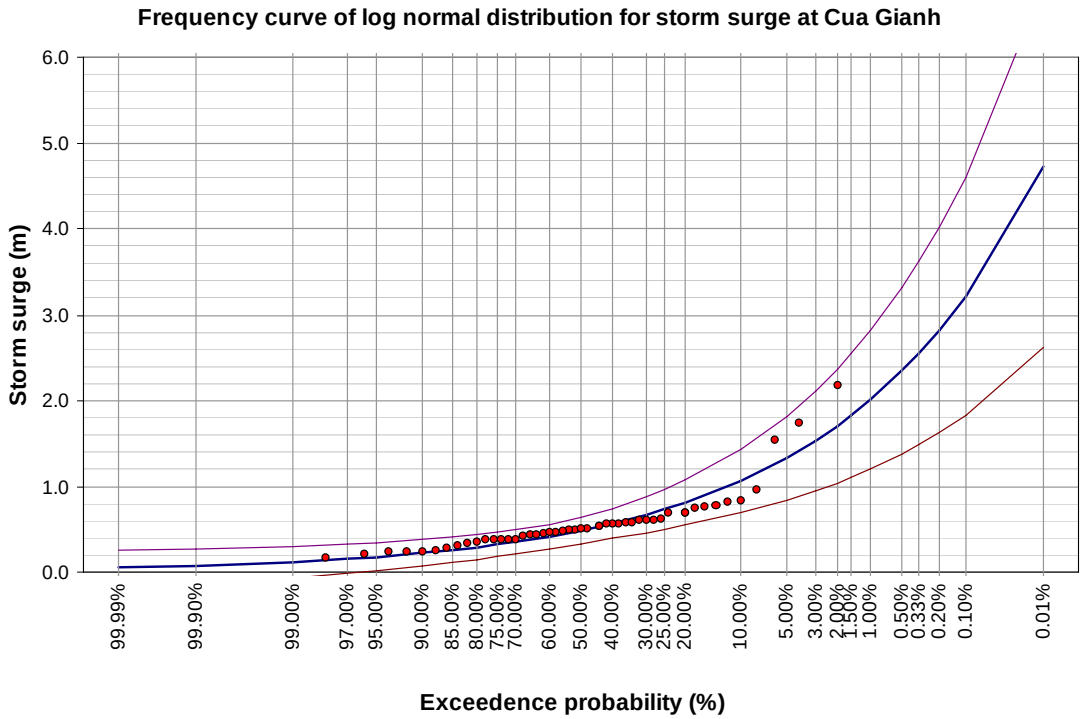

Figure C-23. Log-normal distribution for storm surge at Cua Gianh

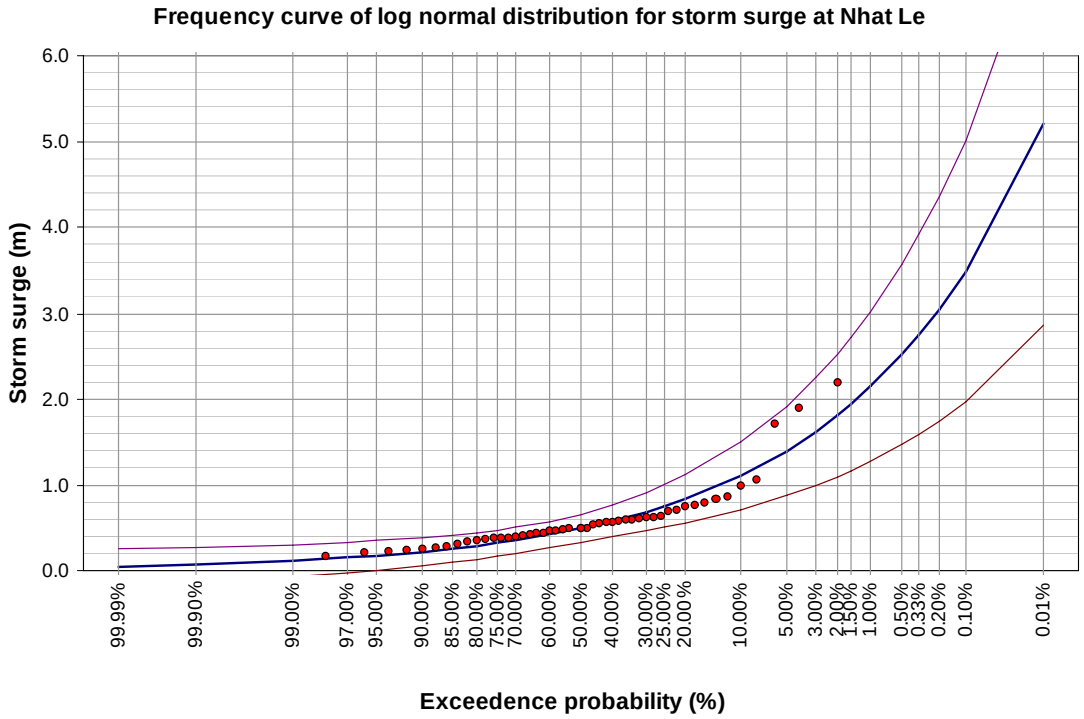

Figure C-24. Distribution for storm surge at Nhat Le

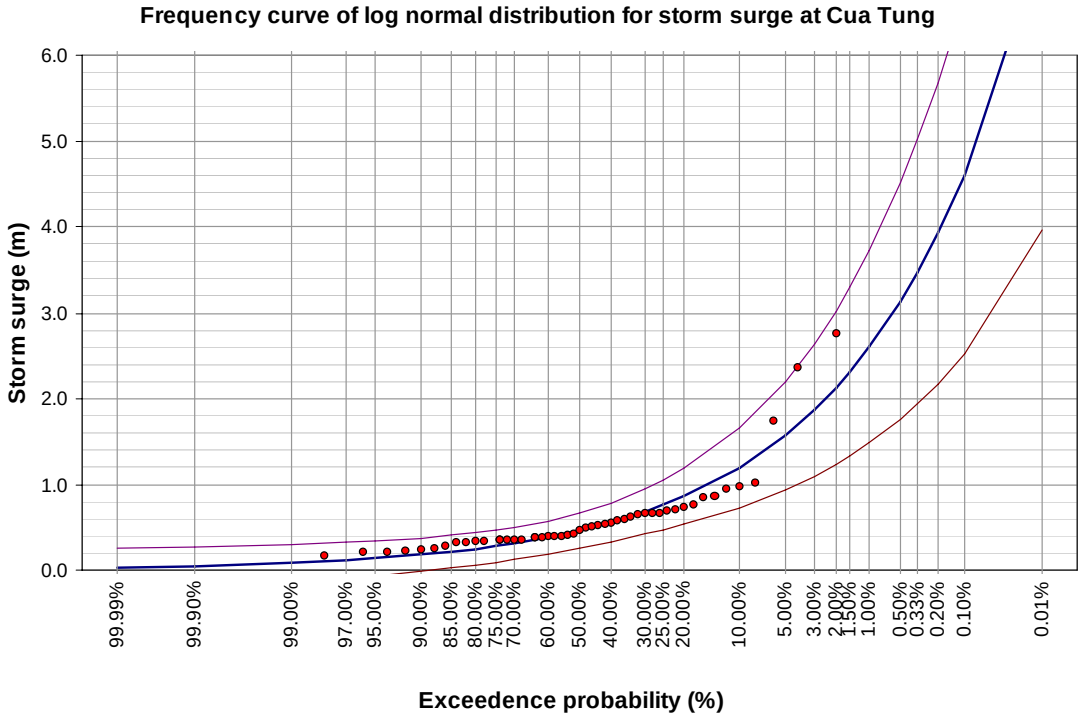

Figure C-25. Log-normal distribution for storm surge at Cua Tung

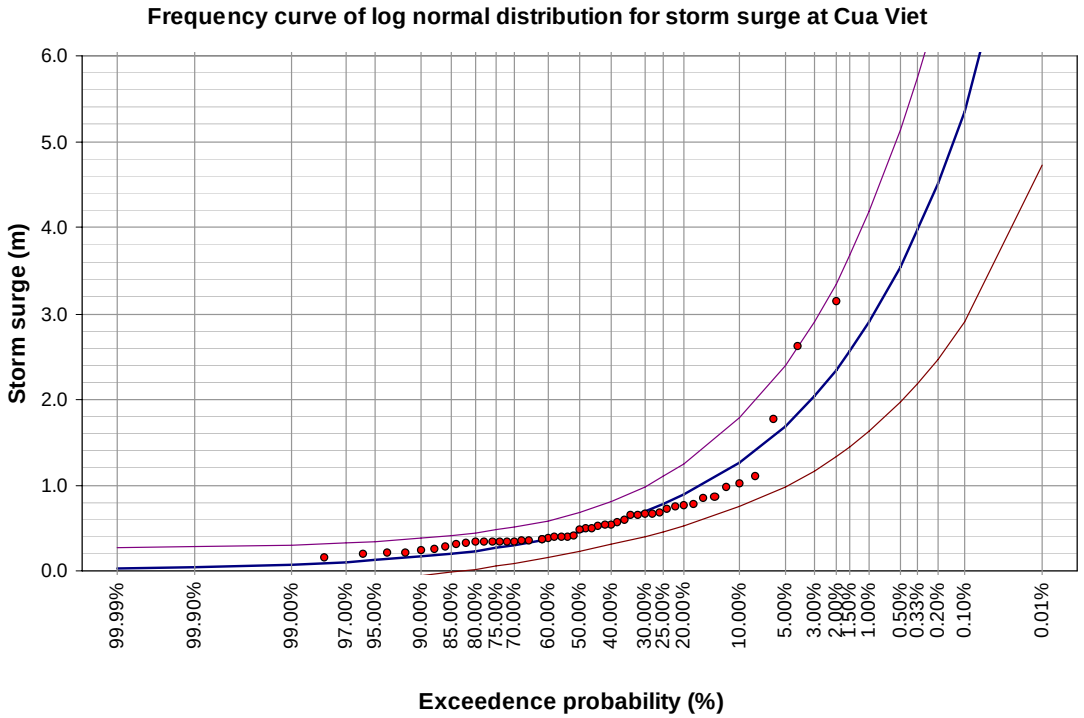

Figure C-26. Log-normal distribution for storm surge at Cua Viet

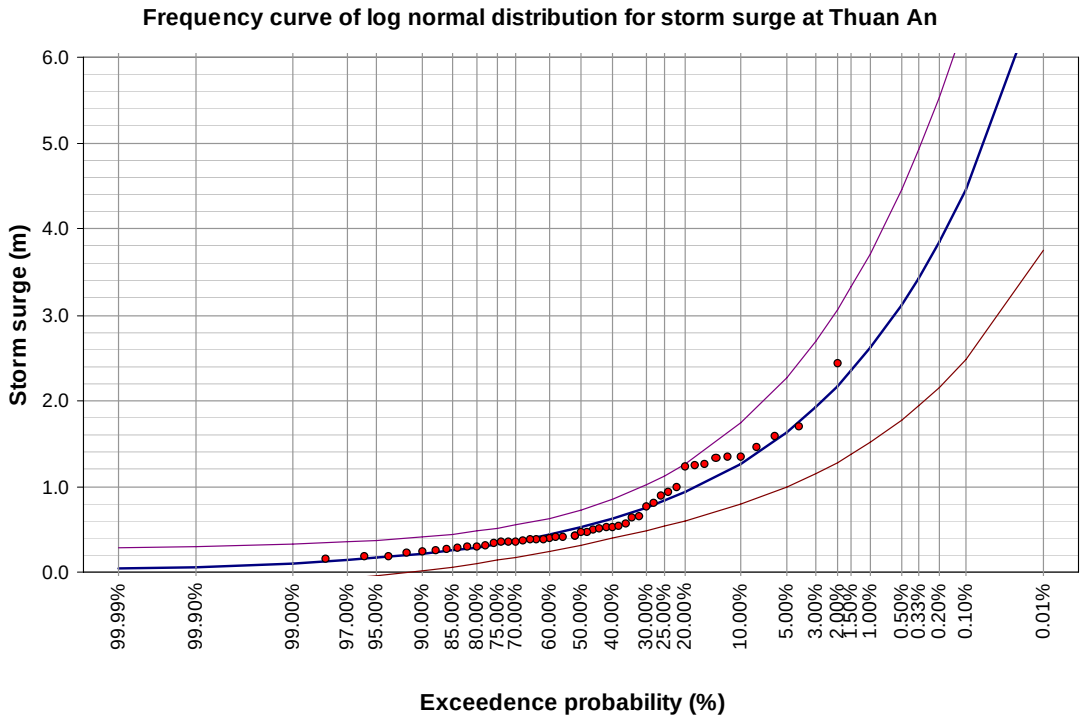

Figure C-27. Log-normal distribution for storm surge at Thuan An

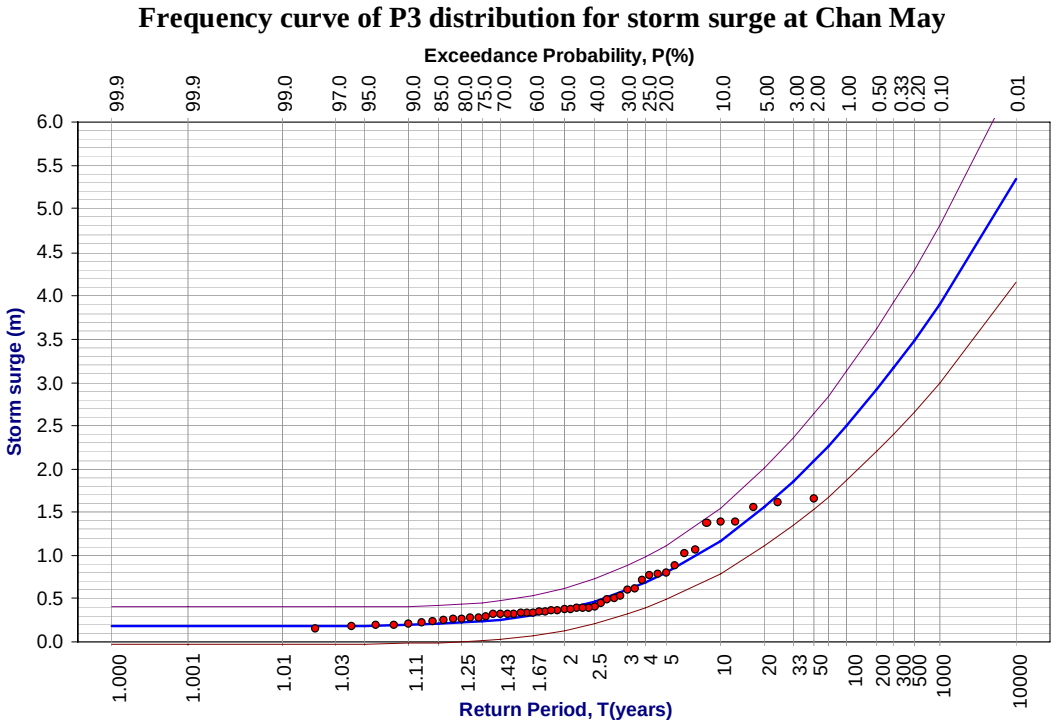

Figure C-28. Pearson type III distribution for storm surge at Chan May

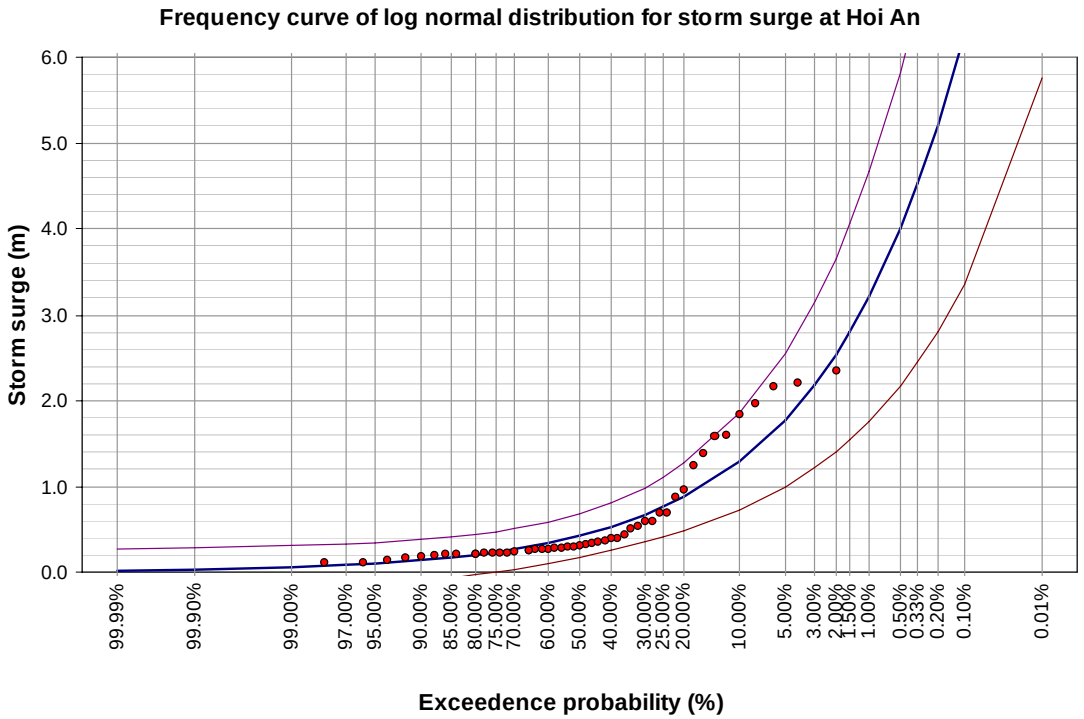

Figure C-29. Log-normal distribution for storm surge at Hoi An

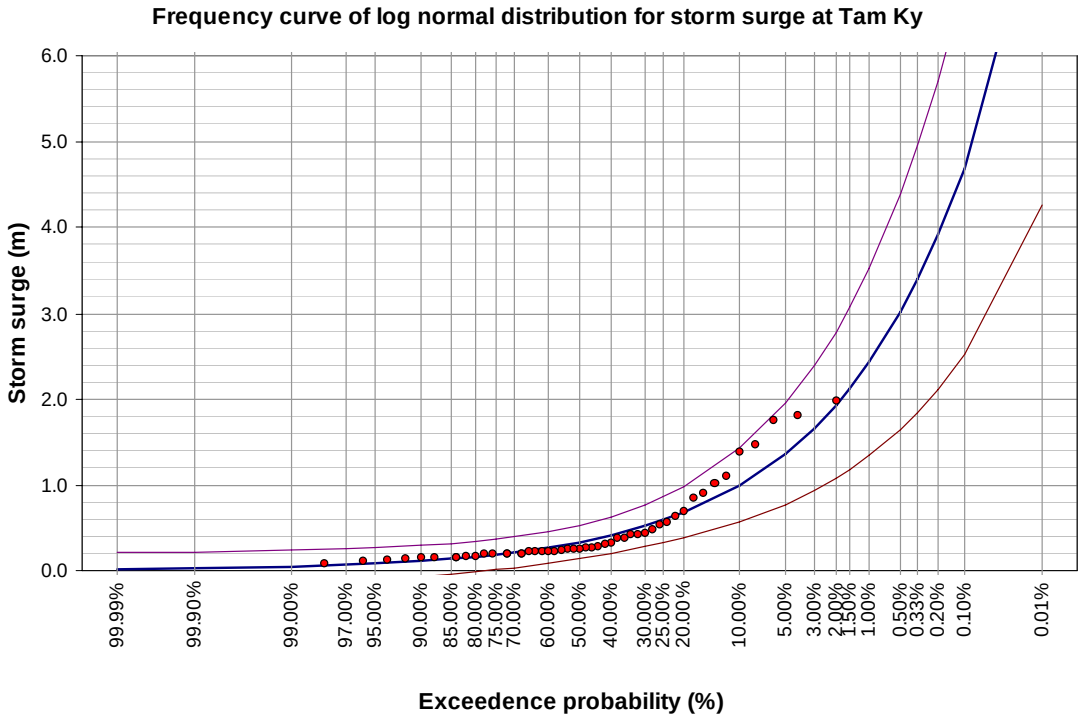

Figure C-30. Log-normal distribution for storm surge at Tam Ky

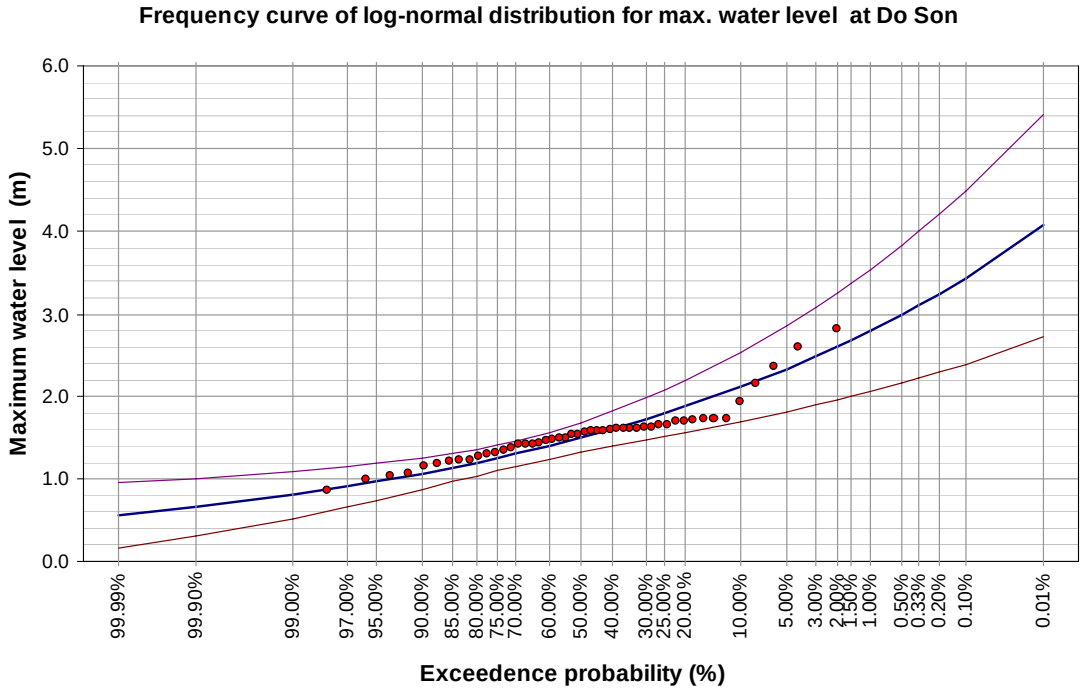

Figure C-31. Log-normal distribution for maximum water level at Do Son

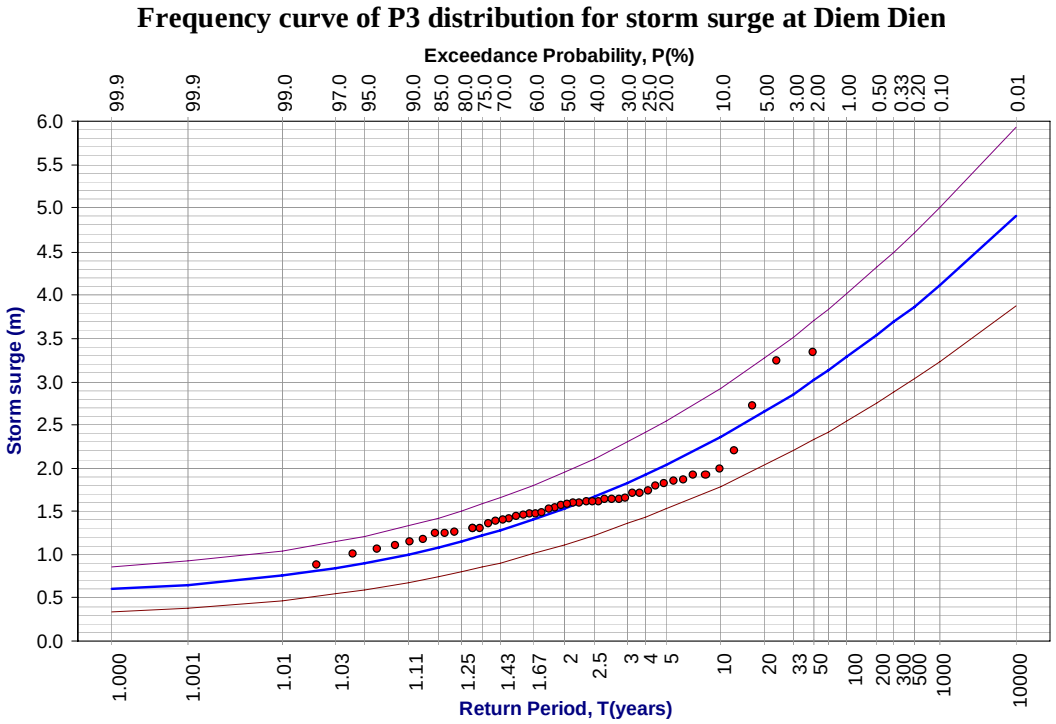

Figure C-32. Pearson type III distribution for maximum water level at Diem Dien

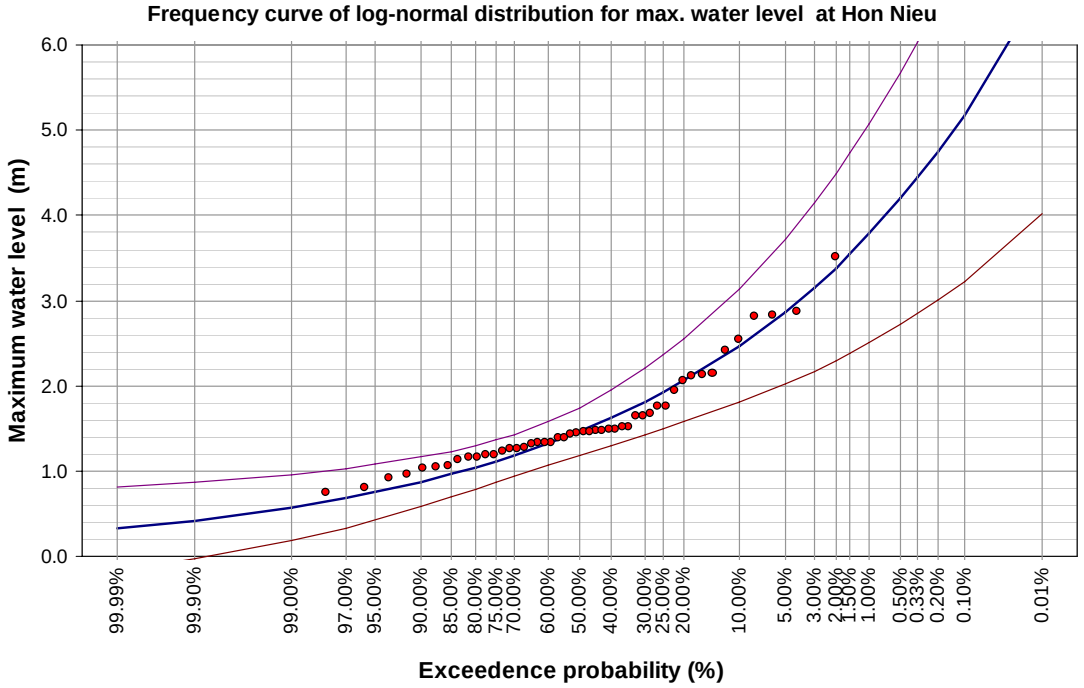

Figure C-33. Log-normal distribution for maximum water level at Hon Nieu

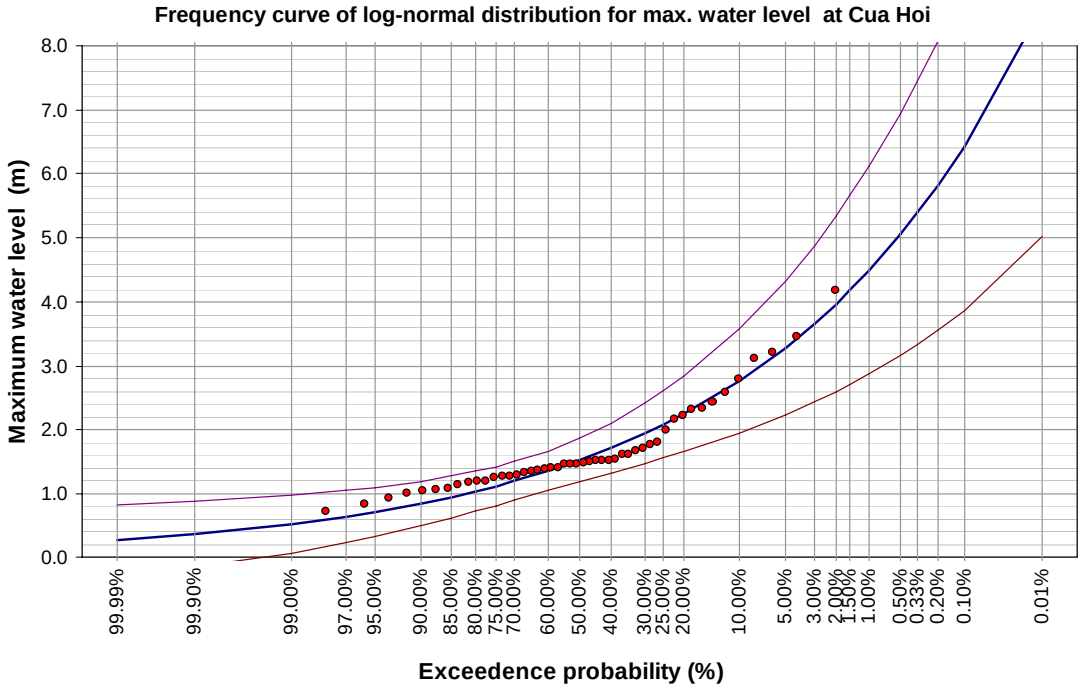

Figure C-34. Log-normal distribution for maximum water level at Cua Hoi

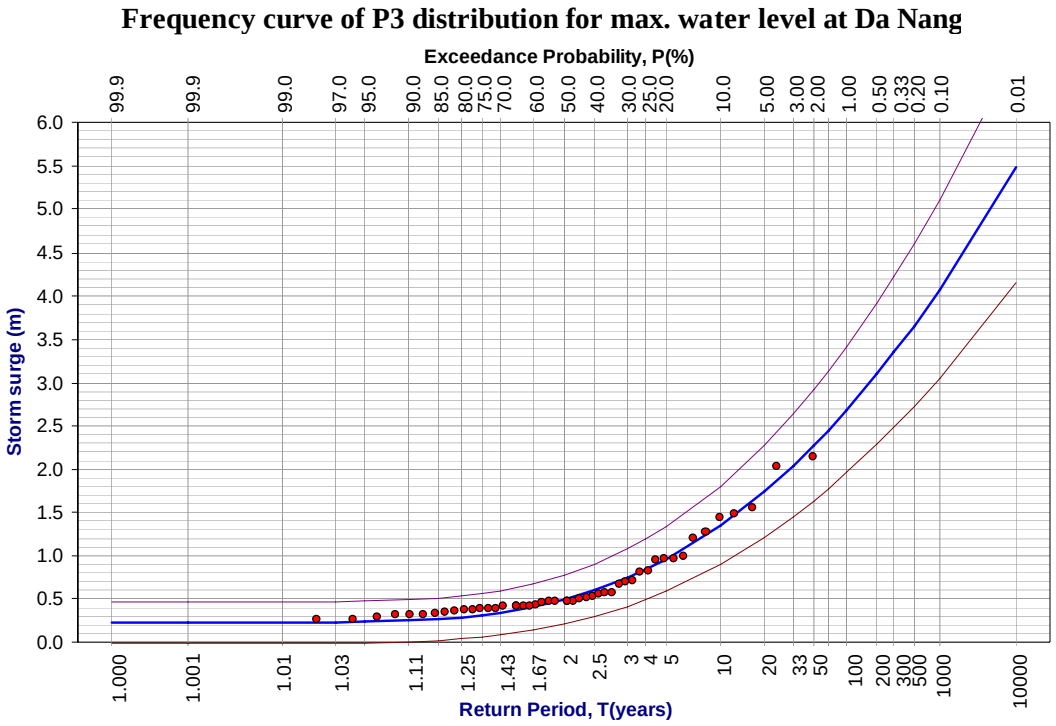

Figure C-35. Pearson type III distribution for maximum water level at Da Nang

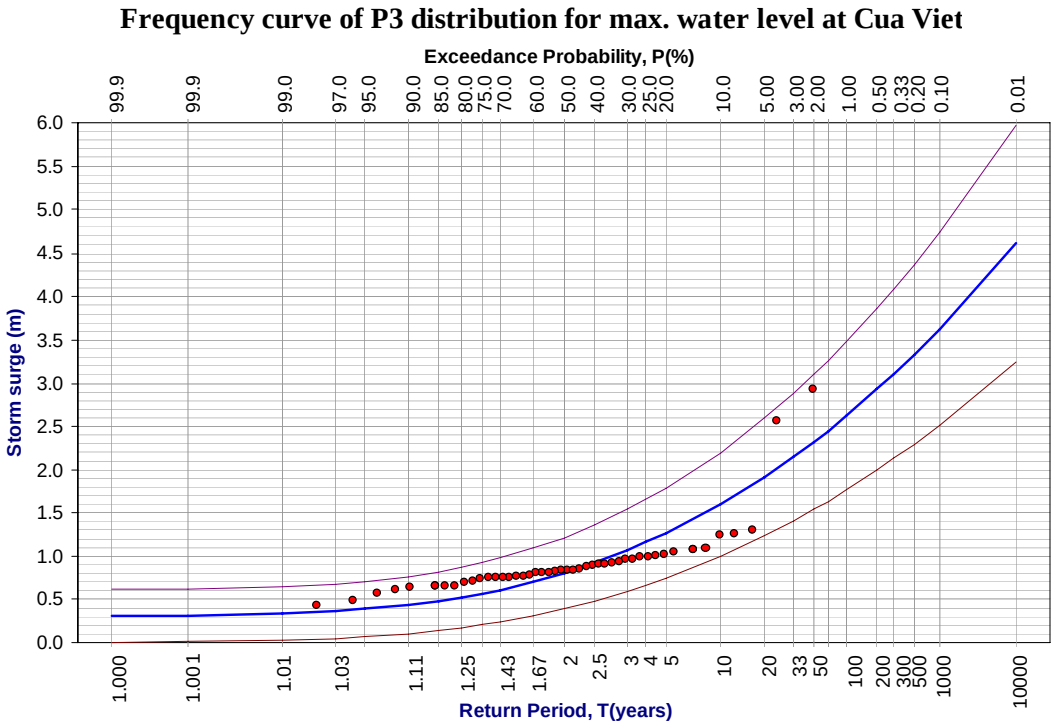

Figure C-36. Pearson type III distribution for maximum water level at Cua Viet